An Examination of the Neuropharmacology of Dependence

A Thesis submitted for the degree of MD to the University of Edinburgh

By

Dr. Mark Robert Crawford Daglish, B.Sc., M.B.Ch.B., M.R.C.Psych.

Acknowledgements

I could not have completed any of this work on my own. The list of those who have contributed is long. I would particularly like to thank those who have stuck with me for the duration of the process both at home and at work. My wife Dr. Constanze Schulz, whose own battle with a thesis I now more fully understand, has supported me in more ways that I have ever thanked her for; an oversight I hope this acknowledgement goes some way to redressing. My mentors, friends and "bosses" David Nutt and Anne Lingford-Hughes are entirely to blame for me ever starting this work in the first place. All three of the above are to blame for me ever finishing.

Thanks are due to all my colleagues and co-authors for their substantial contributions to the research and manuscripts that resulted. PET research is undoubtedly a team sport. Tim Williams, Jan Melichar, Judy Myles, Sue Wilson, Aviv Weinstein and Andrea Malizia have helped drive forward the addiction imaging programme in Bristol. Lindsay Taylor and Robin Holmes have been invaluable in keeping me focused on making image analysis possible in Bristol and providing the input to fill the large gaps in my knowledge. Paul Grasby and Alexander Hammers have provided similarly sage advice, knowledge and science from the PET Psychiatry group at Hammersmith Hospital.

Lastly I owe a debt of thanks to all those "willing volunteers" from the drug treatment services who participated in the studies. They tolerated being dragged out of bed at unpleasantly early hours, long journeys with only me for company, piles of questionnaires, being stuck with large needles and irradiated in return for a picture of their brain. Without exception they were engaged in the science, insightful in their comments that helped us to understand our results and genuinely interested in helping to make things better for future generations of drug users.

I certify that this thesis is my own work. The research contained within was completed as part of a research group. This thesis contains my contribution to the work of the group. None of this work has been submitted for any other degree.

Papers published from work contained in this thesis are:

Daglish M, Weinstein A, Malizia A, Wilson S, Melichar J, Britten S, Brewer C, Lingford-Hughes A, Myles J, Grasby P & Nutt D. Changes in regional cerebral blood flow elicited by craving memories in abstinent opiate-dependent subjects. *American Journal of Psychiatry* (2001) **158**: pp. 1680-1686.

Daglish MRC, Weinstein A, Malizia AL, Wilson S, Melichar JK, Lingford-Hughes A, Myles JS, Grasby P & Nutt DJ. Functional connectivity analysis of the neural circuits of opiate craving: "more" rather than "different"?. *NeuroImage* (2003) **20**: pp. 1964-1970.

Daglish MR, Williams TM, Wilson SJ, Taylor LG, Eap CB, Augsburger M, Giroud C, Brooks DJ, Myles JS, Grasby P, Lingford-Hughes AR, Nutt DJ. Brain dopamine response in human opioid addiction. *British Journal of Psychiatry* (2008) **193**: pp. 65-72.

Dr. Mark Daglish

B.Sc., M.B.Ch.B., M.R.C.Psych.

2009

Table of Contents

1 Introduction

1.1 Planned scope of thesis – neuroimaging dependence

Drugs of abuse alter the neurochemistry of the human brain. This is axiomatic, for if they did not, they would be inactive and hence not abused. My interest in the study of the neurobiology of dependence has centred on the use of the techniques of functional neuroimaging to examine the responses and changes of the living human brain to the processes of substance misuse. As one would expect, this thesis therefore follows that path. After a brief description of the social history of substance misuse, it is intended to begin with an explanation of the variety of techniques available today. This will not be an exhaustive, nor complete, list but will restrict itself to those techniques that feature in the rest of the thesis. A complete list and descriptions of the relative merits of them all would be sufficient to fill an entire thesis alone.

Following on from the description of neuroimaging techniques, this thesis will discuss the previous use of these to the field of opioid addiction and dependence. As the final chapter will be largely discussing the common findings and changes in neurobiology found across the spectrum of drugs of abuse, this review will not be confined solely to the study of opioid dependence; however, all the research work carried out for this thesis focused entirely on this disorder.

The middle section of this thesis will focus on the empirical research carried out using Positron Emission Tomography (PET) techniques to examine the neurobiology

of opioid dependence. There are two separate studies contained within this section; each beginning with a detailed discussion of the scanning and analysis techniques developed and used, and each using a different sub-type of PET imaging to examine different components of the disorder.

The final chapter will attempt to draw together the results from the review of the published literature with the experimental results. The aim is to show the increasing parallels being found from different methodologies examining different drugs of abuse and hence provide evidence for core underlying neurobiological changes that are implicated in the central concept of addiction.

1.2 A brief history of substance misuse

Man has been using and abusing psychoactive substances since the dawn of time. The commonality of the search for psychoactive substances across different continents and cultures suggests a form of social convergent evolution. Across all cultures and substances, there is also a pattern of social constraint defining acceptable manner of use. In addition to opium, khat, peyote, coca leaves and paste, and alcohol all have accepted patterns of use for example. However, some users stray outside of these social boundaries and are labelled as pathological. Intriguingly, for many of these substances the psychological state of dependence is common across the different substances.

The opium poppy (*Papaver somniferum*) has been domesticated for at least 8,000 years. The Sumerian language from Mesopotamia in 3,000 BC contains an ideogram

'the plant of joy' which denotes the opium poppy. Its medicinal use has been recorded for almost as long. Over 700 different medications containing poppy juice extract were found recorded on a medical papyrus dating from Thebes in 1551 BC. More modern preparations like opium tincture (laudanum), and possibly even morphine, date from the mid 17th Century. Descriptions of physical dependence on opiates also begin to appear in the medical literature from this time.

> 'So necessary an instrument is opium in the hand of a skillful man, that medicine would be a cripple without it; and whosoever understands it well, will do more with it alone than he could well hope to do with any single medicine. To know it only as a means of procuring sleep, or of allaying pain, or of checking diarrhoea, is to know it only by halves. Like a Delphic sword, it can be used for many purposes besides. Of cordials, it is the best that has hitherto been discovered in nature. I had nearly said it was the only one.'
>
> Thomas Sydenham (quoted in Davenport-Hines, 2004, p.13)

Morphine was first recorded under that name from the early years of the 19th Century. First reliably synthesised in Paris, it was marketed as a powerful analgesic and cure for opium dependence. The use of injected opiates followed with the invention of the hypodermic some half-century later.

Edinburgh has a long and illustrious history of involvement in the opiate story. One of the largest early opium dealers was a graduate of Edinburgh medical school. William Jardine and his company smuggled Indian opium to China amassing great profits in the first half of the 19th Century. Dr. Alexander Wood, in Edinburgh, developed one of the earliest described treatments for morphine dependence and opium eating in the 1850s. Unfortunately his "cure" was based upon a protocol of

morphine injections with the newly invented hypodermic syringe. A former Physician Superintendent of the Royal Edinburgh Asylum, Thomas Clouston, specialised in the treatment of opiate addiction. He was also one of the first to describe the treatment of cocaine addiction at the end of the 19th Century (Davenport-Hines, 2004).

C.R. Alder Wright first synthesised diacetyl-morphine from morphine in 1874. It was then almost completely ignored until Felix Hoffmann, the creator of aspirin, re-synthesised heroin (the new name for diamorphine) from morphine in 1898. Heroin, the "*heroisch*" drug, contrary to popular myth, was not invented to fight morphine and opium dependence. It takes its name from the German word "*heroisch*" meaning powerful or heroic. It was initially marketed by Bayer as a cough suppressant and treatment for respiratory illnesses more powerful than morphine.

Although the concept of dependence was described over many centuries, its scientific study began much later. The first epidemiological study of opium dependence was by Terry & Pellens (1928). A study they conducted for the, beautifully named, United States Bureau of Social Hygiene.

1.3 The techniques of neuroimaging

The focus of this thesis is on neuroimaging the neurobiology of opioid dependence. I will begin, therefore, with a description of the techniques of neuroimaging. The primary division of these techniques of neuroimaging is into the basic categories of

structural or functional.

1.3.1 Structural imaging

Structural imaging is not used in this thesis, except where is has been used to facilitate the analysis of functional imaging. Structural imaging can be used to provide additional anatomical information, which the lower resolution of most functional imaging techniques is often lacking.

The two main techniques in this category are Computed Tomography (CT) and Magnetic Resonance Imaging (MRI).

1.3.1.1 Computed Tomography (CT)

Computed axial tomography, as it was then known, was first used in the early 1970s at Atkinson Morley's Hospital in Wimbledon, London. Its inventors, Sir Godfrey Hounsfield and Allan Cormack, were awarded the Nobel Prize for their work in 1979. The principle itself is fairly straightforward. The implementation of the process however, had to await sufficient computing power to handle the computations required for image reconstruction. It is reported that the first ever CT image took 9 days to acquire and reconstruct. Thankfully the target was an inanimate object, not a patient.

Images are acquired as a series of x-rays taken at multiple angles. These are then reconstructed into slices by a process of iterative reconstruction akin to solving of the classical "magic square" mathematical puzzle (see Figure 1.1).

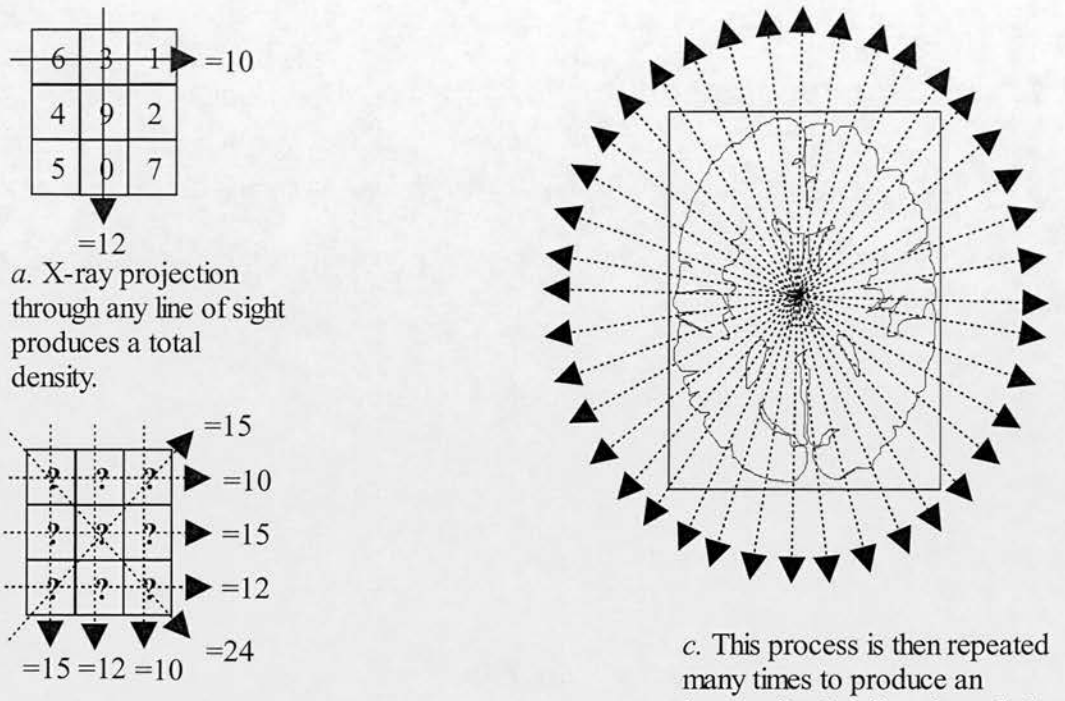

Figure 1.1: Fundamentals of CT Scanning

More recently there have been many improvements in the technique that have reduced the quantities of radiation required to acquire images. Speed, and the production of true 3D images, has also been boosted by the use of spiral scanning sequences (e.g. Hu, 1999). While still used extensively in a clinical setting, because of the widespread availability, speed of image acquisition and low cost, its research use is still limited by the radiation exposure inherent in any x-ray based technique.

In the last few years combined PET / CT scanners have been produced. These enable accurate co-registration of structural CT scans and functional PET images. These

have been developed mainly for clinical use in oncology and neurology.

1.3.1.2 Magnetic Resonance Imaging (MRI)

1.3.1.2.1 History of MRI

The first description of the process of Nuclear Magnetic Resonance (NMR, now called MRI) as a potential *in vivo* imaging technique was by Damadian (1971). He described the differences in T1 & T2 relaxation times between tissue types. The process of using these tissue differences to create clinically useful images such as those used today was taken up by Sir Peter Mansfield (e.g. Grannell & Mansfield, 1975) in Nottingham and Paul Lauterbur in the USA (e.g. Kramer *et al.*, 1981); both of whom were awarded the 2003 Nobel Prize.

1.3.1.2.2 Physics of MRI

MRI is based on the principle that all atomic nuclei are charged and spinning. The combination of these properties requires that they therefore also have a magnetic field. When placed in a very strong magnetic field they will align themselves with this external field. These strong fields are only now possible through the use of superconductors requiring extremely low temperatures. The majority of the bulk of a modern MRI scanning is the liquid helium cooling system. Once the nuclei have aligned with the magnetic field, they can then be perturbed, or knocked out of alignment, by a brief electromagnetic pulse. After the pulse they will relax back into alignment with the static magnetic field releasing measurable energy as they do so. The rate at which they relax is dependent on the magnetic environment surrounding

the nuclei at the time. In most common biological nuclei however, there are an even number of protons, e.g. ^{12}Carbon, ^{16}Oxygen and ^{14}Nitrogen. The MRI effect requires an odd number in the nucleus which is why most current neuroimaging MRI techniques are tuned to measure the responses of ^{1}Hydrogen nuclei; although ^{31}Phosphorus can also be used. Using ^{1}Hydrogen gives a very clear picture of water distribution in the body tissues which is excellent for imaging brain, as the skull is relatively poorly seen in comparison to brain tissue; clearly this is markedly different to CT where bone has a much larger contrast. By adding a gradient to the surrounding magnetic field it then becomes possible to use this gradient to determine the location of any relaxation signal within the field, aiding signal detection and image reconstruction.

There are a very large number of different adaptations and scanning protocols that can be employed to differentiate different tissues. These are produced by use of different pulse sequences and tuning of the detector aerials. The original classical MRI uses T1 relaxation times, which are in the order of 1000ms and are best for distinguishing grey and white matter; T2 times are also commonly used in brain scanning because of their ability to produce high contrast between CSF and brain tissue. Improvements continue to be made with higher field strength magnets with steeper gradients and faster pulse sequences. These act to improve signal to noise ratios, increase spatial resolution and remove unwanted signal from tissues like blood.

1.3.1.2.2.1 Voxel Based Morphometry (VBM)

This is a technique for the systematic and automated analysis of differences in brain structure (Ashburner & Friston, 2000). MRI images are required with high spatial resolution and good contrast between grey matter, white matter and cerebro-spinal fluid (CSF). Each image is warped to fit a standardised space and then segmented into the three main tissue types, with non-brain tissue being excluded. These maps have voxel values that represent the concentration of tissue within the voxel. In many ways this can be thought of also as an index of the proportion of cells within the voxel that belong to the specified tissue class. These maps are then smoothed before being compared between groups.

A further refinement has been proposed, usually referred to as "optimised VBM" (Good *et al.*, 2001), where the tissue concentration maps are convolved with the parameters used to warp the images into standard space to produce modulated tissue maps. In such a modulated map the value of each voxel can be conceptualised as the volume that voxel would have occupied in native patient space. This means that when comparing images between groups the outcome is regions where the *volume* of target tissue is statistically different, rather than where the *concentration* of the target tissue is different. The target tissue in question can be grey matter, white matter, or even CSF.

Table 1.1: Advantages and Disadvantages of MRI & CT

	CT	MRI
Cost	Cheap	Moderately cheap
Typical acquisition time	3-10mins whole head	7-30mins whole head
Availability	Very widespread	Fairly widespread and increasing
Tissue contrast	Best for bone vs. soft tissue vs. air	Best for soft tissue type discrimination
Typical spatial resolution	0.7 x 0.7 x 2-10mm	0.5 x 0.5 x 1 mm
Repeatability	Limited by radiation exposure	Unlimited
Physical constraints	Usually open and easily accessible	Can be very enclosed
Contra-indications	Nil	Metallic implants or foreign bodies. Electronic implants.
Image problems	Poor in areas close to bone	Areas of distortion possible associated with eye movements, swallowing or sinuses.
Radiation exposure	Average 1.5mSv per brain scan (Mettler *et al.*, 2000)	Nil

1.3.2 Functional imaging techniques

1.3.2.1 Functional Magnetic Resonance Imaging (fMRI)

1.3.2.1.1 History of fMRI

The first paper demonstrating the use of fMRI to image changes in neuronal function associated with a task was published in 1992 (Kwong *et al.*, 1992). All the basic elements of current fMRI are nicely described in the paper including the need for averaging over multiple acquisitions to discern the signal. In essence, fMRI is a

subset of MRI. It is based on the differing magnetic properties of oxy- & deoxy-haemoglobin. When neurones are active they are thought to increase the blood flow through surrounding capillaries (Kwong *et al.*, 1992). The increase in the delivery of oxygenated blood exceeds that required by the neuronal tissue, resulting in a relative increase in the amount of oxy-haemoglobin. This alters the response of surrounding hydrogen nuclei to the MRI imaging technique. This variable response is labelled the Blood Oxygen Level Dependent (BOLD) response. Newer pulse sequences and techniques continually increase the possibilities of this technique.

1.3.2.1.2 Advantages and disadvantages of fMRI

fMRI has many advantages. Images can be acquired over a short time span, in the order of hundreds of milliseconds for a whole brain image. No radiation exposure is required. A structural image can be acquired within the same scanning session helping to localise any signal measured by fMRI. These advantages mean that experimental subjects can be scanned repeatedly over a short period of time in order to discern the blood flow changes that accompany any concomitantly reported or induced psychological state. The ability to repeat this many times helps to improve the signal-to-noise ratio of the technique as it allows averaging of responses. Time-locking the scan acquisition to a repeated event also allows for event-related or evoked fMRI BOLD responses to be measured. This functions in a similar manner to evoked potentials in the electroencephalography (EEG) field. Obviously, fMRI is not without its drawbacks. The largest problems are related to the practicalities of

the scanner. All fMRI scans are extremely noisy. Subjects or patients always have to wear headphones, making verbal communication difficult. This can be reduced by the use of "sparse" acquisition protocols, where the image is acquired over a condensed period of time, with gaps interspersed. In addition to being noisy, the scanner environment is frequently enclosed, making the presentation of any visual stimuli difficult. Also the strong magnetic fields surrounding the scanner and the pulsed high-frequency radio waves mean that any equipment used in the scanner room must conform to tight rules of electrical screening.

In comparison with PET techniques, described later, fMRI has a number of advantages. The possibility for rapid acquisition times allows for better temporal resolution. The absence of any radiation exposure, allowing repeated scanning, leads to better statistical power with larger sample numbers. However, fMRI does suffer from some of the similar problems to MRI, with signal drop-out (esp. near sinuses). This is more marked in fMRI due to the faster switching times required. Fluctuations in the magnetic field also lead to image ghosting related to subject movement, e.g. swallowing or eye movement echoes or just ordinary head movement. There is also the issue of low frequency aliasing of high-frequency noise, e.g. respiratory and pulse rate, as demonstrated in Figure 1.2. There are techniques for avoiding, or minimising the impact of, these problems, but it is beyond the scope of this thesis to discuss these in any detail.

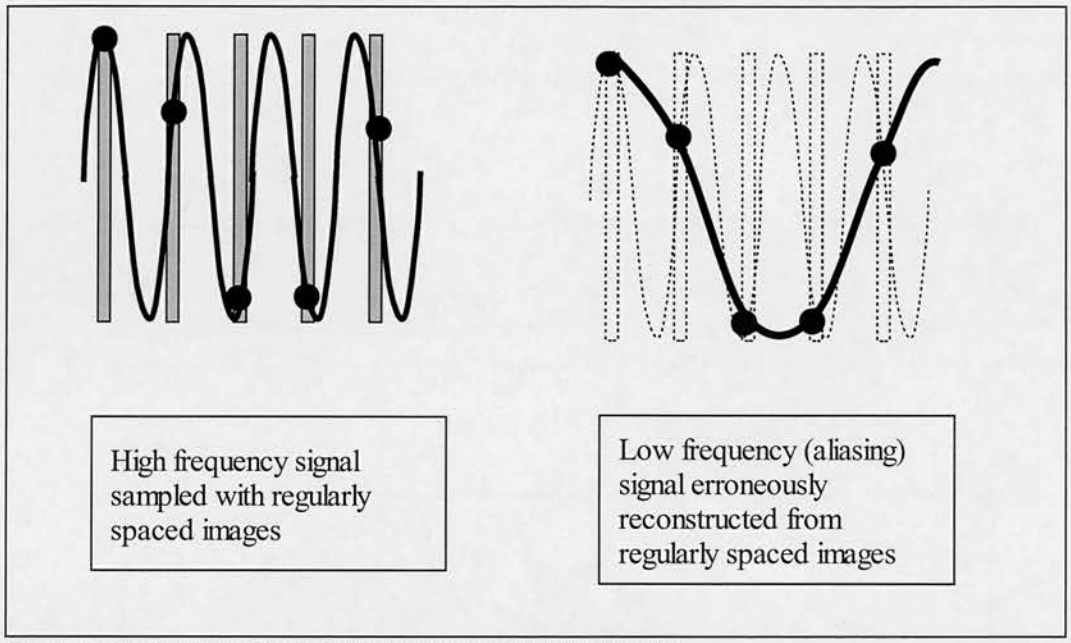

Figure 1.2: Aliasing of high frequency noise in fMRI images

1.3.2.2 Positron Emission Tomography (PET)

1.3.2.2.1 History of PET

The early history of PET is briefly described, along with nuclear magnetic resonance in Brownell *et al.*, (1982). As with CT, the theory was understood for a considerable period of time before the necessary computational power became available to allow the theory to be put into practice.

1.3.2.2.2 Physics of PET

Positron Emission Tomography relies on the injection of tracer molecules labelled with positron emitting radio isotopes. The positron is an anti-matter equivalent to an electron. Once released from a decaying nucleus it will diffuse into surrounding

tissues for a short distance before colliding with an electron. When this happens the two particles undergo a mutual annihilation releasing a dipole of two photons of gamma radiation at 180° with an energy of 511 keV (kilo-electron volts). Using a ring of detectors it is possible to use these two properties of a specific energy and a pair of photons being released simultaneously, to distinguish these annihilation events from background radiation and scattered photons released from events outside of the field of view of the detector ring.

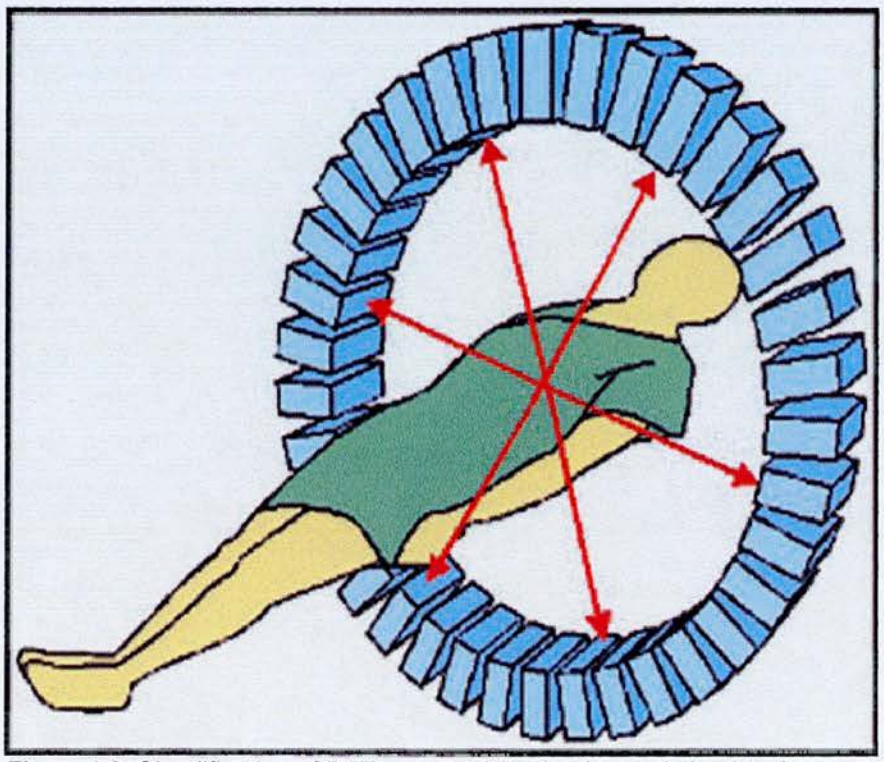

Figure 1.3: Simplification of PET camera detector ring and simulated gamma dipoles from isotope decay

The positron emitting isotopes routinely used for PET are ^{15}Oxygen, ^{11}Carbon and ^{18}Fluorine. These have half-lives of 122 seconds, 20.39 minutes and 109.77 minutes respectively. Images are acquired in one of two modes: frames or list-mode. For the

very short lived isotope ^{15}Oxygen images are usually acquired as a single frame, as a snapshot of cumulative signal distribution over the whole scan. For the longer-lived isotopes, the older form of data collection, in frames, is still used, but decreasingly often. This has the detector ring gather the sum of photons detected for a set period of time. Early in the scan when there is plenty of signal and tracer levels are changing rapidly, these time frames are usually fairly short, in the order of 30 seconds. Later, as the quantity of radiation and signal reduces exponentially and the rate of change declines, then the time frames typically lengthen out to 5 minutes.

With the increase in computing power it is now possible to acquire images in list-mode. In this case, every single event detected by the detectors is individually logged with its time. The usual technique is then to sum the data into time frames as for frame acquisitions and then proceed to image reconstruction. Because the time of data acquisition has also been recorded it is possible to redefine the timing of the frames after the scan, instead of before. They can then be selected based on the actual time curve of the signal, rather than the expected time curve. As yet this technique is still not fully exploited, but in theory it also allows for correction of subject movement within the scan in an almost transparent manner before the data is reconstructed into a dynamic sequence of 3D images.

The techniques of image reconstruction most commonly used are filtered back-projection (FBP) (Kinahan & Rogers, 1989) and Ordered-Subset Expectation-Maximisation (OSEM) (Hudson & Larkin, 1994). FBP is most frequently used for research scans, where quantitative data is required, but OSEM is often used in the

commercial, clinical environment due to improved lesion detection (Lartizien *et al.*, 2003).

Once the images are reconstructed they can be calibrated and further analysed in a number of different manners. Further discussion of this will be postponed until later in the thesis and discussed for each tracer used individually.

1.3.2.2.3 Measures of cerebral activation

The use of PET scanning depends entirely on the tracer that is injected. Radio-labelled water containing $H_2{}^{15}O$ can be used to follow blood flow, as can carbon monoxide ($C^{15}O$). The short half-life of ^{15}O of approximately 122 seconds, allows for repeated scanning over a short period of time and the capture of specific cognitive states. Closely related to this is the use of ^{18}F-fluoro-deoxy-glucose (^{18}FDG). This tracer is taken up into cells and trapped in proportion to their glucose use; giving a proxy measure of metabolic activity. The technique has the advantage of allowing injection of the tracer to occur outside of the scanner environment, which may make studying of certain psychological states more feasible. However, the much longer half-life of ^{18}F means that the temporal resolution is much lower, in the order of tens of minutes. On the other hand, the image quality is substantially better as more data per scan can be acquired. This yields better signal to noise ratios for a single scan for ^{18}F, but the repeat scanning used with $H_2{}^{15}O$ enables averaging of data to redress this balance. Despite this, fMRI has largely replaced $H_2{}^{15}O$ PET for imaging cerebral activation.

1.3.2.2.4 Measures of neurotransmitter systems

This is the field where PET continues to dominate. Using other tracers labelled with either ^{11}Carbon or ^{18}Fluorine it has become possible to measure indices of neurotransmitter function. A large number of possible tracers have been developed around the world. Depending on the neurotransmitter system under study it has become possible to study many aspects of neuronal signalling. Tracers exist to measure transmitter synthesis, post-synaptic binding and re-uptake. I shall describe only those of interest later in this thesis. ^{11}C-Raclopride is a specific antagonist at the dopamine D_2 receptor. It has been shown to bind selectively to this receptor and to be sensitive to the levels of endogenous dopamine (Laruelle *et al.*, 1997). For the opioid system there are two main tracers used. ^{11}C-Diprenorphine is an antagonist which labels all three opioid receptor subtypes (mu, kappa and delta) (Frost *et al.*, 1986; Jones *et al.*, 1999) and ^{11}C-Carfentanyl is a selective mu-receptor agonist (Frost *et al.*, 1990). As described above, depending on the PET scanner and tracer used, PET imaging has a temporal resolution ranging from tens of seconds to a few hours; which is clearly less than that available with fMRI. In the cases of ^{11}Carbon and ^{18}Fluorine the resolution is in the order of tens of minutes. However, in most cases and specifically with ^{11}C-Raclopride and ^{11}C-Diprenorphine, it does allow for absolute quantitation of tracer binding which more readily allows comparison between scans and between individuals. The scanning is also silent, which means that communication with the patient or research subject is easier and the environment less distracting to the experiment. As well as the temporal resolution, spatial

resolution is also not as good as with fMRI. Even the best PET scanners for humans cannot resolve structures several millimetres across, although more is possible with small animal systems.

1.3.2.3 Single Photon Emission Tomography (SPET)

Single Photon Emission Tomography (SPET) pre-dates CT as an imaging modality used to image the living human brain. The first paper on using SPET to examine cerebral blood flow was published in 1975 (Kuhl *et al.*, 1975). SPET has the advantage of being considerably cheaper than PET and hence far more widely available; however, the spatial and temporal resolution is poorer. The principle of injecting a radio-labelled tracer is that same as for PET, however the isotopes are different. In this case, the isotopes emit single photons of gamma radiation. The two most commonly used isotopes are ^{99m}Technetium (^{99m}Tc) and ^{123}Iodine (^{123}I). The single photons of gamma radiation are usually picked up by two or three rotating detector heads. The 3D image slices are reconstructed from these rotating heads in a manner similar to that used for CT. As with PET there are also a wide range of tracers using either ^{99m}Technetium or ^{123}Iodine for the study of several neurotransmitter systems.

For measuring blood flow, and hence cerebral activation, the tracer ^{99m}Tc-hexamethylpropylene amine oxime (^{99m}Tc-HMPAO) is used. It is irreversibly absorbed in proportion to blood flow in the minutes following the injection. As with ^{18}FDG PET, it is possible to inject tracer outside of the scanner environment and

during a period of exposure to stimuli or tasks of interest (Sharp *et al.*, 1986). The other main tracers of interest for this topic are ^{123}I-Iomazanil and ^{123}I-Iodobenzamide (^{123}IBZM). ^{123}I-Iomazanil binds to the $GABA_A$-benzodiazepine receptor (Höll *et al.*, 1989) and ^{123}IBZM to the dopamine D_2 receptor (Kung *et al.*, 1989).

1.4 The current state of neuroimaging in dependence

PET, SPET and fMRI together have produced a considerable body of research to aid the understanding of the fundamental mechanisms of addiction and dependence. The most striking finding is that different research groups studying different populations of drug users using different methodologies repeatedly report the same brain regions as being significant. The exact roles of individual brain regions are the topic of considerable ongoing debate. A brief outline of suggested functions is shown in Table 1.2. The multitude of imaging studies behind this table is discussed in the following section, with particular emphasis on studies of heroin users. Studies of other drugs will be mentioned only where they shed light on the processes of opioid addiction.

Table 1.2 An outline of the brain regions implicated in addiction and their proposed functions

Anterior Cingulate / Medial Pre-frontal gyri	Attention & emotional salience of drug related stimuli
Orbito-frontal cortex	Urge to use & loss of control
Hippocampus & Amygdala	Memory & learning
Ventral Striatum	Reward prediction
Thalamus	Rush & hedonic response
Hypothalamic & brainstem nuclei	Autonomic & endocrine responses

As alluded to above, a large number of differing neuroimaging techniques have been used to study addiction. In the interest of clarity I shall first discuss studies examining brain structure. In this section I will also include studies of brain function where these studies seek to examine evidence of deficits in function *un*related to the process of addition itself. For example, this section will include studies of perfusion or glucose metabolism at rest. The remaining functional neuroimaging studies can be divided into two major groups; those that examine cerebral activation and those examining neurotransmitter function. The former group will also include some studies of perfusion or glucose metabolism, but in this case where the task or activation is related to the process of addiction, such as cue-induced craving.

1.4.1 Neuroimaging studies of structure or basic function

There are problems when attempting to study long term structural changes in the brains of heroin users. The biggest problem that clouds the interpretation of most studies is the tendency for heroin users to use other drugs that may also have neurotoxic effects. Even when users are only buying heroin on the street it may be contaminated with any number of potentially harmful additives. Differentiating the effects of the active diamorphine from these other constituents may prove impossible as they are unknown, unquantified and the amounts used will be strongly correlated with the lifetime exposure to heroin. Unusual, but obvious examples of potential confounds would be infective emboli from endocarditis secondary to poor injecting practice or AIDS-related dementia. The few systematic studies of structural changes

have tended to find evidence of only subtle changes, if anything, which are always open to the criticism that they are pre-morbid and perhaps an indication of a predisposition to drug dependency problems.

Table 1.3 Structural and perfusion imaging studies in addiction

Study	Population	Technique (and task)
Aasly *et al.*, 1993	Poly drug users	MRI
Adams *et al.*, 1993	Alcoholics	FDG at rest
Amass *et al.*, 1992	Mixed cocaine, heroin & poly-drug	1.5T MRI
Bae *et al.*, 2006	Methamphetamine users and controls	MRI
Besson *et al.*, 1981	"Alcoholic cerebral disorder"	MRI/NMR
Bolla *et al.*, 2003	Cocaine users	OFC decision making gambling task
Bolla *et al.*, 2004	Abstinent cocaine users vs controls	$H_2{}^{15}O$ PET on Stroop
Botelho *et al.*, 2006	Heroin users & historical controls	HMPAO SPET at rest
Cala *et al.*, 1978	Alcoholics	CT
Cala *et al.*, 1980	Alcoholics	CT
Carlen *et al.*, 1978	Alcoholics	CT
Carlen *et al.*, 1981	Alcoholics	CT
Carlen *et al.*, 1984	Alcoholics	CT
Cascella *et al.*, 1989	Poly drug users	CT
Cascella *et al.*, 1991	Poly drug users	CT
Chick *et al.*, 1989	Alcoholics	MRI
Christensen *et al.*, 1996	9 male polydrug users	^{31}P-MRS
Cowan *et al.*, 2003	MDMA users	VBM on MRI
Danos *et al.*, 1998a	Opiate patients in withdrawal but on methadone	HMPAO SPECT
Danos *et al.*, 1998c	Opiate dependent	CT
Danos *et al.*, 1998b	Heroin dependent	HMPAO-SPET (in withdrawal)
Di Sclafani *et al.*, 1995	Older abstinent alcoholics	MRI
Ersche *et al.*, 2005a	Amphetamine and opioid users and control	$H_2{}^{15}O$ PET (Gambling task)
Ernst *et al.*, 2000	Methamphetamine	MRS
Fox *et al.*, 1976	Alcoholics	CT
Galynker *et al.*, 2000	Opiate-dependent subjects	FDG-PET
Gerra *et al.*, 1998	Detoxed Opiate users	HMPAO SPET
Gilman *et al.*, 1990	Alcoholic with and without cerebellar damage	FDG
Hagel *et al.*, 2005	Heroin smokers with spongiform leucoencephalopathy	CT & MRI
Handelsman *et al.*, 1993	HIV drug users	0.3T MRI
Haselhorst *et al.*, 2002	Long-term IV heroin	^{1}H-MRS
Hill & Mikhael, 1979	Heroin and alcohol	CT
Holman *et al.*, 1991	Cocaine (polydrug) users	HMPAO SPET
Holman *et al.*, 1992	Cocaine users and AIDS dementia	HMPAO SPECT
Holman *et al.*, 1993	Heroin and Cocaine users	HMPAO SPECT
Hwang *et al.*, 2005	Methamphetamine	HMPAO
Jacobsen *et al.*, 2001	Cocaine	Quantitative morphology
Kao *et al.*, 1994	Amphetamine users	HMPAO
Kaufman *et al.*, 1999	Methadone maintained opiate users	^{31}P-MRS
Kim *et al.*, 2005	Methamphetamine	FDG
Kim *et al.*, 2006	Methamphetamine	VBM
Kivisaari *et al.*, 2004	IV heroin users and controls	MRI

Kosten *et al.*, 1998	Abstinent cocaine-alcohol users	rCBF
Kroft *et al.*, 1991	Alcohol dependent women	MRI
Krystal *et al.*, 1995	Opiate users vs controls	HMPAO SPECT (after naloxone)
Levin *et al.*, 1994	Polydrug abusing women	HMPAO SPECT
Levin *et al.*, 1995	Polydrug users treated with buprenorphine	rCBF
Liu *et al.*, 1995	Polydrug users	MRI
London *et al.*, 1989	2 Heroin addicts & 3 heroin users	FDG
Lyoo *et al.*, 2004	Cocaine & opiate	MRI
Lyoo *et al.*, 2006	66 opioid-dependent + alcohol	VBM with MRI
MacKay *et al.*, 1993	Cocaine-dependent polysubstance abusers	?MRS
Mander *et al.*, 1989	Alcohol withdrawal	MRI T1 times
Mann *et al.*, 1993	Alcoholics	CT
Mena *et al.*, 1994	Cocaine intoxication	review of CT SPECT & MRI data
Meyerhoff *et al.*, 1995	Alcohol abuse and HIV	MRS
Oh *et al.*, 2005	Methamphetamine	MRI of corpus callosum
Pascual-Leone *et al.*, 1991	Cocaine	CT
Pezawas *et al.*, 1998	Opiate addicts	CT
Pezawas *et al.*, 2002	Opiate users	HMPAO SPECT at rest
Pfefferbaum *et al.*, 2000	Alcoholics	MRI
Rose *et al.*, 1996	Heroin users & controls	HMPAO SPET
Rumbaugh *et al.*, 1980	Case series of 6 mixed trauma & drug use & monkey studies	CT
Siew *et al.*, 1993	Cocaine and heroin users	MRI
Silveri *et al.*, 2004b	Start of methadone	^{31}P-MRS
Strang & Gurling, 1989	Long-term heroin users	CT low resolution
Tumeh *et al.*, 1990	Cocaine users	IMP-SPECT
Volkow *et al.*, 1988a	Cocaine	PET perfusion
Volkow *et al.*, 1988c	Cocaine/heroin case series	MRI
Weber *et al.*, 1993	Crack users	IMP-SPECT

1.4.1.1 CT and MRI studies

Almost from the beginning CT scanning was used to examine the effects of alcohol on the brain. In the earliest studies they report atrophy as evidenced by enlarged ventricles and widened sulci (e.g. Carlen *et al.*, 1978; Fox *et al.*, 1976). However, these reported effects were seen in subjects with clinically evident cognitive impairment or neurological sequelae. Aberdeen was one of the early pioneers in the clinical use of MRI scanning. Being Scottish, they applied this new technique to the study of alcoholics very early on. They showed that T1 relaxation times were acutely decreased in alcohol intoxication followed by a rebound increase during withdrawal and after six weeks of abstinence (Besson *et al.*, 1981). The effect was more marked in the frontal grey matter than in the parieto-occipital region. However,

the study number was small, with only 6 alcoholics and 3 controls, and no statistical testing was undertaken. Nevertheless, the results were suggestive of a dehydration effect during acute intoxication and a component of water intoxication in delirium tremens. Over many subsequent studies, chronic exposure to excessive alcohol has become well known to cause cerebral atrophy (e.g. Chick *et al.*, 1989; Mander *et al.*, 1989, see Table 1.3).

The first study I could identify where an attempt was made to use neuroimaging to examine the effects of heroin use on the brain in living people was a CT study from 1979 (Hill & Mikhael, 1979). For an early study, the number of subjects is impressive, at 42 men; this comprised 15 alcoholics, 15 heroin users and 12 controls. As expected from the age of the study, the methodology for examining the images was crude by today's standards, however still better than several subsequent studies. Measures of ventricular and brain area in each image slice were calculated to produce a ratio, but sulcal widening was assessed only by visual inspection. Despite this, no significant differences were detected between the three groups. This study also included neuropsychological testing of the research subjects, which showed impairments in both groups, although of different patterns. Unfortunately, no attempt was made to relate the neuropsychological deficits to structural changes. The only other opioid addiction study reported for the next 10 years is a case series of 6 individuals who underwent CT scanning for a variety of clinical reasons including head trauma, who also had a history of mixed substance misuse and abnormal CT scans (Rumbaugh *et al.*, 1980). Unsurprisingly, given the clinical histories of head

trauma and clinical indications for the head CT scan, there was a common finding of cerebral atrophy.

After the 10 year gap an increasing number of studies have been published examining the structural effects of drug use. The first study after the gap compared the brain CT scans of 23 men with a history of poly-substance misuse against matched controls (Cascella *et al.*, 1989). They showed that severity of alcohol consumption predicted ventricle to brain ratio, i.e. atrophy, where heroin and other drugs did not. In an expanded sample reported later, 40 polydrug users were compared to age-matched controls (Cascella *et al.*, 1991). These men used a wide mixture of drugs, most notably cocaine, alcohol and heroin. This time the analysis was slightly more advanced, with calculation of ventricle:brain ratios and third ventricle width, alongside visual classification of cortical atrophy. These measures of brain damage again showed the strongest relationship with measures of alcohol consumption, particularly with the amount consumed per session. Heroin use showed no association with any of the measures of abnormality on CT scanning.

A case series of CT scans on 3 heroin users and 2 addicts was reported, but I have been unable to acquire the article (London *et al.*, 1989). A group from London attempted to examine the effects of very long-term heroin use (Strang & Gurling, 1989). Their cohort of 7 users had all been using heroin in excess of 20 years and were maintained on injectable diamorphine prescriptions. They were able to ascertain dose histories for the past 20 years in all subjects, giving an abnormally accurate estimate of total lifetime exposure. Unfortunately the imaging data were not

so detailed. Brain image data was acquired in 6-7 slices of low resolution CT and analysed by visual inspection and rating. Three of the 7 subjects showed moderate to severe atrophy with a fourth showing enlarged ventricles, but it was not related to any drug history variables or level of cognitive performance on a wide battery. These results are difficult to further quantify as the control group have no brain image data reported. The authors, themselves, also make the point that this is a very unusual population and may be the survivors of a much larger group, where those with problems died out at a younger age.

There then followed another ten year gap in CT imaging studies, although during this time Danos *et al.* (1998c) used CT to examine structural changes in the brain of 9 heroin addicts and 9 patients with "neurotic depression" as a control group. They demonstrated a 42% increase in the volume of external CSF space in the opioid-dependent group compared to the depressed controls and a 33% increase in internal CSF space. This was a statistically significant difference between the groups controlling for age as a potential confound, as age was found to be strongly correlated with CSF volumes. However, there was no correlation with duration of heroin addiction. This result partly contradicts the results from Hill & Mikhael, (1979), in that they agree on the lack of effect of heroin but disagree on the effect of alcohol. Also in 1998 another group used CT to examine "volume loss" in 21 opiate-dependent patients, this time compared to an equal number of healthy control subjects (Pezawas *et al.*, 1998). This group used a variety of linear and volumetric measures of CSF volume to show evidence of substantial increases in opiate

dependence. They also showed that reduced brain volume in the frontal lobes was associated with decreased length of voluntary abstinence from opiates. They went on to hypothesise that impaired frontal lobe function, and its resultant poor decision making, may be a causal factor in relapse.

Gradually, over time CT has been replaced by the better suited modality of MRI. As reported above, the earlier studies examined the effects of alcohol on brain structure. However, a literature on the effects of opioids on the brain has slowly developed. One early study undertook a study of MRI regional T1 and T2 times in a cohort of opioid and/or cocaine dependent subjects (Amass *et al.*, 1992). They compared three groups of volunteers. The control group had 13 age-matched volunteers to compare to 10 detoxified addicts previously dependent on heroin and /or cocaine, and to 4 poly-drug users still actively using drugs. Alcohol was a potential confound in this study; two of the recently detoxified group had current alcohol dependence and the poly-drug using group also used alcohol. They attempted to reduce the effect of alcohol on the results by recruiting social drinkers into the control group, but clearly this is only a partial solution. By this time, imaging techniques and hardware had improved, such that they were able to use a 1.5 Tesla MRI scanner to acquire the images. The images were analysed in a two stage process. Initially there was a qualitative analysis of the structural images. One drug user and two controls were excluded for sulcal widening, a further four drug users and one control were excluded for T2 hyper-intensities. Therefore only 9 drug-dependent and 10 control subjects remained and the distinction between drug users recently detoxified and

current poly-drug users was not maintained. Unfortunately, no mention is made of associations between these qualitative abnormalities and drug use or alcohol history. With the remaining 19 subjects they found no significant differences in T1 or T2 times in any of the five basal ganglia regions studied. There was also no significant effect from alcohol consumption. From this they conclude that the MRI technology available at that time was inadequate to demonstrate the micro-structural changes in the brain resulting from chronic opioid use. Given that they also failed to identify any changes correlated to level of alcohol consumption, their conclusion is probably correct. One other clear possibility is that the qualitative procedure excluded all those with drug or alcohol related damage, leaving only a select population with no changes and resulting in a false negative finding.

The sequelae of HIV infection on structural MRI changes in drug users has also been studied (Handelsman *et al.*, 1993). In this study of 28 male drug users, they used 0.3 Tesla MRI and visual inspection of the images to measure cortical atrophy. They showed that the level of cortical atrophy was correlated with the stage of HIV infection. Unfortunately, although the cohort recruited consisted of approximately equal numbers of methadone-maintained and heroin-using volunteers, the effects of this on the MRI images were not reported. They also collected drug use and lifetime exposure data, but only reported that this did not differ between the different groups of HIV severity.

Probably the first systematic study of MRI brain scans in drug users was in 1993 (Aasly *et al.*, 1993). Opioid users made up approximately half of their cohort of 23

drug users, who encompassed users of cannabis, cocaine, solvents and amphetamines, and all were heavy alcohol users. They used a quantitative analysis to examine cerebellar and ventricular sizes alongside visual inspection for gross atrophy or white matter hyper-intensities (WMH). In the quantitative analysis the only reported differences in the MRI scans of the drug users compared to a control cohort were an 18% decrease in size of the cerebellum and a trend toward larger lateral ventricles. There was no difference in the incidence of WMH between drug users and controls, but the drug users were 5 times more likely to be diagnosed with cerebral atrophy (30% vs. 6%). Importantly these changes were thought to be related to the effects of alcohol rather than the effects of any of the other abused drugs in this cohort. In 4 of their cohort, the cerebellar changes related to subclinical signs of cerebellar ataxia. The worst affected subject also had the greatest degree of cerebellar shrinkage on MRI.

The earliest significant change in brain structure associated with opioid and cocaine use demonstrated by MRI is an increase in pituitary volume (Siew *et al.*, 1993). This study of eight cocaine & heroin users showed a 190 mm^3 (35%) mean increase in pituitary volume in the drug dependent group compared to a matched control group. Not only was this a large increase, but there was no overlap between the groups at all. These changes were found in the absence of measurable changes in blood hormone levels. As a consequence of the known effects of opioids and stimulants on prolactin and ACTH secretion, the authors suggested that these volumetric changes were most likely to be related to anterior pituitary lactotroph and corticotroph

hyperplasia in response to opioid and cocaine use. Only 2 years later a study of 10 polydrug users and 10 healthy controls showed no difference in brain ventricle size on MRI scans (Liu *et al.*, 1995). This was despite 4 of the 10 polydrug users drinking in excess of recommended levels. However, the later study estimated only ventricular volume and ventricular:brain ratios, so it would not have detected enlargement of the pituitary gland. More recently, but still using visual rating of MRI scans, the finding of mild generalised atrophy has been replicated in IV heroin users (Hagel *et al.*, 2005). In this case 17 heroin users were more likely to have enlarged ventricles than the same number of age-matched controls. In this study the prevalence of co-morbid alcohol problems was much reduced, removing this significant potential confound, but there was a higher incidence of benzodiazepine dependence.

White matter hyper-intensities (WMH) on MRI scanning have been shown in addicts for a number of drugs. They are generally thought to represent focal areas of brain damage resulting from a number of different pathological processes. In an early case series of MRIs in cocaine / crack and heroin users both of the heroin users showed WMH compared to 1 of the 5 cocaine users (Volkow *et al.*, 1988c). Curiously, one of the cocaine users with a normal MRI also showed hypoperfusion of the frontal cortex on PET scanning. Bae et al (2006) showed that there was an increased incidence of WMH in male methamphetamine users compared to a control group, but not in female users. There was also evidence of a dose-dependent relationship, with heavier lifetime use of methamphetamine associated with more severe and more

numerous WMH lesions. The majority of lesions were in frontal regions and deep white matter. In the largest study, (Lyoo *et al.*, 2004) compared the incidence of WMH in 32 cocaine users, 32 opiate users and 32 healthy controls. As in their later study, described below, most co-morbidity was excluded with the notable exceptions of alcohol dependence and diabetes mellitus. These are significant flaws in the study as WHM are thought to be particularly associated with microvascular lesions. As predicted, they showed that WMH incidence was significantly higher in the cocaine users in deep white matter and insular regions, but not in peri-ventricular regions, when compared to both the opiate and control groups. The opiate group, who also had less alcohol dependence, were significantly worse than controls only when all regions were analysed together; they showed a trend in deep white matter, but no difference in other regions. In general, across both drug using groups, the WMH lesions tended to be more frequent in frontal regions. Most recently in a study of fMRI and MRS a larger number of opioid using subjects (4 out of 30), compared to none in the control group, had to be excluded due to a high incidence of WHM (Yücel *et al.*, 2007).

The most comprehensive study of structural effects of heroin addiction so far is that by Lyoo *et al.*, (2006). This was a much larger study than any previous, with 66 opioid-dependent subjects and 48 age-matched controls. 2 opioid users and 1 control were removed for cortical atrophy or ventricular enlargement and a further 2 subjects for motion artefacts in the images. The entire opioid group were methadone maintained and the authors excluded anyone with dependence on anything else

except nicotine & alcohol. The authors do not state how many of the 63 patients had current alcohol dependence, but a significant proportion had past histories of dependence on cocaine (27%), cannabis (29%) and alcohol (35%). This study used a technique referred to as "non-optimised" Voxel Based Morphometry (VBM) described earlier, therefore examining tissue density differences, rather than volume differences. The results were a finding of decreased grey matter density in medial frontal, and in the insula and superior temporal cortices in the opioid-dependent group. The authors state that sub-analyses, excluding those patients with previous co-morbid dependence on other substances, produced similar findings.

1.4.1.2 Perfusion and metabolism studies

Although not strictly structural imaging techniques, perfusion or metabolism scans using either MRS, PET or SPET can be used to demonstrate possible structural changes in the brain, especially when performed in a resting state. When used to show patterns of activation in response to non-addiction related tasks they can also shed light on potential drug-induced deficits in cerebral structure and function.

The technique of phosphorus magnetic resonance spectroscopy (^{31}P-MRS) can be used to derive measures of bioenergetic status, and markers of cell membrane integrity and turnover. Long term methadone treatment has been shown to be associated with disturbances in bioenergetic status (decreased levels of phosphocreatine) and phospholipid levels (elevated phosphomonoesters (PME) and phosphodiesters (PDE)) compared to a control group (Kaufman *et al.*, 1999). It was

also shown that the methadone group who were most affected were those who had received treatment for the shortest time. The authors interpret this as possible evidence that methadone treatment helps to normalise the abnormalities produced by heroin use and dependence. Alternatively, both their patient groups were continuing to use illicit drugs as shown by 26% positive urine screens. So perhaps it is the ability of methadone to prevent recurrent withdrawal states that is improving these cerebral metabolic markers. It is worth noting that the pattern of abnormalities found quite closely resembled that found in chronic ischaemia. Given the findings in other studies of areas of hypoperfusion in heroin users, they argue that this is a possible cause of the ^{31}P-MRS abnormalities. It may also be evidence of subclinical degrees of neuronal cell loss as has also been suggested in the structural studies described at the start of this chapter.

To further test this, the same group went on to study another 43 heroin addicts at different times after transfer to methadone (Silveri *et al.*, 2004b). The whole group findings were very similar with a general reduction in the bioenergetic marker phosphocreatine and an increase in PDE, across the methadone groups compared to controls. However, the PME changes were not replicated. The effects of duration of methadone were not as expected. The phosphocreatine actually started equivalent to the control group in the first week of methadone before falling over the next 3 weeks of methadone treatment. The PME levels showed an almost linear increase with time on methadone and there was no difference in PDE levels between methadone groups. Again, this contradicts the earlier study. There was also no evidence of correlations

with measures of previous drug use.

Using the related technique of ^{1}H-MRS to assess levels of N-acetylaspartate (NAA), (Haselhorst *et al.*, 2002) studied neuronal viability in 12 heroin-dependent patients maintained on methadone(10) or heroin(2) and 12 matched controls. They only examined two voxels of 20x20x20mm in the medial and lateral frontal lobes, but the difference in proportion of grey and white matter in these two regions allowed them to draw inferences about differential effects in these different tissue types. They showed a significant decrease in NAA level in medial frontal lobe, which was equivalent to an estimated reduction in NAA in grey matter. There were a few problems with this study, most notably the co-morbidity of the patients, where 1 patient had Generalised Anxiety Disorder and another had paranoid Schizophrenia. Nevertheless, the group results showed no outliers suggesting a relatively robust effect of long-term heroin use.

The perfusion studies have also supplied evidence that there may be chronic low-level ischaemia disrupting the metabolism of the brain in opioid users. One study of 27 abstinent former heroin users and 9 healthy controls, demonstrated a number of regions of significant hypoperfusion compared with healthy control subjects as well as a trend for a global decrease in CBF in the abstinent group using resting HMPAO SPET scans (Gerra *et al.*, 1998). However, as found in the MRS study above, these changes were not related to the substance abuse history, but rather to other co-morbid diagnoses of depression or antisocial personality disorder. Specifically, significant hypo-perfusion in the right frontal and left temporal cortices was associated with co-

morbid depression and hypo-perfusion in the right frontal lobe was also associated with "antisocial tendencies".

These hypoperfusion deficits following chronic heroin were also seen in another HMPAO SPET study from the same year (Danos *et al.*, 1998b). They scanned 16 heroin users in their first week of inpatient detoxification. At the time of scanning 13 of the 16 were on oral methadone substitution. Unfortunately it is not possible to tell from the paper whether the subjects were in the process of complete detoxification from opioids using a reducing methadone regime, or simply in transition from heroin to methadone. There was no control group in this study, but the number of areas of hypoperfusion reported was substantial. 11 of the 16 patients had at least one region of hypoperfusion according to visual inspection of the images. Bilateral temporal lobe regions were most likely to be affected, followed by frontal and then parietal areas. For those subjects who were also on methadone the degree of hypo-perfusion was inversely related to the methadone dose. In other words, those on higher methadone doses had smaller decreases in perfusion. Interpretation of these results is difficult. The lack of information in the paper means that the effects of acute withdrawal symptoms, long-term heroin use and acute methadone dose are impossible to disentangle. They do report a lack of correlation between opioid withdrawal scores and rCBF, but the scale used is relatively insensitive and any perfusion changes need not be closely reflected in the subjective responses.

The finding of perfusion deficits in cerebral regions seems to be a consistent finding. There is an earlier HMPAO SPET study showing similar focal and multifocal

perfusion deficits in 9 of 10 heroin users and none of the matched control group (Rose *et al.*, 1996). Although this study also used visual ratings to measure the effects of the heroin use, there were several important differences in the methodology. The heroin users in this study were a surprisingly clean sample with no histories of significant co-morbidity or other dependencies. In contrast to the other studies above, we are also explicitly told that they were all detoxifying off heroin with the use of clonidine and were drug free at the time of scanning. The visual ratings were repeated by multiple blind raters. Encouragingly, the abnormal scans all showed improvement at 3 weeks abstinence. However, this does raise the possibility of the hypoperfusion being a side-effect of the clonidine, which is known to lower blood pressure and pulse rate.

Krystal et al (1995) also showed a reduction in rCBF in a population receiving chronic methadone treatment. In this study the effects are much easier to attribute to specific states. 10 methadone-maintained heroin users and 10 matched controls were scanned with HMPAO-SPET after saline or naloxone injections. The effects of the naloxone are described later, but the between-group differences in rCBF following saline injection give information on the effects of chronic methadone. Specifically the methadone group showed significantly less rCBF compared to controls in the parietal and frontal cortices, with a non-significant trend in the temporal cortex. They also showed significantly increased rCBF compared to controls in the thalamus bilaterally. Compared to the later study (Rose *et al.*, 1996) it shows a consistent finding of decreased rCBF, but some mild disagreement over the localisation of the

effects.

There are two studies, by the same group, on the effects of the opioid partial agonist buprenorphine on rCBF using HMPAO-SPET in male cocaine dependent polydrug users (Holman *et al.*, 1993; Levin *et al.*, 1995), who also examined baseline perfusion in the same population (Holman *et al.*, 1991). In the earlier study, the authors examined 18 polydrug users. Of these, 7 met criteria for current opioid dependence in addition to their cocaine dependence. Given that 16 of the 18 patients had perfusion abnormalities we can be sure that at least some of the opioid users had abnormalities. Unfortunately, no data was presented or reported for the opioid using subgroup. The pattern of distribution of these focal hypoperfusion deficits was widespread, but with sparing of the cerebellum and occipital cortex. The same group examined a comparison group of 13 cocaine dependent women, 4 of whom also had opiate dependence (Levin *et al.*, 1994). In contrast to the men, they only found statistically significant hypoperfusion deficits compared to controls in the subgroup with dual dependence.

In both the buprenorphine studies they looked at its effects on abstinent comorbid heroin and cocaine addicts (Holman *et al.*, 1993; Levin *et al.*, 1995). The earlier study contained 10 patients and the latter study 15 patients who were all undergoing methadone-assisted withdrawal from cocaine and heroin before transfer onto buprenorphine. Although not explicitly reported, it can be deduced that all 35 patients, from both studies, had hypoperfusion deficits in early abstinence. Measured levels of rCBF in these regions of hypoperfusion increased by 24% in the first 3

weeks after detoxification in the first study. The effects of buprenorphine in both studies are reported in the next section, but it is interesting to note here that the second study had a placebo arm. In patients taking placebo there was a non-significant increase in the number of hypoperfusion defects by day 5 but this had resolved to a non-significant decrease by day 21 after detoxification.

More recently these findings have been replicated in a cohort of heroin users (Botelho *et al.*, 2006). This was a cleaner cohort of just heroin users; all were dependent on heroin with only a subset showing sporadic use of other substances. Again, the main finding was of widespread hypoperfusion on HMPAO SPET scanning at rest. There was a slightly different spread in the pattern of most extensive hypoperfusion. In this study the largest deficits were seen in the orbito-frontal and temporal cortices. In terms of attribution of cause this study does not attempt to place the origins of the hypoperfusion at the door of other co-morbidities. In this case the authors suggest that the aetiology lies in the combination of heroin use and tobacco smoking. In common with other studies there was also no evidence of recovery in the one subject who underwent repeat scanning after 10 weeks of abstinence.

In contrast to the above studies that report deficits, at least two studies have demonstrated increased function at rest in opioid users (Galynker *et al.*, 2000; Pezawas *et al.*, 2002). In the first of these studies, they used the technique of ^{18}FDG-PET to measure regional cerebral glucose metabolism (rCMRglu) in methadone-maintained opioid users, a group who were previously maintained on methadone and

a control group (Galynker *et al.*, 2000). At rest, they found an increase in rCMRglu in the anterior cingulate gyrus in both current and previous methadone maintained groups compared to controls. They argue that this may be a prolonged effect of opioid dependence, or possibly evidence of a pre-existing pathology related to risk of developing opioid addiction. No attempt was made to look for dose effects on this change in metabolic rate. In the second, larger, study they used HMPAO-SPET to demonstrate an increase in rCBF in twenty-one current opioid users at rest (Pezawas *et al.*, 2002). The significant increases compared to controls were in the superior frontal, central and parietal cortices. However, they also demonstrated decreases in the inferior frontal, occipital and temporal cortices, and basal ganglia. The most interesting finding was a correlation between duration of opioid dependence and the decrease of rCBF in the mesio-frontal cortex.

One group has used $H_2{}^{15}O$-PET to examine cerebral function on a gambling task (Bolla *et al.*, 2003) and a standard colour Stroop task (Bolla *et al.*, 2004) in abstinent cocaine users. They showed that the cocaine users had increased levels of activation during the gambling task in the right orbito-frontal cortex (OFC) and decreased activation in the right dorso-lateral prefrontal cortex (DLPFC) and left medial prefrontal cortex (MPFC). Additional, unpredicted, effects were noted with increased activation in left putamen and postcentral gyrus, and decreased activation in right superior parietal lobule, the left medial frontal gyrus, left middle temporal gyrus, and the right cerebellum, again compared to the levels of activation to the task in the control group. The region in the right OFC was shown to have levels of

activation that correlated with performance scores on the gambling task in both groups, in the absence of performance differences between the groups. A measure of drug use also showed negative correlation with activity in the left OFC. The later study showed that cocaine users had an attenuated increase in function in the left anterior cingulate and right pre-frontal cortices when naming colours incongruent to the words when compared to controls. They also showed an increase in right anterior cingulate cortex. Surprisingly, but as in the gambling task, they found no performance difference between the control and cocaine using groups on this task either. Taking both studies together the authors argue that cocaine use is associated with abnormal levels of functioning, increased or decreased, in multiple brain regions while performing tasks that require decision making and attentional load. Whether increased or decreased activation corresponds to changes in efficiency of processing or inability to activate damaged regions remains as unclear in these studies as it does in many others.

Expanding further on this, another group later used the same imaging technique of $H_2{}^{15}O$-PET to examine the different responses of current opioid or amphetamine users with ex-users and a control group (Ersche *et al.*, 2005b). In this case the task was based on the Cambridge Gambling Task where subjects have to choose between high risk and low risk options to win or lose points. Again, in the scanner environment and with smaller numbers, they failed to find the expected deficit in functioning in the drug using population that had been previously found. In agreement with the other study above, there was a distinct opposite pattern of

activation in the left OFC and right DLPFC between controls and drug users. They found only trends in differences between the opioid and amphetamine users, and between current and former drug users. The potential explanations put forward in this paper highlight the possible effects of poor impulse inhibition or altered affective processing of stimuli that may result from, or predispose to, drug addiction.

Lastly, the case report literature is littered with reports of the potential neurotoxic effects of the use of "street" opioids. Two main types of neurological insult are reported most commonly, a spongiform leucoencephalopathy (Celius & Andersson, 1996) and hypoxic injury related to the respiratory depression of opioid overdose (Vila & Chamorro, 1997). The spongiform leucoencephalopathy reported is characterised by oedema of white matter in either the cerebrum or cerebellum, sometimes also effecting grey matter. At the microscopic level there is swelling and vacuolation of the myelin sheaths but sparing of the axons. The leucoencephalopathy tends to occur sporadically and it has therefore been suggested that it may be related to a neurotoxic contaminant rather then the heroin itself. There has been a recent review that also highlights additional findings on diffusion-weighted MRI (Hagel *et al.*, 2005). They argue that the phenomenon is linked to heroin smoking only, not injecting, and can also be fatal in some cases. There are also reports of ischaemic infarcts, which may be related to embolic phenomena, either thrombo-embolic, infective micro-emboli associated with the increased risk of endocarditis in intra-venous drug abuse, or foreign bodies from injection of insoluble contaminants.

1.4.2 Cerebral activation studies

Cerebral activation studies use a variety of the techniques described above to determine patterns of increased or decreased brain activity in any given state. The studies described below use the techniques of fMRI, perfusion PET or SPET using blood flow tracers, or metabolic PET using ^{18}FDG. In this section the studies discussed focus on the activation of the brain in response to drug, drug related stimuli or withdrawal specifically, rather than the studies at rest described in the section before. Again, the discussion is focused on opioid based studies unless other studies related to specific effects of interest to the study of opioid relevant processes.

Table 1.4Previous neuroimaging activation studies in addiction

Study	Population	Technique	Stimulus
Adinoff *et al.*, 2001	Cocaine users	HMPAO SPECT	Procaine
Adler *et al.*, 1997	Healthy volunteers	$H_2{}^{15}O$-PET	Fentanyl and pain
Anderson *et al.*, 2006	Cocaine users	fMRI	Cue-responses in cerebellum
Becerra *et al.*, 2006	Healthy volunteers	fMRI	Morphine
Breiter *et al.*, 1997	Cocaine users	fMRI	Cocaine
Brody *et al.*, 2002	Smokers	^{18}FDG-PET	Cigarette craving
Brody *et al.*, 2004a	Smokers	^{18}FDG-PET	Bupropion on cue induced anterior cingulate activation
Casey *et al.*, 2000	Healthy volunteers	$H_2{}^{15}O$-PET	Fentanyl +/- pain
Childress *et al.*, 1999	Cocaine users & Healthy volunteers		Cue induced cocaine craving
Christensen *et al.*, 2000	Cocaine users	Proton Density MRI	Cocaine
Daniel *et al.*, 1991	Schizophrenics	^{133}Xe SPECT rCBF	Amphetamine
De Wit *et al.*, 1991	Healthy volunteers	^{18}FDG-PET	Diazepam
Ernst *et al.*, 1997	Healthy volunteers	^{18}FDG-PET	Dex-amphetamine
Firestone *et al.*, 1996	Healthy volunteers	$H_2{}^{15}O$-PET	Fentanyl
Forman *et al.*, 2004	Heroin users and Healthy volunteers	fMRI	Go/NoGo task
Garavan *et al.*, 2000	Cocaine users & Healthy volunteers	fMRI	Cue-induced cocaine craving
Gilman *et al.*, 1996a	Alcoholic	^{18}FDG-PET & ^{11}C-Flumazenil	Disulfiram
Grant *et al.*, 1996	Cocaine users		Cue induced craving
Honey *et al.*, 2003	Healthy volunteers	fMRI Connectivity	Variety of drugs including sulpiride, methylphenidate, diazepam etc.
Johnson-Greene *et al.*, 1997	Alcoholics	^{118}FDG-PET	Before and after relapse
Jones *et al.*, 1991	Chronic pain patient	$C^{15}O_2$	Morphine
Kaufman *et al.*, 1998a	Cocaine	DSC-MRI	Cocaine
Kilts *et al.*, 2001	8 Crack using men	$H_2{}^{15}O$-PET	Cocaine craving

Kosten *et al.*, 2006	17 cocaine users in double-blind sertraline trial	fMRI	Cocaine cues (predicted relapse)
Krystal *et al.*, 1995	Methadone users	SPECT	Naloxone
Kufahl *et al.*, 2005	Cocaine users	fMRI	Cocaine
Langleben *et al.*, 2008b	Heroin users	rCBF	Heroin craving
Lee TM *et al.*, 2005	Heroin users and Healthy volunteers	fMRI	Impulsivity task
Leppä *et al.*, 2006	Healthy volunteers	fMRI	Remifentanil
Levin *et al.*, 1998	Healthy volunteers	fMRI	Photic stimulation after alcohol
Li *et al.*, 2000	Cocaine dependent	fMRI connectivity	Cocaine
London *et al.*, 1990a	Polydrug users	^{18}FDG-PET	Morphine
London *et al.*, 1990b	Cocaine users	^{18}FDG-PET	Cocaine
Lorenz *et al.*, 2000	Healthy volunteers	perfusion MRI	Remifentanil
Maas *et al.*, 1998	Cocaine users	fMRI	Cue-induced cocaine craving
Martin *et al.*, 1992	Chronic organic brain disorders from alcohol	^{18}FDG-PET	Rest
Martin-Soelch *et al.*, 2001	Methadone users	$H_2{}^{15}O$-PET	Reward task
Mathew *et al.*, 1985	Healthy volunteers	rCBF	Diazepam
Mathew, Wilson, 1986	Healthy volunteers	^{133}Xe SPECT rCBF	Alcohol
Mathew *et al.*, 1996	6 Cocaine users	^{133}Xe SPECT rCBF	Before & after cocaine
Mathew *et al.*, 1997	Marijuana smokers	$H_2{}^{15}O$-PET	Marijuana
Matthew *et al.*, 1995	Healthy volunteers	$H_2{}^{15}O$-PET	Benzodiazepine
Matochik *et al.*, 1993	ADHD adults	^{18}FDG-PET	Stimulants
McClernon *et al.*, 2005	Abstinent smokers	fMRI	Smoking cues
Modell & Mountz, 1995	Alcohol	SPECT rCBF	Alcohol craving
Moeller *et al.*, 2004	MDMA users	fMRI	Working memory task
Pearlson *et al.*, 1993	Abstinent cocaine users	HMPAO SPECT	Cocaine
Risinger *et al.*, 2005	Cocaine users	fMRI	Cocaine
Sano *et al.*, 1993	Healthy volunteers	rCBF	Alcohol
Schlaepfer *et al.*, 1998	Opiate users	rCBF	Opiates
Sell *et al.*, 1997	Opiate users	fMRI	Heroin craving
Sell *et al.*, 1999	Opiate users	$H_2{}^{15}O$-PET	Heroin craving
Sell *et al.*, 2000	Opiate users	$H_2{}^{15}O$-PET	Heroin craving
Silveri *et al.*, 2004a	Healthy volunteers	T2 MRI	Methylphenidate
Stapleton *et al.*, 2003	Smokers and Healthy volunteers	^{18}FDG-PET	Nicotine
Stapleton *et al.*, 1995	Poly drug users	^{18}FDG-PET	Placebo (cocaine)
Streeter *et al.*, 1998b Or Streeter *et al.*, 1998a	Healthy volunteers with alcoholism family history	MRI with gadolinium contrast after	Alprazolam
Streeter *et al.*, 2005	Cocaine users	GABA-MRS	Venlafaxine or pramipexole
Theodore *et al.*, 1986 Neurology 36(1):60-64	Healthy volunteers	^{18}FDG-PET	Barbiturates
Tiihonen *et al.*, 1994	Healthy volunteers	rCBF	Alcohol
van Dyck *et al.*, 1994	Buprenorphine users	HMPAO SPECT	Naloxone precipitated opioid withdrawal
Veselis *et al.*, 1997	Healthy volunteers	rCBF	Midazolam
Volkow *et al.*, 1988b	Alcohol intoxication	$H_2{}^{15}O$-PET	Alcohol
Volkow *et al.*, 1990b	Healthy volunteers	^{18}FDG-PET	Alcohol
Volkow *et al.*, 1991b	Cannabis users	^{18}FDG-PET	Tetra-hydro-cannabinol
Volkow *et al.*, 1991a	Cocaine dependent	^{18}FDG-PET	Cocaine withdrawal
Volkow *et al.*, 1992b	Alcoholics	^{18}FDG-PET	Rest
Volkow *et al.*, 1992c	Cocaine users	^{18}FDG-PET	Rest
Volkow *et al.*, 1993a	Cocaine users	^{18}FDG-PET & ^{11}C-Raclopride	Rest
Volkow *et al.*, 1993b	Alcoholics	^{18}FDG-PET	Lorazepam
Volkow *et al.*, 1994	Alcoholic in recovery	^{18}FDG-PET	Rest
Volkow *et al.*, 1995b	At risk for alcoholism	^{18}FDG-PET	Lorazepam
Volkow *et al.*, 1996a	Marijuana users	^{18}FDG-PET	Before & after marijuana

Volkow *et al.*, 1997b	Healthy volunteers	^{18}FDG-PET	Methylphenidate
Volkow *et al.*, 1997d	Alcoholics	^{18}FDG-PET	Lorazepam
Volkow *et al.*, 1998b	Healthy volunteers	^{18}FDG-PET	Methylphenidate
Volkow *et al.*, 1998c	Cocaine users	^{18}FDG-PET	Benzodiazepine
Volkow *et al.*, 1999b	Cocaine users	^{18}FDG-PET	Cocaine craving & methylphenidate
Volkow *et al.*, 2000b	Cocaine users	^{18}FDG-PET	Alcohol
Volkow *et al.*, 2001	Methamphetamine users	^{18}FDG-PET	
Volkow *et al.*, 2003	Healthy volunteers	^{18}FDG-PET	Expecting methylphenidate
Volkow *et al.*, 2005	Cocaine users vs Healthy volunteers	^{18}FDG-PET	Methylphenidate
Volkow *et al.*, 2006	Healthy volunteers	^{18}FDG-PET	Low dose alcohol
Wagner *et al.*, 2001	Healthy volunteers	$H_2{}^{15}O$-PET	Remifentanil
Wallace *et al.*, 1996	Cocaine users	rCBF on	Cocaine
Walsh *et al.*, 1994	Heroin users	^{18}FDG-PET	Buprenorphine
Wang *et al.*, 1994	Healthy volunteer	rCBF after	Methylphenidate
Wang *et al.*, 1998	Female alcoholics	^{18}FDG-PET	
Wang *et al.*, 1999b	Healthy volunteers	^{18}FDG-PET	Lorazepam
Wang *et al.*, 1999a	Cocaine users^{18}FDG	^{18}FDG-PET	Cocaine craving
Wang *et al.*, 2000	Healthy volunteers	^{18}FDG-PET	Alcohol
Wang *et al.*, 2004	Long abstinent methamphetamine users	^{18}FDG-PET	Rest
Wendt *et al.*, 1994	Healthy volunteers	rCBF	Alcohol
Wexler *et al.*, 2001	Cocaine users	fMRI	Cocaine craving
Wik *et al.*, 1988	Alcoholics and Healthy volunteers	^{11}C-glucose	
Wise *et al.*, 2002	Healthy volunteers	fMRI	Pain on/off remifentanil
Wolkin *et al.*, 1987	Healthy volunteer and Sz	^{18}FDG-PET	Amphetamine
Wrase *et al.*, 2002	Alcoholics and Healthy volunteers	fMRI	Alcohol and neutral cues
Yücel *et al.*, 2007	Heroin users	^{1}H-MRS and fMRI	Task on methadone or buprenorphine

1.4.2.1 Acute response to drug

One of the most obvious ways to study the effects of drugs of abuse is to give known doses of drug and measure the effects. This idea has been tried with research subjects being given opioid drugs while imaging the resultant effects in the brain. Unfortunately there are many practical problems and constraints that have to be dealt with resulting from the process of functional neuroimaging. One of the largest problems is the nature of the scanner environment. Much work has been done that shows that the "set and setting" in which a drug is taken heavily influences the subjective effects of the drug. Animal work also suggests that there are differences in effect dependant on whether the drug is experimenter-administered or self-

administered.

Another major problem relates to the stage of dependence the subject population is at during the study. A significant minority of these studies are done on healthy ("opiate naïve") volunteers. This may be the most straight forward trial to run, however there is considerable doubt as to how generalisable any findings would be to the understanding of addiction. Given the nature of addiction and dependence, it is highly unlikely that opioids or other drugs of abuse are having identical effects on those with long-standing addiction as on those who have never used the drug before. Aside from the complex issues of neuroadaptation and altered responses to drug, there is also the much simpler question of equivalent doses. Tolerance is often so marked in those with opioid addiction that the minimum dose required to get an effect would be fatal to an opioid-naive volunteer.

If the subjects are actively dependent then their recent drug use will impinge heavily on any neuroimaging results as opioids can take many days to fully washout from the brain. If the subjects are in treatment then they are likely to be maintained on long-acting substitute opioids like methadone, which take even longer to washout. If the subjects are opioid-free then this is almost certainly going to be as a result of detoxification with permanent abstinence as the long-term goal, in which case the ethics of administration of an opioid require very careful scrutiny. Inevitably a compromise between scientific rigour and practical and ethical considerations has to be achieved. Therefore the results of all neuroimaging studies using this type of paradigm need to be interpreted in the light of such a compromise.

There are a few studies of the acute effects of opioid drugs in healthy volunteers using functional neuroimaging. One group has used $H_2{}^{15}O$ PET to measure regional cerebral blood flow (rCBF) in healthy volunteers in response to acute doses of fentanyl at rest (Firestone *et al.*, 1996) and on acute pain (Adler *et al.*, 1997). Fentanyl was shown to consistently increase rCBF in the anterior cingulate cortex, irrespective of whether the subject was in pain or resting. In the first study, in the resting state, fentanyl also produced increases in rCBF in the prefrontal and orbito-frontal cortices and caudate nucleus. Fentanyl also caused decreases in rCBF in the thalamus, frontal, temporal and cerebellar regions. Interestingly the effect of fentanyl on rCBF changes induced by pain was to augment the increase in rCBF in the supplementary motor area and left inferior frontal cortex. No global effects were detectable in either study as this is removed at the modelling stage and cannot be properly quantified without calibration from an arterial input function. These findings of increased anterior cingulate activation to fentanyl in healthy volunteers was later replicated (Casey *et al.*, 2000). Although they measured subjective hedonic responses to the fentanyl, there was no evidence of rCBF changes correlated with this response. Jones *et al.*, (1991) also studied the effects on rCBF of an analgesic dose of morphine in a single patient with chronic pain. In this case morphine induced increases in rCBF in similar areas, specifically the anterior cingulate, prefrontal cortex, caudate and putamen. Increased rCBF was also seen in the insular cortex contralateral to the site of the pain and ipsilateral temporal cortex. However, an fMRI study of the effects of remifentanil in healthy volunteers showed an almost

opposite effect (Wise *et al.*, 2002). In this study the increases in BOLD signal from a noxious stimulus were significantly attenuated by the opioid infusion in both the insular and anterior cingulate cortices. Unfortunately, it is not possible to directly compare the studies as the absolute effects of remifentanil were not studied and the analysis was restricted to brain regions activated by the pain stimulus.

A subsequent fMRI study of the effect of morphine on healthy volunteers has already neatly summarised the brain systems implicated in the actions of opioids (Becerra *et al.*, 2006). In this study healthy volunteers underwent fMRI scanning during infusions of morphine and saline placebo. The authors present a collection of previous work looking at the overlap between patterns of activation and deactivation in response to morphine with those of other stimuli that elicit particular subsets of the effects. For example the pattern of deactivation in thalamus and a selection of cortical areas from morphine matches that seen in response to another sedative drug, propofol. Of more specific interest to the study of addiction was the increase in BOLD signal in nucleus accumbens, orbito-frontal cortex, putamen, hippocampus and extended amygdala. They also noted a decrease in BOLD signal in the anterior cingulate gyrus, thalamus and peri-aqueductal nucleus. In this study they also presented the time course of the responses to morphine, demonstrating another advantage of fMRI's temporal resolution. A similar method was used to study the fMRI responses to the ultra-short acting opioid remifentanil (Leppä *et al.*, 2006). The six healthy volunteers in this study showed a widespread BOLD response to the remifentanil infusion. The largest response, by a considerable margin, was in the

precuneus. In general the BOLD responses for the activated brain regions divided into two groups. The cortical regions responded to the remifentanil infusion with a rapid increase in activation followed by an exponential decay matching the subjective experiences reported. By contrast, the sub-cortical regions showed a much slower increase in activation followed by a plateau phase before a slow decline.

All of the above studies have detailed the effects of opioids on regional brain activation patterns. There is one study that has used contrast-enhanced perfusion MRI to measure the effects of opioid on absolute measures of rCBF (Lorenz *et al.*, 2000). This study demonstrated that as well as the regional effects reported elsewhere, there was a global increase in CBF although this was minimal in occipital cortex and white matter.

As can be seen from the above summaries of multiple studies, the effects of acute doses of opioids in healthy volunteers can be contradictory. This may be partly explained by a number of factors. The effects of measuring absolute versus relative changes can lead to differences in results as shown (Lorenz *et al.*, 2000). If the whole brain shows a global increase, but some areas increase by a smaller amount than the average then this can be seen as a relative decrease in rCBF. However, there is another effect that we have not yet considered, that of dose. One study has studied the effects of two doses of remifentanil on rCBF in healthy volunteers (Wagner *et al.*, 2001). This study showed that low and moderate doses can have opposing effects on rCBF within the same individual. This effect was observed in a group of healthy

volunteers who should all have a similar lack of opioid tolerance. If we then add the difficulties of trying to calculate equipotent doses of different opioids to compare between studies we can see why some results may be contradictory. As will be seen later in this section, this will become even more complex when differing levels of opioid tolerance have to be considered both within and between different study populations.

Study	Stimulus	cortical											subcortical					
		Ant Cingulate	Post. Cingulate	Med Frontal	DLPFC	Inf frontal	somatosensory	supplementary motor	precuneus	Temporal	occipital	Insula	thalamus	caudate	putamen	hippocampus	amygdala	cerebellum
Firestone *et al.*, 1996	fentanyl $H_2{}^{15}O$ PET	↑	↓	↑	-	↓	-		↓	-	↓	-	-	↑	-	(↓)	-	↓
Casey *et al.*, 2000	fentanyl $H_2{}^{15}O$ PET	↑	-	-	-	-	-		-	↑	↑	-	-	-	-	-	-	-
Becerra *et al.*, 2006	morphine fMRI	-	-	-	↓	↑	↓		-	↓	-	-	↓	↑	↑	↑	↑	↓
Leppä *et al.*, 2006	remifentanil fMRI	↑	↑	↑	-	↑	-		↑	↑	-	↑	↑	↑	-	↑	↑	↑
Lorenz *et al.*, 2000	remifentanil perfusion MRI	-	-	↑	-	↑	-	↑	↑	-	↑	-	↑	↑	↑	-	-	-
Adler *et al.*, 1997	fentanyl $H_2{}^{15}O$ PET	↑	↓							↓			↓					
Wagner *et al.*, 2001	remifentanil (low) $H_2{}^{15}O$ PET			↓	↑			↑										↓
	remifentanil (moderate) $H_2{}^{15}O$ PET	↑	↑	↑					↑		↑							

Table 1.5: Healthy volunteer responses to opioids. "↑" =increased activation "↓"=decreased activation "-"=no change, empty square means the region not reported.

Study	Stimulus	cortical										subcortical					
		Ant Cingulate	Post. Cingulate	Med Frontal	DLPFC	Inf frontal	somatosensory	precuneus	Temporal	occipital	Insula	thalamus	caudate	putamen	hippocampus	amygdala	cerebellum
Casey *et al.*, 2000	fentanyl $H_2{}^{15}O$ PET	↑					↓				-	↓					↓
Adler *et al.*, 1997	fentanyl $H_2{}^{15}O$ PET	-				↓	-					-					
Jones *et al.*, 1991	morphine $C^{15}O_2$ PET	↑		↑					↑		↑		↑	↑			
Wise *et al.*, 2002	remifentanil fMRI	↓									↓						

Table 1.6: Responses to opioids of subjects in pain."↑" =increased activation "↓"=decreased activation "-"=no change, empty square means the region not reported.

Overall the pattern of responses observed in healthy volunteers matches what would be expected from the known pharmacological properties of opioids; there are inhibitory effects in areas rich in opioid receptors and downstream activation in dopamine rich areas released from inhibition. In addition there are responses in areas known to be implicated in the circuits of pain perception and affect.

Bearing in mind what we have said above, the studies of the effects of acute opioid doses have generally either looked at the effects in users who were currently abstinent or who were currently actively dependent. Schlaepfer *et al.*, (1998) studied the effects of two opioids with different receptor profiles on rCBF using HMPAO SPET. The opioids studied were hydromorphone which is a μ full agonist, and butorphanol which is a μ partial-agonist and a κ full agonist. This study allows us to see the differential effects of opioid action on different receptor subtypes on both subjective mental state and rCBF simultaneously. Butorphanol produced subjective

results of "bad effects" and "LSD-like effects" with a diffuse pattern of activation of rCBF, especially in the anterior temporal lobes. Hydromorphone produced euphoriant effects and increased rCBF in the anterior cingulate, thalamus and amygdala regions.

The effects of acute doses of morphine on regional cerebral metabolic rate of glucose (rCMRglu) were studied by London *et al.*, (1990a). As has been demonstrated in several paradigms, morphine induced a global decrease in cerebral activity as measured by CMRglu using ^{18}F-fluorodeoxyglucose (^{18}FDG) with PET scanning. These changes were widespread throughout the brain, with many regions showing significant reductions in the frontal, parietal and temporal cortices. Anterior cingulate region, caudate nucleus and amygdala also showed significant reductions. Of all these regions, only four showed any significant correlation with the subjective measures of morphine effects that were taken during the scan. Both the paracentral lobule and left cerebellar cortex showed positive correlations with the subjective response and two regions in the occipital cortex showed negative correlations. There is an obvious discrepancy between these studies with one showing increases in rCBF and the other showing decreases in rCMRglu. These may be explained by the differences in the method of correction for global changes between the two studies, as regions that show a smaller reduction in rCBF than the decrease in the whole brain will appear as increases in rCBF when the global changes are partialled out of the statistical model. However, there are other possible explanations for the differences related to timing of the acute drug dose with the injection of radio-tracer, or

differences between glucose metabolism and blood flow, for example.

In a similar study, Sell et al (1997) used fMRI to examine the acute effects of heroin injection in users maintained on methadone and heroin. They only examined the effects of the drug on responses to photic stimulation. The effect of the heroin on the visual cortex was to decrease the blood oxygen level dependent (BOLD) response to the photic stimulation. This is consistent with the reported effects of morphine to reduce global cerebral metabolism, but not consistent with the reported lack of effect in the visual cortex in the same study (London *et al.*, 1990a). However, another later opioid study did show a reduction in occipital lobe activity (Walsh *et al.*, 1994). An identical effect has been reported with alcohol (Levin *et al.*, 1998). In a later study, Sell et al (1999) used PET to study rCBF changes in response to heroin and heroin-related cues. In this study heroin injection caused increases in rCBF in the brain stem, at the level of the peri-aqueductal grey matter (PAG) and the ventral tegmental area (VTA).

The effects of buprenorphine, an opioid mu partial agonist and kappa antagonist, have been studied (Walsh *et al.*, 1994). This study used ^{18}FDG to examine rCMRglu in polydrug abusers using a placebo-controlled, double blind design. Buprenorphine produced a global decrease in cerebral metabolism, as is consistent with the effects of other opioids reported above. The regions most affected were medial thalamus, orbito-frontal cortex and hippocampus. However, there were very few regions that did not show some reduction in rCMRglu in response to the buprenorphine injection. Surprisingly, given the results from other studies (e.g. London *et al.*, 1990a) the

amygdala was one of these regions that did not show a response. However, while this may reveal a difference in the effects of morphine and buprenorphine, or the experimental setting, it may well represent differences in the statistical methods of analysis and the effects of use of different statistical thresholds used to guard against false positive results.

The main finding with imaging studies of the effects of acute doses of abused drug is the overlap in the regions affected, irrespective of the drug given. In general, acute doses of drugs of abuse cause a global decrease in brain activation as measured by ^{18}FDG PET scanning. This occurs with opioids (London *et al.*, 1990a; Walsh *et al.*, 1994), nicotine (Stapleton *et al.*, 2003) and stimulants (London *et al.*, 1990b). The opioid study is described above, but the stimulant study reports the widespread effect of cocaine injection, which caused a reduction in rCMRglu in every brain region studied, except the cerebellum and pons. The same effect has been shown using ^{133}Xe SPET where amphetamine reduced global blood flow at rest in patients with schizophrenia (Daniel *et al.*, 1991). Cocaine has been shown to increase the velocity of blood flow, including cerebral blood flow, but concurrent reduction in cerebral blood volume, presumably related to vasoconstriction (Kaufman *et al.*, 1998a; Kaufman *et al.*, 1998b). ^{133}Xe SPET also demonstrated acute increases in CBF following intravenous cocaine in contrast to the other studies (Mathew *et al.*, 1996). This study also showed a correlation between subjective intoxication and right parietal rCBF. The reasons for these discrepancies are not obvious, but may relate to dose of cocaine as well as imaging technique. The same group also showed acute

increased in rCBF following infusions of delta-9-THC (Mathew *et al.*, 1997). There were global increases, but also regional increases, particularly in bilateral frontal regions, insula, anterior cingulate gyrus, right amygdala and hippocampus.

What is not clear, is whether these apparent reductions in brain activation are true representations of decreased neuronal demand for blood flow (measured by $H_2{}^{15}O$ or ^{99}Tm-HMPAO) or energy (measured by ^{18}FDG), or perhaps reduced tracer delivery secondary to vascular constriction caused by the drug. There is at least one study that argues against this interpretation (Ernst *et al.*, 1997), it showed an acute increase in ^{18}FDG following intravenous amphetamine. However, this was not done at rest, and perhaps more likely represents an interaction between dex-amphetamine and the cognitive task given.

Against this background of decreased activation, acute doses have still been shown to produce relative increases in brain activation in specific regions. Again, the pattern emerges that multiple different drugs affect common areas. For example, acute doses of an abused opioid (hydromorphone, Schlaepfer *et al.*, 1998) and cocaine (Breiter *et al.*, 1997) have produced relative increases in brain activation in the anterior cingulate, thalamus and amygdala. Because methylphenidate is also a dopamine re-uptake inhibitor like cocaine, it has been used to mimic the effects of cocaine in cocaine users and has induced activation in the basal ganglia and orbito-frontal cortex (Volkow *et al.*, 1999b). This activation was also shown to correlate with drug-induced craving for cocaine.

Alcohol appears to be the "odd one out" in its acute effects on blood flow. Probably

as a direct result of its vasodilator effects it appears to produce acute increases in CBF (Mathew & Wilson, 1986; Newlin *et al.*, 1982). The early methodology used in this study makes it difficult to reliably identify regional effects, but the increases in rCBF appear more pronounced in frontal regions and in the right hemisphere.

Injected cocaine, rather than a substitute, was shown in one study to induce activity, as measured with fMRI, in three distinct temporal patterns (Breiter *et al.*, 1997). Subjects reported an initial "rush" in response to the cocaine that correlated with the time course of activation in the basal forebrain, ventral tegmental area (VTA), insula cortex, thalamus, prefrontal cortex and caudate bilaterally, plus the right cingulate cortex. The VTA is one of the two sites of dopamine neuron cell bodies and the origin of the ascending meso-cortico-limbic dopamine pathway, long implicated in substance misuse. A later network also appeared, related to the subjective experience of "craving", involving the nucleus accumbens (NAcc), amygdala and right parahippocampal gyrus. Interestingly, these are regions frequently found with cue-exposure paradigms. A later, more sophisticated, study also showed patterns of activation that differed between craving and high following cocaine injections (Risinger *et al.*, 2005). Specifically, high showed positive correlations with caudate, posterior cingulate and cerebellar regions. It was negatively correlated with craving, which was associated with activation in Nucleus Accumbens, orbito-frontal cortex and anterior cingulate cortex. The discrepancies may relate to the later study involving the effects of multiple cocaine injections, thereby altering the relationship between expectation of the next dose, acute drug effects and subjective states from

the previous dose.

A later study using a similar paradigm, but different fMRI imaging sequence, showed a different pattern of BOLD response to IV cocaine infusions. In comparison to a saline infusion, the cocaine infusion induced increased BOLD signal in the orbito-frontal cortex, with some lesser activation in the anterior insula and dorso-lateral pre-frontal cortex. There were also cocaine induced decreases in basal ganglia, including the ventral striatum, ventral tegmental area, amygdala and posterior orbital gyrus (Kufahl *et al.*, 2005). As before, attempts were made to relate the measured BOLD response to the subjective experiences of "High" and "Craving". In this case there was much more overlap in regions associated with each rating scale. The "high" scale was temporally associated most with changes in the Nucleus accumbens and anterior orbito-frontal cortex. The "craving" scale was more tightly associated with a wider area in the orbito-frontal gyrus.

Study	Stimulus	cortical											subcortical						
		Ant Cingulate	Post. Cingulate	Med Frontal	DLPFC	Inf frontal	somatosensory	supplementary motor	precuneus	Temporal	occipital	Insula	thalamus	caudate	putamen	hippocampus	amygdala	midbrain	cerebellum
Schlaepfer *et al.*, 1998	butorphanol HMPAO SPET									↑									
	hydromorphone HMPAO SPET	↑											↑				↑		
London *et al.*, 1990a	morphine ^{18}FDG	↓			↓		↓	↓	-	↓	↓	↓	-	↓	↓	↓	↓		↓
Sell *et al.*, 1997	heroin fMRI											↓							
Sell *et al.*, 1999	heroin $H_2{}^{15}O$ PET																	↑	
Walsh *et al.*, 1994	buprenorphine ^{18}FDG	↓	↓	-	-	↓	-	-	↓	↓	↓	↓	↓	↓	↓	↓	-	↓	↓

Table 1.7: Responses to opioids in opioid dependent subjects. "↑" =increased activation "↓"=decreased activation "-"=no change, empty square means the region not reported.

1.4.2.2 Acute drug withdrawal

There are fewer studies examining the effects of acute withdrawal than the effects of prolonged use or acute doses, but they show a matching tendency for global activation to increase during withdrawal from both cocaine (Volkow *et al.*, 1994) and opiates (van Dyck *et al.*, 1994). However, precipitated opioid withdrawal appears to have little consistent effect on rCBF (Krystal *et al.*, 1995).

It is well known that administration of an opioid antagonist (e.g. naloxone or naltrexone) to an opioid-dependent individual will precipitate the opioid withdrawal syndrome by displacing the agonist (e.g. heroin or methadone) from the receptors.

HMPAO SPET has been used to study the effects of naltrexone precipitated withdrawal from buprenorphine on rCBF (van Dyck *et al.*, 1994). They showed no significant changes in rCBF in response to the withdrawals compared to the placebo condition, but did show that rCBF in the anterior cingulate region was inversely associated with the severity of the opioid withdrawal induced. Krystal et al (1995), in the study already mentioned above, also looked at rCBF changes in response to naloxone precipitated withdrawals in subjects maintained on methadone. There was a significant reduction in global CBF in the methadone group, with no reduction in the control group (Krystal *et al.*, 1995). Surprisingly, the control group showed a significant decrease in rCBF in the right parietal cortex and a significant increase in temporal cortex in response to naloxone, where the methadone group showed no regional changes at all.

1.4.2.3 Craving & neural circuits

The above studies related to acute responses to doses of drug or acute withdrawal. However, there is an extensive literature on the responses to drug-related stimuli. Such stimuli have been shown to provoke a variety of physiological and cognitive responses. Craving is a term often used by opiate dependent individuals to explain their relapses to heroin use, but it has proved difficult to define this term rigorously in a scientific context (Pickens & Johanson, 1992; Robinson & Berridge, 1993). Although not explicitly used in ICD-10 (World Health Organization, 1992) or DSM-IV (American Psychiatric Association, 1994), both systems refer to "a persistent

desire" or "strong desire or sense of compulsion" when defining the dependence syndrome.

Cue-responsivity, or cue-exposure has been repeatedly used to study craving. The term refers to the ability of situations, drug paraphernalia and mood states or memories associated with previous drug use to effect the desire to use the drug (Childress *et al.*, 1988b). Responses to such cues can be drug-like, drug opponent or withdrawal-like and may lead to the subjective experience of craving and/or the re-initiation or perpetuation of drug-seeking behaviour (Koob, 2000). Consequently, the issue of cue-responsivity has received much attention offering possible avenues for relapse prevention treatment (Dawe *et al.*, 1993).

A multitude of different combinations of imaging techniques and craving induction paradigms have been studied. Most of this work has been restricted to cocaine craving with only much smaller amounts focused on other drugs like alcohol, opioids or cigarettes. The variety of craving-induction paradigms has been extensive. Some studies have used video stimuli showing drug related activities, such as buying or using the drug (e.g. Childress *et al.*, 1999; Garavan *et al.*, 2000; Maas *et al.*, 1998), others have used handling drug related paraphernalia and some have used both (e.g. Brody *et al.*, 2002; Grant *et al.*, 1996). Some studies went further and either administered, or promised to allow later consumption of, the drug (e.g. Grant *et al.*, 1996).

Previous work by my predecessor in the Psychopharmacology Unit has shown that craving for drugs, in individuals who were dependent, can be induced by using a cue-

exposure paradigm of autobiographical scripts (Weinstein *et al.*, 1997) even in individuals who have remained abstinent from opiates for at least one year (Weinstein *et al.*, 1998). Similar work has been done elsewhere since (e.g. Kilts *et al.*, 2001).

As shown above, in Table 1.7, for responses to acute doses of opioid, the pattern of brain activity demonstrated by craving studies is varied. This is not surprising given the wide variety of methodologies and subject groups. There are, however, several brain areas that are reported to show activations consistently across paradigms, particularly the dorso-lateral pre-frontal cortex (Brody *et al.*, 2002; Grant *et al.*, 1996; Maas *et al.*, 1998), anterior cingulate cortex (Brody *et al.*, 2002; Childress *et al.*, 1999; Kilts *et al.*, 2001; Maas *et al.*, 1998; Risinger *et al.*, 2005; Sell *et al.*, 1999; Wexler *et al.*, 2001), amygdala (Childress *et al.*, 1999; Garavan *et al.*, 2000; Grant *et al.*, 1996; Kilts *et al.*, 2001) and orbito-frontal cortex (Brody *et al.*, 2004a; Brody *et al.*, 2002; Childress *et al.*, 1999; Risinger *et al.*, 2005; Sell *et al.*, 2000; Stapleton *et al.*, 1995; Volkow *et al.*, 1999b; Wang *et al.*, 1999a). One study using fMRI also showed activation in the anterior cingulate with cocaine related stimuli in subjects who reported no subjective experience of craving (Wexler *et al.*, 2001).

Stapleton *et al.*, (1995) showed that an injection of placebo cocaine produced an increase in rCMRglu in the orbito-frontal cortex. The authors reported the study as showing that rCMRglu was altered in polydrug users compared to controls. In fact, the subjects were all recruited as part of a study examining the effects of cocaine injections on rCMRglu uptake in polydrug users. The control subjects had placebo

injections on every occasion, but the polydrug users were given cocaine or placebo injections in a randomised, double-blind manner. The authors are reporting a comparison of the placebo scans of controls and drug users. While also reporting reduced uptake in the occipital cortex of the drug users, they report increased rCMRglu in the orbito-frontal, superior frontal, superior temporal and insular cortices. Nearly all these regions have been reported to be activated in craving in at least one other study.

Very few of the above cited studies of craving have examined opioid, or specifically heroin, craving; nearly all have been concerned with cocaine craving. Only two published studies have actually looked at heroin craving (Langleben *et al.*, 2008a; Sell *et al.*, 1999; Sell *et al.*, 2000). In the earlier study (Sell *et al.*, 1999; Sell *et al.*, 2000), heroin users were shown neutral or heroin related videos before and after an injection of heroin or placebo. In this way it was possible to look at both the effects of heroin, video cues for heroin and the interaction between the two. Subjects each had 6 scans using $H_2{}^{15}O$-PET on two separate days, one for heroin and the other for the placebo injections. As predicted, the drug-related video induced an "urge to use" heroin which attenuated with repetition, and the heroin induced a significant "high". The subjective "urge to use" correlated with rCBF in prefrontal cortex, specifically in inferior frontal cortex and orbito-frontal cortex. An unpredicted finding, which remained highly significant following correction for multiple comparisons, was a strong positive correlation with a posterior cingulate region corresponding with the right precuneus. A further unpredicted finding was a significant correlation between

urge and bilateral reductions in neural response in the occipital cortex. Subjective "high" ratings showed correlation with the hippocampus bilaterally, but these did not survive correction for multiple comparisons. Absolute cerebral blood flow was not measured, but the drug-related video induced increased rCBF in the brainstem surrounding the peri-aqueductal grey matter and the ventral tegmental area in a similar manner to heroin itself. Unlike the heroin, the drug-related video also provoked increased rCBF in the left insula and bilateral cerebellar cortices. The interaction effects are harder to describe, but the effect of the drug-related video on the anterior cingulate, left dorso-lateral pre-frontal cortices and the left extended amygdala were significantly modulated by the level of activation in the brainstem provoked by the heroin injection. This type of interaction is termed a psycho-physiological interaction and will be dealt with in more detail in the next section on connectivity.

The second study, of 25 methadone-maintained former heroin users, used fMRI to examine the effect of methadone on craving responses to heroin related visual stimuli (Langleben *et al.*, 2008a). Most of the subjects were scanned at two time points; the first was 90minutes pre-methadone and the second 90 minutes post-methadone dose. The first analysis of the effects of the heroin-related stimuli produced activation in the familiar regions of anterior cingulate, orbito-frontal and insular cortices as well as the amygdala and hippocampus. What was particularly interesting about this study was that the responses in the left and right orbito-frontal cortex, insulae and hippocampal complex, and the left amygdala were reduced by methadone; although

the effect in the orbito-frontal cortex was relatively small. By contrast, the anterior cingulate effect of the stimuli was not significantly altered by the methadone. The authors argue that this may explain the reduced effects of methadone on craving, mediated via the orbito-frontal and anterior cingulate cortices, compared to the larger effects on perceived interoceptive state, mediated by the amygdala and insula areas.

1.4.2.4 What is connectivity – effective and functional?

Traditionally, studies of neural activation using functional neuroimaging have used analysis techniques designed to demonstrate whether or not a region is activated by a specific task or stimulus. Connectivity concerns linkage between such brain regions. The technique was originally applied to EEG and single-unit recording data analysis. There have been two particular types of connectivity that have been described: functional and effective (Gerstein & Perkel, 1969 as cited in Friston *et al.*, 1993). Functional connectivity is the simpler form, based on temporal correlation between levels of activity in the brain regions. The premise is that brain regions involved in the same function will tend to be activated at the same time and deactivated at the same time. Therefore, activation levels in such areas should be temporally correlated. Obviously, searching for such correlations requires a time-series of brain images such as is acquired in typical fMRI or water-PET studies.

Effective connectivity is more complex. It requires a pre-defined, usually anatomically derived, model of interconnections between the brain regions to be specified. These connections are then examined using mathematical techniques such

as dynamic causal modelling or structural equation modelling to assign strengths and directions of modulation to the connections (see Buchel & Friston, 1997; Friston, 2002a; Friston, 2002b; Hampson *et al.*, 2002; Mechelli *et al.*, 2002 for examples). Both techniques of measuring connectivity can be further expanded to examine changes in the level of connectivity resulting from external manipulations, for example drug administration or psychological task (Friston *et al.*, 1997; Honey *et al.*, 2003).

1.4.2.5 Functional connectivity studies in dependence

To date, very few connectivity analyses have been carried out on functional neuroimaging studies of substance misuse. The first was carried out by Sell et al (Sell *et al.*, 1999); who found activation in the midbrain in response to both a drug-related video and an injection of heroin. They also carried out an analysis of functional connectivity looking for regions showing a psycho-physiological interaction. This describes the situation where either the correlation between two regions is modulated by a psychological condition, or where neural activation in response to a psychological stimulus is modulated by the level of activation in another brain region. They report three areas where activity correlated with the level of midbrain activation only during the drug-related video; specifically these regions were the anterior cingulate and left dorso-lateral prefrontal cortices, and the left extended amygdala. All of these are regions that other studies have implicated in drug cue-responsivity. Heroin also appeared to alter the relationship between the level of rCBF in the anterior cingulate and basal forebrain regions. The authors

suggest that this could be interpreted as heroin altering the manner in which these brain areas respond to the presentation of drug-related stimuli via its effects on midbrain activation.

Although not explicitly a study examining substance misuse, another group have shown that methylphenidate tends to decrease both functional and effective connectivity in a cortico-striatal-thalamic circuit activated by a spatial memory task (Honey *et al.*, 2003) and by nicotine (Jacobsen *et al.*, 2004).

Cocaine also decreases local functional connectivity within brain regions (e.g. Motor cortex, visual cortex) (Li *et al.*, 2000). This study focused on correlations of activity between voxels within the same localised region over the course of "spontaneous" fluctuations in activity in a "resting" state. This analysis was conducted following injections of saline and cocaine. The regions examined were specifically chosen to be areas where there was minimal dopamine innervation. The authors suggest that these measured decreases in local functional connectivity may be due to dopamine effects on microvasculature or decreases in neuronal firing. Dopamine has known effects on vascular walls in the brain (Krimer *et al.*, 1998), however it is also known that cocaine decreases regional cerebral glucose metabolism (London *et al.*, 1990b) which supports the cause being a simple decrease in "spontaneous" fluctuations resulting in less measurable connectivity.

Some studies have examined the structural element of connectivity due to fears of the neurotoxicity of some abused drugs. Cocaine has been demonstrated to produce white matter lesions suggesting that this is one possible mechanism of altered

connectivity which is particularly associated with stimulant misuse (Lim *et al.*, 2002). Using diffusion tensor imaging to examine white matter integrity, specific disruption was noted in the orbito-frontal cortex of cocaine users. This region has been implicated in the compulsive nature of drug craving and drug seeking behaviours (Volkow *et al.*, 2004a). The possibility of functional impairment of the orbito-frontal cortex has been supported by data showing impairment in human drug users in decision making functions related to orbito-frontal cortex at a level between that of normal controls and patients with brain injuries in the orbito-frontal cortex (Rogers *et al.*, 1999).

1.4.3 Ligand studies

Table .1.8 Previous neuroimaging ligand studies in addiction

Study	Subjects	Ligand	Binding site
Bergström *et al.*, 1998	Single female back pain patient and rats on fentanyl	^{123}I-beta-CIT	DAT & SERT
Farde *et al.*, 1994	Healthy men on alcohol and alcoholics	^{11}C-Flumazenil	GABA-A
Fowler *et al.*, 1989	Healthy human & baboon	^{11}C-cocaine	DAT
Gilman *et al.*, 1996a	Alcoholics on/off disulfiram	^{18}F-FDG & ^{11}C-Flumazenil	GABA-A
Gilman *et al.*, 1996b	Controls & Chronic alcoholics +/- cerebellar degeneration	^{18}F-FDG & ^{11}C-Flumazenil	GABA-A
Greenwald *et al.*, 2003	Buprenorphine users, dose response	^{11}C-Carfentanil	mu-opioid
Greenwald *et al.*, 2007	Buprenorphine users, duration of action	^{11}C-Carfentanil	mu-opioid
Hagelberg *et al.*, 2002b	Healthy volunteers after alfentanil	^{11}C-Raclopride	D2/3
Hagelberg *et al.*, 2004b	Alfentanil in healthy subjects	^{11}C-FLB 457	D2/3
Hietala *et al.*, 1994	Controls and abstinent Alcoholics	^{11}C-Raclopride	D2/3
Jacobsen *et al.*, 2000	Cocaine abstinence	^{123}I-β-CIT	DAT & SERT
Kaasinen *et al.*, 2004b	Healthy volunteers	Caffeine expectation and ^{11}C-Raclopride	D2/3
Kaasinen *et al.*, 2004a	Healthy volunteers	Caffeine ^{11}C-Raclopride	D2/3
Kling *et al.*, 2000	Users on methadone	^{18}F-Cyclofoxy	Mu,kappa-opioid
Laine *et al.*, 1994	Controls, alcoholics at 4 days and 4 weeks abstinence	^{123}I-β-CIT	DAT & SERT
Laine *et al.*, 1999	Alcohol withdrawal	^{123}I-β-CIT relationship to MADRS score	DAT & SERT
Laine *et al.*, 2001	Controls and Alcoholics	^{123}I-β-CIT and sensation seeking	DAT & SERT
Laruelle *et al.*, 1995	Controls	^{123}I-IBZM after	D2/3

		amphetamine	
Laruelle *et al.*, 1996	Controls and Sz	^{123}I-IBZM after amphetamine	D2/3
Lingford-Hughes *et al.*, 1998	Alcoholics	^{123}I-Iomazenil	GABA-A
Lingford-Hughes *et al.*, 2000	Alcoholics women	^{123}I-Iomazenil	GABA-A
Litton *et al.*, 1993	Controls and alcoholics	^{11}C-Flumazenil	GABA-A
Malison *et al.*, 1995	Cocaine addicts	^{123}I-β-CIT after cocaine	DAT & SERT
Malison *et al.*, 1998	Cocaine abstinence	^{123}I-β-CIT	DAT & SERT
McCann *et al.*, 1998	Ex-MDMA users, Controls	^{11}C-McN5652	SERT
Melichar *et al.*, 2005	Users on methadone	^{11}C-Diprenorphine	Mu, kappa & delta - opioid
Nyback *et al.*, 1994	Smokers and controls	^{11}C-nicotine	Showed no use as tracer
Pauli *et al.*, 1992	Controls on/off alcohol	^{11}C-flumazenil	GABA-A
Rourke *et al.*, 1997	Smokers, current & abstinent	^{123}I-IMP SPECT	
Schlaepfer *et al.*, 1997	Cocaine users on IV cocaine	^{11}C-Raclopride	D2/3
Shi *et al.*, 2008	Heroin ex-users, methadone users, controls	^{11}C-CFT with craving	DAT
Smith *et al.*, 1998a	Controls +/- ketamine infusion	^{11}C-Raclopride	D2/3
Volkow *et al.*, 1990a	Cocaine users 1 week and 1 month abstinent, Controls	^{18}F-N-methylspiroperidol	D2
Volkow *et al.*, 1992a	Control	^{11}C-cocaine (whole body, not just brain)	DAT
Volkow *et al.*, 1993a	Cocaine users & controls	^{18}F-FDG and ^{11}C-Raclopride	D2/3
Volkow *et al.*, 1995a	Controls	^{11}C-methylphenidate & ^{11}C-cocaine	DAT
Volkow *et al.*, 1996b	Controls +/- methylphenidate	^{11}C-d-threo-MP	DAT
Volkow *et al.*, 1996c	Alcoholics & Controls	^{11}C-d-threo-MP & ^{11}C-Raclopride	DAT & D2/3
Volkow *et al.*, 1996d	Detoxed cocaine & controls	^{11}C-cocaine & ^{18}F-N-methylspiroperidol	DAT & D2
Volkow *et al.*, 1996e	Controls +/- IV methylphenidate	^{11}C-methylphenidate	DAT
Volkow *et al.*, 1997c	Controls +/- methylphenidate	^{11}C-Raclopride	D2/3
Volkow *et al.*, 1997a	Cocaine users on cocaine	^{11}C-Cocaine	DAT
Volkow *et al.*, 1998a	Controls and baboon +/- methylphenidate	^{11}C-Cocaine	DAT
Volkow *et al.*, 1999c (replicated in Volkow *et al.*, 2002a)	Controls	^{11}C-Raclopride predicts methylphenidate effects	D2/3
Volkow *et al.*, 1999a	Controls	^{11}C-cocaine after methylphenidate	DAT
Volkow *et al.*, 1999d	Controls on methylphenidate	^{11}C-Raclopride correlated with high	D2/3
Volkow *et al.*, 2000a	Cocaine users on cocaine (nasal v. smoked v. IV)	^{11}C-Cocaine	DAT
Volkow *et al.*, 2002b	Controls and abstinent alcoholics (6 weeks & 4 months)	^{11}C-Raclopride	D2/3
Volkow *et al.*, 2004b	Controls maths task & methylphenidate	^{11}C-Raclopride	D2/3
Wang *et al.*, 1995	Chronic cocaine users	^{18}F-N-methylspiperone	5-HT2
Wang *et al.*, 1997a	Cocaine users & controls	^{11}C-Cocaine	DAT
Wang *et al.*, 1997b	Opiate dependent before and after naloxone	^{11}C-Raclopride	D2/3
Wu *et al.*, 1997	Cocaine & controls	^{18}F-DOPA	DOPA uptake
Zubieta *et al.*, 1996	Cocaine dependent & controls	^{11}C-Carfentanil	mu-opioid
Zubieta *et al.*, 2000	Buprenorphine users	^{11}C-Carfentanil	mu-opioid

1.4.3.1 Dopamine

The majority of imaging studies in addiction looking at neurotransmitter systems, as opposed to activation, have focussed on the role of Dopamine. There are probably two main reasons for this. Most of the work has been done in the USA where cocaine (and crack) use are the largest problem in terms of illicit drug use. It is known that this drug works predominantly at the dopamine synapse, like other stimulants. There has, therefore, been a deliberate focus by the National Institute for Drug Abuse on funding studies of dopamine dysfunction in stimulants users (Volkow, Director of NIDA, personal communication). In addition to this, there are also many more PET and SPET tracers available to study the dopamine system than any other. ^{18}F-DOPA can be used to measure the uptake of dopamine pre-cursor into pre-synaptic neurons. ^{11}C-cocaine and ^{11}C-d-threo-methylphenidate have both been used to measure Dopamine-Transporter (DAT) activity in the pre-synaptic neuron. Many tracers have been used to measure post-synaptic dopamine receptor availability, specifically ^{11}C-Raclopride, ^{11}C-FLB and ^{18}F-N-methylspiroperidol have been used in the studies of addiction (see Table .1.8).

In the case of ^{11}C-Raclopride, and the additional tracer ^{11}C-PhNO, it is also possible to measure changes in availability of receptors caused by changes in extra-cellular dopamine concentration. This technique relies on the binding of the radio-tracer being dependent on the density of unoccupied or "available" receptors. This density will be dependent on the number of receptors and the concentration of other ligands that are able to occupy the receptor. In the case of the dopamine-D2 receptor the

competing ligand can be endogenous dopamine or exogenous drug. In this way, changes in tracer binding can reflect either changes in dopamine or receptor occupancy of a drug. This technique has been useful in demonstrating the receptor occupancy of antipsychotic medication as an example (e.g. Kapur *et al.*, 1998). The relationship between endogenous dopamine release and tracer binding is much more complex with estimates of the sensitivity varying widely (see Laruelle, 2000b for review).

1.4.3.1.1 Dopamine studies in opioid dependence

For many years it has been known that animals will self-administer opioid drugs into certain specific regions of the brain. The two main regions for which the best evidence has accumulated are the ventral tegmental area (VTA) and the nucleus accumbens (NAcc) (Wise & Hoffman, 1992). These regions, along with the PAG and the medial forebrain bundle (MFB) are part of the meso-cortical-limbic dopaminergic pathway. This pathway has been implicated as a general reward pathway for diverse stimuli (e.g. sex and food) as well as drugs of abuse (Nutt, 1996). It is thought that opioids exert their addictive properties by "hi-jacking" this natural reward pathway by causing excessive release of dopamine within the pathway that is not subject to the same homeostatic regulation as the natural rewards (Robinson & Berridge, 1993).

There is evidence from animal studies that opioids do release dopamine in this pathway. Using microdialysis techniques, it has been possible to measure extra-

cellular dopamine levels in distinct anatomical regions in response to opioid drugs (Cadoni & Di Chiara, 1999; Wise *et al.*, 1995). For example, opioid micro-injections into the VTA stimulate the release of dopamine in the NAcc in rats (Devine *et al.*, 1993), and systemic opioids have similar effects (Cadoni & Di Chiara, 1999). Further evidence of the role of dopamine in the rewarding effects of opioids is provided by the ability of dopamine antagonists to partially block the ability of opioids to act as unconditioned stimuli in animal studies (e.g. Longoni *et al.*, 1998).

Using the PET tools mentioned above, it is now possible to examine dopamine system function in humans, in particular human opioid addicts. One of the most consistent findings in PET studies of addiction is the down-regulation of Dopamine D_2 receptor tracer binding in users of many drugs. It has been repeatedly demonstrated in cocaine users (e.g. Volkow *et al.*, 1993a; Volkow *et al.*, 1990a; Volkow *et al.*, 1996d) and is also seen in abstinent alcoholics (Hietala *et al.*, 1994; Volkow *et al.*, 2002b). This effect occurs in the absence of changes in the pre-synaptic dopamine transporter, that can be measured with ^{11}C-d-threo-methylphenidate (Volkow *et al.*, 1996c). Of particular relevance to this thesis is the finding of decreased dopamine function in opioid dependent subjects (Wang *et al.*, 1997b). Although this was primarily a study of the effects of naloxone on the dopamine system (discussed below) it also examined baseline ^{11}C-Raclopride binding. Opioid dependent subjects showed significant reductions of 18% and 14% in the putamen and caudate nuclei respectively. As well as this post-synaptic deficit, chronic heroin users have also been shown to have a pre-synaptic deficit. ^{11}C-CFT is

a cocaine derivative that binds to the dopamine transporter and has shown decreased binding in current and past heroin users (Shi *et al.*, 2008).

There is not the same volume of studies examining the acute effects of opioids on dopamine as there are for the dopamine effects of stimulants. In fact, this was the reason for undertaking the study described in Chapter 5 of this thesis. Nevertheless there are two useful studies from the same group examining the dopaminergic effects of alfentanil in healthy volunteers (Hagelberg *et al.*, 2004b; Hagelberg *et al.*, 2002b). In the earlier study alfentanil infusion provoked a 6% increase in ^{11}C-Raclopride binding in basal ganglia. The second study used ^{11}C-FLB457 to demonstrate increased binding in cortical regions. In both cases this increase in tracer binding would be taken as evidence of decreased dopamine release. In the second study the results also showed a correlation between change in tracer binding and the euphoric effect of the alfentanil. It is worth noting that these were studies of analgesic effect and all subjects received a painful stimulus at the end of the scan. What effects this may have had on their state of mind during the scanning session is not discussed in the papers.

The effects of naloxone-precipitated withdrawals on the dopamine system have also been studied as mentioned above (Wang *et al.*, 1997b). In the opioid-dependent group studied, naloxone did not significantly change ^{11}C-Raclopride binding compared with placebo. However, the sub-group who received the higher dose of naloxone, when analysed separately, did show a decrease in ^{11}C-Raclopride binding. This is not what would be expected, as this result would tend to suggest an increase

in synaptic dopamine levels in withdrawal where animal studies have found a decrease using microdialysis techniques (Acquas *et al.*, 1991). The explanation for this difference is not obvious. It may be that the results represent true inter-species differences in opioid withdrawal effects, or may reflect the difference in the experience of withdrawal from a self-administered drug on which you are dependent and an experimentally administered drug over which you have no control. Lastly, it is not always possible to exclude the effects of changes in blood flow (and hence tracer delivery and washout) from changes in radio-tracer binding-sites in PET scans.

1.4.3.2 Opioids

The opioid receptor system is characterised by three basic forms of the receptor mu (μ), delta (δ) and kappa (κ). There are further sub-divisions of these sub-types but this level of detail is not required here. Fully demonstrating the distribution of the different opioid receptor sub-types is not yet possible in humans *in vivo*, due to the lack of sufficient selective tracers, but has been demonstrated using autoradiographic techniques *in vitro* (Cross *et al.*, 1987). The different anatomical distribution of the three subtypes in the human brain is summarised in Table 1.9. The same authors also highlighted the major differences between the pattern in humans and other mammals.

Brain region	Mean total specific ligand binding (fmol/mg protein)	Component (%)		
		μ	δ	κ
Thalamus	202	74	11	15
Temporal cortex	149	44	6	50
Claustrum	115	32	8	61
Caudate nucleus	112	49	3	48
Substantia nigra	63	40	16	13
Putamen	58	43	22	34
Globus pallidus (lat)	14	43	29	29
Globus pallidus (med)	7	43	57	<1

Table 1.9: Distribution of opioid receptor subtypes in the human brain. (After Cross et al., 1987).

The various subtypes of the opioid receptor are thought to mediate different components of the actions of opioids, both external and endogenous. In particular the μ receptor is thought to mediate the analgesic and euphoric effects of opioids, as well as the addictive properties.

1.4.3.2.1 Functional neuroimaging of the opioid system in normal volunteers

The basic mechanisms of PET & SPET have been described in the first section of this chapter. From this it should be apparent that in order to examine the characteristics of the opioid system in the CNS the primary pre-requisite is the availability of suitable neuroimaging tracers. There are three main PET ligands that are used to label this system, each with its own advantages and disadvantages. To date there are no SPET ligands for the opioid system that have been used in humans, but there are agents in development in animals which show promise (see Table 1.10).

Ligand	Imaging type	Receptor profile	Species
^{11}C-Diprenorphine	PET	μ, δ, κ, - antagonist	Human & animal
^{123}I-Diprenorphine	SPET	μ, δ, κ, - antagonist	Animal
^{11}C-Carfentanil	PET	μ - agonist	Human & animal
^{11}C-Methylnaltrindole	PET	δ – antagonist	Human & animal
^{123}I-Naltrindole	SPET	δ – antagonist	Animal
^{18}F-Cyclofoxy	PET	μ, κ - antagonist	Human & animal
^{123}I-Cyclofoxy	SPET	μ, κ - antagonist	Human & animal
^{11}C-Buprenorphine	PET	μ - partial agonist κ - antagonist	Animal

Table 1.10 Currently available radiotracers for SPET & PET

PET studies of the opioid system in normal volunteers have confirmed the post-mortem study findings that opioid receptors are extremely widespread in the human brain. Using ^{11}C-Diprenorphine, which labels all the opioid receptor sub-types, it is possible to demonstrate the normal distribution of opioid receptors in healthy volunteers (Jones *et al.*, 1988). The main areas of concentration of opioid receptors are found in the thalamus, caudate nucleus, and temporal, frontal and parietal cortices (see Figure 1.4 of a normal ^{11}C-diprenorphine scan). There is very little binding of tracer in the occipital cortex as would be expected from the low levels of opioid receptor in this area.

^{11}C-carfentanil can be used as a more selective μ - opioid receptor tracer to show the distribution of this sub-type alone. The modelling of this tracer is more problematic

due to its faster dissociation from the receptor than ^{11}C-diprenorphine and synthesis problems increasing the percentage of unlabelled (cold) ligand, but the distribution is as expected from post-mortem studies with the largest signal present in the thalamus (see Figure 1.4). There is relatively less binding in the cingulate and frontal cortex compared to ^{11}C-diprenorphine as further evidence of the increased numbers of δ- and κ- opioid receptors in these areas (Frost *et al.*, 1990).

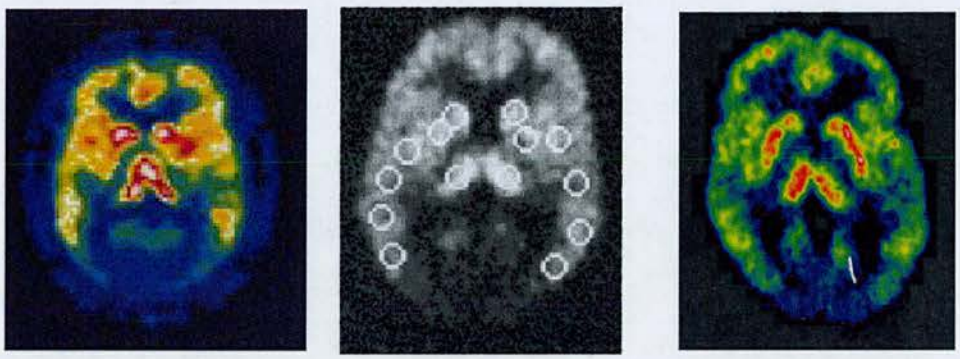

^{11}C-Carfentanil ^{18}F-Cyclofoxy ^{11}C-Diprenorphine

Figure 1.4: Differing distributions of mu, delta & kappa opioid receptors

More recently a relatively new PET ligand, ^{11}C-methylnaltrindole, has been used to demonstrate the distribution of the δ- opioid *in vivo* in humans (Smith *et al.*, 1999). As predicted from the *in vitro* studies, there was a high level of tracer binding in the putamen and caudate, intermediate binding in the frontal, parietal, occipital and cingulate cortices, and lower binding in the thalamus and cerebellum.

The opioid system is not a static entity. The number and distribution of opioid binding sites has been shown to vary with age, gender (Zubieta *et al.*, 1999) and, for women, phase of the menstrual cycle (Smith *et al.*, 1998b). The density of binding sites for many receptor systems changes with age, but the opioid system is unusual in that the density generally increases with age. A further complication is that the age

related changes are not uniform throughout the brain and they are gender dependent. Age and gender related effects were shown in prefrontal, anterior cingulate, temporal and parietal cortices. Age related effects were also found in the putamen and gender related effects in the caudate nucleus and the cerebellum. Age-by-gender interaction effects were also found in the amygdala and thalamus. It is therefore important that comparisons of opioid receptor measures between groups ensure adequate matching of these confounding factors.

The next section deals with the effects of acute doses of opioid drugs on the brain in healthy volunteers. However, there are other non-drug interventions that have shown measurable effects with functional neuroimaging of the opioid system. This system has long been implicated in the perception of pain and a site of action for potent analgesics. Chronic pain and the removal of chronic pain have been shown to alter the pattern and density of available binding sites for opioid PET ligands (Jones *et al.*, 1994). They showed that in patients with chronic arthritis the levels of ^{11}C-Diprenorphine binding decreased when the patient was in pain and increased when scanned during pain-free periods. They suggest that this was an effect of endogenous opioids being released to a greater degree during pain, thereby decreasing the number of available binding sites for the tracer. A similar increase in ^{11}C-Diprenorphine binding was seen in patients with trigeminal neuralgia following surgical intervention to terminate their pain when they were scanned before and after the procedure (Jones *et al.*, 1999).

1.4.3.2.2 Functional neuroimaging of acute effects of opioids in normal volunteers

Before it is possible to fully understand the effects of opioid drugs in dependent users it is necessary to understand what these drugs are doing in the normal healthy volunteer. The most thorough neuroimaging study of the acute pharmacokinetics of commonly used opioids was carried out on the rhesus monkey (Hartvig *et al.*, 1984). This group gave rhesus monkeys a range of ^{11}C-labelled opioids and imaged the distribution and kinetics using PET. The drugs used in this study were heroin, morphine, codeine and pethidine. Due to the low spatial resolution obtainable from PET scanning at that time the results were only differentiated into whole brain, nose, extra-cranial soft tissue and pituitary regions. One of the most striking results from this study is the large difference in kinetics between the whole brain and the pituitary. Following intravenous administration, the peak level of morphine in the pituitary was reached after 5 minutes compared with 10 minutes for the whole brain. The level of uptake into the pituitary region was also almost double that in the rest of the brain. This study also showed that elimination half-lives for these opioids were not the same in brain, extra-cranial soft tissue or plasma. Morphine elimination half-life from the brain is substantially longer than from other tissues. Conversely, pethidine showed rapid uptake and elimination from brain with much longer plasma half-life. The authors suggested that this may be the result of differences in the lipophilic characteristics of the drugs studied; for example, pethidine has higher lipid solubility than morphine, which explains its faster brain uptake, but not the slower plasma

elimination. This is a clear example of functional neuroimaging helping to explain clinical anomalies like the shorter duration of analgesic action of pethidine compared to morphine despite its much longer plasma half-life.

1.4.3.2.3 Functional neuroimaging of acute effects of dependent subjects

The opioid system has, unsurprisingly, also been the subject of some investigation of its role in dependence. There is an emerging pattern from the data that suggests the opioid system is implicated in more than just dependence on opioid drugs. ^{11}C-Carfentanil has been used to study the μ-opioid receptor in cocaine dependence. ^{11}C-Carfentanil binding was elevated in cocaine users in early withdrawal compared to a control group (Zubieta *et al.*, 1996). The binding levels correlated with subjective cocaine craving in four brain regions: amygdala, anterior cingulate cortex, frontal cortex and temporal cortex. These increases in binding showed some evidence of normalisation when re-scanned some 4 weeks after detoxification. The authors highlight that opioid and dopamine systems are thought to have some degree of antagonistic relationship with the brain. This is supported by the reciprocal finding in early abstinence of increase opioid receptor tracer binding and decreased dopamine receptor tracer binding.

The finding of increased opioid receptor availability in withdrawal is becoming a generic finding across drugs of abuse. Work by the group in Bristol, of which I was a member, has shown increased binding of ^{11}C-Diprenorphine in alcohol and

methadone withdrawal (Williams *et al.*, 2007). Increased opioid receptor availability in opioid withdrawal was also shown with ^{11}C-Carfentanil (Zubieta *et al.*, 2000).

This same study has also been able to demonstrate the occupation of μ-opioid receptors by buprenorphine (Zubieta *et al.*, 2000). Buprenorphine is a relatively new substitute opioid treatment. It is a partial agonist at the μ-opioid receptor and antagonist at the κ-opioid receptor. This has been replicated by the same group, who have also gone on to show the dose – occupancy relationship for buprenorphine (Greenwald *et al.*, 2003) and the duration of occupancy (Greenwald *et al.*, 2007).

Attempts to image receptor occupation by the more traditional substitute opioid – methadone, have not produced such clear results. Using ^{18}F-Cyclofoxy, a PET tracer that labels both μ-opioid and κ-opioid receptors, methadone has been shown to reduce tracer binding by up to 32% in a dose dependent manner (Kling *et al.*, 2000). However, work in our unit did not find any effect of methadone treatment on opioid receptor availability using ^{11}C-Diprenorphine (Melichar *et al.*, 2005).

2 Opioid Craving

The intention in this study was to extend previous work on mental imagery and cue-induced heroin craving that had been carried out in a clinical laboratory setting (Weinstein *et al.*, 1997). As detailed in chapter 1, many neuroimaging studies have been carried out in cocaine craving, with a few in alcohol, nicotine and heroin craving. A larger volume of work exists, describing studies of cue-exposure and its use to induce craving for addictive drugs. The aim of the study was to map the neural activation patterns that were associated with the phenomena of heroin craving. At the time of its inception no other study had yet done this. Following the use of cue-exposure studies in the treatment of craving it was anticipated that autobiographical scripts of distinct past episodes of craving would be a powerful induction paradigm. This had already been shown in the clinical laboratory (Weinstein *et al.*, 1997). Work from the United States of America had already shown that exposure to cues that predicted drug availability was also able to induce craving and that these responses could be extinguished by repeated exposure to the stimuli in the absence of drug (see Childress *et al.*, 1988a for review). The implication of this was that it would be ethically possible to use drug-related cues to induce craving in abstinent users, provided these cues were not followed by exposure to the drug. It was anticipated that this exposure should induce heroin craving, but that this would reduce with repeated exposure to the stimuli, thereby not provoking relapse.

The specific hypotheses that this study was designed to test were that:

1. autobiographical memories of previous episodes of heroin craving would

induce heroin craving within the scanner environment, as it had in the clinical laboratory;

2. craving would be associated with detectable changes in regional cerebral blood flow as measured by PET, using the tracer $H_2{}^{15}O$;
3. there would be a correlated pattern of subjective changes in heroin craving, physiological responses and rCBF changes.

2.1.1 Methods

2.1.2 Subjects:

Power calculations are frequently problematic with neuroimaging studies. The variables required for estimating power are frequently unknown. The modelling to date suggested that below six subjects was unlikely to have sufficient power to detect anything other than very large changes in rCBF. Between six and ten subjects power increases in an approximately linear fashion and above twelve subjects is where the power to subject number relationship curve begins to flatten out (Friston *et al.*, 1996). The target number for subjects was therefore set at 10-12 subjects.

In an ideal situation, all subjects would have been previously addicted to heroin, but have used no other drug. In practice this is an impossible requirement as poly-drug use is by far the norm in this population. Nicotine addiction is an almost ubiquitous state in heroin users (Clemmey *et al.*, 1997). In practice the best compromise between removing possible confounding variables and on the other hand creating an unrepresentative or non-existent sample was to require a past history of opioid addiction and exclude any subjects with previous addiction to, or very heavy use of, anything other than nicotine. As PET imaging requires radiation exposure we were

also required by the National Radiological Protection Board (NRPB) and Administration of Radioactive Substances Advisory Council (ARSAC) to set a minimum age limit of 25 years. In order to avoid the confounding effects of withdrawal on our measures of rCBF we required a minimum of 10 days opioid free prior to scanning. However, we wished to examine the effects of duration of abstinence so we aimed to recruit subjects who had been abstinent for a range of time periods.

As well as excluding a past or present history of addiction to other drugs we also excluded concomitant use of any psychotropic medication or the presence of any current or past serious psychiatric diagnosis, any history of severe head trauma or current acute medical condition likely to alter rCBF. We did not exclude anyone with a diagnosis of personality disorder as this is too common a form of co-morbidity and to do so would again make the sample unrepresentative of the population. With the difficulties inherent in requiring abstinence from all potentially confounding medications a compromise was reached in each case, with the aim to have the subjects as medication and drug free as possible. In practice this meant a minimum duration of abstinence from illicit drug use to produce a negative urine drug screen.

Using these inclusion and exclusion criteria we recruited twelve subjects, eleven of whom were male. In keeping with the ARSAC requirement, the age range was from twenty-seven to forty-five years with a mean age of 34.4 years. All subjects were recruited from local drug treatment agencies: NHS, non-statutory and private. All subjects reported suffering cravings for heroin since achieving abstinence according

to their keyworker at the respective treatment agency. All subjects had a history of previous opioid dependence of mean duration 7 years with a range 4 months to 20 years. In all cases, opioid dependence included time addicted to heroin and at least one period of substitution with methadone. No subject had a history of use of buprenorphine. Urine testing confirmed that all were opioid free at the time of the study. The duration of abstinence from opioids prior to taking part in the study was between 10 days and 3 years for all subjects. In the case of the first nine subjects this data had to be recovered by a retrospective search of their case notes as it had not be collected at the time of the scan. In two cases it was not possible for me to trace their old case notes as they had been recruited from a private clinic. Only an approximate estimate had been recorded in the subject details and this was used in all subsequent analyses. For the remaining ten subjects, where precise data was available, the mean duration of abstinence was 8.25 months. All subjects were right handed. Of the twelve subjects, seven had a previous history of abuse of other drugs. None of them were currently using other illegal drugs at the time of the study. This was also confirmed by urine testing. Despite the inclusion / exclusion criteria, two of the subjects were taking selective serotonin re-uptake inhibitor antidepressants and one was taking anticonvulsants. One other subject was taking the anti-cholinergic drug oxybutinin for detrusor instability. This study was approved by the three local ethics committees covering the scanner and recruiting clinics, and by ARSAC. After complete description of the study, written informed consent was obtained from all participants. All subjects were also given a subject information sheet and a letter sent

to their General Practitioner informing them of their patients' participation in the study.

2.1.3 Protocol:

All subjects participated in the study for one day only. In each case this day followed a standardised format. Subjects were collected from their residence in the morning, where an initial dipstick urine test was done to exclude recent use of illicit drugs. We then transported them to the cyclotron unit at Hammersmith Hospital, London. For those subjects recruited by myself, they also completed a checklist of demographic details and provided information on past and recent drug use, including alcohol and tobacco. On arrival at the unit, subjects were given breakfast while the scanning suite was prepared.

During the pre-scan interval all subjects recorded two audio-taped stimuli. This was done in an identical manner to the previously published study in the clinical laboratory setting (Weinstein *et al.*, 1997). Each script was of two minutes duration and recounted a single specific episode from their past. In one case the script concerned an episode when they experienced a strong craving for heroin and the other was of a neutral episode. Subjects were specifically told to focus on describing the feelings, both emotional and physical, of the craving they experienced during the episode they were recounting. Care was also taken to ensure that subjects also described a similar level of details of their chosen neutral episode. Each stimulus was recorded by the subject in conversation with the researcher. In all cases, this was

done in such a way that only the subject's own voice was heard during the two minute period recorded and used as a stimulus. Stimuli were recorded in a private office within the cyclotron unit using a standard microphone attached to a mono cassette recorder. At this point subjects were permitted a last pre-scan cigarette and then shown the scanner environment and reminded of the exact scanning protocol that would be followed. This meant that all subjects were approximately 1 hour since their last cigarette at the time scanning began.

Prior to commencing the scanner session, all subjects completed the Heroin Craving Questionnaire (Tiffany, unpublished as used in Weinstein *et al.*, 1997). Immediately prior to scanning, all subjects were escorted to the bathroom and requested to empty their bladder. At this point a second urine sample was taken which was sent to the local NHS clinical laboratory for confirmatory analysis for illicit drugs by EMIT assay and HPLC. All these analyses were subsequently reported as negative for cannabis, opioids including heroin and methadone, cocaine, amphetamine and benzodiazepines.

Each scanning session followed the same protocol. Subjects were put into the scanner by the radiographer and made comfortable. Their head was restrained in position using padded foam and Velcro straps attached to the scanner bed. We used laser cross-hairs to mark their position in the scanner aperture. The scanner gantry was tilted to an orientation which produced maximal coverage of the whole brain within the 10cm field of view in the inferior-superior axis, but contained the entire cerebellum and orbito-frontal cortex. In practice this required tilting the scanner top

posteriorly by approximately 15 degrees. Subjects were also fitted with a single ear-piece in their right ear. This was connected to the cassette recorder for playback of the audio stimuli.

At this point subjects were also connected to a Finapres® using the finger-probe for continual recoding of pulse and blood pressure.

Subjects then underwent a 12 run PET scan of regional cerebral blood flow (rCBF) using the tracer $H_2{}^{15}O$, with a slow bolus technique. For each scan we injected approximately 10mCi of radio-labelled water over 20 seconds. There was a 10-minute gap between runs, with the total scan lasting 2 hours. A brain dedicated Siemens/CTI (Knoxville, USA) ECAT 953b PET camera was used, operating in high sensitivity 3D mode (Spinks *et al.*, 1992). During each of the 12 runs the subject listened to one of the two previously recorded audio taped scripts. Each drug-related and neutral script was presented six times, in random order. Image acquisition began 90 seconds after the beginning of the script to allow craving to be induced in response to the stimulus. Images were acquired in a single 90 seconds frame. Radioactivity counts acquired during this time frame predominantly reflect changes in rCBF during the rising phase of radioactivity in the head which typically lasts 30-45 seconds.

After each run, the subjects completed 6 visual analogue scales (VAS) of:

> At this moment the intensity of my craving for heroin is ...
> At this moment my urge to take heroin is ...
> At this moment I feel this happy ...

At this moment I feel this sad ...

At this moment I feel this anxious ...

At this moment the vividness of the script is ...

Each scale ranged from 0 to 100 and was anchored at 0 with "not at all", at 25 with "a little", at 50 with "quite a bit", at 75 with "very" and at 100 with "the most I could be" as described previously (Weinstein *et al.*, 1997). Subjects were instructed to respond with the number most closely matching their current state. At the end of all 12 runs, subjects completed the Heroin Craving Questionnaire again, in order to assess the overall level of craving and the multiple aspects of craving including control over drug use, outcome expectancies and avoidance of withdrawal. See figure (Figure .2.1) for a graphical representation of the scanning protocol timings.

Figure .2.1 Timing of Opioid Craving Scan Protocol

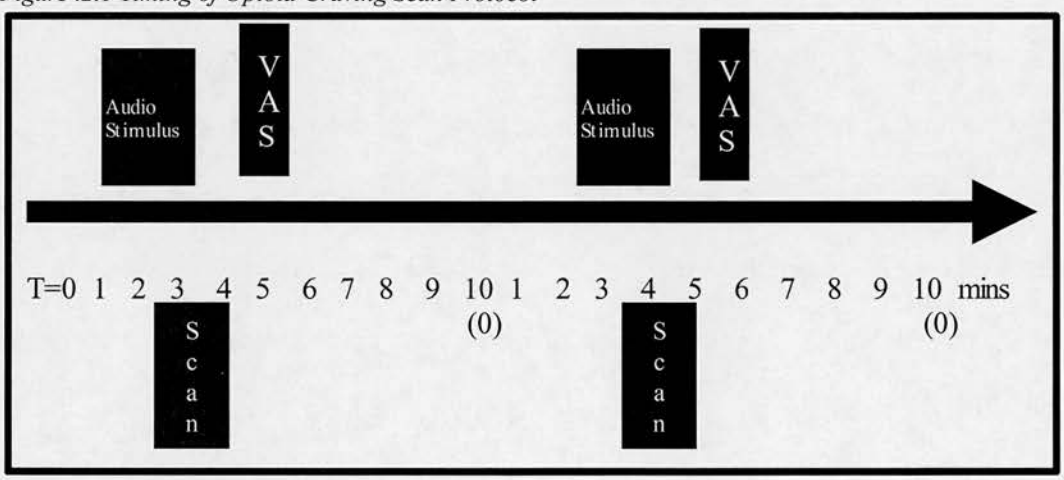

2.1.4 Image Analysis:

2.1.4.1 Patterns of activation

The PET images of rCBF were analysed using SPM99 (Wellcome Department of Cognitive Neurology, London) implemented in Matlab® 6.5.1 (Mathworks). The 12

images for each subject were realigned to a mean image for that subject. This partially corrects for motion of the subject between the 12 scans. Realigned images were normalised to a standardised template $H_2{}^{15}O$ PET image derived from the Montreal Neurological Institute (MNI) template, using windowed sinc interpolation. The resultant realigned normalised images were then smoothed with a Gaussian function at 12mm full width half maximum. This was chosen as three times the size of the image voxel dimensions. This smoothing removes a degree of any remaining mismatch between subjects after normalisation and also ensures a more normal distribution of the residual errors in the subsequent statistical analysis (Friston, 1995).

For the statistical analysis the images were analysed using a cognitive subtraction and a correlational analysis. For the cognitive subtraction a condition comparison was carried out with the audio taped scripts (drug-related or neutral) determining the conditions. For the correlational analysis the "crave" and "urge to use" VAS scores were averaged to produce a more normally distributed composite "crave/urge" scale. This composite "crave/urge" scale was then used as a covariate of interest to examine areas of rCBF that co-varied with this scale. This second analysis was restricted to include only those subjects that reported craving in response to the cue-exposure stimuli. This resulted in 4 subjects being excluded from this analysis since their "crave/urge" scales did not vary from zero throughout the scanning session. To include those subjects who did not report any craving, i.e. whose VAS scores did not vary, would contravene the basic assumptions of normal distribution that underlie the

statistics in SPM, which uses the General Linear Model (Friston, 1995).

In the SPM99 analyses, time from the start of the first scan was entered as a covariate of no interest to take account of any rCBF changes that were related to non-specific factors. All covariates were centred around subject means, and entered with a subject-specific fit. Global cerebral blood flow effects were removed by ANCOVA model allowing a subject-specific fit. The threshold for statistical significance for all analyses was set at $p<0.05$ after correction for multiple comparisons for either peak change in rCBF or the size of the activated cluster.

In a further analysis, the contrast, or difference, images for each subject comparing the effects of the two conditions were entered into a further 2^{nd} level analysis to examine the effects of duration of abstinence. The two subjects for whom duration of abstinence was not precisely known were excluded.

2.2 Results

2.2.1 Subjective measures:

Craving was induced by the cue-exposure paradigm in 8 out of the 12 subjects (66%) as shown by changes in the VAS scores. As can been seen in Figure 2.2 these 8 subjects (labelled as "cravers") showed a consistent pattern of higher "craving" and "urge to use" scores in response to the drug-related script than the neutral script, but this pattern attenuated with repetition of the scripts. The same figure shows the distinct flatline response of the 4 subjects who showed no craving response (labelled

the "non-craver" group). Figures 2.2-2.6 show the subjective responses on all the VAS scales. In all cases the craver and non-craver subsets, and the whole group are shown in their responses to both the neutral and drug-related stimuli.

On the combined "craving / urge to use" scale the whole group of subjects reported a significantly higher score in response to the craving stimulus at all but the last repetition of the stimuli (see Table 2.1). If the sub-group of those who did not show a craving response (the "non-cravers") are excluded then the comparison is still significant after the 1st, 3rd and 4th repetitions. For the "non-cravers" the difference is never significant. The duration of abstinence from opiates did not predict the craving response to the stimuli, nor did it correlate with the degree of craving induced.

Wilcoxon signed-rank parameter	**Stimulus Repetition**					
	1	**2**	**3**	**4**	**5**	**6**
W+	43.5	26.5	36	36	26	39
W-	1.5	1.5	0	0	2	6
N	9	7	8	8	7	9
p ≤	0.0078	0.0031	0.0078	0.0078	0.0469	0.0547

Table 2.1: Wilcoxon paired signed-rank tests for "Craving / Urge to use" combined scale. W+, W- and N are the raw statistics calculated as part of the Wilcoxon test, i.e. the positive and negative rank differences and the number of non-tied pairs.

As well as this statistical evidence that craving was successfully induced in at least 8 subjects there was also qualitative evidence. Several subjects spontaneously reported feeling craving in a manner very similar to when they were using heroin. A few subjects were noted by the experimenters as exhibiting transient signs of opioid withdrawal brought on by the stimuli, for example enlarged pupils and goose-flesh.

Figure 2.3 shows the effect of the stimuli on the "Happy" VAS. Subjects all showed lower scores in response to the drug related stimuli but the effect is visibly smaller in the "non-craver" group. The difference between stimuli never achieves significance however when all 12 of the subjects were studied. There is no difference when only the "cravers" are included in the analysis.

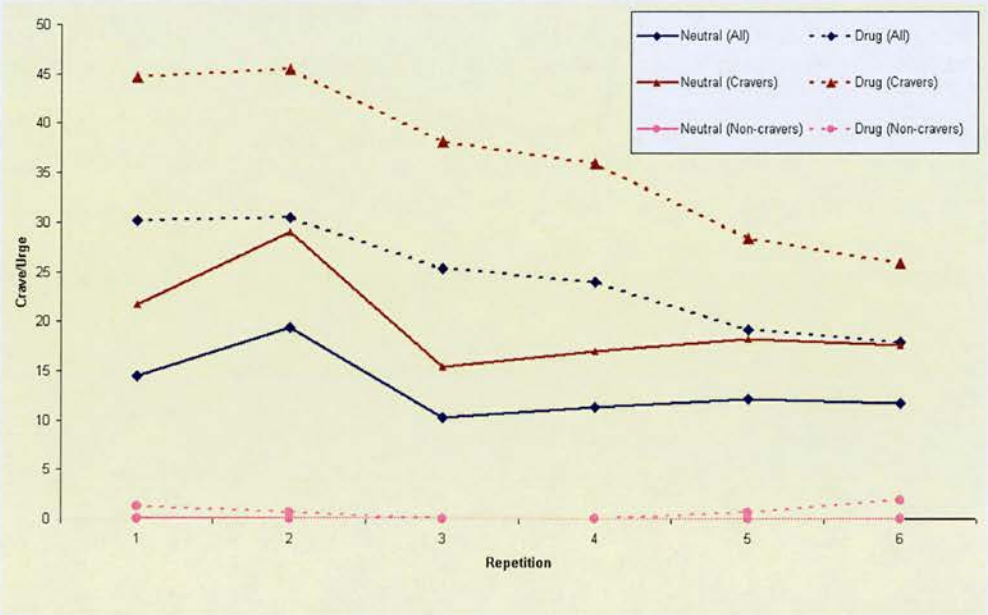

Figure 2.2: Craving / Urge combined VAS scale. Sub-groups divided into Cravers (n=8) and non-cravers (n=4).

The "sad" VAS scores are shown in Figure 2.4. They show a reciprocal pattern to the "happy" VAS scores with all subjects generally scoring higher in response to the craving stimulus. For the group as a whole this is only significant for the first two repetitions (1st repetition: W+46.5, W-8.5, N=10, $p \leq 0.04883$; 2nd repetition: W+45, W-0, N=9, $p \leq 0.00396$). This effect still remained significant for the "cravers" subgroup on the 2nd repetition (W+36, W-0, N=8, $p \leq 0.007812$).

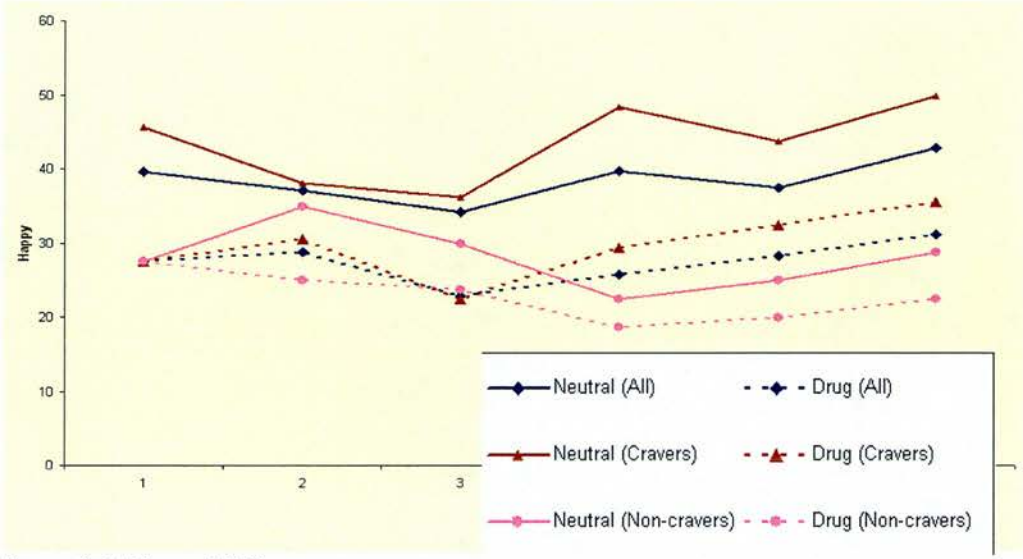

Figure 2.3: Happy VAS scores

A very similar effect was reported on the "anxiety" VAS. Although the magnitude of the differences between the stimuli were a little smaller than on the sad VAS, as can be seen in Figure 2.5, there was greater consistency across the subjects. As a result, for the group as a whole, the differences between the two conditions were significant at the 1st, 2nd and 4th repetitions (1st repetition: W+51, W-4, N=10, $p \leq 0.01367$; 2nd repetition: W+46.5, W-8.5, N=10, $p \leq 0.04883$; 4th repetition: W+63.5, W-2.5, N=11, $p \leq 0.00293$). For the "cravers" sub-group, the difference only remains significant at the 1st repetition (W+32.5, W-3.5, N=8, $p \leq 0.03906$).

The final VAS was "vividness". Here there were, importantly, no visible trends of significant differences between the two stimulus conditions. There was a slight trend for the "non-craver" group to be slightly higher on this scale than the "craver" sub-group.

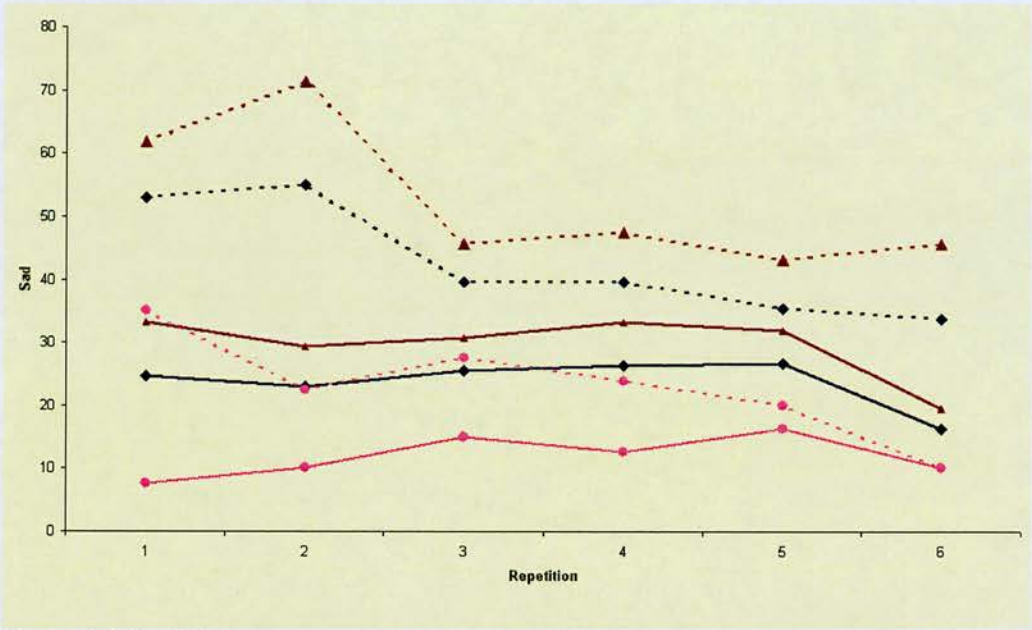

Figure 2.4: Sad VAS scores

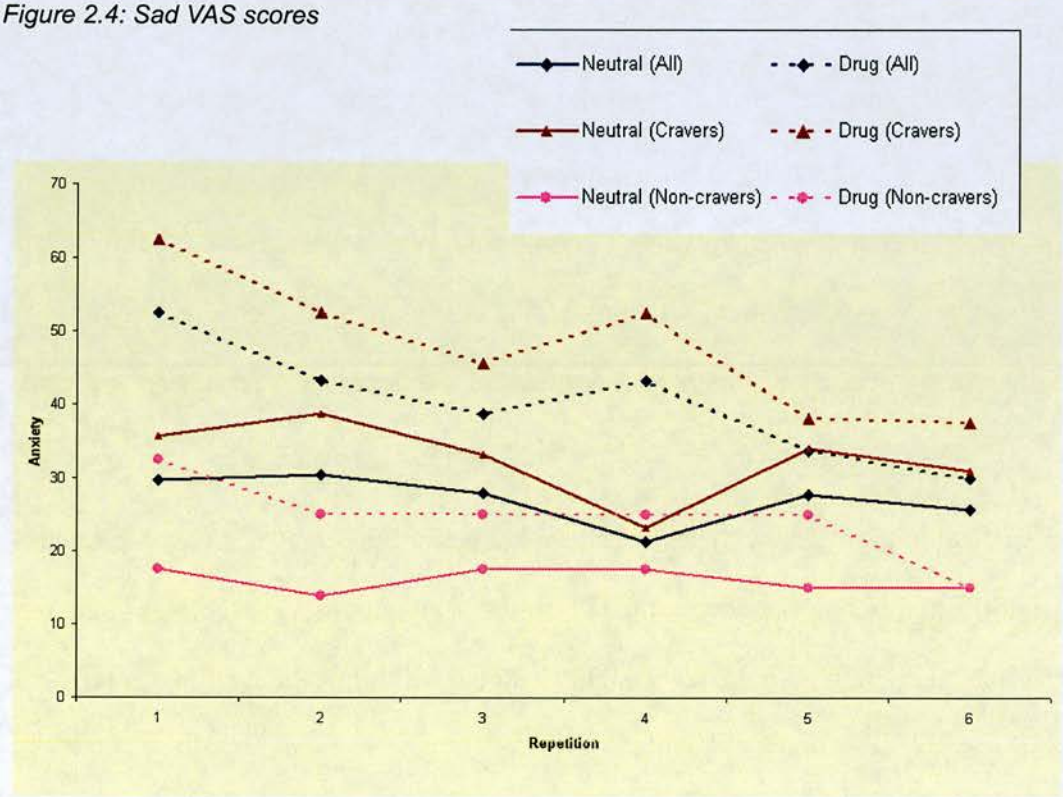

Figure 2.5: Anxiety VAS scores

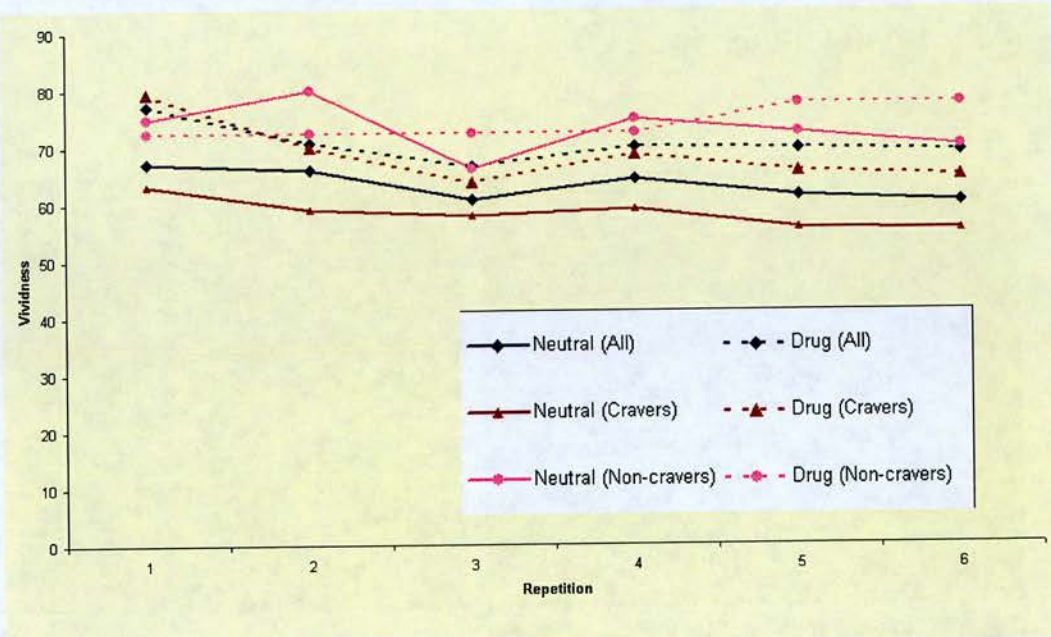

Figure 2.6: Vividness VAS scores

2.2.2 Image analysis:

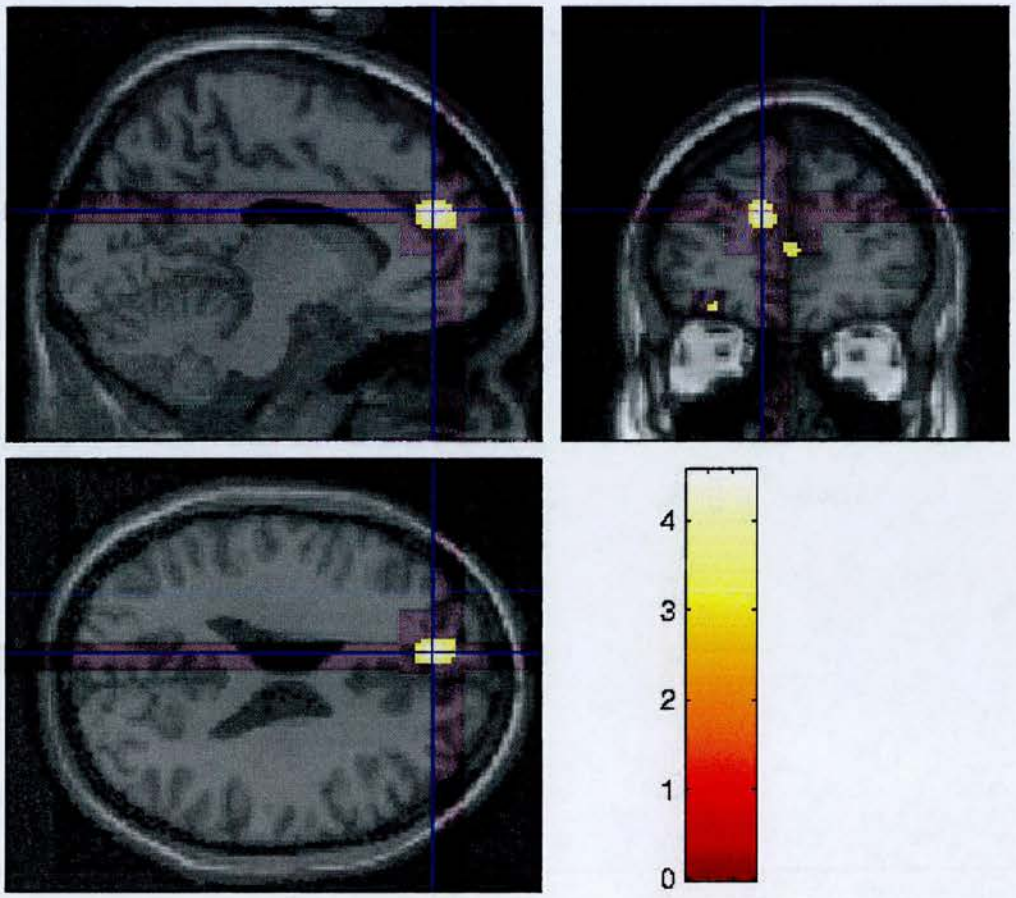

Figure 2.7: Activation in the left Anterior Cingulate and medial pre-frontal gyri. Comparison of drug related with neutral stimuli

Analysis of the rCBF images revealed two main results. In the cognitive subtraction of conditions the scans were divided into "drug-related" or "neutral" determined by the stimulus script. The contrast between these conditions revealed a single significant cluster of voxels ($t= 4.53$, cluster size = 297 voxels, spatial extent $p<0.01$ corrected for multiple comparisons) showing an increase in rCBF in an area overlying the left medial pre-frontal region and adjacent left anterior cingulate cortex (Talairach atlas co-ordinates -10,46,24 mm) (see Figure 2.7). Figure 2.8 shows the

effect sizes for each stimulus in each subject. From this it can be seen that there is a consistent activation in response to the drug related stimulus across all the subjects, both those who craved, and those who did not.

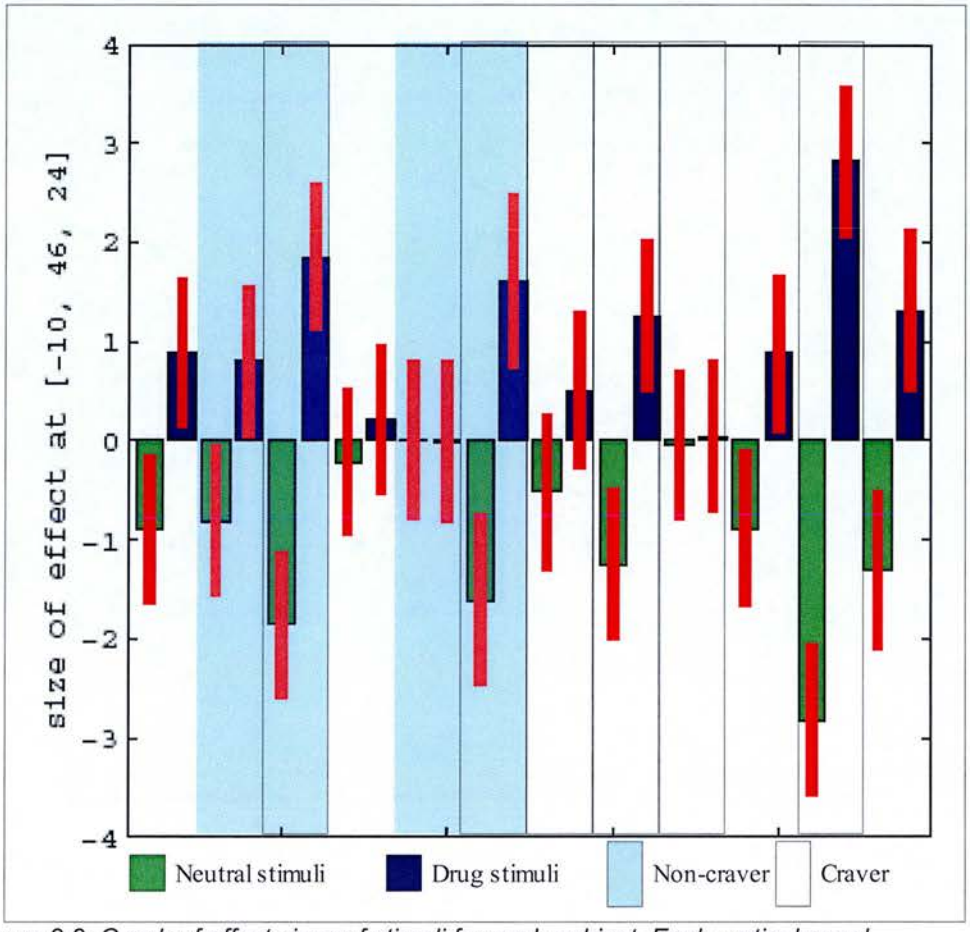

Figure 2.8: Graph of effect sizes of stimuli for each subject. Each vertical panel represents one subject and each bar represents the effect size for that subject in that condition with red error bars.

The duration of abstinence showed a significant positive association with the size of the difference in rCBF responses between the two conditions in this anterior cingulate region (Talairach co-ordinates –8,38,18 mm, t=7.69, cluster size = 10 voxels, peak height p=0.018, spatial extent p<0.001 corrected for multiple

comparisons). This implies that the longer the duration of abstinence from opiate drugs, the larger the change in rCBF between the conditions (see Figure 2.9).

The reverse contrast of these two conditions, looking for areas of relative decrease rCBF in response to the drug-related stimulus, showed significant bilateral decreases in rCBF in the primary visual cortex (Talairach co-ordinates +/-14,-90,20 mm, t=3.99 (Right) & 4.02 (Left), cluster size = 193 (Right) & 241 (Left) voxels, spatial extent $p<0.05$ corrected for multiple comparisons) and the right extra-striate cortex (Talairach co-ordinates 30,-80,30 mm, t=3.96, cluster size = 378 voxels, spatial extent $p<0.005$, corrected for multiple comparisons). These can be seen in Figure 2.10.

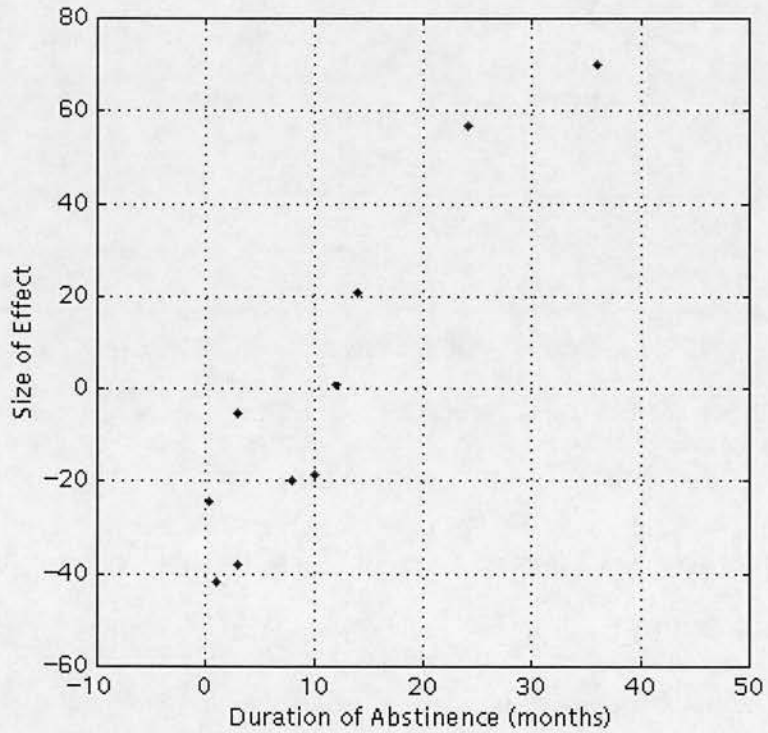

Figure 2.9: Correlation between Anterior Cingulate activation and duration of abstinence.

As stated in the methods, the correlational analysis used only the images from the eight subjects who exhibited a craving response to the drug related stimuli. As shown in Figure 2.11, a single region in the left orbito-frontal cortex (Talairach co-ordinates -26,44,-14 mm) was found to co-vary positively with the composite "crave/urge" score (t= 5.19, cluster size = 157 voxels, peak height $p<0.05$ corrected for multiple comparisons). There were also multiple areas in the occipital cortex that negatively co-varied significantly with the composite "crave/urge" scores. The most significant area was in the right occipital cortex (Talairach co-ordinates 12,-90,22 mm, t=5.31, cluster size = 890 voxels, spatial extent & peak height $p<0.01$ corrected for multiple comparisons). Visually this was very similar to Figure 2.10.

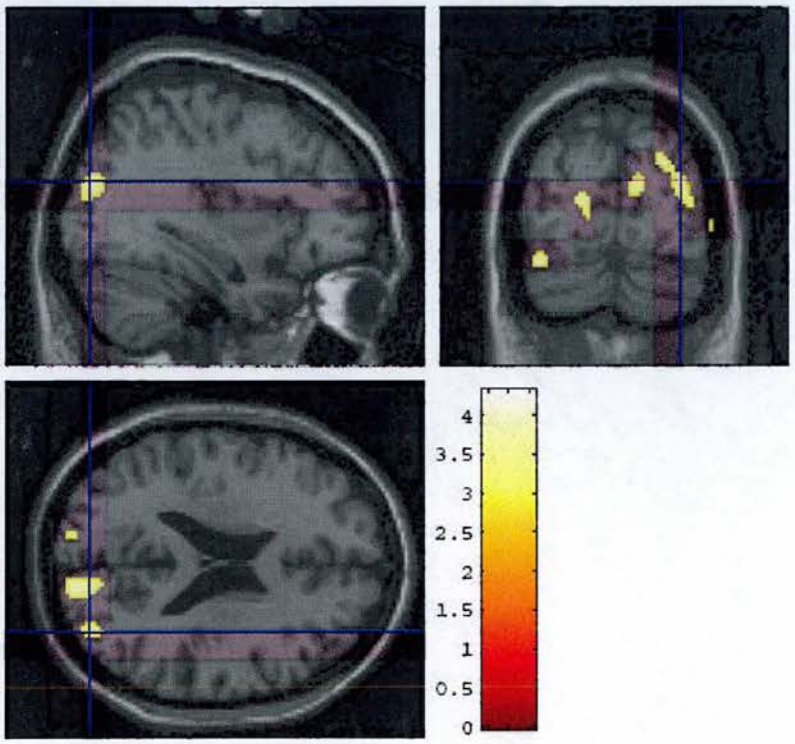

Figure 2.10: Areas of brain activation greater in response to the neutral stimulus.

The region of the orbito-frontal cortex which correlated with the "craving/urge" scale did not show a significant activation in the condition comparison and similarly the region in the left medial pre-frontal and anterior cingulate that showed a significant activation in the condition comparison did not show a significant association with the "crave/urge" scale.

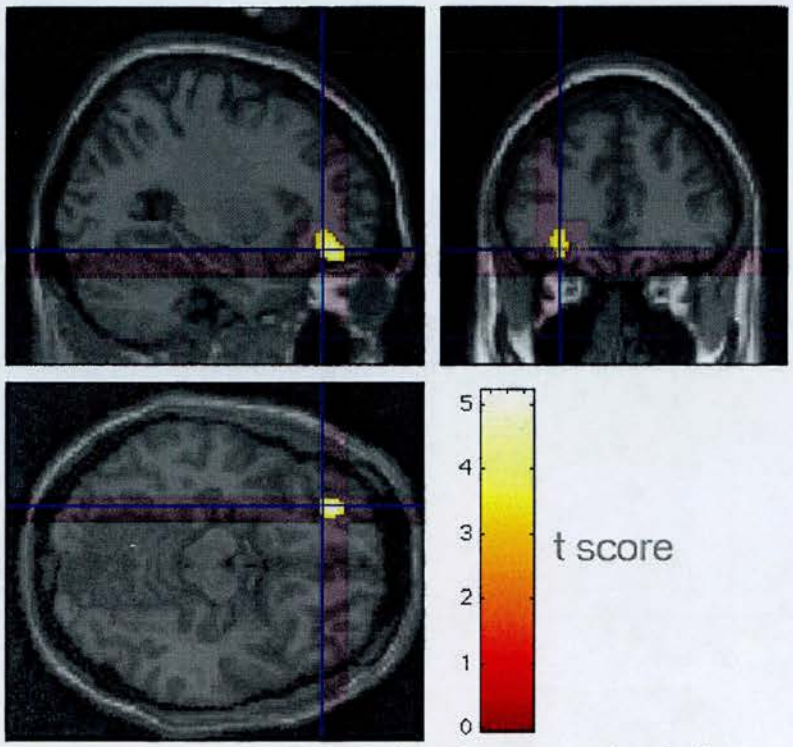

Figure 2.11: Activation in left orbitofrontal cortex correlated with heroin craving

3 Circuits of Opioid Craving

This chapter will focus on an extensive re-analysis of the data from the previous chapter on imaging heroin craving. The techniques used were developed for use in fMRI within the SPM software package. Prior to this study there had only been one published paper using similar techniques in PET imaging in heroin use (Sell *et al.*, 1999). This study provided the inspiration to extend our previous work to examine areas of the brain that appeared to be part of a functionally connected circuit with the primary regions of activation in the Anterior Cingulate and Orbito-frontal cortices.

3.1 Methods

3.1.1 Subjects and protocol:

Data for this study was derived from the same subjects as detailed in the previous chapter. In brief, this was 12 abstinent former heroin addicts. The data for each subject consisted of 12 PET scans of regional cerebral blood flow (rCBF) using the tracer $H_2{}^{15}O$. Half the scans were acquired following presentation of a craving related audio stimulus and half following a neutral stimulus.

3.1.2 Image analysis:

3.1.2.1 Patterns of activation

The PET images of rCBF were analysed using SPM99 (Wellcome Department of

Cognitive Neurology, London). The 12 images for each subject were realigned to a mean image for that subject. This partially corrects for motion of the subject between the 12 scans. Realigned images were normalised to a standardised template $H_2{}^{15}O$ PET image derived from the Montreal Neurological Institute (MNI) template (Evans *et al.*, 1993), using windowed sinc interpolation (Ashburner *et al.*, 1999). The resultant realigned normalised images were then smoothed with a Gaussian function at 12mm full width half maximum. This was chosen as three times the size of the image voxel dimensions.

For the statistical analysis the images were analysed using a cognitive subtraction and a correlational analysis. For the cognitive subtraction a condition comparison was carried out with the audio taped scripts (drug-related or neutral) determining the conditions. For the correlational analysis the "crave" and "urge to use" VAS scores were averaged to produce a more normally distributed composite "crave/urge" scale. This composite "crave/urge" scale was then used as a covariate of interest to examine areas of rCBF that co-varied with this scale. This second analysis was restricted to include only those subjects that reported craving in response to the cue-exposure stimuli. This resulted in 4 subjects being excluded from this analysis since their "crave/urge" scales did not vary from zero throughout the scanning session. To include those subjects who did not report any craving, i.e. whose VAS scores did not vary, would contravene the basic assumptions of normal distribution that underlie the statistics in SPM, which uses the General Linear Model (ref).

In the SPM99 analyses, time from the start of the first scan was entered as a covariate of no interest to take account of any rCBF changes that were related to non-specific factors. All covariates were centred around subject means, and entered with a subject-specific fit. Global cerebral blood flow effects were removed by ANCOVA model allowing a subject-specific fit. The threshold for statistical significance for all analyses was set at $p<0.05$ after correction for multiple comparisons for either peak change in rCBF or the size of the activated cluster.

3.1.2.2 Functional connectivity analysis

The basic patterns of activation analysis above yielded two main areas of activation; activation in the left anterior cingulate gyrus in response to the opiate related stimulus compared to the neutral stimulus in all subjects and activation in the left orbito-frontal region was also shown to be correlated with subjective craving reported by the 8 (66%) subjects who craved. For each of these two regions, SPM99 was used to extract the 1st eigenvariate from all voxels within a radius of 10mm of the peak of activation for each scan. This is done in SPM99 by taking the matrix of data containing the time series data for all voxels within this 10mm sphere and subjecting them to singular value decomposition. The 1st eigenvariate is therefore a time-series of values derived from the singular value explaining most of the variance in the activated cluster from the first analysis.

The purpose of using an eigenvariate is to condense the data and remove some of the noise, while retaining the maximum possible of the underlying information. To aid

this noise reduction process still further, the time-series data subjected to this singular value decomposition was not the raw scan data itself, but time-series derived from the General Linear Model implemented in the original analysis. Specifically, the time-series data used was adjusted to remove the effects of no interest, in this case the global mean and time from scan start. At the end of this process this left two time-series eigenvariables for each of the 12 subjects, one from the anterior cingulate region and one from the orbito-frontal cortex. Figure 3.1 shows the 1st eigenvariate from the orbito-frontal cortex as an example time-series.

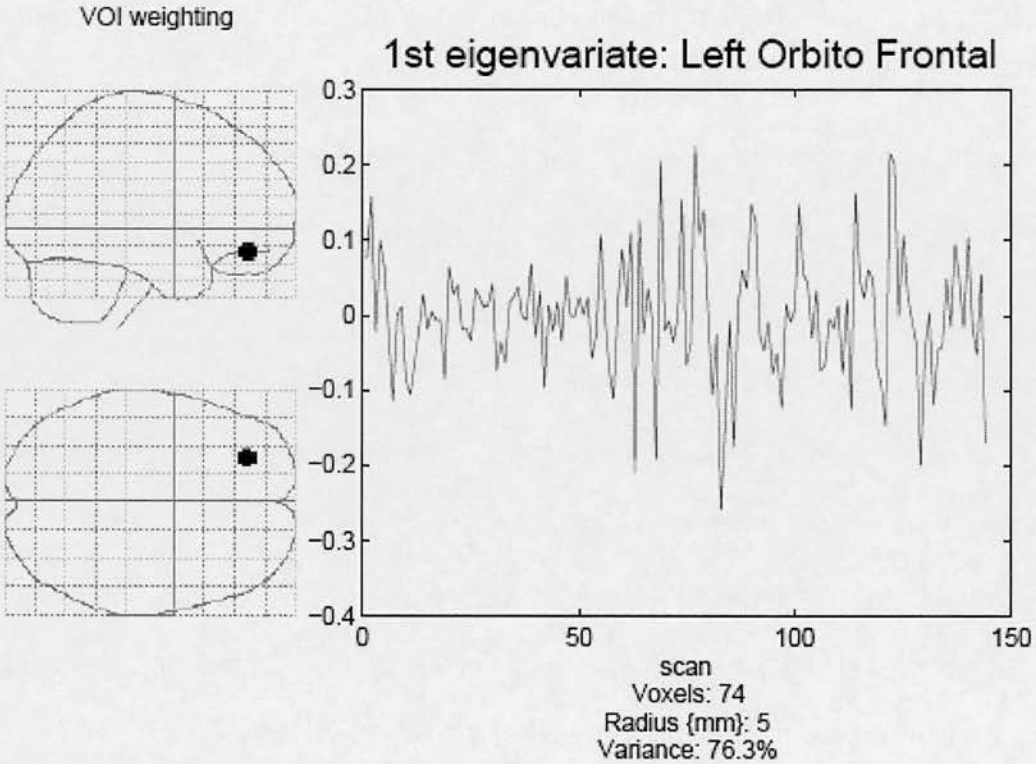

Figure 3.1: Graph of the 1st eigenvariate drawn from the left orbito-frontal cortex. As can be seen, this accounts for 76.3% of the variance within the sphere

These two variables were then entered into SPM99 analyses. In each case the covariate was centred around the subject mean and modelled with a covariate by subject interaction. As before, the time in minutes from the start of the scanning session and the global mean were entered into the model allowing a subject-specific fit.

For each eigenvariate, three separate analyses were performed; a simple association, an interaction with scan condition (neutral or drug related stimulus) and an interaction with subject group ("craver" of "non-craver"). Subject group was determined post-hoc by whether or not the subject demonstrated a craving response to the stimuli. In the first analysis the eigenvariate alone was entered into SPM99 as described above. This tests for brain regions where activity is functionally connected with the AC or OFC region.

In the next analyses two separate methods were used to test for brain regions where the scan condition or subject group modulated the correlation of activity with the covariate. This type of analysis has been termed a psycho-physiological interaction (Friston *et al.*, 1997). Firstly an interaction variable was calculated by multiplying the eigenvariate by 1 or –1 depending on the condition or group. This was entered into an SPM99 analysis along with the main variable of condition or group. In the second interactions method, the conditions or groups and the eigenvariate were entered into a combined analysis where the variable was centred around the condition or group mean and interactions tested for by contrasting the difference between the covariance of the brain activity between the two conditions.

The threshold for statistical significance for all analyses was set at $p<0.05$ after correction for multiple comparisons for either peak change in rCBF or the size of the activated cluster. In all cases the analysis uses 12 scans per subject with no differentiation made between intra- and inter- subject variance measures. As such, this is a fixed-effects analysis and consequently any statistical inference extends only as far as the subjects in this study.

3.2 Results

3.2.1 Circuits results

Two networks of neural activation related to the primary areas found from the previous analysis are shown in Figures 3.2 and 3.3. The first network (Figure 3.2) is of regions where rCBF is associated with activity in the left Anterior Cingulate (AC) region (Brodmann Area, BA 32). A positive association with middle temporal gyrus was found on the ipsilateral (left) side (-62, -8, -18mm, BA21, cluster $p=0.003$, voxel $p=0.003$). This was a consistent association across all 12 subjects. There was a consistent negative relationship between the AC and posterior visual areas (BA 18 right (28, -92, 8, cluster $p<0.001$, voxel $p=0.026$) & BA 19 bilateral (left -16, -86, 18, cluster $p<0.001$, voxel $p=0.014$) (right 28, -72, 34, cluster $p=0.032$, voxel $p=0.257$)). In BA 19 on both sides there was a significant modulation of the negative association with AC activity by the scan condition and BA 18 on the right side. Finally for this circuit there was a significant modulation of the association between the AC region

and left BA 3 (-34, -24, 36, cluster p=0.713, voxel p=0.043) depending on the presence or absence of a subjective craving response; i.e. an interaction with subject group.

The circuit associated with rCBF in the left orbito-frontal region (BA 11) is depicted in Figure 3.3. As with activity in the AC region there was a negative association between the OFC and posterior visual cortex bilaterally (BA 17/18 left (-14, -86,2 cluster p<0.001, voxel p=0.081) & BA 17 right (8, -80, 14, cluster p<0.001, voxel p=0.041)). A similar negative association was seen in right BA 37 (52, -60, 0, cluster p=0.02, voxel p<0.001).

There was a significant association between the left and right OFC (BA 11) only for those who craved in response to the drug-related stimulus (26, 48, -18, cluster p=0.230, voxel p=0.038). The same pattern was seen in the left parietal region BA 48 (-36, 20, -2, cluster p=0.002, voxel p=0.194). This region also showed a significant modulation of the association dependent on the subject group. For all subjects there was a positive association between activity in the left OFC (BA 11) and left posterior insular cortex (BA 41, -26, -38, 10, cluster p=0.006, voxel p<0.001).

The scan condition was shown to have a significant modulatory effect on the association between activity in the left OFC (BA 11) and two sub-cortical regions. Specifically, this result was seen in the brainstem – centred in the area of the red nucleus (0, -16, -8, cluster p=0.170, voxel p=0.025) and the left hippocampus (-20, -36, 4, cluster p=0.092, voxel p=0.034). In these two areas no main association with either the OFC activity or scan condition was observed. Figure 3.4 shows the

association between the left OFC and brainstem regions for each subject, in particular the change in slope between the craving and neutral conditions in the 12 subjects.

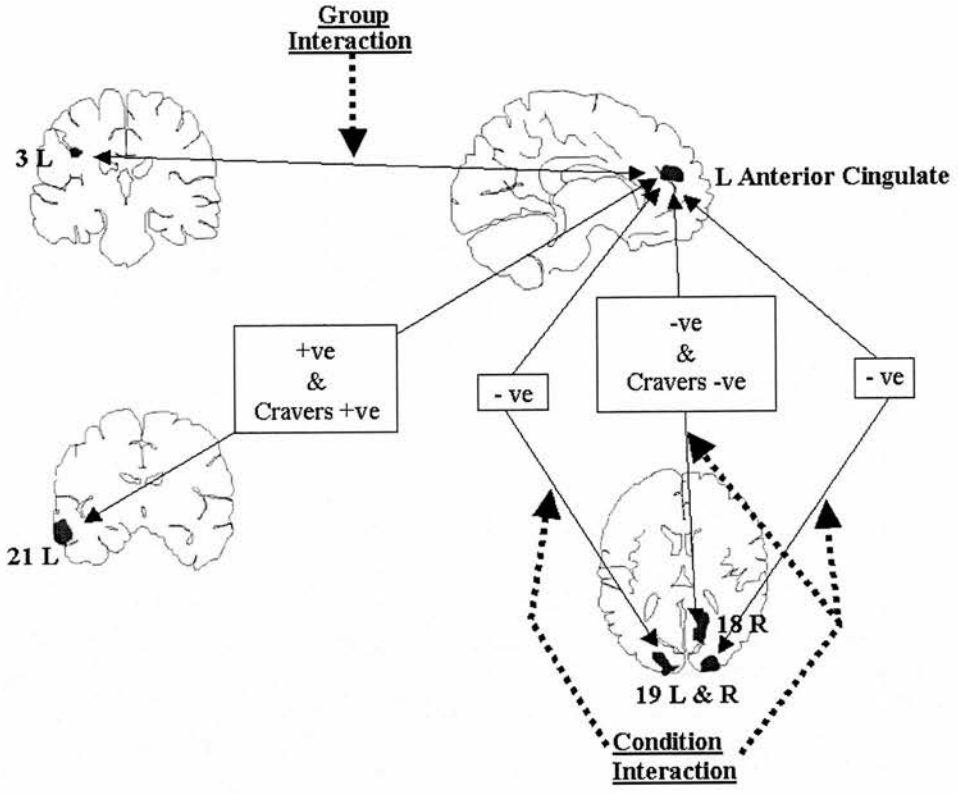

Figure 3.2Functional Connectivity of Left Anterior Cingulate Activation in Opiate Craving. Solid arrows represent main effect correlations in activation; the boxes describe the subjects groups showing the effect. Dotted arrows represent interactions between the correlation and either group or condition.

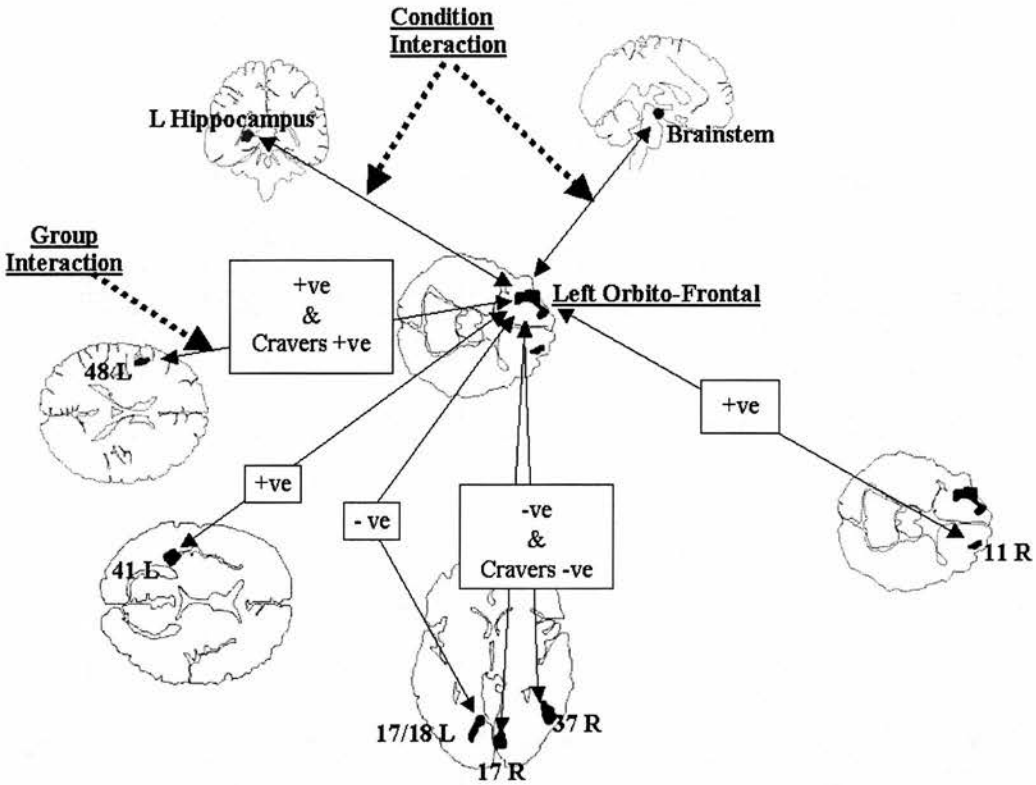

Figure 3.3 Functional Connectivity of Left Orbito-Frontal Cortex Activation in Opiate Craving. Solid arrows represent main effect correlations in activation; the boxes describe the subjects groups showing the effect. Dotted arrows represent interactions between the correlation and either group or condition.

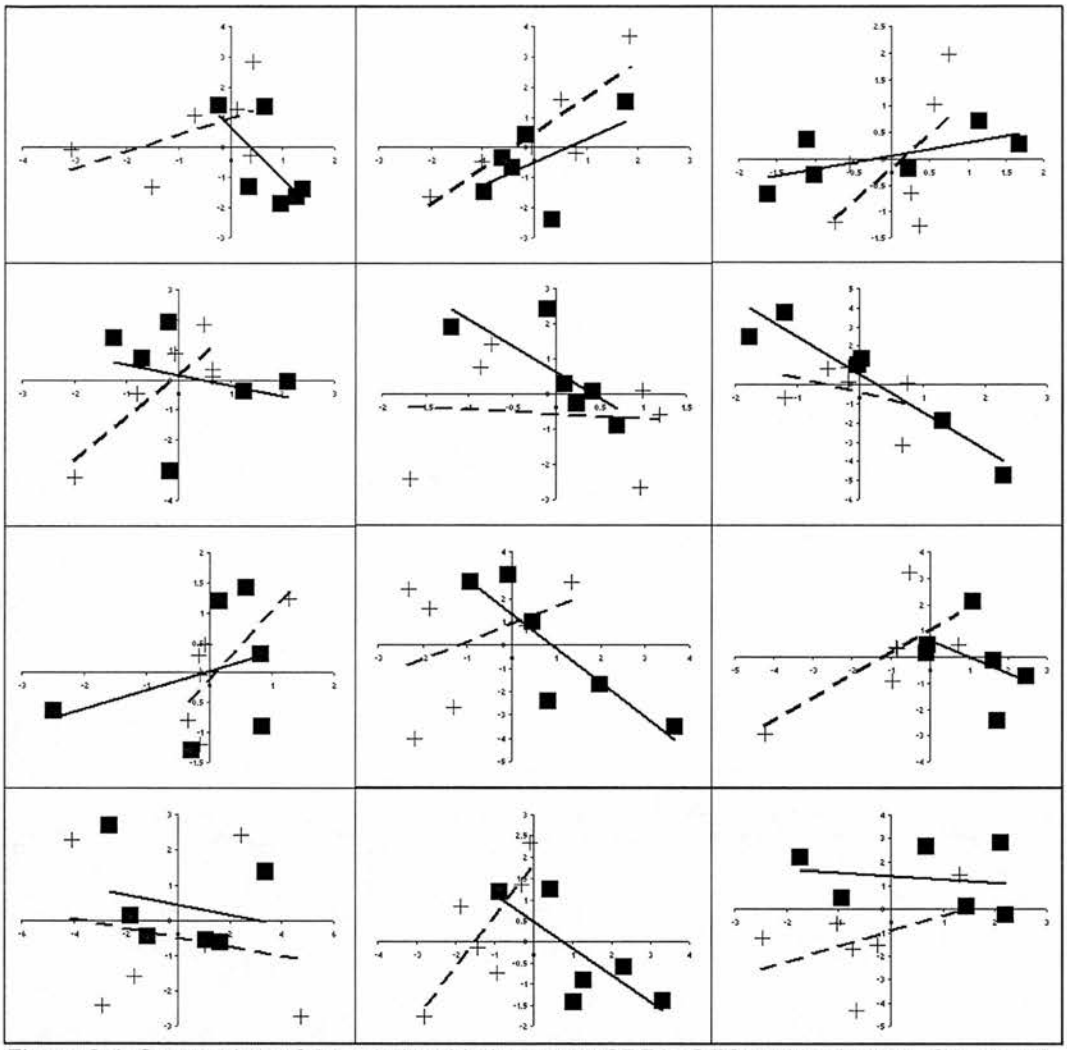

Figure 3.4: Scatterplots of the relationship between rCBF in OFC and brainstem. One panel per subject. Squares are "craving" scans and crosses are "neutral" scans

4 Measuring Dopamine Response with ^{11}C-Raclopride

4.1 Introduction

There are few good PET tracers. In the dopamine system the range available is bigger than many other systems. Almost the entire process of dopaminergic neurotransmission can be imaged with PET tracers:

Dopamine synthesis can be estimated from ^{18}F-DOPA (Barrio *et al.*, 1990). The dopamine re-uptake pump has been imaged with ^{11}C-RTI-121 (Hume *et al.*, 1996), ^{11}C-cocaine (Gatley *et al.*, 1994), ^{11}C-PE2I (Jucaite *et al.*, 2006) and ^{11}C-WIN-35,428 (Villemagne *et al.*, 1998). Post-synaptic dopamine-D_1 receptors ^{11}C-SCH-23390 (Maziere *et al.*, 1992), ^{11}C-NNC 756 (Karlsson *et al.*, 1993); dopamine-D_2 receptors with ^{11}C-Raclopride (Farde *et al.*, 1985), ^{11}C-(-)-NPA (Hwang *et al.*, 2000), ^{11}C-(+)-PHNO (Ginovart *et al.*, 2006) in striatum, ^{11}C-FLB 457 extra-striatal only (Halldin *et al.*, 1995); Dopamine-D_3 receptors with ^{18}F-fallypride (Mukherjee *et al.*, 1996).

At the time the studies for this thesis were undertaken the only tracers available to us were ^{18}F-DOPA and ^{11}C-Raclopride. We wished to investigate the release of dopamine in opioid addiction. ^{11}C-Raclopride was the obvious choice as a PET ligand for these studies as it had already been shown to be sensitive to release of endogenous dopamine by amphetamine (Carson *et al.*, 1997).

4.2 Characterisation of ^{11}C-Raclopride

Raclopride is a substituted benzamide from the same chemical family as the anti-psychotic drug sulpiride. It has been shown to be a selective competitive antagonist at the dopamine-D2 receptor. It has a high affinity and selectivity for Dopamine-D2 receptors, with a K_D of 1.2nM and low non-specific binding. Over 90% of the injected dose reaches the brain unmetabolised (Kohler *et al.*, 1985).

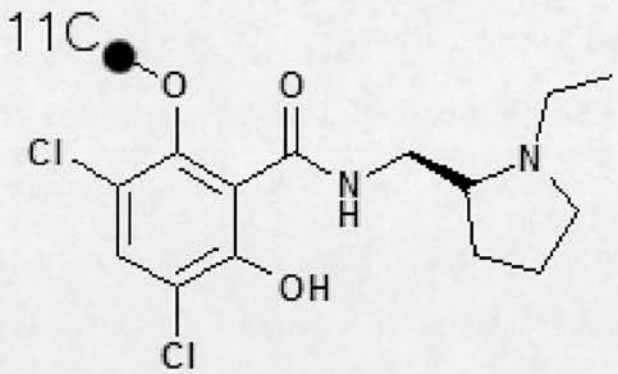

Figure 4.1: Chemical structure of ^{11}C-Raclopride showing the position of the ^{11}C isotope atom.

The standard method of modelling ^{11}C-Raclopride has become the simplified reference tissue model to yield a measure of Binding Potential (BP) (Gunn *et al.*, 1997). This is derived from earlier work comparing different methods of parameter estimation for modelling of ^{11}C-Raclopride (Lammertsma *et al.*, 1996).

4.2.1 Protocol

4.2.2 Image acquisition

4.2.2.1 Scanner characteristics

For all our ^{11}C-Raclopride studies, data was acquired on a brain dedicated CTI/Siemens EXACT3D (model 966) scanner. This was a prototype scanner developed by CTI, Knoxville Tennessee, USA with 6 detector rings as opposed to the usual 4 rings. Full specification is detailed elsewhere (Spinks *et al.*, 2000), but the main advantages of this scanner are increased sensitivity by a factor of 2.5 over the HR+ and enlarged axial field of view to 23.4 cm. This enables acquisition of whole brain images. Being able to obtain whole brain images is particularly useful for ^{11}C-Raclopride studies, as good visualisation of the cerebellum is needed for modelling of the tracer. Scanner efficiency is relatively high at 5.8%. The higher sensitivity and use of 3D mode increase the detection of scatter to about 42% of the total counts detected, requiring greater correction. Using the techniques of filtered back-projection with a ramp filter and standardised scatter correction, the in-plane resolution of the scanner is reported as 4.8mm FWHM at the centre of the field of view, increasing to 8.4mm FWHM.

4.2.2.2 Listmode acquisition

The full specification of listmode acquisition on the 966 PET camera is described in the same reference as the scanner specification above (Spinks *et al.*, 2000).

Listmode means that each pair of co-incident photons of radioactivity detected are recorded with a time-stamp and other data. This allows for later rebinning of the data into frames whose specification can be determined *post hoc*. The advantage of this being that the frame duration and start times can be determined following an examination of the total radioactivity counts in the data after scanning has finished. Previously, the frame definitions had to be determined in advance, which meant that if the tracer injection was late, or the time activity curves were not as expected then sampling frequency of the frames may not be optimal for modelling of the data. Using listmode the optimal frame definitions can be determined from the data.

Using a system known as Polaris® it is possible to also log the exact position of the subject's head at the time that photon was detected (Bloomfield *et al.*, 2003). This system uses fiducial markers fixed to a skullcap worn by the subject and tracked by laser. Subject to certain constraints it is therefore theoretically possible to correct for head movement before the data is even rebinned into sinograms, let alone reconstructed back into 3D images. At the time we began our PET scanning studies with ^{11}C-Raclopride, this system was not reliably implemented. We therefore decided not to use Polaris® motion correction on our data, despite it being acquired with listmode.

4.2.2.3 Experiment image acquisition protocol

Each scanning session began with the acquisition of a 5 minute transmission image using a standard rotating ^{137}Cs isotope source. Emission scans were then acquired

following a bolus injection of 120MBq ^{11}C-Raclopride over 30 seconds. Images were acquired for 90 minutes using listmode acquisition. The sinograms were created from the listmode data following rebinning into 26 frames starting with a variable duration background frame then short initial frames extending to 5 minutes toward the end of the scanning session [1*15sec, 1*5sec, 1*10sec, 1*30sec, 4*60sec, 17*300sec]. Images were reconstructed using filtered back projection with a ramp filter using the process whose general principles were described in Chapter 1. A matching pair of images was created for each scan, one with measured attenuation correction from a transmission image, and the second with no attenuation correction to be later used for correction of subject head movement.

4.2.3 Image analysis methodology

4.2.3.1 Motion correction

PET images using ligands that bind to specific targets, like receptors, routinely take 60-120 minutes to acquire. This time is required to allow some form of delineation of the tracer kinetics within the target tissue region as described in the section on modelling the tracer. This length of scanning brings with it the problem of movement. During scanning subjects are routinely restrained with a variety of different techniques. In some centres, subjects are fitted with a helmet which can then be strapped to the scanner bed, others use a fitted thermoplastic face mask to reduce head movement. Many techniques have been employed at Hammersmith Hospital, but experience has lead us to use a combination of foam pad and soft straps

over the forehead to restrict movement during the scan.

The main problem caused by head movement is blurring of the image. This is exactly the same as the blurring seen with ordinary photographs with long exposure times and moving objects. As the dynamic PET images are acquired as a series of frames movement can be separated into movement within a frame and movement between frames.

Movement within a frame will cause that frame to be blurred. If that frame has been acquired as a single frame, then that blurring is essentially permanent. If the frame has been acquired by rebinning of data acquired in listmode, then it is theoretically reducible as described above. In fact, in listmode the distinction between within-frame and between-frame movement does not apply, as all data can be motion corrected before the data is rebinned into frames.

Aside from blurring of the image, head movement will also cause a mismatch between the dynamic emission scan and the transmission scan that precedes it. The transmission image is acquired by rotating a standard radioactive source around the object to be scanned. In effect this creates a low resolution CT scan of the head. This image is used to derive the parameters for attenuation correction on the emission image. Therefore, if the transmission and emission scans are out of alignment, then the correction applied to the emission scan will be incorrect. This has particularly noticeable effects in regions where tissues with different attenuation characteristics are in close proximity, for example, inferior orbito-frontal cortex (Brett *et al.*, 1999). In the case of ^{11}C-Raclopride this is a negligible effect as all of

the important signal comes from the basal ganglia. In these areas tissue attenuation is relatively homogeneous.

4.2.3.2 Correction of between-frame movement

If data have been acquired directly into sinograms and frames, or rebinned into frames from listmode without Polaris® motion correction, then between-frame motion correction is the only possibility. Correction for head movement begins with the prerequisite step of quantifying the extent of movement. As has been alluded to above, it is possible to track the movement of the head using an external system. The coordinates and parameters of this movement can then be applied to the brain image data. However, as we were not using the Polaris® system, this was not possible with our data set. We therefore had to use the information contained in the image data itself to derive the movement parameters. Techniques for this kind of motion correction had been described for $H_2{}^{15}O$-PET and fMRI for some time (e.g. Friston *et al.*, 1989). The extension of the use of these techniques into ligand-PET was just beginning to be used and described as our studies were under way.

In the case of $H_2{}^{15}O$-PET and fMRI each image in a dataset has a very similar overall structure and contrast. In ligand PET this is not always the case. Particularly in the case of tracers, like ^{11}C-Raclopride, where the specific binding is highly localised to a small region, the distribution of signal within the image will dramatically change as the scan progresses (see Figure 4.2). In this case it is very likely that the realignment algorithm will incorrectly attribute changes in tracer distribution as movement

(Dagher *et al.*, 1998). Therefore correction for this false movement will increase the misalignment between frames instead of reducing it.

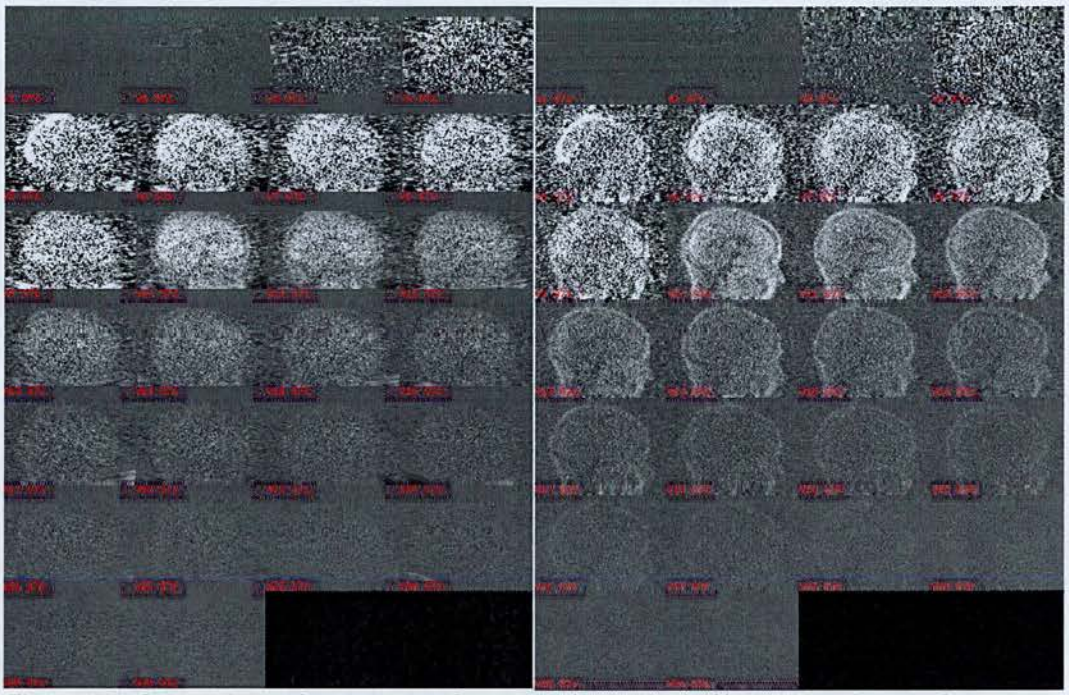

Figure 4.2: Comparison of Attenuation Corrected (Pane A - Left) and Non-Attenuation-Corrected (Pane B - Right) Sagital Sections of every time frame in an exemplar scan. Note the increased anatomical information on the right and the dramatic changes in tracer distribution through the scan.

Three main techniques have been employed for dealing with movement within ^{11}C-Raclopride, aside from the early years, where it was simply ignored. The easiest technique is to remove subjects who moved too much from subsequent inclusion in the analysis. This technique may certainly be appropriate in cases where there is sufficient remaining data to maintain statistical power and where the exclusion rate is approximately equal between any groups or conditions being studied. This raises the common problem of movement that is correlated with either the task or condition

being studied, or associated with any diagnosis under examination.

The two, more involved, techniques for motion correction are either to use an idealized PET image as a template for realignment or to use images with greater structural information and less tracer redistribution, for example images that have not been corrected for attenuation (see Figure 4.2 above, pane B). The technique of using an idealised PET image has been largely proposed by the Brain Imaging Centre at the Montreal Neurological Institute, Canada (Zald *et al.*, 2004). In this technique, an MRI image is obtained for each subject. This image is then divided into specific tissue types. For each tissue type an idealised time-activity curve is calculated. This is then combined with the MRI image to produce an 4D image which is effectively an idealised PET image, where the various tissue types have ideal time-activity curves. The 4D PET image can then be realigned on a frame-by-frame basis to the matching frame in the idealised PET image. In this way, each frame of the dynamic 4D PET image should end up in the same space as the MRI image and, by extension, in the same space as each other. The main drawback to this technique is that the boundaries of tissue with different binding profiles for the tracer are not always easily determined in a structural image. This can lead to inaccurate realignment of the PET images at different stages of the scan session. In particular, differences in the realignment between frames will worsen any motion effects or introduce artefactual correction for non-existent motion. We, however, have developed the technique of using non-attenuation corrected images.

4.2.3.3 Use of non-attenuation corrected images

Initially dynamic PET images are reconstructed to 4-dimensional images. The software for realigning images was originally developed to realign a time series of images. Therefore, before processing the 4D images were separated into a series of 3D images, with one image per frame. This was achieved using standard brain image software, MRIcro (http://www.mricro.com). Previously, where this had been attempted at all, motion correction of ^{11}C-Raclopride images at the MRC Cyclotron Unit, Hammersmith Hospital, had used "mpr" software. This uses a standardised method for image co-registration called mutual information. Unfortunately, in "mpr" the algorithms are implemented in 2D only. This means that movement within an axial plane (i.e. left to right, or anterior to posterior, or roll) can be measured, but movement between planes, or pitch and yaw, cannot be corrected.

To overcome this problem, I used the SPM2 (Wellcome Dept. Cognitive Neurology) software package implemented in Matlab® (The Mathworks). The realignment algorithms have been shown to be very effective at detecting and correcting movement in a time series of water-PET or fMRI scans. SPM2 also detects and corrects motion in 3 planes, as well as rotations about all 3 axes. The difficulty was that SPM2 is written to apply the motion correction only to the images from which the movement parameters were derived. SPM2, like its predecessor SPM99, uses a system of files for storing image information. The images themselves are stored in a standard format known as Analyze® 7.5 (AnalyzeDirect.com) that is commonly used for medical images. This format defines a binary image file containing the matrix of

data, combined with a header file which describes the format of the binary file and contains many parameters concerning the image. For example, the header file contains information on the image orientation, voxel sizes, date of the scan and any scaling factors required. In addition to these 2 files, SPM2 adds a third file which contains a matrix defining the translation from voxel-space (measured in voxels within the image) to world-space (measured in millimetres from a standard reference point, where the anterior commissure crosses the midline by convention).

I then realised that SPM2 could be used to realign the non-attenuation corrected image frames to correct for movement. The translations required for this correction were then stored in the associated data files. These files could then be renamed to match the files containing the attenuation-corrected images. Once that procedure had been established it made it possible to begin optimising the process for detecting and correcting movement.

The obvious starting point was to include all time frames in the process. The realignment module of SPM2 runs as a two stage process. The first process is to realign all images to the space defined by the first image specified. All these realigned images are then averaged to produce a mean image. In the second pass, all images are then realigned to the space defined by the mean image. Obviously, the mean image will be in the same space as the first image in the sequence due to the effects of the first pass of the process. Once all the images have been realigned to the mean image the distance and direction of movements and rotations are displayed.

When all time frames were included in the process it very quickly became clear, from

the display of movement parameters, that there was an apparent large movement in every scan between frames one to four. This is illustrated in Figure 4.3 pane A. Often the calculated movements were so large that they would have required the subject to have moved outside of the scanner field of view, or to hover 2cm above the scanner bed (e.g. pane B). Clearly, these detected movement parameters were not physically possible, and therefore must be incorrect and an artefact. This is a concrete example of the risks outlined by Dagher *et al.* (1998)

Visual inspection of the images (see Figure 4.2 top row in both panes) showed that the tracer distribution in the early frames was markedly different from the rest of the frames. This is not surprising as the first frame in the dynamic image is always a variable duration background frame. This means that the frame only contains background radiation levels and ends when the tracer is injected. It therefore cannot contain any tracer signal or brain image to which subsequent images can be aligned. The next three frames are all of very short duration – 30 seconds – and contain few counts as the tracer is only just starting to be delivered to the brain. I therefore, sequentially removed these early frames from the realignment process until the movement parameters stabilised. This is illustrated in Figure 4.3 panes A-E. It can be seen that this stabilisation occurred once frames 1-4 were removed from the process.

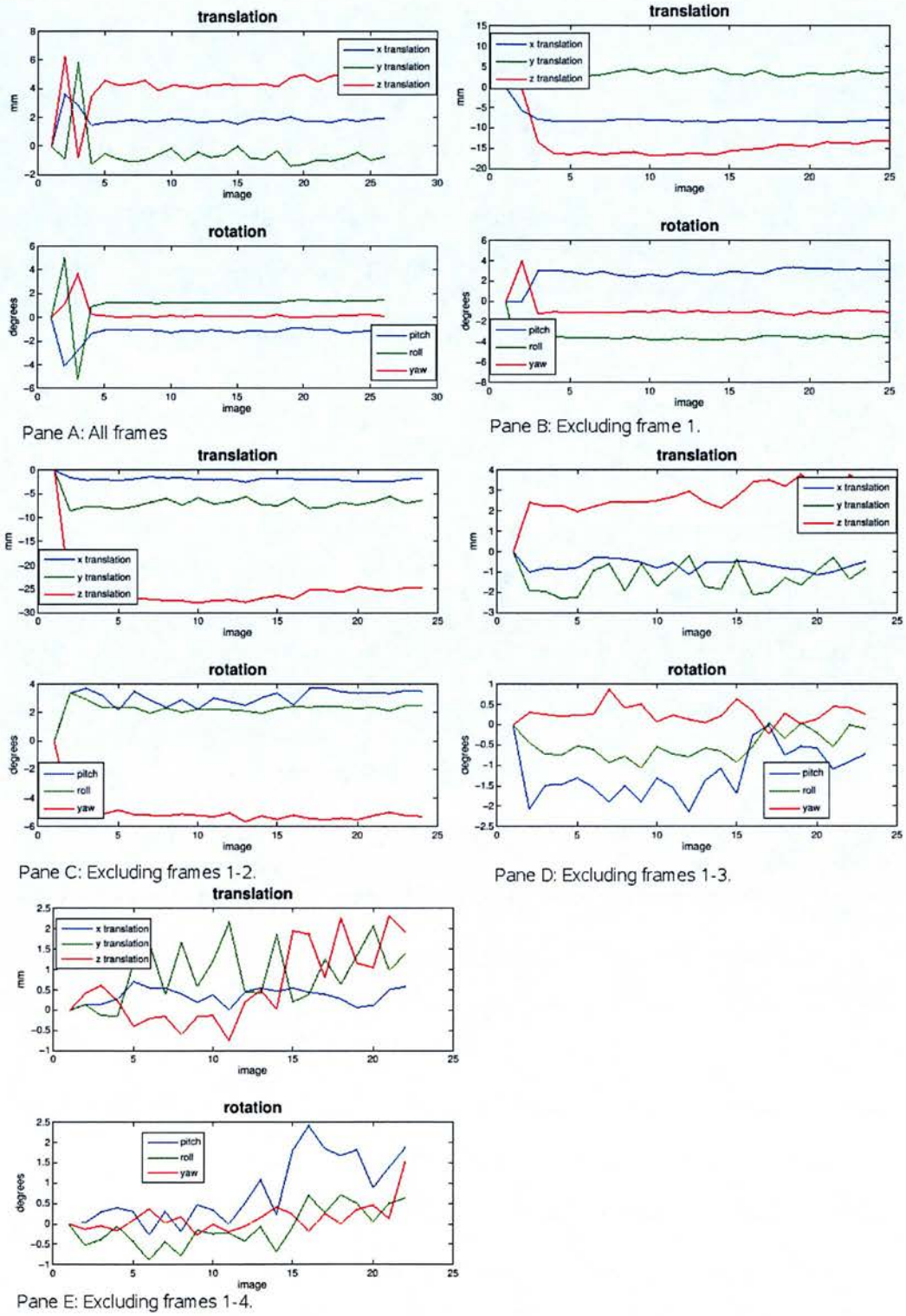

Figure 4.3: Estimation of movement parameters for exemplar scan excluding successive early frames.

Excluding frames 1-4 from the realignment is unlikely to detrimentally affect the correction for movement. Frame 1 is background only and frames 2-4 are a total of 30 seconds duration together, which means only 30 seconds remains uncorrected for movement. This is a very small proportion of a scan lasting 90 minutes. It is also not unreasonable to assume that the majority of head movement will occur in the later part of the scans as subjects become less comfortable over time.

Once the movement parameters have been determined and saved in the associated files, they are then copied to be applied to the attenuation-corrected images. Like the non-attenuation corrected images, these dynamic 4D images have been separated into a series of 3D image volumes. These movement parameters then have to be incorporated into the 3D images to perform the correction of motion. This is accomplished within SPM2 again, using the reslice routines. During the reslice procedure the user is required to chose a resampling method. Resampling of the image is required because the translations and rotations require movement of the image by a non-integer number of voxels. The intensity of the image is only defined at the resolution of the image voxel sizes. Therefore data needs to be interpolated to represent the intensity of a given voxel after movement from the surrounding voxels.

There are several algorithms that can be used for this interpolation. In general the trade-off between methods is one of speed against accuracy. The quickest and easiest

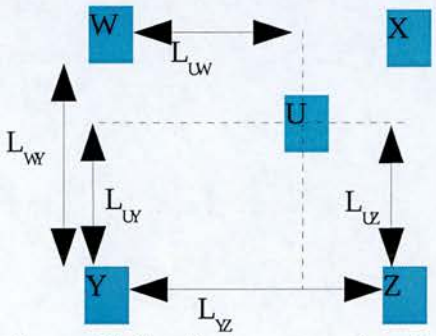

Figure 4.4: Graphical representation of bilinear interpolation

interpolation method is simply to substitute the intensity value from the nearest known value. This simply requires working out which voxel in the original image is closest to the position of the new voxel whose value requires to be established from interpolation. The distance from any new interpolated voxel to the surrounding voxels can easily be determined using Pythagoras theorem in 3 dimensions.

As computing power has increased the ability to use more computationally intensive interpolation algorithms has also increased. The next methods up the scale of computation load are bilinear and then trilinear interpolation. The bilinear method is shown graphically in Figure 4.4 and the equation is presented in Equation 1. The trilinear method is simply an extension of the bilinear method into 3 dimensions. Unfortunately, although computationally straightforward, this algorithm results in some loss of higher frequency information (Ashburner & Friston, 2003). It is also susceptible to local noise in the image as it relies on a relatively small number of voxels (only 8 in 3 dimensions) to derive the intensity value for the interpolated voxel. As a result, and with the benefit of increased computing power, more complex and accurate techniques have been developed.

$$U = \left(Y * \frac{L_{UW}}{L_{WY}} + W * \frac{L_{UY}}{L_{WY}} \right) * \frac{L_{UX}}{L_{YZ}} + \left(X * \frac{L_{UZ}}{L_{XZ}} + Z * \frac{L_{UX}}{L_{XZ}} \right) * \frac{L_{UW}}{L_{YZ}}$$

Equation 1: Bilinear interpolation - The value of the Unknown voxel "U" where W,X,Y and Z are the intensity values for the nearest voxels in each direction. LWY is the length of the line from W to Y. In words this equates to the sum of each nearby voxel weighted by its distance from U.

With increased computer power the standard interpolation algorithm used for PET

data has now become windowed-sinc (Ashburner & Friston, 2003). The main advantage of this algorithm is that it no longer relies on a single voxel in any given direction to derive the interpolated data; this, of course, makes the algorithm less likely to propagate spikes of noise within the image. Sinc interpolation uses all of the voxels within the entire image to generate the value of the interpolated voxel. This would be both computationally expensive and more complex than necessary. To reduce the computational load to manageable levels, the volume of included voxels is constrained to a set 3 dimensional window. Each voxel is again weighted by its distance from the target voxel to be derived. The formula for doing this in each dimension is shown in Equation 2. The window is applied to this formula by restricting I to include only voxels where d_i is less than a specified distance.

$$U=\sum_{i=1}^{I} v_i \frac{\frac{\sin(\pi d_i)}{\pi d_i}\frac{1}{2}(1+\cos(2\pi d_i / I))}{\sum_{j=1}^{I}\frac{\sin(\pi d_j)}{\pi d_j}\frac{1}{2}(1+\cos(2\pi d_j / I))}$$

Equation 2: Sinc interpolation - The value of the Unknown voxel U, where vi is the value of the ith voxel and di is the distance from U to the ith voxel

For image modalities with greater spatial resolution, such as fMRI, even windowed-sinc is usually considered too coarse. For these situations the interpolation is carried out using Fourier methods. In these cases the data are transformed before the interpolation is carried out, then the reverse transform is applied to restore the image. As this is not generally applied to PET data, and has not been used in these studies, I will not describe these methods here, but would direct the reader to the SPM2 reference (Ashburner & Friston, 2003).

In common with all data-derived procedures, proper validation of this procedure for motion correction would require knowledge of the true magnitude and direction of the subject head movement during the scan. Unfortunately, this is an unknown quantity. Therefore an alternative estimate of the utility of motion correction had to be found. The purpose of motion correction is to decrease the noise in the measures of radioactivity in the tissues of interest. An index of the level of noise can be estimated from the time activity curves of the regions of interest in the brain. In an ideal situation the time activity curves for the brain regions of interest would be smooth and noise free. Where there has been a sharp movement of the head the change in the region of the brain sampled in a set location will cause a step change in the time activity curve. Ideally motion correction should reduce any such steps in the curve. This can be inspected visually, but is difficult to quantify.

In order to sample the regions of interest in the brain for validating the motion correction an unbiased automated procedure for defining and delineating these regions had to be developed. This procedure will be described below in this chapter. At this point it is simply necessary to state that an automated procedure was used to sample the 7 regions of the brain that are of interest in ^{11}C-Raclopride scans, namely: putamen, caudate and ventral striatum bilaterally and the grey matter of the cerebellar cortex.

Using these defined regions each subject's dynamic ^{11}C-Raclopride images were sampled to yield mean and standard deviation of values of radioactivity in the region for each time frame for each scan. This was done for each scan both before and after

motion correction had been applied. An example of the derived data is shown in Figure 4.9.

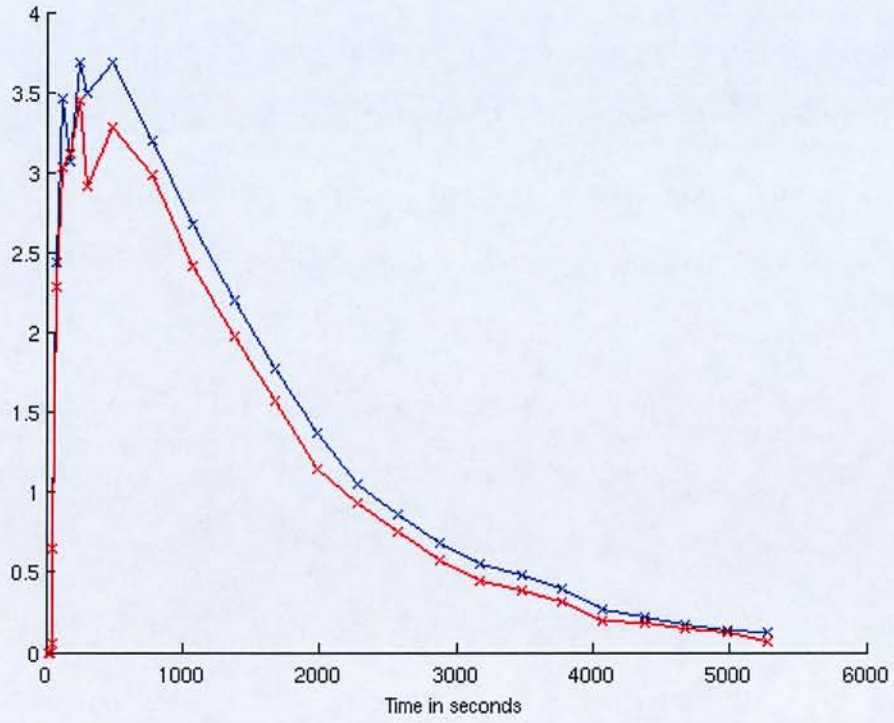

Figure 4.5: Plot of mean activity in left caudate from an example image demonstrating the effect of motion correction on time activity curves. (Raw data in RED, realigned data in BLUE.)

I attempted to use the "string length" of the curve as a measurement of the size and number of such step changes in the curve. In order to do this I wrote a small Matlab script to take the time activity curve and calculate the string length. As can be seen from Figure 4.5, the string length is given by the simple equation in Equation 3(1).

$$\text{string length} = \sum_{t=1}^{scanend} \sqrt{\Delta t^2 + \Delta a^2} \qquad (1)$$

$$\text{string length} = \sum_{t=1}^{scanend} \sqrt{\Delta (t/1000)^2 + \Delta a^2} \qquad (2)$$

Where: Δt is the change in time and Δa is the change in activity over that time.

Equation 3: Calculation of string length using Pythagoras theorem.

The initial values obtained for the string length were in the order of five to six thousand, but the differences between string lengths for different regions or between scans were in the order of 0.1 to 0.9. I realised this was because the scan duration was effectively a constant, but also very large in comparison to the activity values. I therefore scaled the time index as shown in Equation 3(2). This modification yielded values of around ten, but preserved the level of variability at 0.1 to 0.9. However, examining the results it became clear that this was not a good measure of the effectiveness of motion correction. As the steps in the time activity curve were removed this did indeed reduce the string length but this was variably offset by the effect seen in Figure 4.9 of higher peak values for activity which increased the Δa component of the function. This meant that the string length could go up or down for any given curve after motion correction depending on the balance of these two opposing effects. More importantly, it was not a clear good measure of the "quality" of the time-activity data.

I therefore considered the problem from a different angle. If the motion correction is working then the VOI definitions should be more accurately sampling the tissues desired. Therefore the voxels within the VOIs should be more homogeneous. This increased homogeneity should be reflected in a lower standard deviation of the

voxels within the VOI. Sampling the VOIs as described above yields a standard deviation as well as a mean value. This gives a standard deviation for each frame within the dynamic image. These standard deviations could be plotted against time in an analogous manner to the mean activity as shown in Figure 4.9, but some form of summary measure incorporating the entire scan was more useful. A simple mean standard deviation was unlikely to be a good measure as it would be overly influenced by early frames that have high count levels and relatively large variability due to the short frame length. I needed to derive some form of weighted mean of the VOI standard deviations for the whole scan. There was already an established technique for weighting in use at the MRC Cyclotron Unit. The weight for each frame is derived from the frame duration, the number of true counts in the frame and total number of frames in the image as given in Equation 4.

$$\text{The weight for the } i\text{th frame } W(i) = N \frac{length(i)/truerate(i)}{\sum_{j=1}^{N} length(j)/truerate(j)}$$

Where: length(i) is the length of the ith frame, N is the number of frames and truerate(i) is the rate of true counts (not random counts) per second during the ith frame.

Equation 4: Formula for calculating frame weightings

The weighted mean of the standard deviations is then easily calculated as the mean of the standard deviations multiplied by their respective weighting factors then divided by the number of frames. The effect of the motion correction is shown in Table 4.1. Testing whether this was a significant improvement in the data required the selection of an appropriate statistical test for this data. Clearly the data are paired as each scan has values before and after motion correction. It is possible to calculate

paired student's t-tests for each VOI, but then the question of correction for multiple comparisons arises. The obvious Bonferoni correction would be overly conservative given that the data are clearly highly correlated. I therefore calculated a Hotelling's t-squared multivariate statistic for the dataset as a whole ($T2 = 745.6$, $F=88.3$, $p<0.0001$) showing that the differences are significant overall. Individual paired student's t-tests for the separate VOIs showed that they were all significant $p<0.0001$ uncorrected. Therefore, they would remain significant at the $p<0.05$ level even after a full Bonferoni correction.

When analysing this data I decided to treat the scans as independent events even though the majority of subjects had two scans. The reason for this is that the between and within subject variances in PET data are roughly equivalent and that the effects of motion correction should be independent of the subject. This will have increased the power of the statistical test by increasing the degrees of freedom, but could be argued to decrease the generalisability of the results.

		Raw (mean VOI stdev ± stdev)	Realigned (mean VOI stdev ± stdev)	%difference (95% CI)
Caudate	left	0.299±0.037	0.277±0.036	7.3 (6.6 - 8.0)
	right	0.300±0.036	0.278±0.033	7.4 (6.5 - 8.2)
Putamen	left	0.313±0.038	0.293±0.036	6.2 (5.5 - 6.9)
	right	0.310±0.037	0.292±0.032	5.8 (4.5 - 7.1)
Ventral striatum	left	0.298±0.034	0.278±0.028	6.4 (5.3 - 7.6)
	right	0.298±0.037	0.280±0.030	6.0 (4.9 - 7.1)
Cerebellum		0.219±0.023	0.203±0.020	7.0 (6.2 - 7.8)

Table 4.1: Effect of motion correction on weighted means of the VOI standard deviations.

This reduction in VOI heterogeneity combined with visual inspection of the raw and

realigned TACs gives a reasonable level of evidence that the motion correction procedures reduce the noise introduced into the data by movement.

Interpolation of the data during reslicing of the images will necessarily result in a degree of smoothing of the image. For trilinear interpolation the level of smoothing will be dependent on the original "noisiness" of the image and on the closeness of the movement to a multiple of the voxel dimensions. In other words this can explained as the amount of smoothing will be at its least if the movement is exactly a multiple of the voxel dimensions as no interpolation will be required. Conversely, the interpolation will be maximal when the translation is exactly "n" and a half voxels, where "n" is any integer. When windowed-sinc interpolation is used, the level of smoothing is a constant, irrespective of the magnitude of the movement. The presence of this smoothing secondary to interpolation is the rationale for deciding whether or not to motion correct all images or just those with evidence of movement. Some colleagues have argued that it is better to leave as much data as possible in its original raw state (personal communication), however, I take the view that all data need to be processed in the same way to avoid a potential bias. This is particularly the case where the amount of movement may be correlated with the effect of interest. In our studies we have often been studying the effect of stimuli that could easily be argued to cause potential movement; for example we have presented drug related stimuli to abstinent ex-users or injected doses of opioid agonist. Therefore it was decided to apply motion correction to all our ^{11}C-Raclopride data.

4.2.3.4 Automation of VOI sampling methods

There are already published criteria for defining the main regions in the basal ganglia where ^{11}C-Raclopride is specifically bound (Mawlawi *et al.*, 2001). However, simply drawing these regions on each frame of each image would be both prohibitively time consuming and sensitive to bias or inaccuracies. This required the development, in parallel with development of the above motion correction, of a technique for automated delineation of brain volumes of interest (VOIs). The first step was to delineate the important regions on a template image derived from the ICBM dataset (Evans *et al.*, 1993). We used the template from the SPM2 software derived from a normal dataset of T1-weighted MRI images transformed into the standard space of the ICBM template. Using the published criteria (Mawlawi *et al.*, 2001) we outlined the putamen, caudate and ventral striatum on the template image (see Figure 4.6). In addition we outlined the grey matter of the cerebellar cortex (see Figure 4.7).

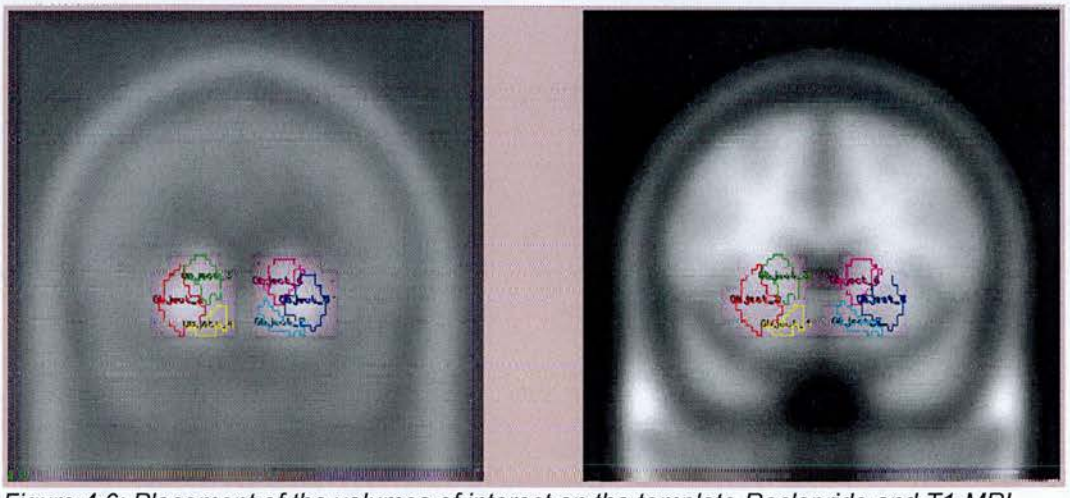

Figure 4.6: Placement of the volumes of interest on the template Raclopride and T1-MRI images. (Putamen - red and dark blue; caudate - green and pink; ventral striatum - yellow and cyan).

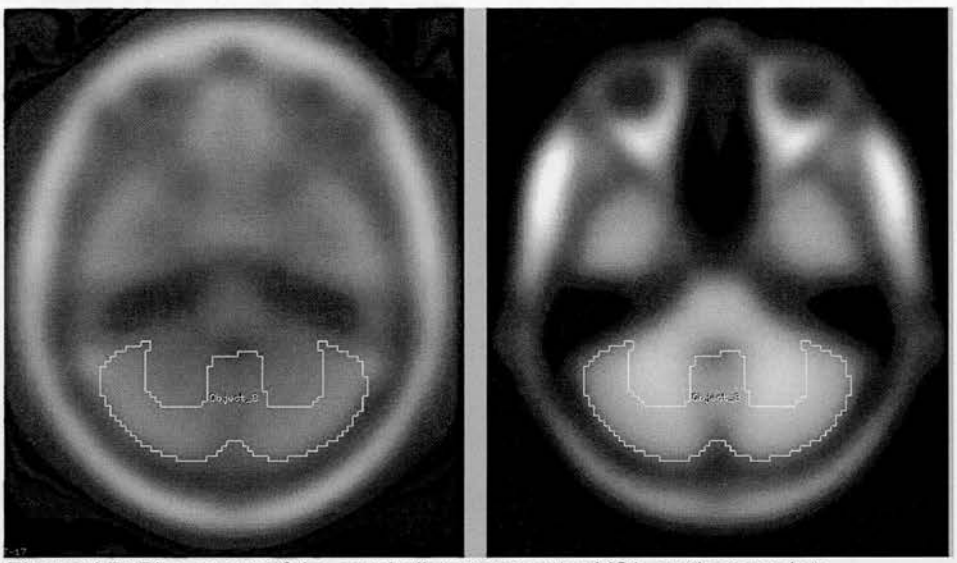

Figure 4.7: Placement of the cerebellar grey matter VOI on the template Raclopride and T1-MRI images.

It was then necessary to find a way of transferring the VOI definitions onto the brain image for each subject. SPM2 provides a "normalization" function (Ashburner & Friston, 1999) which is used to warp subjects' images into the standard stereotactic space defined by the ICBM template. In order to do this it requires an image from the subject with good anatomical information and a matching template image. This can be done is several different ways. If each subject has both a PET image and a good resolution structural MRI image then the commonest method is to co-register the PET and MRI image for the subject, so that they are in the same space. As we are dealing with the same underlying structure, i.e. the same brain produced both images, this is a rigid body transformation. SPM2 provides a routine for doing this co-registration step (Ashburner & Friston, 1997).

Co-registration between images from different modalities is not as straightforward as registration of images in the same modality. Images of the same brain in the same

modality would be expected to have peaks and troughs of intensity levels in the same anatomical locations. This is not the case for images from different modalities. As can be seen in Figures 4.6 & 4.7, the pattern of high and low intensity voxels in T1-weighted MRI images and ^{11}C-Raclopride images is very different. In a T1 image the peak intensities are in white matter, with grey matter being somewhere between white matter and cerebro-spinal fluid in intensity. In a ^{11}C-Raclopride PET image the peak intensity is in the striatum, with little else in the rest of the brain. This means that co-registering the images is not as simple as just minimising the difference between them.

The algorithms within SPM2 used for inter-modality image co-registration are based on three different techniques, Mutual Information, Joint Entropy and Normalised Mutual Information. The latter, normalised mutual information, has been shown to produce the most robust co-registration between MRI and PET data, especially where there is a large field of view as we get from our PET scanner (Studholme *et al.*, 1999). The technique of mutual information co-registration is derived from communications and information theory. Such algorithms were originally developed to measure the quality of a signal transmitted and received. Put simply, a complex image will contain a large amount of information, whereas a blank picture will contain very little information. Similarly, entropy can be thought of as the converse of complexity. In this context it can be considered as a measure of the uniformity of an image; again illustrated by a grey image having greater entropy than a black & white checker-board.

If the information contained within an image is represented as a set then the Venn diagram in Figure 4.8 can be used to illustrate the various mathematical techniques for solving the problem of inter-modal image co-registration. In the case of Mutual Information the images are moved such as to maximize the Mutual Information – i.e. the green area. In the case of Joint Entropy techniques the algorithms seek to minimize the Joint Entropy – i.e. the orange area. In the examples below it can be seen how such techniques would maximise the overlap between the images, i.e. find the best co-registration. Unfortunately the images are not always as well behaved as the Venn diagrams. Often there will be one image that contains a field of view covering less than the whole brain. It is also common for the image to contain a large area of non-brain within the field of view. This has been shown to reduce the chance of these algorithms finding the genuine best solution to the problem (Studholme *et al.*, 1999). The same authors show that "normalising" the search for the minimum joint entropy by incorporating information on the marginal entropies yields an algorithm that is more robust to both these conditions and to the condition of poor starting estimates for the required translation.

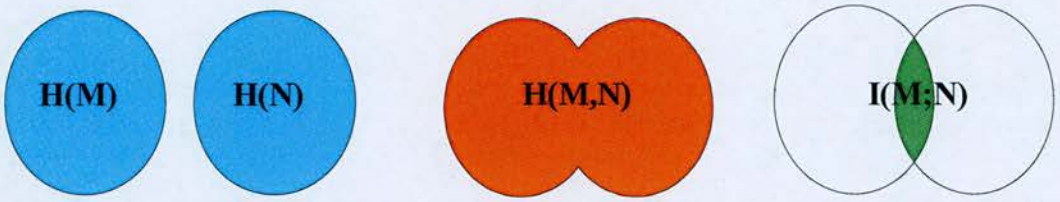

Marginal Entropy (blue) = $H(M) + H(N)$
Joint Entropy (orange) = $H(M, N)$
Mutual Information (green) = $I(M; N) = H(M) + H(N) - H(M, N)$
Normalised Mutual Information = $Y(M; N) = \frac{H(M) + H(N)}{H(M, N)}$

Figure 4.8: Venn diagram illustrating set theory representation of Mutual Information and Joint Entropy

Once the PET and MRI images are in the same space it is then possible to "normalise" the structural image to a matching structural template provided by SPM2. The warping parameters derived for the MRI image can then be applied to the PET image.

However, in our case we did not have good quality structural MRI scans available for all subjects. We had acquired standard T1 structural MRI brain images on every subject using the clinical scanner at the local hospital in Bristol. Unfortunately there was a long delay of 2 years in obtaining the required computer access to retrieve the raw data from the clinical scanner. It was only at this point that it became apparent that the images contained insufficient contrast to permit analysis. The images produced contained only approximately 100 distinct shades of grey; this is plenty for printing on X-ray film and for clinical use. The image analysis algorithms require a minimum of 256 intensity levels for analysis. We were able to rapidly develop a enhanced acquisition protocol once we had access to the raw image data, but not in

sufficient time to permit re-scanning of the early subjects in the study. We were therefore unable to use an identical MRI-based analysis for all subjects.

This meant that the ideal solution was to "normalise" the subjects' PET images directly to a matching PET template image. This approach would require PET images with good anatomical information and the creation of a matching template image. The images available with the most anatomical information were the weighted mean images from the non-attenuation corrected images used in the movement correction procedure above. What was therefore required was to create a matching template image in standard space.

4.2.3.4.1 Creating a template ^{11}C-Raclopride image

We had good quality MRI images for several of the later subjects used in our experiments. It was therefore possible to use these subjects in a bootstrap procedure to begin the creation of the template. For each subject with a good quality MRI, the MRI image was co-registered to the mean non-attenuation corrected image using SPM2 co-registration routines. The MRI images were then used to derive normalisation parameters for each of these subjects. The parameters were then applied to the PET images. This yielded a collection of PET images in a close approximation of standardised space. I visually inspected all images at every step of this process to ensure that the co-registration and normalisation had succeeded. The next step was to produce a first-pass ^{11}C-Raclopride template image. This requires the production of a "soft mean". In words, a soft mean equates to the sum of data in

a given voxel over all images, divided by the number of images with data in that voxel. This can be easily produced using the image calculation facility in SPM2 and Equation 5.

$$'softmean' = \frac{(I_1 + I_2 + \ldots + I_n)}{(eps + (I_1 != 0) + (I_2 != 0) + \ldots + (I_n != 0))}$$

Where I_n is the value in the nth image and '!=' means 'not equal'. The eps term is the smallest possible non-zero number, inserted to prevent 'division by zero' errors in voxels where there is no data in any image.

Equation 5: Calculation of a "soft mean".

This soft mean image was then smoothed with a Gaussian kernel of 6mm at Full-Width-Half-Maximum. This smoothing has been shown to improve the registration of images to a template by better allowing for anatomical differences between individuals (Ashburner & Friston, 1999).

It would be possible to use this "first-pass" mean image as a template, but the fear is that normalisation parameters would be more accurate for those subjects whose images contributed to the template image than for the others. This could potentially cause a bias in the outcome. To overcome this problem I put the data through a "second-pass" of template creation. In this phase I took the first-pass template and normalised all subjects' mean non-attenuation corrected images to this template. Then, using the same formula, I created a second-pass template from the newly created normalised images. In this way, all subjects contributed equally to the creation of the template image.

4.2.3.4.2 Applying the VOIs to subject images

For each subject, I took the non-attenuation-corrected mean image and normalised it

to the template created above. This generates warping parameters describing the transformation from subject space to standard space. The VOI definitions are in standard space. The two alternative procedures that could be applied are to warp the subject's PET images into standard space using these parameters, or to invert the parameters and warp the VOI definitions into the same space as the subject's images. Each method has its advantages and disadvantages. Warping the subject's images has one less step, the inversion of the parameters. Also, if all images are warped into standard space it enables easier comparison between subjects. However, as described above for the motion correction process, each resampling of the PET data necessitates interpolation of the data and subsequent loss of resolution.

The normalisation process begins with a 12-parameter affine transformation of the subject's image into the same space as the target template image (Ashburner & Friston, 1999). This process accounts for the differences in position, orientation and global size between the two images. In effect it spins and slides the subject's image into the same orientation as the template using 9 parameters, then uses the remaining 3 parameters to describe scale factors in each dimension accounting for differences in overall size. The second phase of the process uses a series of basis functions to describe the non-linear warping required to account for the localised differences in brain shape between the images. In earlier versions of SPM, e.g. SPM99, the parameters describing the basis functions were found which minimised the sum-of-squares difference between the subject's and template images. This process took no account of the anatomical feasibility of these warps, making the process vulnerable

to unstable results where the subject's brain had localised anomalies or could become trapped in localised minima. In SPM2 and later there is a dual cost function that seeks to minimise both the sum-of-squares difference between the images and a measure of the anatomical likelihood of the warping parameters. This second component of the cost function is referred to as the "regularisation" of normalisation. It is based on the Bayesian probability of the warping parameters. This refers to the posterior probability of the parameters given the calculated parameters from the minimisation of the sum-of-squares and the prior probability. As more eloquently described elsewhere (Ashburner & Friston, 1999), in an ideal situation the prior probabilities would be derived from some concept of the "brain-ness" of the image, but this is difficult to quantify. Instead, the prior probabilities are derived from the "membrane energy" of the warping parameters. In essence this is a measure of the degree to which the subject's brain image will be "stretched out of shape". Ultimately the combined dual cost function derives the warping parameters producing the best match between the images with the least warping of the subject's image to do so.

The next step is to invert these warping parameters. This can't be done directly. It is easy to invert the 12-parameter affine components, but the non-linear warping parameters and coefficients of basis functions which are not easily inverted. However, there is an additional toolbox available with SPM2 called the deformation toolbox (Ashburner *et al.*, 2000). This toolbox takes the warping parameters from the normalisation and converts them into a deformation field image which can be

inverted. The deformation field produced by conversion from the warping parameters is a matrix of the same dimension as the warped image but with each voxel containing a vector describing the movement required for that voxel to accomplish the warping. The same toolbox was then used to invert the deformation field. This inverse deformation field was then applied to the VOI definitions in standard space. This final step required some modification of the code.

4.2.3.4.3 Warping the VOI definition images

The VOIs are delineated in Analyze®. Routinely they are stored as "Object files", which is a proprietary format. In order to be warped to match the subject's image, they first need to be converted into a format that SPM2 can read and manipulate. Analyze® itself is able to convert these VOI definitions into an image file where the voxel value is an integer representing the VOI that voxel is a part of. The inverted deformation field created above can be applied to this VOI image using the deformation toolbox. However, the resampling of the image uses trilinear interpolation as described above. This results in non-integer values in some voxels. This makes it impossible to return the warped VOI images back into Object files. The only way to maintain integer-only values in the image is to use "Nearest neighbour" interpolation. The choice of trilinear interpolation is hard-coded into the SPM2 source code (as shown in Codeblock 1), which therefore had to be modified.

Codeblock 1: Original SPM2 function - spm_applydef_ui.m

```
function spm_applydef_ui(P,PT)
% Applies a deformation field to an image
%_____
% @(#)spm_applydef_ui.m          1.4 John Ashburner 04/03/24
if nargin<2
        n = spm_input('Number of subjects','+0', 'n', '1', 1)';
        for i=1:n
        P{i}  = spm_get(1,{'*y_*.img','noexpand'},['Select deformation field ' num2str(i)]);
        PT{i}  = spm_get(Inf,'*.img',['Image(s) to warp (' num2str(i) ')']);
        end;
else
        n = length(P);
        if n ~=length(PT)
        error('Must have matching deformation / files list cell arrays as inputs to spm_applydef_ui')
        end
end
spm_progress_bar('Init',n,'Applying deformations','subjects completed');
for i=1:length(P),
        Pi = [repmat([P{i} ','],3,1) num2str([1 2 3]')];
    spm_applydef(Pi,PT{i});
    spm_progress_bar('Set',i);
end;
spm_progress_bar('Clear')
return;
%_____
function spm_applydef(VD,VI)
if ischar(VD), VD = spm_vol(VD); end;
if ischar(VI), VI = spm_vol(VI); end;
VO = VI;
for i=1:length(VO),
        VO(i).fname   = prepend(VO(i).fname,'w');
        VO(i).dim(1:3) = VD(1).dim(1:3);
        VO(i).mat     = VD(1).mat;
        if ~isfield(VO,'descrip'), VO(i).descrip = ''; end;
        VO(i).descrip  = ['warped ' VO(i).descrip];
end;
VO = spm_create_vol(VO);
for p=1:VD(1).dim(3),
        M  = spm_matrix([0 0 p]);
        x1 = spm_slice_vol(VD(1), M, VD(1).dim(1:2),1);
        x2 = spm_slice_vol(VD(2), M, VD(1).dim(1:2),1);
        x3 = spm_slice_vol(VD(3), M, VD(1).dim(1:2),1);
        for i=1:length(VI),
        M   = inv(VI(i).mat);
        y1  = M(1,1)*x1+M(1,2)*x2+M(1,3)*x3+M(1,4);
        y2  = M(2,1)*x1+M(2,2)*x2+M(2,3)*x3+M(2,4);
        y3  = M(3,1)*x1+M(3,2)*x2+M(3,3)*x3+M(3,4);
        img  = spm_sample_vol(VI(i),y1,y2,y3,1);
        VO(i) = spm_write_plane(VO(i),img,p);
        end;
end;
VO = spm_close_vol(VO);
return;
```

I decided that the best way to implemented this change was to permit user selection of the interpolation algorithm. SPM2 can also be run using commands issued from within a script. Any such script would not expect to have to choose the interpolation algorithm, so I had to ensure that I maintained this interface. I achieved this by setting trilinear interpolation as the default choice in the graphical interface and not require the parameter to be passed as an input argument to the function, but allow it to be passed. The resultant code is shown in Codeblock 2 with much of the unaltered code snipped out.

Codeblock 2: Modified spm_applydef_ui.m (with unchanged elements snipped for brevity)

```
function spm_applydef_ui(P,PT,interp)
% Applies a deformation field to an image
%
% Changes made by Mark Daglish 04/11/19
% Wanted to allow different interpolation levels so
% 1: interp added to function call
% 2: If no vargin then full gui with P (array of deformation fields)
%    PT (array of images to warp) and interp (level of interpolation)
%    are required to be specified.
%   If P & PT are defined, but not interp, then assume someone is expecting
%    John's original program and set interp=1 as default.
%   If P, PT & interp are specified then use them & skip GUI.
% 3: Calls to spm_slice_vol and spm_sample_vol changed to include
%   interp variable
%_____________________________________________________________________
% @(#)spm_applydef_ui.m            1.4 John Ashburner 04/03/24
if nargin<3
        if nargin == 2;
                interp=1;
        else
                n = spm_input('Number of subjects','+0', 'n', '1', 1)';
                for i=1:n
                P{i}   = spm_get(1,{'*y_*.img','noexpand'},['Select deformation field ' num2str(i)]);
                PT{i}  = spm_get(Inf,'*.img',['Image(s) to warp (' num2str(i) ')']);
%       Option to change interpolation method added by Mark Daglish 04/11/18
                interp = spm_input('Interpolation Method?','+1','m',...
                        ['Nearest Neighbour|Trilinear Interpolation|',...
                        '2nd Degree B-spline|3rd Degree B-spline|4th Degree B-spline|',...
                        '5th Degree B-spline|6th Degree B-spline|7th Degree B-spline'],...
                        [0 1 2 3 4 5 6 7], 2),
% ----------End of change----------
                end;
        end;
<< code snipped>>
%       Change to include interpolation in call to spm_applydef
        spm_applydef(Pi,PT{i},interp);
        <<code snipped>>
%_____________________________________________________________________
function spm_applydef(VD,VI,interp)
        <<code snipped>>
% Changed to include interp variable in calls to spm_slice_vol & spm_sample_vol
for p=1:VD(1).dim(3),
        M  = spm_matrix([0 0 p]);
        x1 = spm_slice_vol(VD(1), M, VD(1).dim(1:2),interp);
        x2 = spm_slice_vol(VD(2), M, VD(1).dim(1:2),interp);
        x3 = spm_slice_vol(VD(3), M, VD(1).dim(1:2),interp),
                        <<code snipped>>
        img  = spm_sample_vol(VI(i),y1,y2,y3,interp);
        <<code snipped>>
```

Once implemented, the new code allowed application of the inverse deformation field to the standardised VOIs. I also applied the deformation to the template 11C-Raclopride image. The end product of this process is to produce a map of the VOIs that had been defined in standard space now warped into the same space as the individual subject's images. By comparing the subject's mean non-attenuation-corrected image with the warped template image it was possible to do a rough check on the success of the normalisation and inversion process. The, now warped, VOI image can then be converted back into an Object file using Analyze®. A sample result of this process is shown in Figure 4.9. These can then be used to sample the subject's dynamic image to obtain time-activity curves for the seven VOIs. It is these time-activity curves that were sampled and plotted above to test the effects of motion correction.

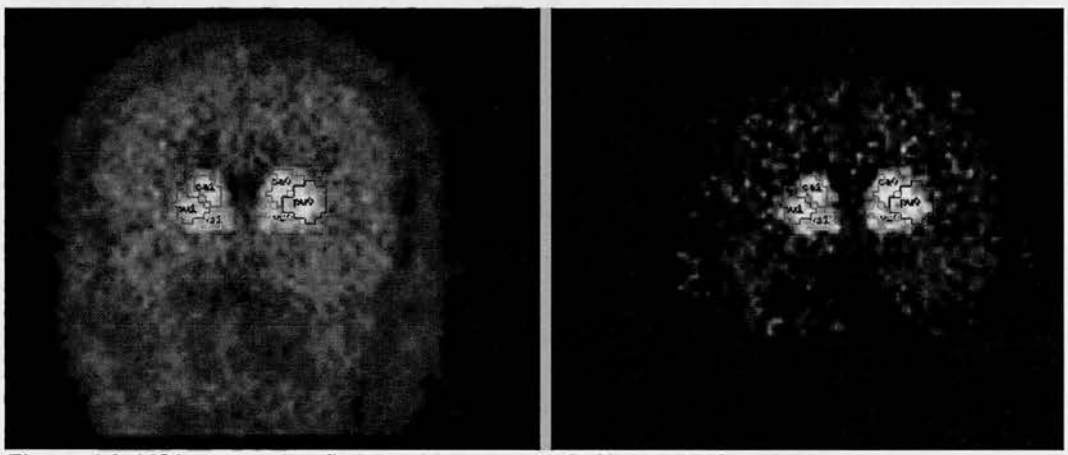

Figure 4.9: VOIs warped to fit the subjects mean (left) and BP (right) image.

4.3 Modelling of ^{11}C-Raclopride

When analysing ligand PET images the concentration of radioactivity in the tissue is the quantity measured by the scanner. Some measure of the availability of the binding site is the measure of interest. It is the modelling of the tracer that enables us to get from one to the other.

4.3.1 The simplified reference tissue model

This modelling technique for ^{11}C-Raclopride was first described by Lammertsma & Hume, (1996). ^{11}C-Raclopride has been previously shown to have no specific binding outside of the basal ganglia (Kohler *et al.*, 1985). This means that it is possible to model the tracer using the simplified reference tissue model. Modelling of any tracer binding requires some form of input function that describes the delivery of the tracer into the target region. Generally, this can be described using a three-compartment model, as illustrated in Figure 4.10. The nominal compartments are plasma plus the three tissue compartments: free, non-specifically bound and specifically bound tracer. Assuming reversible binding, each compartment has two rate constants associated with in describing influx and efflux from the compartment, yielding a total of six rate constants.

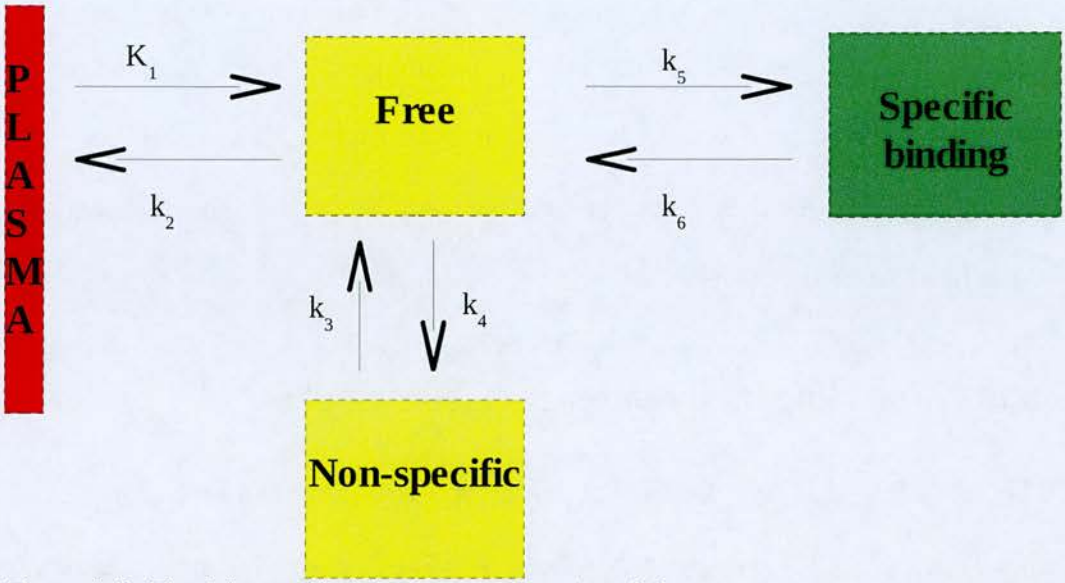

Figure 4.10: The fully specified three compartment model

This model requires estimation of six parameters and requires knowledge of the amount of radio-labelled parent compound tracer in the arterial blood supply. The parameters of interest are only k_5 and k_6, or the ratio k_5/k_6. Therefore if the free and non-specifically bound compartments can be reliably estimated in a brain region lacking specific binding it it possible to reduce the model to a reference tissue model using four parameters (see Figure 4.11). This is possible because the specific binding compartment does not directly connect with the plasma compartment. However, the reference tissue model does make the assumption that the effective delivery of tracer to the free and non-specific binding compartments are the same in both target and reference regions. Mathematically this is expressed as $K_1/k_2 = K'_1/k'_2$. These parameters are dependent on delivery of the tracer to the region by the plasma and the effective surface area of the blood-brain barrier at each location. These factors need not be the same in the target and reference regions, but the effect of differences

is assumed to be the same on both K_1 and k_2, thereby preserving the ratio between them.

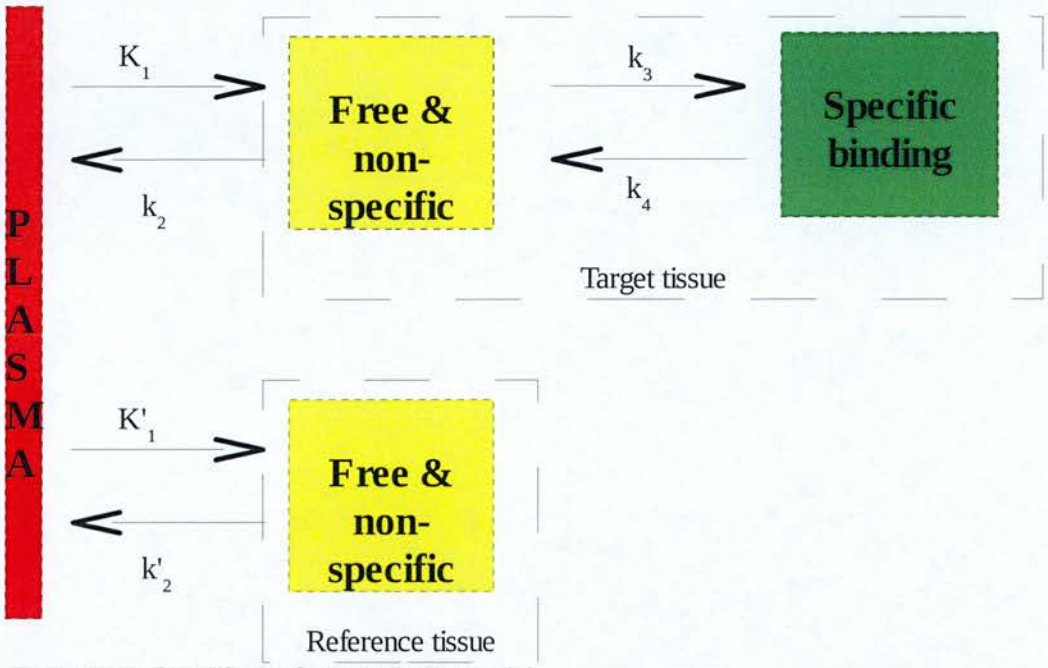

Figure 4.11: Simplified reference tissue model

On initial examination it appears that this model still requires estimation of six parameters (K_1,k_2,k_3,k_4,K'_1,k'_2). Using the equations from Lammertsma & Hume, (1996) reproduced as Equation 6(1-5), it is possible to show that these initial six reduce to four parameters (R_1,k_2,k_3,k_4). Where the tissue concentration C_t is expressed as a function of C_r and the four parameters. Substituting Equation 6(6) gives us a parameter of Binding Potential which is related to the parameters of real interest which are B_{max} and K_D. B_{max} gives a measure of the binding site availability and K_D is a measure of the tracer affinity for the binding site. There is currently some debate amongst experts as to the correct nomenclature for this BP parameter (personal communication). As identified in Equation 6 the reference tissue models all yield a

measure of f_2.BP which is dependent on the free-fraction of tracer in the target tissues. I will generically refer to this parameter as BP, which is one of the conventions currently being used in the literature.

$$\frac{dC_r(t)}{dt} = K_1' C_p(t) - k_2' C_r(t) \quad (1)$$

$$\frac{dC_f(t)}{dt} = K_1 C_p(t) - k_2 C_f(t) - k_3 C_f(t) + k_4 C_b(t) \quad (2)$$

$$\frac{dC_b(t)}{dt} = k_3 C_f(t) - k_4 C_b(t) \quad (3)$$

$$C_t(t) = C_f(t) + C_b(t) \quad (4)$$

$$R_1 = \frac{K_1}{K_1'} \quad \Rightarrow \quad k_2' = \frac{k_2}{R_1} \quad (5)$$

$$BP = \frac{k_3}{k_4} \quad \Rightarrow \quad k_4 = \frac{BP}{k_3} \quad (6)$$

Where: C_r is the concentration in the reference tissue,
C_f is the concentration of free and non-specifically bound,
C_p is the metabolite corrected concentration in plasma,
C_b is the concentration of specifically bound tracer (i.e. the measure of interest) and
C_t is the concentration in the target tissue (as measured by the scanner).
R_1 is the ratio of tracer delivery between target and reference region.
BP is the binding potential - the new measure of interest
(more accurately described as BP. f_2 where
f_2 is the free-fraction of tracer in the target tissue).

Equation 6: Differential equations describing the change over time of the concentration of tracer in each compartment in the reference tissue model.

The simplified reference tissue model (Lammertsma & Hume, 1996) makes further assumptions of the data in order to derive a more straightforward and mathematically stable approximation of BP. If it is assumed that, under tracer conditions, equilibration between C_f and C_b is very fast then they can be effectively modelled as a single compartment. This has been shown to hold for ^{11}C-Raclopride (Farde *et al.*,

1989). This replaces Equation 6(2-3) with Equation 7(1). Including Equation 7(2) with Equation 6 yields the full equation for the simplified reference region model as Equation 7(3).

$$\frac{dC_t(t)}{dt} = K_1 C_p(t) - k_{2a} C_t(t) \quad (1)$$

$$\frac{K_1}{k_{2a}} = \frac{K_1}{k_2}.(1 + \mathrm{BP}) \quad (2)$$

$$C_t(t) = R_1 C_r(t) + \left(k_2 - \frac{R_1 k_2}{1 + \mathrm{BP}}\right) C_r(t) \otimes e^{-\frac{k_2}{1+\mathrm{BP}}t} \quad (3)$$

Where k_{2a} is the effective k_2 for $C_t(t)$.

Equation 7: The equations for the simplified reference region model.

It can be seen that this simplified model now depends on the concentration in the reference tissue and three parameters (R_1,k_2 and BP) of which BP is the parameter of interest. The implementation of this model in terms of computer software is discussed in the next section.

4.3.2 Re-implementation of Receptor Parametric Mapping software

Traditionally, at the MRC Cyclotron Unit in Hammersmith Hospital, the simplified reference tissue model described above was implemented within an in-house software package called "Receptor Parametric Mapping" (RPM). This software was written by Dr. Vin Cunningham and Dr. Roger Gunn.

4.3.2.1 Reformulation of the Simplified Reference Tissue Model

The equation for the simplified reference tissue model is given in Equation 7(3). This is solvable, but computationally intensive and susceptible to noise (Gunn *et al.*, 1997). However, it is possible to linearise the equation to yield Equation 8(1).

$$C_t(t) = \theta_1 C_r(t) + \theta_2 C_r(t) \otimes e^{-\theta_3 t} \quad (1)$$

Where:

$$\theta_1 = R_1 \quad (2)$$

$$\theta_2 = k_2\left(1 - \frac{R_1}{1 + \mathrm{BP}}\right) \quad (3)$$

$$\theta_3 = \frac{k_2}{1 + \mathrm{BP}} \quad (4)$$

This can be restated as:

$$C_t(t) = \theta_1 C_r(t) + \theta_2 B(t) \quad (5)$$

Where:

$$B(t) = C_r(t) \otimes e^{-\theta_3 t} \quad (6)$$

Inserting a term for radioactive decay of ^{11}C gives:

$$\theta_3 = \frac{k_2}{1 + \mathrm{BP}} + \lambda \quad (7)$$

Equation 8: Linearised reformulation of Equation 5(3).

From Equation 8(5) it is clear that $C_t(t)$ is a linear function of $C_r(t)$ and B(t) with two parameters (θ_1 and θ_2). Solving such a linear equation is computationally much more straightforward. The novel approach taken in Gunn *et al.*, (1997) was to generate a range of basis functions ($B_i(t)$) covering the plausible values given the physiological state being described. It is then a linear problem to find the basis function that best fits the observed data and derive the parameters θ_1 and θ_2 and to

yield corresponding values for R_1, k_2 and BP. The only additional component needed in the model is a term to account for the radioactive nature of the tracer, so λ has to be inserted as the decay constant for the ^{11}C isotope to finally give us Equation 8(7).

4.3.2.2 Origins of the software problems to be solved

The majority of the RPM software package runs from within the Matlab® (Mathworks Inc., USA) package. Given the date it was written, the RPM package was written for Matlab® version 5. There have been a number of changes to the Matlab language between version 5 then and version 7.2 now. These required updating of the program files to match the alterations in the language specification. It also used routines for reading and writing brain images from disk taken from SPM96 (Wellcome Dept. Cognitive Neurology) and adapted for use in the package. For some of the more computationally intense operations, the software was written in more efficient, lower level, computer languages like C, C++ and Fortran.

In order to analyse the brain images we acquired, we needed to deploy this software package in Bristol on our own computers. The problem of this was that the computers at the MRC Cyclotron Unit were Sun® computers using the SPARC® architecture. In Bristol we had no Sun® computers and only machines based on the Intel® x86 architecture. This created two main difficulties; firstly any software compiled for the SPARC architecture had to be re-compiled for the x86 architecture; secondly, all the brain images were stored in the wrong endian format. This needs to be explained in more detail.

The software written in Matlab's own language can be run on any machine that Matlab will install and run on. The code written in C, C++ or Fortran needs to be compiled before it will run on any computer. The same source code can be compiled to run on any machine, but the compiled executable program will only run on the architecture it was compiled for. The implication of this is that all the C, C++ and Fortran components of the RPM package needed to be recompiled to run on our computers. Unfortunately, a lot of the source code was either incomplete or missing completely. This meant it had to be re-written to a varying degree before it could be deployed in Bristol. Each of the components that required this work are described in their own sections below.

The second problem was that of the endian format of the brain images and the machines they were to be analysed on. The term "endian" relates to the way numbers are physically stored within a computer's memory. The basic unit of computer memory is the byte. A byte is a number comprising 8 binary digits. The size and precision of the brain image voxel data cannot be stored in a single byte, so the data has to be stored in several bytes. These bytes can be ordered in at least two ways; with the least significant byte first (see Figure 4.12, pane A), which is called "Little endian"; or with the most significant byte first (see Figure 4.12, pane B), which is called "Big endian". This is important because the Sun® computers use Big-endian and the x86 computers use Little-endian formats. The result of this is that if you try to read an unconverted image in the wrong format, it will appear to be white noise. This has been traditionally typified as the "NUXI problem", as the first

attempt to port the Unix language to an other-endian system resulted in the printing of "UNIX" as "NUXI". This gives a simple example of the effects of wrong endian data reading on data. As an amusing aside, the terms big & little endian are purported to be derived from the argument of the Lilliputians in Gulliver's Travels over which end to crack open an egg.

Figure 4.12: Little and Big endian representations of the hexadecimal number 4A3B2C1D.

4.3.2.3 Solving the endian problem

The solution to the endian problem was to re-write the RPM software package to use different routines to read and write brain image data from disk. If the image reading and writing routines could be written to detect the byte-order (or "endian-ness") of the images then this can be corrected as they are read in from disk. In this way the rest of the software need have no knowledge of the image byte-order as the data is automatically represented in memory in the correct format. The easiest way to achieve this was to update the image routines to use those from the recently released SPM2 as opposed to the original SPM96 routines. This updated version of the SPM software package referenced above included improved disk reading and writing routines. In particular, there were two clear advantages. Firstly, the images were handled in a more memory efficient manner and also the byte-order was detected and corrected if necessary as images were read in from disk (i.e. on-the-fly).

The change of versions did mean a re-write of several segments of the RPM software as the Application Program Interface (API) of the SPM image input/output (I/O) routines was also changed with the new version. The API of any software is the rules and conventions governing the passing and retrieving of arguments and the syntax for invoking the routines. If the API remains unchanged with an upgrade of software it will appear to the calling software, or end user, that the software has not changed. Even if it accomplishes its functions in a different manner, these changes will be transparent to the user. Conversely, when the API of a software package changes, then it will require at least some degree of re-writing to regain the previous functionality.

The original RPM software turned out to be using customised versions of some of the SPM96 software as well. The original SPM96 software was written to handle 3D images of a single brain volume. RPM requires the main input image to be a 4D time-series of volumes. In order to more fully understand the nature of the problem, some explanation is required of the format in which the brain images are stored. The images use a format described as "Analyze 7.5" as it was defined by the software package Analyze® (AnalyzeDirect, USA) version 7.5. This format is a widely used method of image data storage. It uses two files to store the brain image. There is a small header file (name.hdr) that contains a number of parameters that describe the associated image. The image data itself is stored in an image file (name.img) that contains only the binary data in the format described in the associated header file.

One of the first tasks for the RPM software when accessing images on disk is to

determine the format of the image. This is done by reading in the header file. Previously the RPM package used a modified version of the SPM96 routine spm_hread.m but this had been replaced in SPM2 by the new routine spm_read_hdr.m. Behind the name change was also a fundamental change in the way the data retrieved from the header file was represented in memory. Previously each item of data, like image dimensions and voxel sizes, was stored in its own variable. With the move to SPM2 the data from each header was stored in a single structure variable containing all the necessary variables within it. The new header I/O routine also returned information on the byte-order of the data. The net result of these changes is that calls went from the form of:

```
[dim,vox,scale,type,offset,origin,descrip] = spm_hread(hdrfilename);
```

to:

```
[hdr, otherendian] = spm_read_hdr(hdrfilename);
```

Where hdr is a structure containing fields like hdr.dim, hdr.vox etc. and otherendian is a flag denoting where byte-swapping is required.

Previously, SPM96 would then take the header information and use it to memory map the associated image disk file, to avoid loading large amounts of data into memory, using a call to spm_map_vol. This mapped image file could then be read using spm_sample_vol. In SPM2 images were no longer memory-mapped until actually read from disk. In the RPM software this was accomplished by a routine

map_dynamic which would create a matrix of memory-mapped 3D volumes from a single 4D image file as shown in Codeblock 3.

```
function V=map_dynamic(P)

% Receptor Parametric Mapping
% Version 1.0 : 20-06-98
% Roger Gunn
%
% John Ashburner's Memory Mapping Routine
%
% memory map of a dynamic image
% FORMAT V=map_dynamic(P)
% P - filename
%_____________________________________________________________________
%
% map_dynamic returns a matrix V identifying a memory mapped dynamic image.
% The matrix V can be used by sample_dynamic.
% Once finished with, it should be unmapped with unmap_dynamic.

P       = P(P~=' ');
Filename = P;
q       = length(P);
if P(q-3)=='.'; P = P(1:(q-4)); end

[DIM VOX SCALE TYPE OFFSET] = spm_hread([P '.hdr']);
if    (TYPE==2) siz=1;
elseif (TYPE==4) siz=2;
elseif (TYPE==8) siz=4;
elseif (TYPE==16) siz=4;
elseif (TYPE==64) siz=8;
else            siz=1;
end

if (length(DIM)==3) DIM = [DIM 1]; end

for fr=1:DIM(4)
        V(:,fr) = spm_map_vol(Filename,[DIM(1:3) VOX(1:3) SCALE TYPE
                OFFSET+prod(DIM(1:3))*(fr-1)*siz]);
end
```

Codeblock 3: Original version of map_dynamic routine.

The new version of RPM had to be adapted to the new format of spm_vol, which replaced spm_map_vol. The revised version is shown in Codeblock 4.

```
function V=map_dynamic(P)
% memory map of a dynamic image
% FORMAT V=map_dynamic(P)
% P - filename
%_____________________________________________________________________
%
% map_dynamic returns a matrix V identifying a memory mapped dynamic image.
% The matrix V can be used by sample_dynamic.
% Once finished with, it should be unmapped with unmap_dynamic.
%
% Hacked by Mark Daglish 3 Jan 2005 to work with SPM2 routines
% spm_map_vol is no longer used, replaced by spm_vol. V remains
% a (num_frames x 1) matrix of structures as described in spm_vol

P       = P(P~=' ');% Remove blanks
Filename = P;
q       = length(P);
if P(q-3)=='.'; P = P(1:(q-4)); end % remove filename extension

[hdr,otherendian] = spm_read_hdr([P '.hdr']); % get the hdr structure

% If it is a 3D image, set the 4th dimension to 1
if ((length(hdr.dime.dim)==4) | hdr.dime.dim(5)==0) hdr.dime.dim = [hdr.dime.dim(1:4) 1]; end

Vols = cell(hdr.dime.dim(5),1);
% As this is a 4D image create a matrix of filenames of the form "filename.img,n"
% where n is the frame number from 1 to number of frames.
for fr=1:hdr.dime.dim(5)
        tmp = [strcat(Filename,',',num2str(fr))];
        Vols(fr)= cellstr(tmp);
end
Vols = char(Vols);
V=spm_vol(Vols);
```

Codeblock 4: Revised version of map_dynamic routine.

Once these changes had been made, the rest of the routine calls to read image data from disk where very straightforward to modify. References to the mapped 4D volume matrix V_old of the form V_old(:,frame) could simply be replaced by V_new(frame). Similarly, the image dimensions were no longer referenced as V_old(1:2,frame), but as V_new(frame).dim(1:2). The other remaining advantage from the new API was that image structures no longer needed to be unmapped, rendering calls to spm_unmap unnecessary.

With the changes in image I/O routines the other remaining task was to update the routines for writing images to disk. Previously, the RPM package did the writing to disk of all the created images. It made more sense to me to use the new SPM2 routines to obviate the need for re-implementing routines that were already in existence. All that was needed was to build a structure describing the volume to be written, as defined by the spm_vol. The data to be written has already been created in a matrix, and so can be written to disk with a call to spm_write_vol.

4.3.2.4 Re-writing the compiled software

The analysis of ^{11}C-Raclopride images using the simplified reference tissue model requires the use of two of the compiled routines within RPM. The Simplified Reference Tissue Model (SRTM) as implemented in RPM, as described in Equation 8.5 and Equation 8.6, uses a series of basis functions generated as a range spanning the likely possible solutions to the model parameters. The routine that generates the basis functions has to implement a convolution function (see Equation 9) which is computationally heavy.

From Equation 8(5) above, the ith basis function $B_i(t) = C_R(t) \otimes e^{-\theta_3 t}$

Where $C_R(t)$ = interpolated activity in reference region at time t.

Expanding over a finite set of discrete time intervals gives us:

$$B_i(t) = k\frac{1-e^{\theta_3}}{\theta_3}\sum_{\tau=0}^{t} C_R(\tau)e^{-(t-\tau)\theta_3}$$

Where k is a constant.

Similarly: $B_i(t-1) = k\frac{1-e^{\theta_3}}{\theta_3}\sum_{\tau=0}^{t-1} C_R(\tau)e^{-(t-1-\tau)\theta_3}$

Which implies: $B_i(t-1)e^{-\theta_3} = k\frac{1-e^{\theta_3}}{\theta_3}e^{-\theta_3}\sum_{\tau=0}^{t-1} C_R(\tau)e^{-(t-1-\tau)\theta_3}$

and therefore: $B_i(t)-B_i(t-1)e^{-\theta_3} = k\frac{1-e^{\theta_3}}{\theta_3}C_R(t)$

Which means that: $B_i(t) = B_i(t-1)e^{-\theta_3} + k\frac{1-e^{\theta_3}}{\theta_3}C_R(t)$

Equation 9: Convolution function for SRTM basis function generation

There originally existed a routine written in Matlab code (see Codeblock 5). It can easily be seen that this implements the final line of Equation 9. For speed this had been converted to C using the Matlab compiler to which we did not have access in Bristol. This left us with two possible solutions: 1) we could continue to use the Matlab code, or 2) I could re-write the code as a C function.

Codeblock 5: Matlab code to implement

```
function convolution=conv(inp,k,theta,t)
        et = exp(-theta);
        prev = 0;
        for i = 1:length(t)
                prev = prev*et + k*inp(i)*(1-et)/theta;
                convolution(i) = prev;
        end
```

The first option of leaving the Matlab® code in use was clearly the easiest. However, as the length of vector 't' is the scan duration in seconds it is frequently in excess of 5,000 and therefore incurred a noticeable time penalty with each image analysis run. Taking the code in Codeblock 5 as a starting point, I re-implemented this in C. Having not programmed in C before, this required the use of some web-based resources and the External Interfaces Manual for Matlab®. The resulting C code is shown in appendix 8.1.2.1. The mathematical explanation for the nature of the convolution is detailed in Gunn *et al.*, (1997) and Equation 9.

The next compiled routine was a much more complex problem. The whole principle of the basis functions approach described above relies on finding the best fit of the model to the observed data from every possible model derived from the basis functions. As demonstrated in Equation 8 this is a linear problem with two parameters (θ_1 and θ_2). In this way, an expected $C_T(t)$ can be derived for every plausible basis function. The best fit to the observed data can then be found using a standard linear least squares method. It was the solution of this problem that was handled by the compiled software routine.

As before, I had a few resources at my disposal to re-implement this solution on our computer system in Bristol. It was possible to trace the original software for the compiled routines in use from a backup store. Unfortunately, this code comprised three files written in a different language, namely C++. This code had been written in 1996 and would now no longer compile due to changes in the accepted standards of the language. Luckily, hidden within the source code was an old version of the

Matlab® code from which it was derived. However, it was soon clear that the M-code was not as sophisticated as the C++ code that was derived from it. In addition, the original M-code was written to make use of the matrix capabilities of the Matlab® environment. In order to re-implement this in C++ the previous programmers had used the object-orientated nature of C++ to create a series of classes of objects that mimicked the matrix and vector structures of Matlab® and implemented equivalent methods. This is not easily mimicked in C. The original C++ files written by Drs. Steve & Roger Gunn are reproduced in Appendix 8.1.

This first step to solving the problem was to re-implement the current solution in Matlab® M-code. This would be much slower than any compiled code, but has the advantage of being much easier to read, write and debug. The code contained in the comments of the C++ source code appeared to provide a solution to the mathematical components of the problem. Specifically, it would take similar input parameters, although not identical as detailed below, and would find the best fitting solution with the associated values for θ_1, θ_2 and θ_3. However, unlike the existing compiled routine it was missing one input argument. This argument was a matrix labelled "mask". From the calling program it was possible to deduce that this parameter contained a binary vector that contained a value of 1 where there was data in the image, according to a user-supplied masking image, and a value of 0 where there was no useful data in the image (i.e. outside the brain).

The only reason for supplying such an input would be to reduce the computational load on the software by only analysing voxels that contain useful data. Given that

the brain image sits in a larger cuboid matrix of non-brain there are large regions where analysis will produce meaningless results at the expense of a large amount of computer processing time. It appeared that this was what the C++ code was using the mask input argument for. Therefore, any solution to re-implement the M-code had to include the "mask" argument to avoid the need to modify the source code in the program calling the routine. The idea being, that it should be possible to substitute one routine for another directly without the rest of the software package being altered, or even aware of the change. Similarly, the substitution should be transparent to the end-user, most particularly in the production of identical end results. In addition, the reduction in computational load would also be maintained.

The new Matlab® M-code for this routine is shown in full in Appendix 8.1.3.2. It was while re-writing the section in Codeblock 6 that I discovered a bug in the original software as shown in Codeblock 7.

Codeblock 6: M-code for allocating default return values

```
RI=zeros(1,ydim);
k2=zeros(1,ydim);
BP=zeros(1,ydim);
index=ones(1,ydim)*(no_basis_functions);
```

The calling program for this routine uses the returned variable "index" to calculate the number of voxels where the solution found is the first or last in the series of possible basis functions. This can be used as a quality check, as an occasion where too large a proportion of the solutions found are in the first or last function suggests that the range of basis functions specified for the tracer is either off-centre or too small. When originally developed and published (Gunn *et al.*, 1997) the only tracers

studied were shown to be adequately modelled by 100 basis functions.

Codeblock 7: Original c++ code showing bug highlighted

```
R(y) = 0.0;
k(y) = 0.0;
BP(y) = 0.0;
ind(y) = 100.0;
```

At some later date the new tracer for the 5-HT_{1a} receptor, ^{11}C-WAY-100635, was added to the tracers modelled using the SRTM. In contrast to the others, ^{11}C-WAY-100635 requires 300 basis functions to be adequately modelled. As can be seen from Codeblock 7, the return value for index where there is no data will be 100. For tracers where the number of basis functions is 100, this value will be 1+(maximum value returned) as "index" usually returns "solution -1". For tracers, like ^{11}C-WAY-100635, where the number of basis functions is greater than 100, this value will no longer be outside the meaningful range of returned values for index. Therefore the code had to be modified to return a signal value that was always outside the meaningful range, i.e. "number of basis functions" as shown in Codeblock 6.

Having corrected this bug the full code could then be implemented as shown in Appendix 8.1. Once this had been done, the code had to be tested. The only truly valid test was to compare the results produced by the original software package and the new re-implementation. Luckily was had a store of ^{11}C-Raclopride images that I had analysed using the software at the MRC Cyclotron Unit. These were acquired for the study detailed in Chapter 5. I was therefore able to re-analyse the images using the new routines and compare the resulting parametric images. I realised that

the C implementation of the routine would have to be tested in the same way, and therefore it made sense to write that code as well before running the test comparisons on both new routines simultaneously. Clearly if the set of three results were all closely matched, then I could be confident of the routines. If the results differed, then the presence of results from all three routines would aid the debugging process. I therefore wrote the C program shown in Appendix 8.1.3.3. As can be seen from the comments within the code, I was able to incorporate a number of enhancements for speed into the C routine. The clearest example is in Codeblock 8.

Codeblock 8: Matlab loop to identify the best solution

```
for i=1:no_basis_functions
    B(:,2)=A(:,i);
    result=bigm((i*2-1):i*2,:)*Wd;
    ssq(i)=sum((weight).*(B*result-data).^2);
end
sol=find(min(ssq)==ssq);
ind=sol(1);
```

In this example the result for each possible basis function is calculated and then the sum-of-squares difference is then calculated and stored in the "ssq" vector. This is then searched for the minimum value, which returns the index of the best fitting basis function. This "find" command is effectively looping through the whole contents of the vector to find the minimum value. As can be seen from Codeblock 9, this can be brought inside the preceding loop for greater computational efficiency. However, it is also clearly visible that the cost is the clarity of the code.

The first run of the code, once the errors had been removed, showed immediately the speed effects of using C rather than Matlab® to handle the computationally heavy

algorithm. Using the Matlab® code the image analysis took approximately 22.5 minutes. The same analysis with the compiled C code took 3.5 minutes.

Codeblock 9: C code illustrating increased computational efficiency

```
for (bf=0 ; bf<nobf;bf++) {
        /* B(:,2)=A(:,bf);
        For each basis function in turn extract the required parameters */
        for (i=0;i<frames;i++) {
                *(B+frames+i)=*(A+bf*frames+i);
        }
        /* result=bigm((bf*2-1):bf*2,:)*Wd; */
        result[0] = 0.0;
        result[1] = 0.0;
        for (i=0; i<2;i++) {
                for (j=0; j<frames; j++) {
                        result[i] += *(bigm+j*2*nobf+(bf*2+i)) * Wd[j];
                }
        }
        /*ssq(bf) = sum((weight).*(B*result-data).^2);
        and calculate the sum of squares difference between the predicted data from the parameters
and the observed data */
        ssq = 0.0;
        for (i=0; i<frames;i++) {
                temp = *(B+i)*result[0] + *(B+frames+i)*result[1] - data[i];
                ssq += temp*temp*weight[i];
        }
        /* sol = find(min(ssq)==ssq); */
        /* Brought finding the minimum sum of squares solution inside the same loop to cut
computational time */
        if (bf == 0) {
                /* Skip checking first time round as minssq starts at 0.0 */
                minssq=ssq;
                sol = bf;
        } else if (ssq < minssq) {
                sol = bf;
                minssq = ssq;
        }
}
```

4.3.2.5 *Testing the results from the new code*

I initially began by comparing the resulting Binding Potential images (BP.img) from the three different version of the code: the original on the Cyclotron Unit system; the Matlab code; and lastly the compiled C-code. The easiest way to do this comparison

was to load the images into the Analyze® software package (AnalyzeDirect Inc., Kansas, USA) and use the image calculator to produce a difference image simply by subtracting one image from the other. I calculated such difference images for all the possible combinations. The results were all very similar between the three images. The first point to note is that the difference images were not entirely blank as would be expected if the BP images were all identical. I firstly looked at the global image characteristics. These are shown in Table 4.2 below. This initial comparison looks very good, especially the mean difference. However, it has to be remembered that a lot of the image matrix is outside the brain, and therefore set to zero. I therefore decided to also look at the differences in the volumes of interest.

Value of difference	Global	Left Putamen	Left Caudate	Left Ventral Striatum	Right Putamen	Right Caudate	Right Ventral Striatum	Cere-bellum
Maximum	0.97504	0.00408	0.00011	0.00281	0.46831	0.00327	0.00011	0.38680
Minimum	-0.8124	-0.08461	-0.08778	-0.05643	-0.09770	-0.07008	-0.04139	-0.65987
Mean	-0.00016	-0.01452	-0.01553	-0.01167	-0.01271	-0.01474	-0.00997	-0.00017
Standard Deviation	0.00455	0.01461	0.01556	0.01207	0.02369	0.01323	0.01105	0.01564

*Table 4.2: Initial comparison of BP value differences between **original** code and **new C** code for one exemplar scan.*

The differences in the VOIs are again reassuringly small. However, it has to be borne in mind that the mean values for the BP images are themselves quite small, typically less than 5. I therefore calculated values of percentage difference between the images using the mean value over both images as the denominator. For these "percentage difference" images it was necessary to exclude the whole image and

cerebellar values from the comparison as these would be expected to be extremely large (approaching infinity) as the expected mean value for the BP images in these regions should be zero. The percentage differences for the same exemplar subject as above in Table 4.2 are shown in Table 4.3.

Value	Left Putamen	Left Caudate	Left Ventral Striatum	Right Putamen	Right Caudate	Right Ventral Striatum
Maximum	2.47%	0.01%	1.09%	34.72%	0.67%	7.45%
Minimum	-3.09%	-2.64%	-2.51%	-4.53%	-2.96%	-2.70%
Mean	-0.69%	-0.75%	-0.64%	-0.60%	-0.73%	-0.52%
Standard Deviation	0.55	0.58	0.57	1.86	0.55	1.03
Number of voxels < -10% or > 10%	0	0	0	2	0	0

*Table 4.3: Percentage differences in BP between **original** and **new C-code** analysis for a single scan*

For the one VOI, right putamen, with 2 voxels that were outside the range -10% to 10% the mean and standard deviation came back to -0.6975% $\pm$ 0.5756 once the two outliers were removed. The small size of the differences between the images led me to suspect that the differences were due to different inaccuracies in the storage of floating point numbers in the two computer architectures. In order to test this hypothesis I first looked at the difference between the BP images from the original C-code run on the MRC Cyclotron Unit computer and the new C-code on the Bristol computer. I then compared the images from the Matlab® code and C-code both run in Bristol, it was clear that these images were identical. This demonstrated that the new C-code and Matlab® code were working identically when run on the same computer. I then compared the original image from the MRC Cyclotron Unit computer and the new Matlab® M-code on the Bristol computer. Unsurprisingly the

results were identical to those in Table 4.2 and Table 4.3. Very similar results were found for the other images, with the differences between the results produced by the two methods being small with the exception of a few isolated voxels, which in some cases fell within the volumes of interest. Nevertheless, these results were sufficiently close to be considered a good enough equivalent implementation of the model to proceed with the image analysis using this re-implemented software.

4.4 The measurement of dopamine release with ^{11}C-Raclopride

As mentioned briefly at the very start of this chapter, ^{11}C-Raclopride has been used to measure dopamine release (e.g. Carson *et al.*, 1997). Now that the mechanics of the analysis of the ^{11}C-Raclopride images has been thoroughly described, the mechanism by which this technique can be used to measure dopamine release needs to be examined.

As described in the very first section of this chapter, Raclopride is a competitive antagonist at the dopamine-D_2 receptor. *In vivo*, in the absence of any other pharmacological challenge, the only competitor for Raclopride at the receptor is endogenous dopamine. As described above, the measure acquired from modelling ^{11}C-Raclopride is the binding potential. This measure is dependent on two core parameters, the B_{max} and the K_D. K_D is the effective dissociation constant for Raclopride from the dopamine-D_2 receptor and, in this context, can therefore be assumed to be a constant. The more interesting contributor to BP is the B_{max}

component. This is a measure of the concentration of free receptors. In the *in vivo* state this will be the density of dopamine-D_2 receptors reduced by the proportion that are unavailable to ^{11}C-Raclopride. Unlike dopamine, ^{11}C-Raclopride will bind to dopamine-D_2 receptors in either the high or low affinity state. As has recently been shown ^{11}C-Raclopride is also able to bind to intra-cellular dopamine-D_2 receptors (Jiang *et al.*, 2006). This means that the only dopamine-D_2 receptors unavailable will be those that are already occupied by dopamine.

There remains some debate over how best to interpret the baseline resting ^{11}C-Raclopride BP. At rest and comparing between subjects any difference in BP value could reflect a difference in dopamine-D_2 receptor density or in resting extra-cellular dopamine. It is not possible with a single scan paradigm to disentangle these two components. Previous studies have shown that two scans using high and low specific activity are able to give better differentiation (Farde *et al.*, 1995; Hietala *et al.*, 1999).

While the exact contributions of individual factors to a single ^{11}C-Raclopride scan binding potential are problematic to elucidate, the interpretation of pairs of scans under different conditions is more clear. Alterations in dopamine function have now been clearly demonstrated to induce changes in ^{11}C-Raclopride binding in a variety of models and species. *Ex vivo* it has been shown that electrically stimulating dopamine neurones will decrease ^{3}H-Raclopride binding but this effect can be blocked by depleting the cells of dopamine or preventing its release (Gifford *et al.*, 1996). Similarly, *ex vivo* rodent studies have demonstrated the ability of

dopaminergic drugs to alter ^{3}H-Raclopride binding. D-amphetamine provokes dramatic dopamine release and induces decreased ^{3}H-Raclopride binding, whereas reserpine induces decreased brain dopamine levels and increases ^{3}H-Raclopride binding (Young *et al.*, 1991).

Extending the tritiated labelled autoradiographic studies into PET with the same raclopride molecule, but now labelled with carbon-11 has produced complementary results. Amphetamine, which provokes dopamine release and blocks its re-uptake and GBR-12909 which blocks dopamine re-uptake, both produce marked decreases in ^{11}C-Raclopride binding potential (Dewey *et al.*, 1993). In the same studies, the authors also gave tetrabenazine as a monoamine depleting agent, expecting it to increase ^{11}C-Raclopride binding. However, it produced an equivalent reduction in ^{11}C-Raclopride binding, which is what would be expected from its actions as a dopamine-D2 receptor antagonist.

The strongest evidence for the specificity of the ^{11}C-Raclopride signal comes from work using simultaneous PET and microdialysis. In this way changes in extra-cellular dopamine concentrations can be related directly to alterations in ^{11}C-Raclopride binding. For obvious reasons, this cannot be done in humans, but has been done in non-human primates (Tsukada *et al.*, 1999). The linear relationship between changes in extra-cellular dopamine concentration and ^{11}C-Raclopride binding in these studies is a very clear argument that this is the main component of the change in ^{11}C-Raclopride signal seen in paired-scan PET studies.

5 Dopamine Response to Opioids

The previous chapter dealt, at some length, with the methodology of ^{11}C-Raclopride PET scanning. In this chapter I will now go on to describe the use of these techniques to examine the effect of opioids on the dopamine system in opioid addicted patients. This chapter will describe a study in two parts. The primary aim of the study was to examine the hypothesis that drugs of abuse, specifically opioids, provoke dopamine release in the ventral striatum in human addicts. The evidence for this theory has been discussed in the introduction to this thesis, Section 1.4.3.1.1. Therefore the hypotheses were that:

1. a dose of opioid agonist would produce a dopamine response measurable by displacement of ^{11}C-Raclopride;
2. and that the amount of dopamine release would be related to the level of subjective and objective intoxication produced by the agonist.

The two arms of the study were identical except for the opioid agonist administered. In the earlier part this was a subcutaneous injection of hydromorphone and in the later part an intravenous injection of diamorphine.

5.1 Methods

Approval was obtained from the relevant local ethics committees, NHS Trust Research Governance committees and the Administration of Radioactive Substances Advisory Committee.

5.1.1 Subjects

Two groups of subjects were recruited, using the criteria below. All subjects were recruited from the local drug treatment agencies. After a full explanation of the study and provision of approved information leaflets, written informed consent was obtained.

5.1.1.1 Inclusion and exclusion criteria

The primary inclusion criterion was addiction to opioids. On this background criterion the exclusion criteria were then developed as required by ethical constraints, regulatory bodies and in order to minimise the heterogeneity of the sample population and remove potential confounds. Therefore subjects had to be aged between 18 and 65 years. The minimum age was determined by the Administration of Radioactive Substances Advisory Committee (ARSAC) consequent upon the radiation dose administered during the PET scans, and the upper limit was an arbitrary divide intended to exclude those with a higher likelihood of cerebral atrophy or Parkinson's disease. In addition, it has previously been shown that opioid receptors (Zubieta *et al.*, 1999) and dopamine receptors (Antonini *et al.*, 1993) change with normal ageing.

We required subjects to be stable on a prescribed dose of methadone of at least 15mg/day. We sought to recruit subjects with a range of methadone doses above this minimum threshold. The 15mg/day threshold was chosen to ensure that subjects would be sufficiently opioid tolerant to be administered 50mg IV diamorphine

without undue risk of overdose. Subjects stable on methadone were chosen as this would give an easily quantifiable measure of their level of opioid tolerance. "On-top" use of heroin was not an exclusion criterion for two reasons. Primarily there was a concern from one of the ethics committees approving the study that we may provoke relapse in patients by administering an opioid agonist; patients using "on-top" heroin could not be considered abstinent and therefore relapse was not a concern. Secondly, and equally importantly, continuing use of heroin meant that an acute agonist challenge was mimicking, as closely as possible within the scanner environment, the current experience of drug use, i.e. acute dose on the background of methadone. As for the craving study described in Chapters 2 and 3, we aimed to get the subjects as drug free as possible, excluding opioids and smoking.

Concurrent use of stimulants, such as amphetamine and cocaine, was also an exclusion criterion at anything other than an occasional level. The rationale for this was that stimulant drugs are known to act directly at the dopamine synapse and would therefore alter the ^{11}C-Raclopride signal we were trying to measure (Cadenas *et al.*, 2004). Stimulant addiction is also known to cause down-regulation of ^{11}C-Raclopride binding (Ginovart *et al.*, 1999; Volkow *et al.*, 1997c) which can take some time to recover. We did permit patients with a past history of stimulant use to enter the study, but excluded those with a history of addiction. It was not possible to exclude all subjects with previous, or even current, occasional stimulant use as this would have excluded all but a very atypical minority of patients from the studies. Very few contemporary heroin addicts have no use of stimulants in the area served

by the Bristol Specialist Drug Service. This has been an increasing trend seen in the national statistics (Chivite-Matthews *et al.*, 2005).

Concurrent or past addiction to any other substance was also an exclusion criterion, with the exception of nicotine. All subjects were current smokers. We permitted a history of heavy alcohol consumption, but not in the past year.

5.1.1.2 Hydromorphone study arm subjects

I recruited nine methadone maintained opioid dependent males from the local drug treatment centre. From a clinical interview and review of their case-notes I confirmed that they all satisfied ICD10 (World Health Organization, 1992) and DSM-IV (American Psychiatric Association, 1994) criteria for opioid dependence. Basic demographic data are displayed in Table 5.1. As well as being on prescribed methadone, all subjects were also continuing to use "street" heroin on top of their prescription to varying degrees. Two were later excluded for testing amphetamine or cocaine positive on urine screening on the day of a PET scan. 1 subject subsequently dropped out after receiving only 1 of the 2 planned PET scans.

5.1.1.3 Heroin study arm subjects

For the second arm of the study I recruited 10 methadone maintained opiate dependent males from local drug treatment agencies. As well as being on prescribed methadone, all subjects were also continuing to use "street" heroin on top of their prescription to varying degrees. One was later excluded for testing cocaine positive

on urine screening. One other subject subsequently dropped out after receiving only 1 of the 2 planned PET scans. Eight remaining subjects completed the study. Basic demographic data are displayed in Table 5.1.

		Hydromorphone Study Arm	**Heroin Study Arm**
Number of subjects recruited		9	11
Number not completing the study		3 (1 single scan, 1 cocaine +ve, 1 amphetamine +ve)	3 (2 single scan, 1 cocaine +ve)
	Age	25, 25 & 27 years	28, 31 & 40 years
	Methadone daily dose	20, 25 & 50 ml/day	35, 45 & 45 ml/day
Number completing the study		6	8
	Age	32.6 ± 5.0 years	34.7 ± 9.7 years
	Methadone daily dose	46.7 ± 13.2 ml/day (Range 35-70 ml/day)	40.6 ± 10.1 ml/day (Range 30-50 ml/day)

Table 5.1: Demographic Data for both ^{11}C-Raclopride study subjects

5.1.2 Protocol

The overall protocol was that subjects attended for two PET scanning sessions. Before each session they completed a variety of questionnaires. Immediately prior to the scan they were administered an injection of opioid or placebo in a double-blind random order cross-over design. During the scanning session visual analogue scales were used to measure subjective effects and saccadic eye movements were used to assess objective effects of the injections. Each element of this protocol is described in more detail below.

As will be seen, a large number of measures were collected. The rationale for this

was that the PET data would measure the dopamine response. We collected physiological and objective measures of intoxication to quantify the effects of the opioid agonists administered. Lastly, we collected data on a number of potential confounding variables so that they could be excluded as the cause of any measured dopamine signal, for example anxiety or depressive mood states.

5.1.2.1 Questionnaires

After being recruited into the study, all subjects completed questionnaires on general health, personality factors and history of drug dependence. The personality questionnaires chosen were the Eysenck Personality Questionnaire - revised (EPQ-R) and the Eysenck Personality Questionnaire – Impulsiveness, Venturesomeness, Empathy (EPQ-IVE) (Eysenck & Eysenck, 1975; Eysenck *et al.*, 1985). These were chosen as well known broad personality inventories. It is known that heroin addicts have a different spread of scores on these scales compared to control populations, generally scoring higher on neuroticism and psychoticism on the EPQ-R (Gossop & Eysenck, 1980). Similarly, drug users have a different distribution of normal scores on the EPQ-IVE (e.g. Butler & Montgomery, 2004). In addition to the personality inventories, each subject completed the MOS-SF36 general health survey (SF-36) (Jenkinson *et al.*, 1996). This was chosen as we had already used the same instrument in a number of addiction related projects within Bristol. We wanted to include a measure of general health as a way of screening for chronic ill health or pain, as these are known to affect the opioid system (Jones *et al.*, 1991).

We gathered three primary measures of drug use, using the Severity of Dependence scale (Gossop *et al.*, 1995), a version of the Obsessive Compulsive Drinking Scale (Anton *et al.*, 1995) modified for use with injecting opiate users (see Law *et al.*, 1997) and a structured drug use history. The Severity of Dependence scale offers a very straightforward measure of the dependency on a number of drugs, which we planned to use to moderate any potential confounding effects on our primary outcome measure. The main purpose of the structure drug history was to ensure compliance with the inclusion and exclusion criteria.

All of the questionnaires were administered just once to each subject as they purport to measure relatively static characteristics. These were augmented by several additional questionnaires used to measure both state of mind on the day of the PET scans and the effects of administered drugs. On each scanning day, prior to scanning, subjects completed the Spielberger State/Trait anxiety inventory (STAI, Spielberger *et al.*, 1983), the Beck Depression Inventory (BDI, Beck *et al.*, 1961) along with a general mood profile visual analogue scale. These questionnaires were chosen as a general screen for potential confounding factors that may interfere with the dopamine signal, such as anxiety or sadness.

In order to capture drug related states of mind, like craving and withdrawal, we also administered four additional scales prior to each PET scan. For craving, we used the Heroin Craving Questionnaire (HCQ, Weinstein *et al.*, 1997) which we had previously used in all heroin craving studies in the unit, including those in chapter 2. We wanted an objective measure to use as an adjunct to the other subjective or self-

report measures. To this end we used a modified version of the Opiate Withdrawal Scale (OWS, Kolb & Himmelsbach, 1938). As baseline measures of possible drug effects we used the Addiction Research Centre Inventory (ARCI, Haertzen, 1974) and the Adjective Checklist (AC, Jasinski, 1977). These four scales (ARCI, OWS, AC, HCQ) and the mood profile were repeated immediately after the PET scanning sessions to assess changes. One last questionnaire was administered asking subjects to classify and rate the strength of the pre-scan injection.

All questionnaires are reproduced in appendix 8.2.

In addition to the above questionnaires on drug use we also conducted a case-note review of drug use histories. We wanted to derive a simple measure that somehow encompassed the past drug use history for each subject. In order to do this we created a rating scale of drug use comprising definitions of duration, quantity and route of drug use for all the commonly abused drugs. Two very experienced addiction psychiatrists (the author and a colleague) then took these ratings scales to derive measures of drug use from the subjects' case-notes for the month and year prior to scanning as well as a total lifetime measure. The two raters completed these ratings independently and then compared the concordance. In cases of disagreement, a mean score was calculated.

5.1.2.2 Visual Analogue Scales (VAS)

In order to assess changes in subjective state during the PET scans we used a verbal form of visual analogue scales. We could not use questionnaires during the scans as

the subjects had to lie supine in the scanner and move as little as possible. We also did not want any confounding motor signal to alter dopamine release in the striatum. We therefore developed a standard technique for presenting written visual scales to the subjects while asking them to respond verbally to with a number corresponding to their current state. The exact scales, as they were presented, are shown in Appendix 2, with the other questionnaires. In this study the scales used were as follows:

1. At this moment I feel this sleepy .....
2. At this moment my urge to take heroin is .....
3. At this moment the intensity of my craving for heroin is .....
4. At this moment I feel this gouched out .....
5. At this moment I feel I am withdrawing .....
6. At this moment I feel this high .....
7. At this moment I feel this much of a rush .....

Subjects were asked to rate themselves on a standard scale for each of the above questions at baseline, before the injection, then at 5 minutes after the injection and at 15 minute intervals thereafter until the end of the scanning session.

For those not *au fait* with the street language of opioid use in Bristol, the term "gouched out" requires some brief explanation. It is a term used to describe the subject experience of opioid intoxication and is in widespread use throughout England. In essence it includes elements of psychological calm, relaxation and sedation, as well as physiological sensations like "pleasant sick" which describes the visceral sensation of opioid intoxication.

5.1.2.3 Physiological measures

Previous work in our unit has shown us that saccadic eye movements are a reliable method for assessing the central effects of psychoactive substances, including opioids (e.g. Melichar *et al.*, 2003). As in the case of the visual analogue scales, the subjects had their saccadic eye movements measured at baseline and then 5 minutes after injection, followed by every 15 minutes until the end of the scan. We used the same saccadic eye movement procedure as in our previous studies. This meant that we sequentially tested eye movements at 35° saccades decreasing to 5° saccades with two repeats at each angle. Data was then interpolated to 30° from all data points. The recorded eye movements were then analysed to produce measures of peak velocity, peak acceleration, peak deceleration and acceleration:deceleration ratio.

Blood samples were taken at baseline for estimation of plasma methadone levels. Further samples were taken 5 and 20 minutes after the scan start for estimation of hydromorphone or heroin metabolite levels. These samples were spun down and frozen for storage on the day of the scan. The samples from both studies were then sent to collaborators in Switzerland for analysis of plasma methadone enantiomers, hydromorphone, diamorphine and their metabolites.

5.1.2.4 Pre-scan interventions

In both arms of the study, subjects were given a pre-scan injection. The injection contained either an active opioid agonist or saline placebo of similar volume. Both the subjects and investigators in the scanning room were blind to the injection

content. One investigator, not in the scanning room, knew the injection content and was carrying naloxone, a specific opioid antagonist, in case of overdose. However, this was never needed. All investigators, but not the subjects, knew that each subject would receive one active injection and one placebo injection in random order prior to the two scanning sessions. Subjects were told that they could receive the active injection on one, both or neither occasion. In this way, at the second scan subjects would still be unable to deduce the content of the injection, even if they had correctly identified the injection at their first scan.

For the first arm of the study, subjects were given a subcutaneous injection 15 minutes prior to the scan start. The active opioid injection contained 10mg Hydromorphone. This is a potent mu-opioid agonist equivalent to approximately 35mg diamorphine. The timing was chosen as we knew from previous studies that hydromorphone SC will have reached its maximal effect by this time.

Preliminary analysis of the first arm of the study revealed that the subjects were only reporting mild to moderate levels of intoxication. This occurred at the same time as hydromorphone for injection became unavailable in the UK. Therefore we revised the protocol for the second arm of the study to use a stronger stimulus, i.e. a larger dose intravenously. As a result, subjects were given an intravenous injection 5 minutes prior to scan start. The active opioid injection contained 50mg diamorphine. At current estimated street purity of 11% this would equate to approximately 0.5 gr "street" heroin. Again, the injection time was chosen to ensure peak drug effects prior to the injection of ^{11}C-Raclopride.

5.1.2.5 Scanning protocol

Each subject underwent 2 PET scans with ^{11}C-Raclopride approximately 1 week apart (range 1-3 weeks). All scans took place at approximately 1pm to avoid temporal effects confounding any differences found between scans. On scan days the first 2 subjects, in the hydromorphone arm of the study, were instructed to take half their usual daily methadone dose at 8 am, i.e. 5-6 hours before scan start. The remainder of the subjects took no methadone prior to scan start. As most subjects took their methadone routinely at around 10am this meant that the majority of subjects were 27 hours after their last dose at the time of scanning.

The PET images were acquired on a brain dedicated Siemens/ECAT HR++ scanner. Following a bolus injection of 120MBq ^{11}C-Raclopride over 30 seconds, we acquired images for 90 minutes. The images were acquired using listmode acquisition, as described in the previous chapter. Dynamic images were rebinned into 26 frames starting with a variable duration background frame then short initial frames extending to 5 minutes [1*15sec, 1*5sec, 1*10sec, 1*30sec, 4*60sec, 17*300sec]. Images were reconstructed using filtered back projection with a ramp filter. A matching pair of images was created for each scan, one with measured attenuation correction from a transmission image, and the second with no attenuation correction.

5.1.3 Analysis methods

5.1.3.1 PET images

The ^{11}C-Raclopride images were analysed as described in some detail in the previous chapter. In brief, the images were corrected for movement using SPM2 with movement parameters derived from non-attenuation corrected images. These motion corrected images were then analysed with the RPM software to produce maps of Binding Potential. We then used automated sampling techniques to derive mean levels of ^{11}C-Raclopride binding in the six regions of interest; namely, left and right caudate, putamen and ventral striatum. These were then compared between scanning sessions using paired t-tests.

5.1.3.2 Questionnaires:

Baseline questionnaires on personality and other unchanging variables like drug history were compared to population norms. State questionnaires performed only once per scan were compared using paired t-tests to examine for between-scan condition differences. State measures completed pre- and post-scan were compared using repeated measures ANOVA with time (pre- vs. post-scan) and condition (placebo vs. drug) as within-subject effects, and drug (hydromorphone vs. heroin) and scan order (placebo scan first vs. drug scan first) as between-subject effects.

5.1.3.3 Visual Analogue Scales (VAS)

VAS were collected at 2 baseline time points and 7 time points following injection of

either opioid or placebo. For each scan I used a trapezoid method to calculate an area under the curve (AUC) measure of change from baseline. These AUC measures were compared using paired t-tests for the effects of the drugs and entered into a repeated measures general linear model analysis to examine for effects and interactions between drug and placebo, and heroin and hydromorphone. All VAS data was also entered into a repeated measures ANOVA with scan condition and time point as the within-subject variables.

5.1.3.4 Physiological data

The intention was to analyse the saccadic eye movement data in a similar manner to the visual analogue data, i.e. as a repeated measures general linear model design with condition and active drug as the independent variables. This proved not to be possible as the main effect of the heroin was to make the subjects too intoxicated to complete the task, particularly at the earlier time points. Therefore only a descriptive summary of the data was possible.

5.2 Results

5.2.1 Subjective measures

5.2.1.1 Personality variables

The personality questionnaire results are presented in Table 5.2. They showed the subjects to be high on scores of Psychoticism, Addiction and Criminality as expected from published studies of drug dependent populations (Gossop & Eysenck, 1980). There was a moderate elevation of mean neuroticism scores of less than one standard

deviation, this was very close to the published data for addicts in treatment. We found a similar result for the psychoticism scale. In contrast, on the extroversion scale our subjects actually scored closer to the general population levels than the addicts' data published. On the Criminality scale our subjects were scoring at levels very close to the report norms for prisoner populations (prisoners: 15.57±5.18) rather than controls (shown in Table 5.2).

In contrast to the EPQ-R, I could find no published studies of the EPQ-IVE in drug using populations. As can be seen from Table 5.2, the small sample studied here scored higher on both Impulsiveness and Venturesomeness, but approximately the same on the empathy scale as published norms for males of similar age.

The SF-36 health measure showed a general poor level of health for our patient sample compared to the general population (Jenkinson *et al.*, 1993). The general population norms are shown in Table 5.2 for males aged 25-34 years. As can be seen from the table, the addict sample scores well below these norms. What is not shown in the table is that the reported mean scores for patients with self-reported long-standing illness also score better than our addict sample. The largest difference was in the Social Functioning scale. The addicts scored around 33 which is about 3.5 standard deviations below the population norm (91.3) and still 1.8 standard deviations below those with chronic illness (80.2). Our sample also scored very poorly on the Mental Health subscale. In this case they were only 2.2 standard deviations below age-matched norms (75.8) and 1.5 standard deviations below the chronic illness population (69.9). On all the other subscales the addict sample scored

at levels very close to the chronic illness population.

The OCDS showed generally high scores on both subscales of obsessive thinking about drugs and compulsion to use drugs. A subsection of those items used in the OCDS-R (Morgan 2004) showed a mean score of 17.5, which was higher than that shown in the original validation study. There was a non-significant trend for the hydromorphone group to score worse than the heroin group (Table 5.2).

Table 5.2Personality and General Characteristics of the Study Samples

Scale		All	Hydromorphone group	Heroin group	Published norms (males only if different)	Addiction population norms (if available)
EPQ-R	Neuroticism	13.5±5.39	16.2±3.35	11.1±5.86	10.5±5.81	15.8±4.67
	Extroversion	13.1±4.73	13.1±4.83	13.0±4.9	12.5±6.0	15.2±4.94
	Psychoticism	10.3±3.6	9.4±4.3	11.0±2.87	7.2±4.6	10.7±4.64
	Lie	5.5±3.55	4.9±3.26	6.1±3.87	7.1±4.28	3.1±2.75
	Addiction	16.5±4.82	18.6±4.72	14.6±4.3	11.6±4.96	19.8±4.96
	Criminality	16.3±5.27	18.3±5.29	14.5±4.79	9.0±4.54	
EPQ-IVE	Impulsiveness	9.7±4.72	8.8±5.43	10.8±3.83	6.6±4.43	
	Venturesomeness	11.5±3.44	10.0±3.92	13.2±1.79	7.6±4.25	
	Empathy	11.2±3.72	12.1±3.14	10.2±4.24	12.0±3.31	
SF36	Physical Functioning	78.3±28.8	81.7±22.1	75.5±34.2	93.9±14.2	
	Role functioning – physical	69.7±31.8	50.0±35.4	84.1±20.2	92.0±23.2	
	Bodily Pain	64.8±24.4	65.5±19.9	64.3±28.2	87.5±17.7	
	General Health	60.7±20.9	61.0±22.6	60.5±20.7	76.7±17.7	
	Vitality	51.9±10.8	46.3±11.9	56.0±8.11	64.5±17.3	
	Social Functioning	33.6±11.5	27.8±12.9	37.9±8.54	91.3±16.3	
	Role functioning – Emotional	71.9±27.8	70.8±27.8	72.7±29.1	87.1±27.9	
	Mental Health	46.0±11.2	41.7±11.1	49.1±10.7	75.8±15.2	
OCDS	Obsessive	9.56±5.99	11.1±4.83	8.0±6.89		
	Compulsion	14.4±7.95	15.4±8.93	13.3±7.21		
	OCDS-R	17.5±9.41	19.1±10.0	15.9±9.06		9.77±6.70

The drug profile data showed good inter-rater agreement with Spearman's rank correlations ranging from 0.35 to 0.846 (median 0.63) for the categorical measures and Pearson's from 0.86 to 0.99 (mean 0.92) for the measures of years of use. The least reliable measure was estimated lifetime stimulant use, although still with a Pearson's r = 0.86. Summary data for the agreed values are presented in Table 5.3 and Table 5.4.

Variable	Hydromorphone		Heroin		All	
	Median	Range	Median	Range	Median	Range
Opiates Last Month	3	2-4	3	3-3.5	3	2-4
Opiates Last Year	3	2-4	3	2-4	3	2-4
Opiates Lifetime	3	2-4	3.5	2-3.5	3	2-4
Tobacco Last Month	3	3-4.5	3.25	3-5	3	3-5
Tobacco Last Year	3	2.5-4.5	3.25	3-5	3	2.5-5
Tobacco Lifetime	3	2-4	3.75	3-5	3.5	2-5
Alcohol Last Month	1.5	0.5-4	1.25	0-2	1.25	0-4
Alcohol Last Year	2.75	2-4	1.5	0-2	2	0-4
Alcohol Lifetime	2.25	1.5-4	2	2-2.5	2	1.5-4
Stimulants Last Month	0	0-2.5	0	0-0.5	0	0-2.5
Stimulants Last Year	1.5	0-2	2	0-0.5	1.75	0-2
Stimulants Lifetime	2	1-3	2.5	0-3	2	0-3
Cannabis Last Month	2	0-4	1	0.3	1.5	0-4
Cannabis Last Year	3	0-4	2.5	0-3	3	0-4
Cannabis Lifetime	3	1.5-4.5	3	0-4	3	0-4.5
Benzodiazepines Last Month	0	0-1	0	0-0.5	0	0-1
Benzodiazepines Last Year	0.5	0-2.5	0	0-1.5	0.5	0-2.5
Benzodiazepines Lifetime	1	0-3.5	0.25	0-2	1	0-3.5

Table 5.3: Measures of Past Drug Use (Categorical Variables)

	Hydromorphone	Heroin	All
Duration of use	**Mean ± SD**	**Mean ± SD**	**Mean ± SD**
Opiates	9.67 ± 4.12	11.81 ± 8.18	10.68 ± 6.24
Tobacco	15.67 ± 6.1	17.4 ± 11.13	16.29 ± 7.86
Alcohol	14.19 ± 4.27	15.75 ± 4.26	14.86 ± 4.18
Stimulants	6.67 ± 5.83	7.68 ± 7.99	7.11 ± 6.63
Cannabis	13.94 ± 6.55	8.00 ± 4.85	11.82 ± 6.51
Benzodiazepines	5.56 ± 7.6	1.38 ± 2.43	4.17 ± 6.53

Table 5.4: Measures of Duration of Past Drug Use (years)

5.2.1.2 Pre-scan state

There was no difference in pre-scan measures of BDI, STAI on drug or placebo days, as can be seen from the data presented below (Table 5.5). There was also no difference in scores between the first and second scans, suggesting an absence of an order effect that could have confounded the results. The mean of BDI scores was in the mild to moderate depression range. Finer analysis of the data showed that the subjects endorsed the items for Insomnia, Sense of Failure, Retardation, Fatigability and Self Accusation most frequently. Clinically, none of the subjects had a diagnosis of depression and the items endorsed could also be explained as side-effects of opioid addiction. The items also mirror the findings on the SF-36 of fairly poor levels of general health.

The scores on the STAI are close to the reported population average of 36±11 for normal volunteers (Spielberger *et al.*, 1983).

Table 5.5: Pre-scan Variables

Scale	All		Hydromorphone group		Heroin Group		
	Placebo day	Drug Day	Placebo Day	Drug day	Placebo Day	Drug Day	
State Anxiety	34.9±11.0	36.9±9.36	40.4±10.6	39.8±9.08	30.9±9.92	34.1±9.25	ns
Trait Anxiety	40.6±10.9	40.4±10.2	47.0±9.41	44.9±10.8	35.5±9.43	36±7.71	ns
BDI	12.7±7.2	12.4±9.45	14.6±8.80	14.1±10.5	11.3±5.82	10.4±8.38	ns

ns = non-significant on repeated measures ANOVA with group (hydromorphone vs heroin) and scan order as between-subject effects and condition (drug vs. placebo) as within-subject effect.

5.2.1.3 Drug effects

The effects of the injection (placebo or active drug) on the Adjective Checklist, ARCI and Opiate Withdrawal Scale are shown below (Table 5.6). Using the repeated measures ANOVA showed that there was a significant time (pre-post scan) by condition (drug vs. placebo) effect on both the agonist and withdrawal subscales of the Adjective Checklist (Agonist F=13.89, p=0.034; Withdrawal F=11.54, p=0.043). Specifically, the active opioids produced an increase in scoring on the agonist scale that was not seen in response to the placebo injections. In addition, the withdrawal subscale showed significant interaction with both the drug (hydromorphone or heroin) and order (placebo first vs. drug first) terms. Inspection of the raw data showed that pre-scan the withdrawal scores were strangely higher in the hydromorphone arm of the study compared to the heroin arm. There is no obvious reason why this should be the case as the subjects were in very similar states in both studies, i.e. about 26 hours after their last dose of methadone. Also there was no such difference on the observer rated withdrawal scale.

The MBG (morphine-benzedrine-group) scale of the ARCI showed a significant condition by time interaction on the repeated measures GLM (F=9.098, p=0.024). This translates as the opioid injection producing a larger increase in the scale compared to the placebo injection. This effect showed a barely significant interaction with order (F=6.02, p=0.050) and a more significant interaction of time by condition by drug by order (F=7.793, p=0.032). The A (amphetamine) subscale also showed a significant time by drug by order (F=16.932, p=0.006) and main time (F=6.58, p=0.04) effect.

Table 5.6: Drug effects of questionnaire ratings

Scale	All				Hydromorphone				Heroin			
	Placebo		Drug		Placebo		Drug		Placebo		Drug	
	Pre	Post	Pre	Post	Pre	Post	Pre	Post	Pre	Post	Pre	Post
Adjective Checklist – Agonist	21±5	19±5	21±7	27±7	19±4	17±2	19±5	29±7	22±6	20±6	23±8	26±8
Adjective Checklist - Withdrawal	9±9	8±6	8±8	8±14	16±9	10±6	13±9	13±2	4±4	7±6	3±3	4±4
ARCI – MBG	6±4	5±2	5±4	6±4	4±2	3±1	3±1	5±5	8±4	6±2	7±4	8±3
ARCI – LSD	4±3	4±2	4±3	4±3	7±2	5±3	6±3	6±4	3±1	3±1	3±1	3±2
ARCI – PCAG	5±3	5±3	5±4	6±4	7±3	7±3	7±4	7±4	5±2	4±2	3±1	4±2
ARCI – BG	6±2	5±2	5±2	5±2	4±2	3±2	4±1	4±2	7±2	6±2	7±2	6±1
ARCI – A	3±3	3±2	3±2	4±3	2±1	2±2	2±2	3±3	4±3	4±2	4±1	5±2
OWS	0±0	0±0	0±0	1±2	0±0	0±0	0±0	1±2	0±0	0±0	0±0	0±0

Examining the raw data for the mood scales showed that the individual subjects had been interpreting the scales in very different ways. The spread of baseline values was extreme, as demonstrated by the standard deviations of the data frequently being an order of magnitude larger than the means. This meant that generating any form of

mean value at any given time-point was unlikely to be representative of the data. Therefore, a difference measure was calculated to show the amount of change in each scale that was reported by each subject in response to the injection. The means of these change scores (post-scan minus pre-scan scores) are summarised below (Table 5.7). These data were still analysed using a repeated measures GLM as this accounts for inter-individual differences in baseline scores and examines within-subject changes in scores.

Table 5.7: Mood changes following injection

Scale	All		Hydromorphone		Heroin	
	Placebo	Drug	Placebo	Drug	Placebo	Drug
	Change (Post-pre scan)	Change (Post-pre scan)	Change (Post-pre scan)	Change (Post-pre scan)	Change (Post-pre scan)	Change (Post-pre scan)
Nervous	0.58±20.6	11.6±29.8	6.88±18.6	1.25±11.2	-4.82±22.1	18.9±37.4
Tired	-4.42±16.9	10.4±32.1	-13.3±20.1	8.00±14.0	3.21±8.83	12.1±40.3
Depressed	-0.38_20.7	8.23±22.5	4.38±24.3	-1.75±24.2	-4.46±18.0	15.4±36.8
Relaxed	6.83±22.2	13.0±22.5	11.0±24.5	2.25±19.0	3.21±21.4	20.7±22.8
Drowsy	1.63±31.4	-11.0±20.5	3.75±12.6	-9.50±16.7	-0.18±42.8	-12.1±24.1
Alert	9.81±65.3	6.56±36.6	-4.58±36.2	6.75±15.9	22.1±83.9	6.43±47.8
Energetic	-17.1±40.6	5.00±31.5	5.42±17.0	23.4±39.0	-36.4±46.0	-5.54±23.1
Clear-headed	-4.04±17.1	12.1±26.3	0.00±13.7	10.3±32.9	-7.50±19.9	13.4±23.4
Sociable	25.3±59.1	2.08±14.7	-4.38±25.9	-0.50±22.0	50.7±69.2	3.93±7.95
Cheerful	-9.23±43.1	1.67±14.7	15.6±22.3	1.75±24.2	-30.5±46.4	1.61±2.77
Irritable	11.2±31.7	7.08±34.5	-1.88±24.3	-0.25±29.6	22.3±34.6	12.3±39.0
Confused	-1.06±16.7	-6.35±17.4	3.54±11.7	-2.75±5.48	-5.00±20.1	-8.93±22.8

HCQ had to be abandoned because the subjects became confused and frustrated with the questionnaire and refused to fill it in.

5.2.1.4 Visual Analogue Scales

The complete VAS data are presented in Figure 5.1. There was a large amount of variability in the responses to the injections and the scanner environment as a whole. Evidence of this can be seen in the large standard deviations on the figures. Due to the high correlations between some of the measures (see Table 5.8), they were combined to form composite scales. Specifically, the "crave" and "urge to use"scales were combined, as were the "high" and "gouched" scales. The correlations between the VAS scales were calculated taking each individual time point as an independent measure. Statistically this cannot be used to argue that these scales are highly intercorrelated in the population as a whole as this method conflates between- and within- subject variance. Nevertheless it is still valid to say that in these subjects as a group the measures are correlated. Reducing the VAS data in this way to five scales instead of seven also reduces the number of statistical tests, and hence the chance of Type I error.

	Urge	Crave	Gouched	Withdrawal	High	Rush
Sleepy	-0.262	-0.263	0.686	-0.035	0.546	0.367
Urge		**0.898**	-0.213	0.588	-0.084	-0.136
Crave			-0.202	0.676	-0.086	-0.136
Gouched				-0.026	**0.818**	0.516
Withdrawal					-0.026	0.007
High						0.526

Table 5.8: Pairwise Pearson's correlation coefficients between VAS scales. Scales to be combined shown in bold.

5.2.1.4.1 Sleepy

Results for the sleepy VAS scale were similar from the repeated measures analysis using all the data, and using the Area-Under-the-Curve measures. For all the timepoint data there was a general effect for sleepiness to increase during the scanning session in both the active and placebo conditions. As a main effect of time the differences were significant at 15, 30, 45 and 60 minutes after injection. There was also a significant main effect of condition ($F=6.64$, $p=0.026$) with the active injection causing more sleepiness. Looking at the time by condition interaction it can be seen that the significant increase in sleepiness occurred at 15 minutes after the injection and continued to the end of the session. There was no time by condition by drug or condition by drug interaction effect. Using the AUC measures, there was a main effect of condition ($F=9.45$, $p=0.011$), but no interaction of condition by drug.

5.2.1.4.2 Crave / Urge

As described above, the "urge to use" and "crave" measures behaved in a identical manner, as has been found in Chapter 2. Examining the individual time-points showed that the combined measure significantly declined with time at all time points. There were no other significant effects. This was surprising as visual inspection of the data showed that in the hydromorphone study the Crave/Urge levels decreased a little in the placebo condition, but decreased more following hydromorphone injection. In the heroin study the measure stayed fairly flat in the placebo condition but reduced to zero for the duration of the scan following heroin injection. The most

likely reason is that the levels were low in the placebo condition and that floor effects prevented statistical separation of the scores after the injections.

5.2.1.4.3 Withdrawal

In both groups, withdrawal ratings started low, and remained so in the placebo condition. However, it was completely reduced to zero by both active injections. There were no statistically significant effects using either analysis technique, which again probably represents a floor effect.

5.2.1.4.4 Gouched / High

As these measures were so highly correlated, the combined scale was analysed. Using the data from all time points there was a significant interaction between time and condition with ratings increasing following active drug and slightly decreased after placebo, which started at 15 minutes after the injection and continued to the end of the session. It was not statistically significant, but there was a short increase in ratings after the placebo injection, but it was of much smaller magnitude than after the active injections. The AUC measure also showed a significant effect of condition, but no interaction with drug. There was a borderline main effect of drug with heroin scores being slightly higher that hydromorphone scores across conditions ($F=4.863$, $p=0.050$).

5.2.1.4.5 Rush

Visual inspection of the data from the "rush" scale showed results as expected.

There was a small, slow steady rise following subcutaneous hydromorphone and a much shorter, higher peak response to intravenous heroin. Statistical analysis showed no time by condition by drug interaction, but the time point data showed a significant condition by time interaction at 15 minutes after injection only. There was, however, a main effect of time at 15, 30 and 45 minutes after the injections. Using the AUC measure, there was a significant increase in rush after the active injection ($F=5.78$, $p=0.035$), but not interaction with drug or main effect of drug.

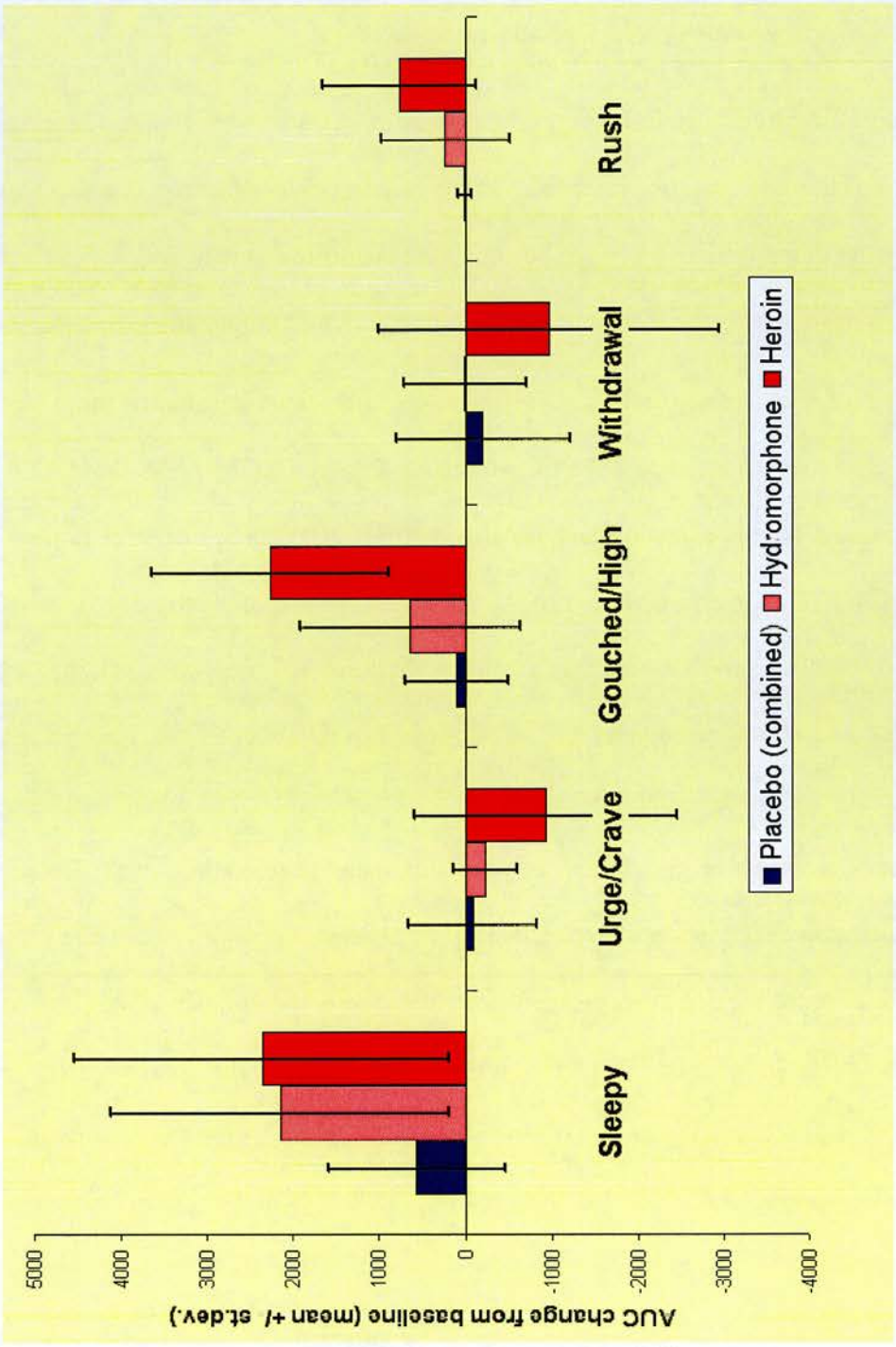

Figure 5.1: Subjective responses to Injection measured by VAS.

5.2.2 Physiological measures

No significant changes in Finapres® measures of any sort were found. Therefore, no more of this data will be presented. There was an observable drop in pulse oximetry after the diamorphine injection, but this was not formally recorded. If such a drop occurred following the hydromorphone injection, it was not noted at the time.

Of the 14 subjects who remained in the study, after the exclusion of those who had only one scan or tested positive for stimulants, 2 were lacking SEM data for the drug scan and 4 for the placebo scan. In all cases this was due to technical failure in the amplifier. However, inspection of the remaining data showed that the most striking effect of the active injections, heroin or hydromorphone, was that the subjects became unable to complete the task. This further reduced the quantity of data available and made further statistical analysis impossible. The picture was the same for all the variables measured: peak velocity, peak acceleration, peak deceleration, acceleration:deceleration ratio and latency. Only data for peak velocity are presented below (Figure 5.2). As can be seen from this figure, the number of subjects capable of performing the task fell from 6/6 to 2/6 immediately following the heroin injection, but gradually recovered to 5/6 subjects by 60 minutes. Conversely, the hydromorphone group showed a drop from 5/5 to 4/5 at 15 minutes post injection and then to 3/5 at 60 minutes, before recovering to 4/5 at the end of the session. For the heroin – placebo group, the number remained at 5/5 throughout and for the hydromorphone – placebo group it fell to 4/5 for most of the readings.

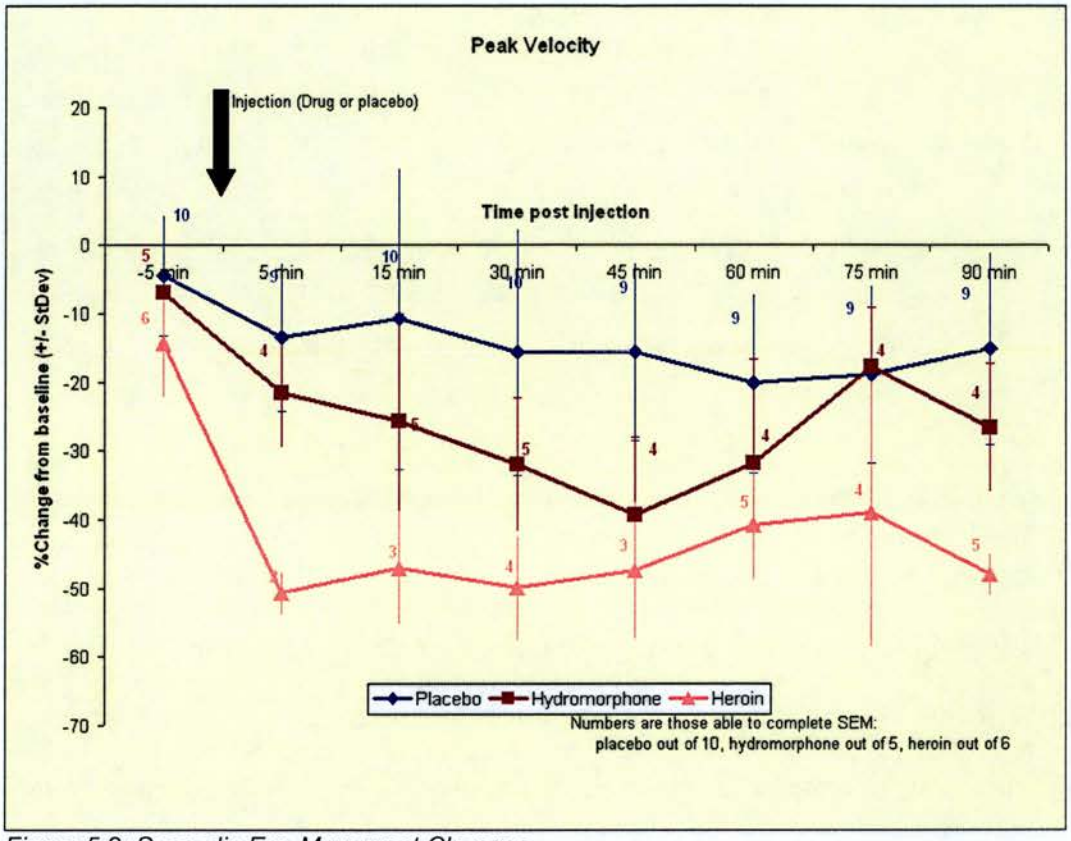

Figure 5.2: Saccadic Eye Movement Changes.

5.2.3 PET results

The mean values for ^{11}C-Raclopride BP are shown in Table 5.9. No significant change in dopamine receptor binding was seen using paired t-test for within-subject comparison between the two conditions in either group or in all subjects together. Using repeated measures ANOVA with condition (active or placebo) as within subject factor and active drug (heroin or hydromorphone) as the between subject factor also showed no main effect of condition nor was there any interaction between condition and active drug.

		Putamen		Caudate		Ventral Striatum	
		Left	Right	Left	Right	Left	Right
Hydro-morphone	Placebo	2.84±0.36	2.88±0.42	2.89±0.36	2.72±0.43	2.52±0.30	2.28±0.22
	Drug	2.76±0.30	2.70±0.36	2.73±0.24	2.61±0.30	2.44±0.14	2.24±0.26
Heroin	Placebo	2.81±0.25	2.79±0.24	2.68±0.26	2.61±0.34	2.49±0.34	2.21±0.33
	Drug	2.89±0.27	2.85±0.29	2.80±0.39	2.73±0.44	2.49±0.36	2.07±0.49
All	Placebo	2.82±0.28	2.83±0.31	2.77±0.30	2.66±0.37	2.51±0.30	2.24±0.27
	Drug	2.84±0.27	2.79±0.33	2.77±0.34	2.68±0.39	2.47±0.34	2.14±0.40
Controls	Nil	2.73±0.47	2.74±0.40	2.62±0.15	2.58±0.21	2.41±0.15	2.31±0.17

Table 5.9: Mean ^{11}C-Raclopride BP for regions of interest for hydromorphone, heroin, combined drug groups and historical control data.

Examining the placebo scans only and comparing these with data from 5 historical controls with a one-way ANOVA showed that there was no difference between the three groups. The full data are plotted in Figure 5.3. As can be seen from this figure, the control subjects, scanned at rest, are evenly interspersed with the hydromorphone and heroin subjects scanned after the placebo injection. The ladder plot also shows no consistent pattern of response to opioid agonist in either group, even though the means for the hydromorphone group might suggest it.

There were no significant correlations between subjective measures and ^{11}C-Raclopride BP. There were several subjects excluded for protocol violations, either completing only one scan or testing positive for stimulant drugs. Figure 5.4 is in the same form as Figure 5.3 but shows the data for all the controls, the included subjects and the excluded subjects. This clearly shows that the single subject excluded for amphetamine positive urine drug screen had markedly lower ^{11}C-Raclopride than any of the other subjects, including those testing positive for cocaine. The full details for

these subjects is shown in Table 5.10.

Subject	Scan	Reason for exclusion	Putamen		Caudate		Ventral Striatum	
			Left	Right	Left	Right	Left	Right
1395	1	Amphetamine in urine	1.90	1.70	1.96	1.82	1.85	1.82
	2	Amphetamine in urine	1.66	1.67	1.75	1.72	1.53	1.42
1538	1	Paired with cocaine scan	2.96	3.02	2.91	2.86	2.93	2.47
	2	Cocaine in urine	2.85	2.84	2.88	2.78	2.80	2.35
1863	1	Single scan only	2.96	2.93	3.19	2.87	2.91	2.52
2369	1	Single scan only	2.41	2.64	2.31	2.17	2.08	1.84
2604	1	Paired with cocaine scan	2.44	2.45	2.53	2.49	2.10	1.82
	2	Cocaine in urine	3.01	2.99	3.16	3.03	2.65	2.15
3119	1	Single scan only	2.59	2.63	2.30	2.43	2.53	2.42

Table 5.10: Individual ^{11}C-Raclopride BP data for scans excluded from the primary analysis

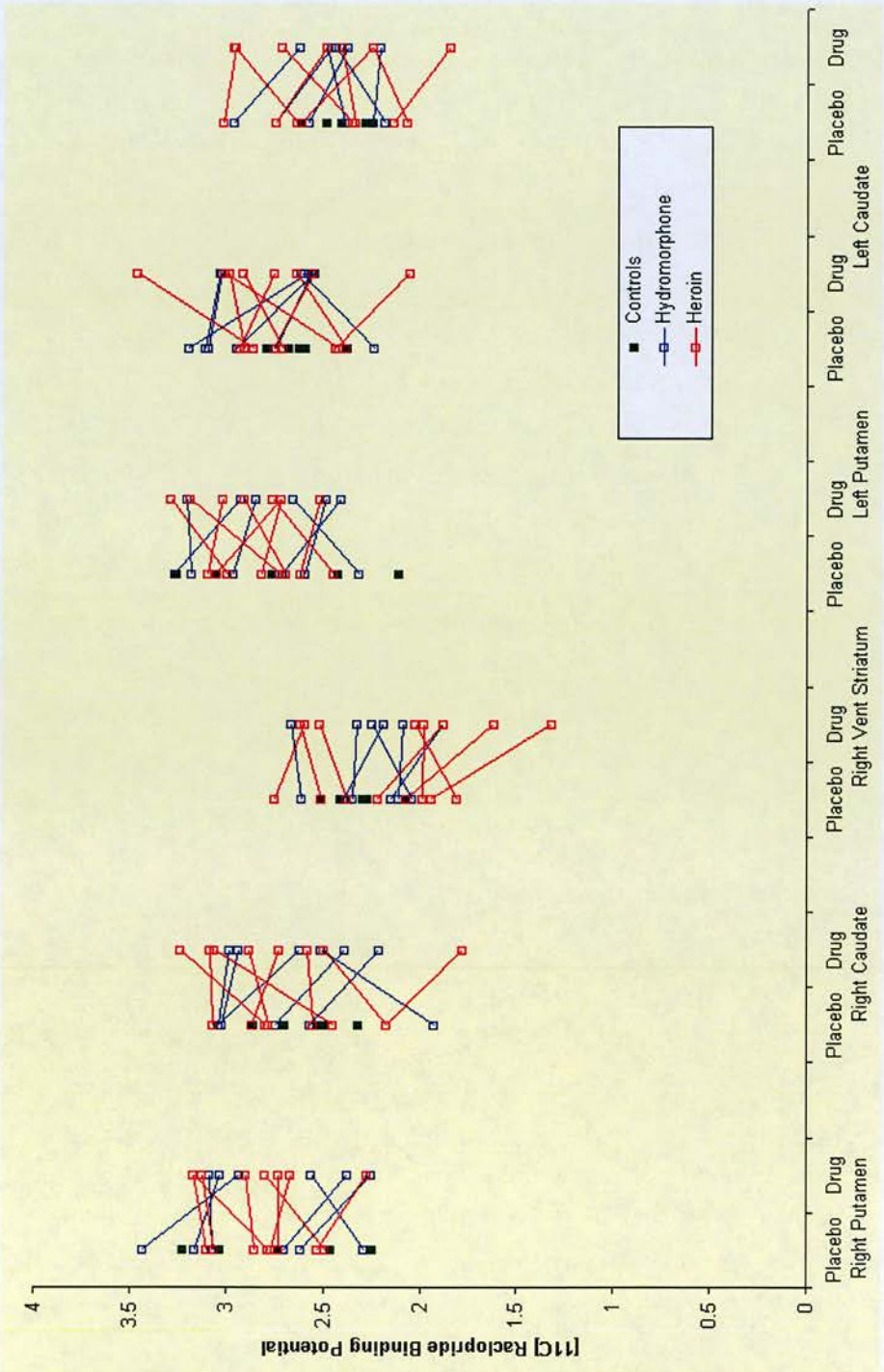

Figure 5.3: Ladder plot of the effect of opioid injection on [11C]Raclopride binding potential. (Each line represents one subject, except for historical controls where each marker is one subject.)

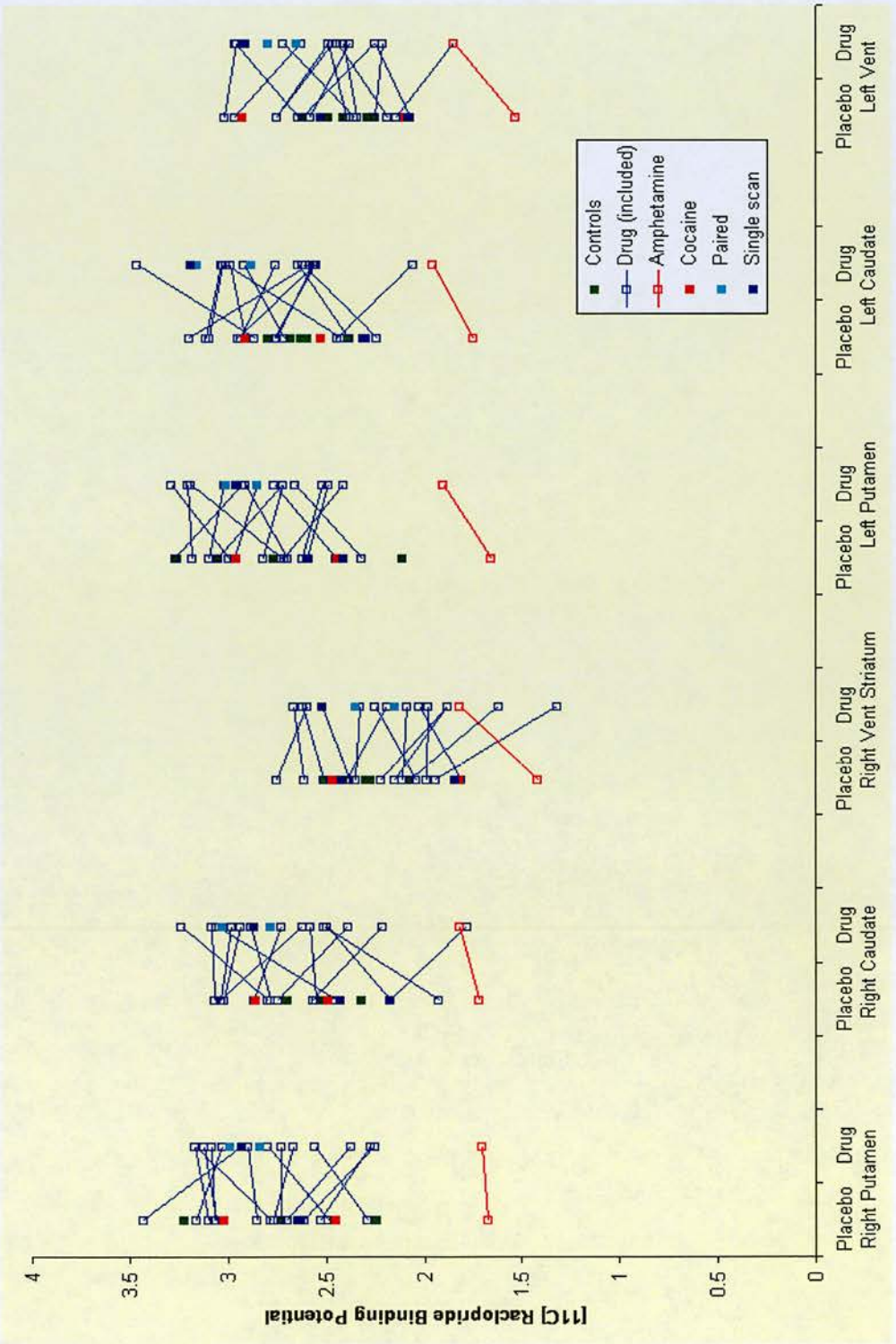

Figure 5.4: Ladder plot showing the BP values for those scans excluded from the primary analysis due to protocol violations. "Paired" are scans where the matching pair tested cocaine positive, but this scan was negative.

6 Discussion

The preceding chapters have presented results from a number of studies and the development of the methodologies required to obtain these results. The first study presented the effects of drug related autobiographical stimuli on brain activation patterns in abstinent heroin addicts. I showed that drug related stimuli activated the left anterior cingulate cortex more than matched neutral stimuli. I also showed that the subjective level of craving experienced as a result of those stimuli correlated with the level of activation in the left orbitofrontal cortex. Both regions were then shown to be part of distributed, functionally connected, networks of activation. There were also consistent areas of deactivation.

I then went on to show the development of enhanced techniques for the analysis of ^{11}C-Raclopride PET images. Using these techniques, I showed that despite significant doses of opioid, there was no measurable release of dopamine in opioid dependent patients given their drug of choice. This was in spite of marked psychological and physiological responses to these pharmacological stimuli.

6.1 Neural substrates of heroin craving

The most significant finding in the present study of heroin craving is of two distinct and dissociable peaks of activation. The results show an activation of the anterior cingulate gyrus and adjacent medial pre-frontal region that occurs in response to a drug-related stimulus, but does not correlate with the subjective craving response to that stimulus. In fact, it occurs even in the absence of such a subjective response. In

addition, we saw an increase in this effect with duration of abstinence. Conversely the orbitofrontal cortex activation is correlated with the subjective response to the stimulus, but is not always present in response to the stimuli themselves.

The different analysis methods could be employed to tease apart this distinction because there was a carry over effect into the neutral scans of craving induced by the drug-related stimuli. Initially this was considered to be a draw back of the study design. It was clear from the VAS that inducing craving worked well for some of the subjects as their reported levels increased rapidly in response to the stimuli. However, turning off the craving was not possible, in effect we were waiting for it to subside almost spontaneously. In addition, the progressive desensitization to the stimuli shown by the subjects also meant that comparing scans by subtraction was not the same as looking at activation with craving.

During the analysis phase it became apparent that I could use this carry over effect to differentiate responses to the stimuli from activation associated with craving. Specifically the cognitive subtraction will be maximally sensitive, and a correlational analysis will be relatively insensitive, to detecting responses to the drug-related stimuli that do not show a carry over effect into the next scan run. Conversely, areas of activation that show a slower response and particularly are slow to wear off will not be modelled well by an "on/off" model as used for the condition comparison, but a correlational analysis will be maximally sensitive to this pattern.

Thus the orbito-frontal cortex (which correlated with the "craving/urge" scale) did not show a significant activation with opioid related cues and similarly the left

anterior cingulate/medial pre-frontal region (activated by opioid related stimuli) did not show a significant correlation with the "crave/urge" scale. Because these prefrontal foci do not overlap spatially and were obtained with fundamentally different analyses these results suggest a true dissociation that brain responses to drug-related stimuli per se may invoke different brain circuits from those involved in the craving induced by these stimuli.

6.1.1 The role of the anterior cingulate

The activation of the left anterior cingulate gyrus has become a consistent finding in many types of functional imaging studies. More significantly, this region has been shown to be activated by other drug related stimuli, but not consistently. There are three other published functional imaging studies of opioid craving. In the first study the level of activation in the midbrain was found to modulate the response of the anterior cingulate to drug related visual cues (Sell *et al.*, 1999). The second study, by the same group, showed no anterior cingulate response but did show an unexpected posterior cingulate activation to a drug related video (Sell *et al.*, 2000).

However, the most recent study showed anterior cingulate activation in response to water but not heroin in thirsty drug users (Xiao *et al.*, 2006). As was noted by the authors of this last study, the literature on imaging heroin craving is small, making it difficult to unpick the potential causes of inconsistencies. In the single fMRI study no attempt was made to measure craving induced by drug related stimuli but only half of the 14 subjects were stated to have reported craving for the heroin (Xiao *et*

al., 2006). This alone is not enough to explain the discrepancy with the current study as the anterior cingulate activation was present in all subjects, whether they reported a subjective craving response or not. In the current study, the experimental protocol was designed to raise the potential salience of drug related stimuli. Specifically, the subjects all knew they had been recruited for a study of heroin craving; they had spent time prior to the scanning session recording the audio stimuli; they completed repeated scales rating their levels of heroin craving and were otherwise undistracted. In the most recent study, the subjects had been subject to a thirst induction paradigm involving water restriction and diuretic administration (Xiao *et al.*, 2006). The authors in this later study did not measure craving levels during the scanning session. It is therefore very likely that the primary preoccupation of the subjects during the scanning session was thirst. It is therefore not surprising that the stimulus that was able to capture their attention primarily was the drink related stimulus. In our study the primary stimuli of interest were likely to be the drug-related stimuli as a result of the clear direction of the focus of the study on heroin craving. What this suggests is that the salience of the stimuli can be inferred from their ability to activate the anterior cingulate. However, this can also be stated as the level of activation of the anterior cingulate being the determinant of the level of salience attributed to a given stimulus, i.e. the direction of causality is unknown.

This interpretation is further supported by the larger number of studies of craving for cocaine and other drugs. Activation of the anterior cingulate has been reported with cue-induced cocaine craving in response to a drug-related video in two studies from

the same group (Childress *et al.*, 1999; Maas *et al.*, 1998), however in the earlier study it is not possible from the published data to further localise the effect to a specific subdivision of the AC. ACC activation in the same pre-genual subdivision has additionally been shown in smokers in response to cigarette cues (Brody *et al.*, 2002). The same group also showed that this activation could be attenuated with bupropion (Brody *et al.*, 2004a).

In our study the focus of activation was located in the pre-genual subdivision of the cingulate cortex. Previous reviews of the functional imaging literature have subdivided the anterior cingulate into a superior-dorsal "executive" region and an "affective" region in the pre- and sub- genual parts of the gyrus (Bush *et al.*, 1998). As can be seen from this paper, the activation peak found in this current study is very close to the localisation of activation in an emotional counting Stroop done by the same authors (Whalen *et al.*, 1998). This argues for the activation in the current study to be related to emotional attention. This is in keeping with the subjective experience informally described by our subjects, who felt that the induction of craving was an emotional stimulus. Tasks that have activated the "executive" region of the AC have usually been tasks of divided attention of other cognitive tasks (Bush *et al.*, 1998), which is much more dissimilar to the stimuli presented in our study. In at least one of the previous studies the AC activation in heroin craving modulated by midbrain responses was inferior to our activation but remains within this 'affective' region (Sell *et al.*, 1999).

Activation in this AC region, as measured by SPET, has additionally been shown to

be inversely correlated with the severity of naltrexone-precipitated opioid withdrawal (van Dyck *et al.*, 1994). It was observed, but not measured, that several of our patients experienced conditioned withdrawal, (e.g. sweating and piloerection) whilst listening to their craving experiences. Therefore an alternative explanation is that the activation of the anterior cingulate (an area which was previously associated with withdrawal and pain) during the craving manipulation in our patients is a manifestation of conditioned withdrawal. However, if this was the case it would be expected that the difference in responses between the opioid stimulus and neutral stimulus conditions would decrease with increasing duration of abstinence, rather than the increase described.

The finding of an increase in the AC activation with increasing time abstinent was an unexpected finding. There was no *a priori* hypothesis, but the expectation would be that heroin addicts early in recovery would show an exaggerated response to drug-related stimuli compared to those with a longer period of abstinence. One theory that may explain the finding is that exposure to stimuli that provoke craving for opioids should become a less familiar experience as the period of abstinence increases. Therefore any habituation to such stimuli should gradually be lost and they would be more arousing or alerting when encountered. Consequently it would not be surprising that regions involved in emotional arousal and attention, such as the anterior cingulate/medial pre-frontal cortex, show increased relative activation to opioid related stimuli with increasing length of abstinence. It could also be that the character of these stimuli moves from appetitive to aversive over time.

Animal models have also demonstrated increases in conditioned responses to drug-paired stimuli over time (Grimm *et al.*, 2003). Rats previously trained to lever press in response to a light stimulus to receive a cocaine reward showed increasing lever-press responses to the same light stimulus as duration of abstinence increased out to 66 days of abstinence. However, the ability of foot shock to reinstate heroin associated lever presses showed an inverted-U shaped pattern over the same time period (Shalev *et al.*, 2001). It is difficult to see whether this confirms or refutes the current results as the cocaine study using conditioned stimuli is closer to the autobiographical stimuli used in our study, however the heroin study using foot shocks has a poorer match in the stimuli but is based on the same drug. Unfortunately the conditioned cue study has not been done with heroin.

6.1.2 The role of the orbito-frontal cortex

Activation in the left orbito-frontal cortex (OFC) showed a positive association with the composite "crave/urge" scale. This association of rCBF activation was present in all 8 subjects who reported a craving response to the stimulus. The absence of statistical activation in this area in the subtraction analysis above argues that the OFC is more directly related to the subjective experience of craving rather than the early processing of the opioid related stimuli. A significantly similar result has been reported showing a correlation between 'urge to use' heroin and rCBF in an adjacent area of the left inferior frontal cortex and an area of the orbito-frontal cortex in the opposite, right hemisphere (Sell *et al.*, 2000). Visual heroin related stimuli have also

more recently been shown to activate the OFC in an fMRI study of heroin users (Xiao *et al.*, 2006). Cocaine craving also correlates with OFC activation, more medially, when precipitated by withdrawal (Volkow *et al.*, 1991a) and in the right OFC when induced by methylphenidate (Volkow *et al.*, 1999b). Bilateral OFC activations are also observed in response to stimuli that elicit cocaine craving (Grant *et al.*, 1996; Wang *et al.*, 1999a). Similar results have also been shown for craving in treated & untreated smokers (Brody *et al.*, 2004a; Brody *et al.*, 2002).

The above data adds to the emerging evidence, from other non-imaging techniques, that the OFC plays an important role in drug dependence (Di Chiara & North, 1992; Wise, 1996). The OFC is linked to the mesolimbic dopamine system that mediates response to reward related stimuli (Koob, 1992), the subcallosal region of the anterior cingulate seen activated in this study (Di Chiara & North, 1992; Koski & Paus, 2000; Wise, 1996) and is connected to the amygdala. Additionally, it receives inputs from various sensory association areas and consequently plays an important role in expectancy and the reinforcing salience of stimuli (Hugdahl *et al.*, 1995; Rolls, 1996; Thorpe *et al.*, 1983). Others have theorized that the OFC, through its connection with the amygdala, may play a role in evaluating the motivational value of stimuli and labelling the emotional experience of craving (London *et al.*, 2000). This hypothesis could explain why this region co-varied with subjective craving measures in our study. Lastly, Volkow has emphasized the role of the OFC as part of the striato-thalamic-orbitofrontal cortex circuit in which dysfunction results in compulsive behaviour and heightened motivation to access a drug of abuse in a

number of her publications (e.g. Volkow & Fowler, 2000). This is supported by evidence that patients with lesions in the OFC perform poorly on tasks of gambling that require synthesis of emotional valence and impulse control for optimal performance (Rogers *et al.*, 1999). Furthermore, amphetamine and opioid dependent patients performed at a level between OFC-lesion patients and a healthy control group. This deficit could be mimicked in the control group using dietary tryptophan depletion.

6.1.3 The role of the sensory cortices

The correlational analysis looking for areas of functional connectivity with the AC region found activity deep in the posterior central gyrus (BA 3) and middle temporal gyrus (BA 21). Neither of these areas is classically thought to be connected to the AC region. However, the functions of these areas do have a possible link with the task condition, which may explain this apparent functional connectivity. Brodmann area 21 is involved in auditory sensory input and this craving experiment used auditory stimuli. The activation in the posterior central gyrus is in the area representing intra-abdominal sensation (Penfield & Rasmussen, 1950). It is therefore plausible that both these areas are activated by heroin related auditory stimuli that may evoke a visceral response in addition to any cognitive response. The heroin related stimuli are likely to engage a greater auditory attention to the stimulus, which would explain the increase in BA21 and the negative correlation between the AC region and visual areas via a cross-modality suppression of visual areas (Figure 3.2). The negative

association between activity in the OFC and posterior visual areas could again be related to cross-modal suppression. Consistent with this result, activation of the primary visual cortex has been shown in response to heroin related visual stimuli (Xiao *et al.*, 2006). Again this demonstrates the ability of drug-related stimuli to command greater responses from early stages of processing within primary sensory cortex. Of course, it remains possible that the relative decrease in rCBF observed in my study in the occipital cortex during the "craving" scans is simply the subjects allowing their attention to wander to gazing around the scanner room while listening to the neutral stimuli. In effect this could produce greater occipital activation during the neutral scan, rather than reduced activation during the craving scan. This is something that could have been examined if we had included a resting control scan; however the precise nature of the cognitive activity occurring during a "resting" state is usually unknown and often impossible to standardise.

This is in keeping with a hypothesis that the pre-genual AC activation is related to the emotional salience / attentional focus to the heroin stimuli which in turn is linked to heightened sensory processing of the stimuli and the physiological effects. These are effects of the stimuli that are likely to be the result of many thousands of unconditioned – conditioned stimulus pairings over many years of substance misuse. In this respect there is therefore no need for this particular activation network of sensory cortices and attentional circuits to be functionally connected to the OFC network also found in the study.

6.1.4 Wider circuits of activation

The nodes in the OFC connection network that activated proportionally with craving also have face validity when considering the nature of the experimental situation. The hippocampus, and temporal regions are implicated in memory or episodic memory. The stimuli used here were autobiographical episodes of craving. The more the script evoked activation in the memory areas the more subjective craving was described. It is difficult to know whether this was an effect of the nature or intensity of the memories for the craving and neutral episodes. There was no reported difference in the "vividness" of the stimuli, which suggests that it was not the richness of the recorded script that accounted for the differences found. What cannot be differentiated with the data available is any possible direction of causality, or effective connectivity.

The brainstem (Red Nucleus) region that was associated with the OFC activity is usually considered to be involved in the integration of motor activity. This region also has projections from the anterior cingulate cortex and cerebellar dentate gyrus. The spatial resolution of PET is not sufficient to differentiate the Red Nucleus from other nearby brain stem nuclei more often implicated in the opioid system, e.g. peri-aqueductal grey matter. Therefore, even though this was the localisation of the peak interaction between stimulus condition and OFC activity the true focus could have been located in other nearby nuclei. However, early reports from a recent fMRI study of video induced heroin craving, with the greater spatial resolution of fMRI, has also shown the red nucleus to be activated in response to drug-related stimuli

(Langleben *et al.*, 2002).

These results suggest that opiate craving and drug related stimuli do not activate "special" brain circuits specific for drug dependence or craving. Instead, the connected networks reported in this study identify circuits related to attention, sensory processing and memory. In other words, drug-dependence circuitry is perhaps associated with a greater degree of activation of regions associated with processing the autobiographical stimuli rather than activating "special" "addiction" regions of the brain. Our results add further support to the theories of addiction that suggest that what makes dependence is the ability of the drug and its related stimuli to "hi-jack" the neural circuits usually activated by attention and motivation and drive them stronger than "normal" rewards and stimuli (e.g. the incentive-sensitisation model, Robinson & Berridge, 1993).

6.1.5 Limitations of the craving studies

A number of caveats apply to the $H_2{}^{15}O$-PET data. The were no control subjects and only 12 subjects in total. The analysis techniques used only a fixed-effects not a random effects statistical design, so we are limited in our conclusions to this particular group of subjects. Small subject numbers and the consequent effects on statistical power are very commonly an issue in PET studies. At the time this study was done 12 subjects was an average number of subjects. There is always a tension between increasing statistical power on the one hand and the requirements of ARSAC to minimise the number of subjects exposed to radiation on the other. In the

case of this study we can be reasonably confident that the subject number was sufficient to detect important patterns of rCBF changes in heroin craving. The activation patterns found were in keeping with many other studies in the literature and made functional sense with substantial face validity.

Only 66% of our subjects reported craving in response to the drug related stimulus, however this is not unusual in the artificial environment of a brain scanner. When all subjects were included in the original correlational analysis an activation was found in the left dorso-lateral pre-frontal cortex (DLPFC). This activation very closely matched one previously found in cocaine craving (Grant *et al.*, 1996). This result was not reported however as inspection of the individual effect sizes for each subject showed that the entire effect was being driven by those four subjects who had a craving score of zero throughout the study. In straightforward terms, this correlation was statistically invalid. The DLPFC activation completely disappeared when these four subjects were removed. It was not possible to exclude this as the cause of the findings in the cocaine study as individual craving scores were not reported.

A weakness of our initial categorical design was the carry over effect of craving into the neutral condition, however we were able to take advantage of this effect by performing a correlational analysis in those subjects who craved to show a differential pattern of activation.

The relationship of the VAS reports of subjective craving used in this study to real behavioural intentions are also open to some question as none of the subjects acted on this craving by relapsing to heroin use. However, the majority of them were

seeking help with craving as part of their on-going treatment and so the experience of craving was well known to them. The gradual habituation to the craving stimuli, shown by the VAS scores, in some of our subjects may also have increased the variance of responses reducing the sensitivity of the cognitive subtraction analysis.

There were minor significant differences in the "vividness", "anxious" and "sad" VAS scales between the two conditions but it is unlikely that these were responsible for the activations reported as no significant rCBF changes correlated with these scales.

It is also necessary to bear in mind the limited spatial and temporal resolution afforded by PET scanning. This technique of examining functional connectivity has allowed us to highlight a network of brain regions implicated in opioid dependence, but it does not allow us to study the nature of the interactions between them. At present this is a map of nodes whose level of activation shows an association. It is not possible to state a causal relationship between activity in connected brain region, or the strength of one, should it exist. This will require further study with techniques better suited to the study of effective connectivity, but where the experimental environment is even less conducive to the state of mind we are trying to study, e.g. fMRI.

6.2 Dopamine

The ^{11}C-Raclopride study reported here is the first study to examine whether opioids increase dopamine levels in human opioid addicts as is seen with other drugs of

abuse. We detected no increase in striatal dopamine levels despite marked subjective and objective opioid effects. Following the injections of diamorphine and hydromorphone the subjects showed slowed saccadic eye movements and a pronounced level of intoxication including "high/gouched" and "rush". There was also a dose-response relationship between these physiological and subjective responses and the opioid injections. This dissociation implies that dopamine may not be critical in mediating the 'high' from opioids in dependent humans and contrasts with a number of pre-clinical studies.

A portion of the animal literature has shown that there is a dopamine response to opioids. In drug naïve rats, single doses of morphine up to 10mg/kg S.C. induced increases in extra-cellular dopamine of up to 200% of baseline in the nucleus accumbens and up to 180% in the caudate nucleus (Di Chiara & Imperato, 1988). Using similar microdialysis techniques an injection of IV diamorphine also induced a similar 260% rise in extra-cellular dopamine in drug naïve rats (Hemby *et al.*, 1995). However, the same study in a second sample of rats showed that after repeated self-administration of heroin the dopamine response was no longer observable. The same group showed that in rats trained to self-administer heroin, cocaine or a heroin/cocaine mixture there was a significant increase in extracellular dopamine following cocaine and heroin/cocaine, but not following heroin alone (Hemby *et al.*, 1999). In a study intended to examine the effects of chronic buprenorphine infusion, acute single doses of heroin were again shown to induce small increases in extracellular dopamine, typically around 150% of baseline (Sorge *et al.*, 2005). The

continual slow infusions of buprenorphine also resulted in increases in baseline dopamine concentrations pre-injection of a similar magnitude after 2 weeks exposure.

Dopamine responses to heroin self-administration have also been measured with greater temporal resolution using the technique of high speed chronoamperometry (Kiyatkin *et al.*, 1993). This technique measures the electrochemical effects of changes in extracellular dopamine concentrations rather than measuring dopamine concentrations directly as with microdialysis. This method has been criticised (Di Chiara 2005, personal communication) but nevertheless this study reports interesting results that may be of relevance to the interpretation of our ^{11}C-Raclopride data. Rats were permitted to self-administer heroin daily. The dopamine electrochemical signal in response to the first injection of each day's session was significant and increased over subsequent days. In contrast, the response to the second and later injections of each day's session was an initial drop in signal lasting approximately 20 minutes that followed a steady crescendo of electrochemical signal up to the moment of the lever press that delivered the heroin injection. Translating this into the situation experienced by our research subjects would suggest that one would expect a dopamine response to the first self-administration of heroin each day, but all subsequent self-administrations would be *preceded* by the dopamine release followed by a post-injection dip in dopamine. However, as suggested by some of the animal literature above, we may see a different pattern of dopamine response, if any, as the heroin was administered to our subjects by the experimenter and not self-

administered.

Relating this element of the pre-clinical animal literature to our human PET studies clearly requires overlooking of a large number of significant assumptions. However, the subjects in our dopamine experiment were clearly well experienced users with long histories of heroin use. That clearly suggests that the experiments with animals pre-exposed to opioids are more likely to match our experiment. All our subjects were on methadone maintenance but, with the exception of the first subjects had received no dose on the scan day until after the PET scans. Initially this would argue that the first injection of the day animal experiments are most appropriate as a model, where dopamine was seen to be released. However, methadone has a long half-life and none of the subjects were showing withdrawal signs or symptoms prior to scanning. This contrasts with the animal models where much shorter acting opioids were used.

This has not been the first study to examine dopamine responses to opioids in humans. The effects of another opioid agonist, alfentanil given by infusion, have been reported in two dopamine receptor PET studies designed to explore analgesia in healthy volunteers (Hagelberg *et al.*, 2004a; Hagelberg *et al.*, 2002a). The first showed a 6% *increase* in ^{11}C-Raclopride binding in the striatum (Hagelberg *et al.*, 2002a). This argues for a possible decrease in extracellular dopamine, contrary to the pre-clinical studies. In the second, ^{11}C-FLB-457 binding was *increased* by a small amount in several cortical regions (Hagelberg *et al.*, 2004a). ^{11}C-FLB-457 is a selective high-affinity Dopamine $D_{2/3}$ receptor ligand that is used to image extra-

striatal receptor availability. The authors were able to show that the increase in ^{11}C-FLB-457 binding was proportional to the euphorogenic effects of the alfentanil. Again, this finding of a suggested decrease in dopamine is contrary to the pre-clinical studies. The authors were unable to account for this discrepancy, other than to consider whether the noradrenergic neuron release of dopamine may contribute to the posterior cingulate signal measured. However, this would not account for the largest decrease which was seen in the thalamus. Our study is different in that we examined the effects of a substantial analgesic dose of hydromorphone and a standard heroin "hit". The doses used in our study were only possible to give because of the pre-existing tolerance to opioids in our methadone-maintained subjects. Had we given such doses to healthy control subjects we would have very likely provoked signs and symptoms of opioid overdose. Secondly our study used addicted individuals who continue to use heroin for its euphoriant effects and were expecting to get such effects from the injected dose used in this study. The experiments described above used healthy volunteers, in the latter study they also were expecting to have the analgesic effect of the alfentanil tested after the PET scan sessions (Hagelberg *et al.*, 2004a; Hagelberg *et al.*, 2002a). However, there was an association with the euphorogenic effects of the alfentanil, so the experiences of the healthy volunteers can't have been entirely negative.

Stimulant drugs and opioids are generally considered to be approximately equal in their ability to cause dependence (Ridenour *et al.*, 2005) and several studies have shown that cocaine and amphetamine measurably reduce ^{11}C-Raclopride binding.

The high dose of heroin given in our second study produced significant subjective effects that were of similar magnitude to those reported from cocaine (Schlaepfer *et al.*, 1997) and amphetamine (Oswald *et al.*, 2005) when given in the scanner environment. Despite this, there was no equivalent effect on ^{11}C-Raclopride binding. That cocaine, amphetamine and methylphenidate induce measurable decreases in human ^{11}C-Raclopride binding is not surprising, as these drugs act directly at the dopamine synapse to increase dopamine levels. However, increases in dopamine release have also been reported with challenges either of drug or behaviours that do not directly release dopamine. These include alcohol (Boileau *et al.*, 2003), smoking (Barrett *et al.*, 2004; Brody *et al.*, 2004b), feeding (Small *et al.*, 2003), playing a video game (Koepp *et al.*, 1998), placebo apomorphine (Fuente-Fernandez *et al.*, 2001) and finger tapping (Badgaiyan *et al.*, 2003).

One important finding to note is that the magnitude of the ^{11}C-Raclopride signal in response to a stimulant challenge is attenuated in chronic cocaine users (Volkow *et al.*, 1997c). In this study the cocaine dependent group showed a 9% reduction in ^{11}C-Raclopride following methylphenidate, whereas the control group showed a reduction of 22%. As was described in the animal literature above, this decreased dopamine response is known to follow the development of dependence on opioids as well.

Baseline levels of ^{11}C-Raclopride binding are also reported to be 11% lower in cocaine users compared to a control group (Volkow *et al.*, 1997c). Similar findings have been suggested in alcoholics (Martinez *et al.*, 2005). However, we did not see a

matching difference between the ^{11}C-Raclopride binding in our subjects during the placebo scan and levels in an historical control group re-analysed with the same methodology. One previous study has reported reduced dopamine D_2 receptor levels of 18% in opioid dependence (Wang *et al.*, 1997b). However, direct comparison with this opioid study is difficult as the protocols and patient populations were different. The protocol involved an injection of either saline or naloxone prior to the scan and the subjects were users of heroin primarily. Contrary to the expectations of the authors, the naloxone injections decreased ^{11}C-Raclopride binding, suggesting an increase in dopamine levels. However, the subjects were reportedly blind to the drug injection, so it is possible that the dopamine signal related to surprise at the unexpected consequences of the injection.

There is additional evidence that the dopamine system is not desensitised in our population. One heroin addict recruited in study 1 who, despite appearing un-intoxicated, subsequently tested positive to amphetamine on urine screening. He had approximately 30% lower ^{11}C-Raclopride BP in all regions compared to all the other subjects (see Figure 5.4). This suggests that the dopamine system in this subject remained sensitive to amphetamine induced reduction in ^{11}C-Raclopride binding. One further possible interpretation is that he had a measurable response to amphetamine because he was not dependent on this drug and had therefore not become desensitised. In addition it also confirms that our scanning and analysis method was able to measure the known effect of amphetamine.

6.2.1 Sensitivity of ^{11}C-Raclopride PET

Another potential difference between the animal microdialysis studies and the human imaging studies is the anatomical resolution. For some time it has been known that the nucleus accumbens has two subcomponents of a core and shell (e.g. Heimer *et al.*, 1991). The subdivisions have different patterns of connectivity, with the medio-ventral shell being connected to the "extended amygdala" and the core connecting to the striato-pallidum (Pontieri *et al.*, 1995). It has also been shown that single doses of experimenter-administered morphine produce increases in extracellular dopamine only in the shell, but not the core, of the nucleus (Pontieri *et al.*, 1995). Again, the level of increase has still been relatively modest, in the order of 200% of baseline. At present, the resolution achievable with PET is in the order of 2-5mm (full-width Half maximum) which is insufficient to distinguish this level of substructure.

In addition to issues of spatial resolution, there is also the issue of sensitivity. Measures of the sensitivity of ^{11}C-Raclopride to changes in extracellular dopamine concentration are highly variable, ranging in estimates from 8:1 to 44:1 (% increase DA to % decrease ^{11}C-Raclopride) and this relationship may vary with the subject and nature of the challenge (see Laruelle, 2000a for full discussion). In brief, it is suggested that Raclopride can bind to a larger pool of dopamine D_2 receptors than dopamine itself. Dopamine binds only to "active" receptors in the high affinity state, where Raclopride will bind to all surface receptors. The net result of this is that ^{11}C-Raclopride PET remains a relatively insensitive tool. Therefore, changes of the comparatively small magnitude reported by microdialysis studies, particularly if

highly localised, would not be readily detectable with ^{11}C-Raclopride PET, even with movement correction and the latest image analysis techniques.

Another potential contribution to the lack of sensitivity of ^{11}C-Raclopride PET to changes in extracellular dopamine in this study is the size of the sample. We recruited and obtained complete data on 14 subjects, excluding those that tested positive for stimulant use. While this seems a small number, it is in keeping with the PET literature. There is also no evidence of a "sub-threshold" trend to our data to suggest that a small dopamine response was emerging. The "ladder plot" (Figure 5.4) shows that the direction of change in the paired scan data was convincingly inconsistent. It could also be argued that with a single subject we were able to demonstrate the known effects of amphetamine on ^{11}C-Raclopride binding.

6.2.2 Theoretical implications for the role of dopamine in opioid dependence

This study raises fundamental questions about the role of dopamine in human opioid addiction. The dissociation of measurable dopamine release and subjective "high" argues against this as a fundamental prerequisite for perception of drugs as rewarding and pleasurable. Certainly, it cannot now be suggested that the magnitude of dopamine release measured in response to stimulants is required for a substance to be "addictive".

One possible unifying explanation is that the level of dopamine release and ^{11}C-Raclopride displacement provoked by stimulants may be correlated with, but not

necessary for, the addictive properties of these drugs. It could be that a dopamine signal in the shell of the nucleus accumbens is required by all drugs of abuse, but that this is too small to be detectable with PET and that the detectable dopamine signal is merely a corollary pharmacological effect of the stimulants. Although on the surface the findings with alcohol and nicotine argue against this, they show weaker effects than those with stimulants. The alcohol data required extreme intoxication (Boileau *et al.*, 2003) and the original nicotine data, that initially showed a large effect, has recently been extended to reveal a much smaller effect that is predominantly seen in subjects with the low dopamine functioning COMT polymorphism (Brody *et al.*, 2006).

It may be that drugs such as nicotine and opioids, that in animals activate dopamine neurons indirectly by switching off an inhibitory GABA inter-neuron in the ventral tegmental area (Garzon & Pickel, 2001), release little, if any, dopamine in the terminal regions, or that dopamine is rapidly taken up into the pre-synaptic terminals. Perhaps blocking dopamine re-uptake, e.g. by a low dose of cocaine, would prevent such uptake and reveal an effect of opioids, as has been suggested by the synergistic elevations shown in rodents (Hemby *et al.*, 1999). However, in the case of opioids there are potential sites, other than the dopamine system, that may mediate their addictive actions. For example, some output regions of the basal ganglia dopamine projections, e.g. the globus pallidus, have high opioid receptor densities that could be the "down-stream" target for mu-opioid agonists (Mitrovic & Napier, 2002).

It has been argued that the role of dopamine is not to signal the rewarding properties

of drugs of abuse, but as a signal related to drug "wanting" - the incentive-sensitisation theory (Robinson & Berridge, 1993). Clinically the subjective response to stimulants includes the component of "wanting", as well as "rush" and "high", with the "wanting" often leading to bingeing. In contrast, subjective responses to opioids are characterised only by "rush", "high" and intoxication, as we found in this study. The drug "wanting" component of opioid addiction is most closely associated with the period between acquisition of the drug and its subsequent consumption. If the dopamine response to drugs of abuse is related to the "wanting" phase rather than the "liking" phase, then it would be expected that dopamine would be associated with acute administration of stimulants, but in the case of opioids the dopamine release would be maximal when drug was expected, not after it has just been administered. It has already been shown that the "craving" induced by cocaine administration activates the dopamine-rich nucleus accumbens, where the "rush" and "high" do not (Breiter *et al.*, 1997). This suggests that, at least in the case of opioid addiction, manipulations of expectation of drug would be a more fruitful area of future research. This explanation certainly ties in with the animal models described above where the predominant dopamine release in experienced animals was in a crescendo associated with lever pressing to receive a conditioned reinforcement rather than to the heroin infusion (Kiyatkin *et al.*, 1993).

Whatever the explanation, the results of this study cannot refute the animal literature which argues dopamine may well be intimately involved in the process of developing addiction to opioids and the drive to seek alleviation of the withdrawal syndrome.

However, our study argues against dopamine having the same supremacy as the causative agent in opioid addiction as has been hypothesised for stimulant addiction. We still face fundamental problems however in marrying up the data from the pre-clinical and human studies due the the very different drug administration histories of the animals and addicts. Ideally one would like to be able to challenge abstinent drug users with opioids and give equivalent doses to drug naïve subjects, neither of which could be ethically justified. Similarly the animal models required to properly mimic the real clinical patterns of drug use observed in patients would take many years to complete. We felt that this study was the best compromise as similar opioid doses given to drug naïve subjects would have caused unacceptable levels of nausea and respiratory depression, and waiting for higher levels of withdrawal to emerge would have had the potential to cause increased subject head movement and other potential confounds.

6.3 Conclusions

Addiction, or substance misuse, is a large social problem worldwide. To date the majority of treatments are empirically derived from experience and evidence from the clinic. Gradually neuroscience is beginning to shed light on the underlying mechanisms of dependence which will pave the way for potential new treatments. The techniques of functional neuroimaging give the ability to visualise neuronal function in the living human drug user and therefore open a window on the understanding of addiction processes unavailable from any other technique.

Positron Emission Tomography (PET) and functional magnetic resonance imaging (fMRI) together have produced a considerable body of research to aid the understanding of the fundamental mechanisms of addiction and dependence. The majority of neuroimaging studies in dependence, to date, have focused on regions of brain activation in response to specific drug related stimuli or on changes in neurotransmitter function.

The studies presented in this thesis have endeavoured to take these established methodologies and extend. The opioid craving study began with a straightforward activation paradigm. It showed that drug-related stimuli and the subjective experience of craving were associated with definable patterns of cerebral blood flow. However, the second component of the study was an extension of existing fMRI analysis techniques into the field of perfusion PET. This cross-fertilisation of analysis techniques yielded new insights into the meaning of these activation patterns and helped to link them to the subjective and observable phenomena of opioid craving. Similarly, the ^{11}C-Raclopride study did not simply report changes in neurotransmitter binding in response to a pharmacological challenge. Instead, this study used combined subjective and functional measures of opioid effect simultaneously with measurement of neurotransmitter function. We also developed automated and enhanced techniques of image analysis to ensure that the data was exploited to its full extent.

The work presented in this thesis was, for me at least, more of an exploration of the ways that imaging methodologies can be extended and applied to the study of the

neurobiology of addiction than it was an actual study of the neurobiology. In effect the journey taught me more than what I found when I arrived at the destination.

7 References

Aasly J, Storsaeter O, Nilsen G, Smevik O, Rinck P. Minor structural brain changes in young drug abusers. A magnetic resonance study. *Acta Neurologica Scandinavica* (1993) **87**: pp. 210-214.

Acquas E, Carboni E & Di Chiara G. Profound depression of mesolimbic dopamine release after morphine withdrawal in dependent rats. *European Journal of Pharmacology* (1991) **193**: pp. 133-134.

Adams K, Gilman S, Koeppe R, Kluin K, Brunberg J, Dede D, Berent S & Kroll P. Neuropsychological deficits are correlated with frontal hypometabolism in positron emission tomography studies of older alcoholic patients. *Alcoholism: Clinical & Experimental Research* (1993) **17**: pp. 205-210.

Adinoff B, Devous,MD,Sr, Best S, George M, Alexander D & Payne K. Limbic responsiveness to procaine in cocaine-addicted subjects. (2001) **158**: pp. 390-398.

Adler L, Gyulai F, Diehl D, Mintun M, Winter P & Firestone L. Regional brain activity changes associated with fentanyl analgesia elucidated by positron emission tomography. *Anesthesia & Analgesia* (1997) **84**: pp. 120-126.

Amass L, Nardin R, Mendelson J, Teoh S & Woods B. Quantitative magnetic resonance imaging in heroin- and cocaine-dependent men: a preliminary study. *Psychiatry Research: Neuroimaging* (1992) **45**: pp. 15-23.

American Psychiatric Association. Diagnostic and Statistical Manual of Mental Disorders (DSM-IV). American Psychiatric Association, Washington DC, 1994.

Anderson CM, Maas LC, Frederick BD, Bendor JT, Spencer TJ, Livni E, Lukas SE, Fischman AJ, Madras BK, Renshaw PF & Kaufman MJ. Cerebellar vermis involvement in cocaine-related behaviors. *Neuropsychopharmacology* (2006) **31**: pp. 1318-1326.

Anton R, Moak D & Latham P. The Obsessive Compulsive Drinking Scale: a self-rated instrument for the quantification of thoughts about alcohol and drinking behaviour. *Alcoholism: Clinical & Experimental Research* (1995) **19**: pp. 92-99.

Antonini A, Leenders K, Reist H, Thomann R, Beer H & Locher J. Effect of age on D2 dopamine receptors in normal human brain measured by positron emission tomography and 11C-raclopride. *Archives of Neurology* (1993) **50**: pp. 474-480.

Ashburner J & Friston K. Multimodal image coregistration and partitioning--a unified framework. *NeuroImage* (1997) **6**: pp. 209-217.

Ashburner J & Friston K. Nonlinear spatial normalization using basis functions. *Human Brain Mapping* (1999) **7**: pp. 254-266.

Ashburner J & Friston K. Voxel-based morphometry--the methods. *NeuroImage* (2000) **11**: pp. 805-821.

Ashburner J, Andersson J & Friston K. High-dimensional image registration using symmetric priors. *NeuroImage* (1999) **9**: pp. 619-628.

Ashburner J, Andersson J & Friston K. Image registration using a symmetric prior--in three dimensions. *Human Brain Mapping* (2000) **9**: pp. 212-225.

Ashburner J, Friston K. Rigid body registration. In *Human Brain Function*. Frackowiak R, Friston K, Frith C, Dolan R, Price C, Zeki S, Ashburner J, Penny W (Eds.). (2003).

Badgaiyan R, Fischman A & Alpert N. Striatal dopamine release during unrewarded motor task in human volunteers. *Neuroreport* (2003) **14**: pp. 1421-1424.

Bae S, Lyoo I, Sung Y, Yoo J, Chung A, Yoon S, Kim D, Hwang J, Kim S & Renshaw P. Increased white matter hyperintensities in male methamphetamine abusers. *Drug & Alcohol Dependence* (2006) **81**: pp. 83-88.

Barrett S, Boileau I, Okker J, Pihl R & Dagher A. The hedonic response to cigarette smoking is proportional to dopamine release in the human striatum as measured by positron emission tomography and [11C]raclopride. *Synapse* (2004) **54**: pp. 65-71.

Barrio JR, Huang SC, Melega WP, Yu DC, Hoffman JM, Schneider JS, Satyamurthy N, Mazziotta JC & Phelps ME. 6-[18F]fluoro-L-dopa probes dopamine turnover rates in central dopaminergic structures. *Journal of Neuroscience Research* (1990) **27**: pp. 487-493.

Becerra L, Harter K, Gonzalez RG & Borsook D. Functional magnetic resonance imaging measures of the effects of morphine on central nervous system circuitry in opioid-naive healthy volunteers. *Anesthesia & Analgesia* (2006) **103**: p. 208-16, table of contents.

Beck A, Ward C, Mendelson M, Mock J & Erbaugh J. An inventory for measuring depression. *Archives of General Psychiatry* (1961) **4**: pp. 561-571.

Bergström KA, Jolkkonen J, Kuikka JT, Akerman KK, Viinamäki H, Airaksinen O, Länsimies E & Tiihonen J. Fentanyl decreases beta-CIT binding to the dopamine transporter. *Synapse* (1998) **29**: pp. 413-415.

Besson J, Glen A, Foreman E, MacDonald A, Smith F, Hutchison J, Mallard J & Ashcroft G. Nuclear magnetic resonance observations in alcoholic cerebral disorder and the role of vasopressin. *Lancet* (1981) **318**: pp. 923-924.

Bloomfield P, Spinks T, Reed J, Schnorr L, Westrip A, Livieratos L, Fulton R & Jones T. The design and implementation of a motion correction scheme for neurological PET. *Physics in Medicine and Biology* (2003) **48**: pp. 959-978.

Boileau I, Assaad J, Pihl R, Benkelfat C, Leyton M, Diksic M, Tremblay R & Dagher A. Alcohol promotes dopamine release in the human nucleus accumbens. *Synapse* (2003) **49**: pp. 226-231.

Bolla K, Eldreth D, London E, Kiehl K, Mouratidis M, Contoreggi C, Matochik J, Kurian V, Cadet J, Kimes A, Funderburk F & Ernst M. Orbitofrontal cortex dysfunction in abstinent cocaine abusers performing a decision-making task. *NeuroImage* (2003) **19**: pp. 1085-1094.

Bolla K, Ernst M, Kiehl K, Mouratidis M, Eldreth D, Contoreggi C, Matochik J, Kurian V, Cadet J, Kimes A, Funderburk F & London E. Prefrontal cortical dysfunction in abstinent cocaine abusers. *Journal of Neuropsychiatry & Clinical Neurosciences* (2004) **16**: pp. 456-464.

Botelho MF, Relvas JS, Abrantes M, Cunha MJ, Marques TR, Rovira E, Fontes Ribeiro CA & Macedo T. Brain blood flow SPET imaging in heroin abusers. *Annals of the New York Academy of Sciences* (2006) **1074**: pp. 466-477.

Breiter H, Gollub R, Weisskoff R, Kennedy D, Makris N, Berke J, Goodman J, Kantor H, Gastfriend D, Riorden J, Mathew R, Rosen B & Hyman S. Acute effects of cocaine on human brain activity and emotion. *Neuron* (1997) **19**: pp. 591-611.

Brett M, Bloomfield P, Brooks D, Stein J & Grasby P. Scan order effects in PET activation studies are caused by motion artefact. *NeuroImage* (1999) **9**: p. S56.

Brody A, Mandelkern M, Lee G, Smith E, Sadeghi M, Saxena S, Jarvik M & London E. Attenuation of cue-induced cigarette craving and anterior cingulate cortex activation in bupropion-treated smokers: a preliminary study. *Psychiatry Research* (2004a) **130**: pp. 269-281.

Brody A, Mandelkern M, London E, Childress A, Lee G, Bota R, Ho M, Saxena S, Baxter,LR,Jr, Madsen D & Jarvik M. Brain metabolic changes during cigarette craving. *Archives of General Psychiatry* (2002) **59**: pp. 1162-1172.

Brody A, Olmstead R, London E, Farahi J, Meyer J, Grossman P, Lee G, Huang J, Hahn E & Mandelkern M. Smoking-induced ventral striatum dopamine release. *American Journal of Psychiatry* (2004b) **161**: pp. 1211-1218.

Brody AL, Mandelkern MA, Olmstead RE, Scheibal D, Hahn E, Shiraga S, Zamora-Paja E, Farahi J, Saxena S, London ED & McCracken JT. Gene variants of brain dopamine pathways and smoking-induced dopamine release in the ventral caudate/nucleus accumbens. *Archives of General Psychiatry* (2006) **63**: pp. 808-816.

Brownell G, Budinger TF, Lauterbur PC, McGeer PL. Positron Tomography and Nuclear Magnetic Resonance Imaging. *Science* (1982) **215**: pp. 619-626.

Buchel C & Friston K. Modulation of connectivity in visual pathways by attention: cortical interactions evaluated with structural equation modelling and fMRI. *Cerebral Cortex* (1997) **7**: pp. 768-778.

Bush G, Whalen P, Rosen B, Jenike M, McInerney S & Rauch S. The Counting Stroop: An Interference Task Specialized for Functional Neuroimaging - Validation Study with Functional MRI. *Human Brain Mapping* (1998) **6**: pp. 270-282.

Butler G, Montgomery A. Impulsivity, risk taking and recreational 'ecstasy' (MDMA) use. *Drug & Alcohol Dependence* (2004) **76**: pp. 55-62.

Cadenas L, Houle S, Kapur S & Busto U. Oral D-amphetamine causes prolonged displacement of [11C]raclopride as measured by PET. *Synapse* (2004) **51**: pp. 27-31.

Cadoni C & Di Chiara G. Reciprocal changes in dopamine responsiveness in the nucleus accumbens shell and core and in the dorsal caudate-putamen in rats sensitized to morphine. *Neuroscience* (1999) **90**: pp. 447-455.

Cala L, Jones B, Mastaglia F & Wiley B. Brain atrophy and intellectual impairment in heavy drinkers--a clinical, psychometric and computerized tomography study. *Australian & New Zealand Journal of Medicine* (1978) **8**: pp. 147-153.

Cala L, Jones B, Wiley B & Mastaglia F. A computerized axial tomography (C.A.T.) study of alcohol induced cerebral atrophy--in conjunction with other correlates. *Acta Psychiatrica Scandinavica, Supplementum* (1980) **286**: pp. 31-40.

Carlen P, Wilkinson D, Wortzman G & Holgate R. Partially reversible cerebral atrophy and functional improvement in recently abstinent alcoholics. *Canadian Journal of Neurological Sciences* (1984) **11**: pp. 441-446.

Carlen P, Wilkinson D, Wortzman G, Holgate R, Cordingley J, Lee M, Huszar L, Moddel G, Singh R, Kiraly L & Rankin J. Cerebral atrophy and functional deficits in alcoholics without clinically apparent liver disease. *Neurology* (1981) **31**: pp. 377-385.

Carlen P, Wortzman G, Holgate R, Wilkinson D & Rankin J. Reversible cerebral atrophy in recently abstinent chronic alcoholics measured by computed tomography scans. *Science* (1978) **200**: pp. 1076-1078.

Carson R, Breier A, De Bartolomeis A, Saunders R, Su T, Schmall B, Der M, Pickar D & Eckelman W. Quantification of amphetamine-induced changes in [11C]raclopride binding with continuous infusion. *Journal of Cerebral Blood Flow & Metabolism* (1997) **17**: pp. 437-447.

Cascella N, Pearlson G, Wong D, Broussolle E, Nagoshi C, Margolin R & London E. Effects of substance abuse on ventricular and sulcal measures assessed by computerised tomography. *British Journal of Psychiatry* (1991) **159**: pp. 217-221.

Cascella N, Wong D, Pearlson G, Nagoshi C & London E. Brain structural abnormalities differentially correlate with severity of alcohol and opioid abuse. *NIDA Research Monograph* (1989) **90**: p. 374.

Casey KL, Svensson P, Morrow TJ, Raz J, Jone C & Minoshima S. Selective opiate modulation of nociceptive processing in the human brain. *Journal of Neurophysiology* (2000) **84**: pp. 525-533.

Celius E, Andersson S. Leucoencephalopathy after inhalation of heroin: a case report. *Journal of Neurology, Neurosurgery & Psychiatry* (1996) **60**: pp. 694-695.

Chick J, Smith M, Engleman H, Kean D, Mander A, Douglas R & Best J. Magnetic resonance imaging of the brain in alcoholics: cerebral atrophy, lifetime alcohol consumption, and cognitive deficits. *Alcoholism: Clinical & Experimental Research* (1989) **13**: pp. 512-518.

Childress A, Ehrman R, McLellan A & O'Brien C. Update on behavioral treatments for substance abuse. *NIDA Research Monograph* (1988a) **90**: pp. 183-192.

Childress A, McLellan A, Ehrman R & O'Brien C. Classically conditioned responses in opioid and cocaine dependence: a role in relapse? *NIDA Research Monograph* (1988b) **84**: pp. 25-43.

Childress A, Mozley P, McElgin W, Fitzgerald J, Reivich M & O'Brien C. Limbic activation during cue-induced cocaine craving. *American Journal of Psychiatry* (1999) **156**: pp. 11-18.

Chivite-Matthews N, Richardson A, O'Shea J, Becker J, Owen N, Roe S & Condon J. Drug Misuse Declared: Findings from the 2003/04 British Crime Survey. Home Office, UK, (2005).

Christensen J, Kaufman M, Frederick B, Rose S, Moore C, Lukas S, Mendelson J, Cohen B & Renshaw P. Proton magnetic resonance spectroscopy of human basal ganglia: response to cocaine administration. *Biological Psychiatry* (2000) **48**: pp. 685-692.

Christensen J, Kaufman M, Levin J, Mendelson J, Holman B, Cohen B & Renshaw P. Abnormal cerebral metabolism in polydrug abusers during early withdrawal: a 31P MR spectroscopy study. *Magnetic Resonance in Medicine* (1996) **35**: pp. 658-663.

Clemmey P, Brooner R, Chutuape MA, Kidorf M & Stitzer M. Smoking habits and attitudes in a methadone maintenance treatment population. *Drug & Alcohol Dependence* (1997) **44**: pp. 123-132.

Cowan R, Lyoo I, Sung S, Ahn K, Kim M, Hwang J, Haga E, Vimal R, Lukas S & Renshaw P. Reduced cortical gray matter density in human MDMA (Ecstasy) users: a voxel-based morphometry study. *Drug & Alcohol Dependence* (2003) **72**: pp. 225-235.

Cross A, Hille C & Slater P. Subtraction autoradiography of opiate receptor subtypes in human brain. *Brain Research* (1987) **418**: pp. 343-348.

Dagher A, Gunn R, Lockwood G, Cunningham V, Grasby P, Brooks D. Measuring neurotransmitter release with PET: methodological issues. In *Quantitative functional brain imaging with positron emission tomography*. Carson R, Daube-Witherspoon M, Herscovitch P (Eds.). 1998. pp. 449-454.

Damadian R. Tumor detection by nuclear magnetic resonance. *Science* (1971) **171**: pp. 1151-1153.

Daniel D, Weinberger D, Jones D, Zigun J, Coppola R, Handel S, Bigelow L, Goldberg T, Berman K & Kleinman J. The effect of amphetamine on regional cerebral blood flow during cognitive activation in schizophrenia. *Journal of Neuroscience* (1991) **11**: pp. 1907-1917.

Danos P, Kasper S, Grunwald F, Klemm E, Krappel C, Broich K, Hoflich G, Overbeck B, Biersack H & Moller H. Pathological regional cerebral blood flow in opiate-dependent patients during withdrawal: a HMPAO-SPECT study. *Neuropsychobiology* (1998a) **37**: pp. 194-199.

Danos P, Kasper S, Grünwald F, Klemm E, Krappel C, Broich K, Höflich G, Overbeck B, Biersack HJ & Möller HJ. Pathological regional cerebral blood flow in opiate-dependent patients during withdrawal: a HMPAO-SPECT study. *Neuropsychobiology* (1998b) **37**: pp. 194-199.

Danos P, Van RD, Kasper S, Bromel T, Broich K, Krappel C, Solymosi L & Moller H. Enlarged cerebrospinal fluid spaces in opiate-dependent male patients: a stereological CT study. *Neuropsychobiology* (1998c) **38**: pp. 80-83.

Davenport-Hines R. The Pursuit of Oblivion. A social history of drugs. Phoenix. London, (2004).

Dawe S, Powell J, Richards D, Gossop M, Marks I, Strang J & Gray J. Does post-withdrawal cue exposure improve outcome in opiate addiction? A controlled trial. *Addiction* (1993) **88**: pp. 1233-1245.

De Wit H, Metz J, Wagner N & Cooper M. Effects of diazepam on cerebral metabolism and mood in normal volunteers. *Neuropsychopharmacology* (1991) **5**: pp. 33-41.

Devine D, Leone P, Pocock D & Wise R. Differential involvement of ventral tegmental mu, delta and kappa opioid receptors in modulation of basal mesolimbic dopamine release: in vivo microdialysis studies. *Journal of Pharmacology & Experimental Therapeutics* (1993) **266**: pp. 1236-1246.

Dewey S, Smith G, Logan J, Brodie J, Fowler J & Wolf A. Striatal binding of the PET ligand 11C-raclopride is altered by drugs that modify synaptic dopamine levels. *Synapse* (1993) **13**: pp. 350-356.

Di Chiara G & Imperato A. Drugs abused by humans preferentially increase synaptic dopamine concentrations in the mesolimbic system of freely moving rats. *Proceedings of the National Academy of Science, USA* (1988) **85**: pp. 5274-5278.

Di Chiara G & North R. Neurobiology of opiate abuse. *Trends in Pharmacological Sciences* (1992) **13**: pp. 185-193.

Di Sclafani V, Ezekiel F, Meyerhoff D, MacKay S, Dillon W, Weiner M & Fein G. Brain atrophy and cognitive function in older abstinent alcoholic men. *Alcoholism: Clinical & Experimental Research* (1995) **19**: pp. 1121-1126.

Ernst M, Zametkin A, Matochik J, Schmidt M, Jons P, Liebenauer L, Hardy K & Cohen R. Intravenous dextroamphetamine and brain glucose metabolism. *Neuropsychopharmacology* (1997) **17**: pp. 391-401.

Ernst T, Chang L, Leonido-Yee M & Speck O. Evidence for long-term neurotoxicity associated with methamphetamine abuse: A 1H MRS study. *Neurology* (2000) **54**: pp. 1344-1349.

Ersche K, Fletcher P, Lewis S, Clark L, Stocks-Gee G, London M, Deakin J, Robbins T & Sahakian B. Abnormal frontal activations related to decision-making in current and former amphetamine and opiate dependent individuals. *Psychopharmacology* (2005a) **180**: pp. 612-623.

Ersche K, Roiser J, Clark L, London M, Robbins T & Sahakian B. Punishment induces risky decision-making in methadone-maintained opiate users but not in heroin users or healthy volunteers. *Neuropsychopharmacology* (2005b) **30**: pp. 2115-2124.

Evans AC, Collins DL, Mills SR , Brown ED, Kelly RL & Peters TM. 3D statistical neuroanatomical models from 305 MRI volumes. *Nuclear Science Symposium and Medical Imaging Conference Proceedings.* (1993) **3**: pp.1813-817.

Eysenck H & Eysenck S. Manual of the Eysenck personality questionnaire. Hodder and Stoughton, London, (1975).

Eysenck S, Pearson R, Easting G & Allsopp J. Age norms for impulsiveness, venturesomeness, and empathy in adults. *Personality and Individual Differences* (1985) **6**: pp. 613-619.

Farde L, Ehrin E, Eriksson L, Greitz T, Hall H, Hedstrom C, Litton J & Sedvall G. Substituted benzamides as ligands for visualization of dopamine receptor binding in the human brain by positron emission tomography. *Proceedings of the National Academy of Sciences of the United States of America* (1985) **82**: pp. 3863-3867.

Farde L, Eriksson L, Blomquist G & Halldin C. Kinetic analysis of central[11C]raclopride binding to D2-dopamine receptors studied by PET - A comparison to the equilibrium analysis. *Journal of Cerebral Blood Flow & Metabolism* (1989) **9**: pp. 696-708.

Farde L, Hall H, Pauli S & Halldin C. Variability in D2-dopamine receptor density and affinity: A PET study with [11C]raclopride in man. *Synapse* (1995) **20**: pp. 200-208.

Farde L, Pauli S, Litton J, Halldin C, Neiman J & Sedvall G. PET-determination of benzodiazepine receptor binding in studies on alcoholism. *EXS* (1994) **71**: pp. 143-153.

Firestone L, Gyulai F, Mintun M, Adler A, Urso K & Winter P. Human Brain Activity Response to Fentanyl Imaged by Positron Emission Tomography. *Anesthesia & Analgesia* (1996) **82**: pp. 1247-1251.

Forman S, Dougherty G, Casey B, Siegle G, Braver T, Barch D, Stenger V, Wick-Hull C, Pisarov L, Lorensen E. Opiate addicts lack error-dependent activation of rostral anterior cingulate.. *Biological Psychiatry* (2004) **55**: pp. 531-537.

Fowler J, Volkow N, Wolf A, Dewey S, Schlyer D, MacGregor R, Hitzemann R, Logan J, Bendriem B & Gatley S. Mapping cocaine binding sites in human and baboon brain in vivo. *Synapse* (1989) **4**: pp. 371-377.

Fox J, Ramsey R, Huckman M, Proske A. Cerebral ventricular enlargement. Chronic alcoholics examined by computerized tomography. *JAMA* (1976) **236**: pp. 365-368.

Friston K. Statistical parametric mapping: Ontology and current issues. *Journal of Cerebral Blood Flow & Metabolism* (1995) **15**: pp. 361-370.

Friston K. Beyond phrenology: what can neuroimaging tell us about distributed circuitry? *Annual Review of Neuroscience* (2002a) **25**: pp. 221-250.

Friston K. Functional integration and inference in the brain. *Progress in Neurobiology* (2002b) **68**: pp. 113-143.

Friston K, Buechel C, Fink G, Morris J, Rolls E & Dolan R. Psychophysiological and Modulatory Interactions in Neuroimaging. *NeuroImage* (1997) **6**: pp. 218-229.

Friston K, Frith C & Frackowiak R. Time-dependent changes in effective connectivity measured with PET. *Human Brain Mapping* (1993) **1**: pp. 69-79.

Friston K, Holmes A, Poline J, Price C & Frith C. Detecting activations in PET and fMRI: levels of inference and power. *NeuroImage* (1996) **4**: pp. 223-235.

Friston K, Passingham R, Nutt J, Heather J, Sawle G & Frackowiak R. Localisation in PET images: direct fitting of the intercommissural (AC-PC) line. *Journal of Cerebral Blood Flow & Metabolism* (1989) **9**: pp. 690-695.

Frost J, Mayberg H, Sadzot B, Dannals R, Lever J, Ravert H, Wilson, Wagner H.N. Jr. & Links J. Comparison of [11C]diprenorphine and [11C]carfentanil binding to opiate receptors in humans by positron emission tomography. *Journal of Cerebral Blood Flow & Metabolism* (1990) **10**: pp. 484-492.

Frost J, Smith A & Wagner,HN,Jr. 3H-diprenorphine is selective for mu opiate receptors in vivo. *Life Sciences* (1986) **38**: pp. 1597-1606.

Fuente-Fernandez R, Ruth T, Sossi V, Schulzer M, Calne D & Stoessl A. Expectation and dopamine release: mechanism of the placebo effect in Parkinson's disease. *Science* (2001) **293**: pp. 1164-1166.

Galynker I, Watras-Ganz S, Miner C, Rosenthal R, Des Jarlais D, Richman B & London E. Cerebral metabolism in opiate-dependent subjects: Effects of methadone maintenance. *Mount Sinai Journal of Medicine* (2000) **67**: pp. 381-387.

Garavan H, Pankiewicz J, Bloom A, Cho J, Sperry L, Ross T, Salmeron B, Risinger R, Kelley D & Stein E. Cue-induced cocaine craving: neuroanatomical specificity for drug users and drug stimuli. *American Journal of Psychiatry* (2000) **157**: pp. 1789-1798.

Garzon M & Pickel VM. Plasmalemmal mu-opioid receptor distribution mainly in non-dopaminergic neurons in the rat ventral tegmental area. *Synapse* (2001) **41**: pp. 311-328.

Gatley S, Yu D, Fowler J, MacGregor R, Schlyer D, Dewey S, Wolf A, Martin T, Shea C & Volkow N. Studies with differentially labeled [11C]cocaine, [11C]norcocaine, [11C]benzoylecognine, and [11C]- and 4'-[18F]fluorococaine to probe the extent to which [11C]cocaine metabolites contribute to PET images of the baboon brain. *Journal of Neurochemistry* (1994) **62**: pp. 1154-1162.

Gerra G, Calbiani B, Zaimovic A, Sartori R, Ugolotti G, Ippolito L, Delsignore R, Rustichelli P & Fontanesi B. Regional cerebral blood flow and comorbid diagnosis in abstinent opioid addicts. *Psychiatry Research: Neuroimaging* (1998) **83**: pp. 117-126.

Gerstein GL & Perkel DH. Simultaneously Recorded Trains of Action Potentials: Analysis and Functional Interpretation. *Science* (1969) **164**: pp. 828 - 830.

Gifford AN, Gatley S. John, Ashby Jr CR. Endogenously released dopamine inhibits the binding of dopaminergic PET and SPECT ligands in superfused rat striatal slices. *Synapse* (1996) **22**: pp. 232-238.

Gilman S, Adams K, Johnson-Greene D, Koeppe R, Junck L, Kluin K, Martorello S, Heumann M & Hill E. Effects of disulfiram on positron emission tomography and neuropsychological studies in severe chronic alcoholism. *Alcoholism: Clinical & Experimental Research* (1996a) **20**: pp. 1456-1461.

Gilman S, Adams K, Koeppe R, Berent S, Kluin K, Modell J, Kroll P & Brunberg J. Cerebellar and frontal hypometabolism in alcoholic cerebellar degeneration studied with positron emission tomography. *Annals of Neurology* (1990) **28**: pp. 775-785.

Gilman S, Koeppe R, Adams K, Johnson-Greene D, Junck L, Kluin K, Brunberg J, Martorello S & Lohman M. Positron emission tomographic studies of cerebral benzodiazepine-receptor binding in chronic alcoholics. *Annals of Neurology* (1996b) **40**: pp. 163-171.

Ginovart N, Farde L, Halldin C & Swahn C. Changes in striatal D2-receptor density following chronic treatment with amphetamine as assessed with PET in nonhuman primates. *Synapse* (1999) **31**: pp. 154-162.

Ginovart N, Galineau L, Willeit M, Mizrahi R, Bloomfield PM, Seeman P, Houle S, Kapur S & Wilson AA. Binding characteristics and sensitivity to endogenous dopamine of [11C]-(+)-PHNO, a new agonist radiotracer for imaging the high-affinity state of D2 receptors in vivo using positron emission tomography. *Journal of Neurochemistry* (2006) **97**: pp. 1089-1103.

Good C, Johnsrude I, Ashburner J, Henson R, Friston K & Frackowiak R. A voxel-based morphometric study of ageing in 465 normal adult human brains. (2001) **14**: pp. 21-36.

Gossop M, Darke S, Griffiths P, Hando J, Powis B, Hall W & Strang J. The Severity of Dependence Scale (SDS): psychometric properties of the SDS in English and Australian samples of heroin, cocaine and amphetamine users. *Addiction* (1995) **90**: pp. 607-614.

Gossop M, Eysenck S. A further investigation into the personality of drug addicts in treatment. *British Journal of Addiction* (1980) **75**: pp. 305-311.

Grannell P & Mansfield P. Microscopy in vivo by Nuclear Magnetic Resonance *Physics in Medicine and Biology* (1975) **20**: pp. 477-482.

Grant S, London E, Newlin D, Villemagne V, Liu X, Contoreggi C, Phillips R, Kimes A & Margolin A. Activation of memory circuits during cue-elicited cocaine craving. *Proceedings of the National Academy of Sciences* (1996) **93**: pp. 12040-12045.

Greenwald M, Johanson C, Bueller J, Chang Y, Moody DE, Kilbourn M, Koeppe R & Zubieta J. Buprenorphine duration of action: mu-opioid receptor availability and pharmacokinetic and behavioral indices. *Biological Psychiatry* (2007) **61**: pp. 101-110.

Greenwald MK, Johanson C, Moody DE, Woods JH, Kilbourn MR, Koeppe RA, Schuster CR & Zubieta J. Effects of buprenorphine maintenance dose on mu-opioid receptor availability, plasma concentrations, and antagonist blockade in heroin-dependent volunteers. *Neuropsychopharmacology* (2003) **28**: pp. 2000-2009.

Grimm JW, Lu L, Hayashi T, Hope BT, Su T & Shaham Y. Time-dependent increases in brain-derived neurotrophic factor protein levels within the mesolimbic dopamine system after withdrawal from cocaine: implications for incubation of cocaine craving. *Journal of Neuroscience* (2003) **23**: pp. 742-747.

Gunn R, Lammertsma A, Hume S & Cunningham V. Parametric imaging of ligand-receptor binding in PET using a simplified reference region model. *NeuroImage* (1997) **6**: pp. 279-287.

Haertzen C. An overview of addiction research center inventory scales (ARCI): An appendix and manual of scales. Government Printing Office, Washington, DC: US, (1974).

Hagel J, Andrews G, Vertinsky T, Heran MKS & Keogh C. "Chasing the dragon"--imaging of heroin inhalation leukoencephalopathy. *Canadian Association of Radiologists Journal* (2005) **56**: pp. 199-203.

Hagelberg N, Aalto S, Kajander J, Oikonen V, Hinkka S, Nagren K, Hietala J & Scheinin H. Alfentanil increases cortical dopamine D2/D3 receptor binding in healthy subjects. *Pain* (2004a) **109**: pp. 86-93.

Hagelberg N, Aalto S, Kajander J, Oikonen V, Hinkka S, Någren K, Hietala J & Scheinin H. Alfentanil increases cortical dopamine D2/D3 receptor binding in healthy subjects. *Pain* (2004b) **109**: pp. 86-93.

Hagelberg N, Kajander J, Nagren K, Hinkka S, Hietala J & Scheinin H. Mu-receptor agonism with alfentanil increases striatal dopamine D2 receptor binding in man. *Synapse* (2002a) **45**: pp. 25-30.

Hagelberg N, Kajander JK, Någren K, Hinkka S, Hietala J & Scheinin H. Mu-receptor agonism with alfentanil increases striatal dopamine D2 receptor binding in man. *Synapse* (2002b) **45**: pp. 25-30.

Halldin C, Farde L, Hogberg T, Mohell N, Hall H, Suhara T, Karlsson P, Nakashima Y & Swahn C. Carbon-11-FLB 457: A radioligand for extra-striatal D2 dopamine receptors. *Journal of Nuclear Medicine* (1995) **36**: pp. 1275-1281.

Hampson M, Peterson B, Skudlarski P, Gatenby J & Gore J. Detection of functional connectivity using temporal correlations in MR images. *Human Brain Mapping* (2002) **15**: pp. 247-262.

Handelsman L, Song,I.S.Losonczy,M., Park S, Jacobson J, Wiener J, Aronson M. Magnetic resonance abnormalities in HIV infection: a study in the drug-user risk group. *Psychiatry Research* (1993) **47**: pp. 175-186.

Hartvig P, Bergstrom K, Lindberg B, Lundberg P, Lundqvist H, Langstrom, Svard H & Rane A. Kinetics of 11C-labeled opiates in the brain of rhesus monkeys. *Journal of Pharmacology & Experimental Therapeutics* (1984) **230**: pp. 250-255.

Haselhorst R, Dursteler-MacFarland K, Scheffler K, Ladewig D, Muller-Spahn F, Stohler R, Seelig J & Seifritz E. Frontocortical N-acetylaspartate reduction associated with long-term IV heroin use. *Neurology* (2002) **58**: pp. 305-307.

Heimer L, Zahm D, Churchill L, Kalivas P, Wohltmann C. Specificity in the Projection Patterns of Accumbal Core and Shell in the rat. *Neuroscience* (1991) **41**: pp. 89-125.

Hemby S, Co C, Dworkin S & Smith J. Synergistic elevations in nucleus accumbens extracellular dopamine concentrations during self-administration of cocaine/heroin combinations (Speedball) in rats. *Journal of Pharmacology & Experimental Therapeutics* (1999) **288**: pp. 274-280.

Hemby S, Martin T, Co C, Dworkin S & Smith J. The effects of intravenous heroin administration on extracellular nucleus accumbens dopamine concentrations as determined by in vivo microdialysis. *Journal of Pharmacology & Experimental Therapeutics* (1995) **273**: pp. 591-598.

Hietala J, Nagren K, Lehikoinen P, Ruotsalainen U & Syvalahti E. Measurement of striatal D2 dopamine receptor density and affinity with [11C]-Raclopride in vivo: A test-retest analysis. *Journal of Cerebral Blood Flow & Metabolism* (1999) **19**: pp. 210-217.

Hietala J, West C, Syvalahti E, Nagren K, Lehikoinen P, Sonninen P & Ruotsalainen U. Striatal D2 dopamine receptor binding characteristics in vivo in patients with alcohol dependence. *Psychopharmacology* (1994) **116**: pp. 285-290.

Hill S & Mikhael M. Computerized transaxial tomographic and neuropsychological evaluations in chronic alcoholics and heroin users. *American Journal of Psychiatry* (1979) **136**: pp. 598-602.

Höll K, Deisenhammer E, Dauth J, Carmann H, Schubiger P. Imaging benzodiazepine receptors in the human brain by single photon emission computed tomography (SPECT). *International journal of radiation applications and instrumentation. Part B, Nuclear medicine and biology* (1989) **16**: pp. 759-763.

Holman B, Carvalho P, Mendelson J, Teoh S, Nardin R, Hallgring E, Hebben N, Johnson K. Brain perfusion is abnormal in cocaine-dependent polydrug users: a study using technetium-99m-HMPAO and ASPECT. *Journal of Nuclear Medicine* (1991) **32**: pp. 1206-1210.

Holman B, Garada B, Johnson K, Mendelson J, Hallgring E, Teoh S, Worth J & Navia B. A comparison of brain perfusion SPECT in cocaine abuse and AIDS dementia complex. *Journal of Nuclear Medicine* (1992) **33**: pp. 1312-1315.

Holman B, Mendelson J, Garada B, Teoh S, Hallgring E, Johnson K & Mello N. Regional cerebral blood flow improves with treatment in chronic cocaine polydrug users. *Journal of Nuclear Medicine* (1993) **34**: pp. 723-727.

Honey G, Suckling J, Zelaya F, Long C, Routledge C, Jackson S, Ng V, Fletcher P, Williams S, Brown J & Bullmore E. Dopaminergic drug effects on physiological connectivity in a human cortico-striato-thalamic system. *Brain* (2003) **126**: pp. 1767-1781.

Hu H. Multi-slice helical CT: scan and reconstruction. *Medical Physics* (1999) **26**: pp. 5-18.

Hudson H, Larkin R. Accelerated image reconstruction using ordered subsets of projection data. *IEEE Transactions on Medical Imaging* (1994) **13**: pp. 601-609.

Hugdahl K, Berardi A, Thompson W, Kosslyn S, Macy R, Baker D, Alpert N & LeDoux J. Brain mechanisms in human classical conditioning: a PET blood flow study. *Neuroreport* (1995) **6**: pp. 1723-1728.

Hume SP, Lammertsma AA, Myers R, Rajeswaran S, Bloomfield PM, Ashworth S, Fricker RA, Torres EM, Watson I & Jones T. The potential of high-resolution positron emission tomography to monitor striatal dopaminergic function in rat models of disease. *Journal of Neuroscience Methods* (1996) **67**: pp. 103-112.

Hwang D, Kegeles L & Laruelle M. (-)-N-[(11)C]propyl-norapomorphine: a positron-labeled dopamine agonist for PET imaging of D(2) receptors. *Nuclear Medicine & Biology* (2000) **27**: pp. 533-539.

Hwang J, Lyoo I, Kim S, Sung Y, Bae S, Cho S, Lee H, Lee D & Renshaw P. Decreased cerebral blood flow of the right anterior cingulate cortex in long-term and short-term abstinent methamphetamine users. *Drug & Alcohol Dependence* (2005) : .

Jacobsen L, D'Souza D, Mencl W, Pugh K, Skudlarski P & Krystal J. Nicotine effects on brain function and functional connectivity in schizophrenia. *Biological Psychiatry* (2004) **55**: pp. 850-858.

Jacobsen L, Giedd J, Gottschalk C, Kosten T & Krystal J. Quantitative morphology of the caudate and putamen in patients with cocaine dependence. *American Journal of Psychiatry* (2001) **158**: pp. 486-489.

Jacobsen L, Staley J, Malison R, Zoghbi S, Seibyl J, Kosten T & Innis R. Elevated central serotonin transporter binding availability in acutely abstinent cocaine-dependent patients. *American Journal of Psychiatry* (2000) **157**: pp. 1134-1140.

Jasinski D. Assessment of the abuse potential of morphine-like drugs (methods used in man). In *Drug addiction I: Morphine, sedative/hypnotic and alcohol dependence*. Martin W (Ed.). (1977). pp. 197-258.

Jenkinson C, Coulter A, Wright L. Short form 36 (SF36) health survey questionnaire: normative data for adults of working age. *BMJ* (1993) **306**: pp. 1437-1440.

Jenkinson C, Layte R, Wright L & Coulter A. The UK SF-36: An analysis and interpretation manual. A guide to health status measurement with particular reference to the Short Form 36 Health Survey. University of Oxford, Department of Public Health and Primary Care, Health Services Research Unit, Oxford, (1996)

Jiang M, Guo W, Scheiren I, Narendran R, Javitch J, Rayport S, Laruelle M. Agonist-mediated internalization of dopamine D2 receptors does not appear to mediate the decrease in benzamides binding potential observed after dopamine surge. *NeuroImage* (2006) **31**: p. T32.

Johnson-Greene D, Adams K, Gilman S, Koeppe R, Junck L, Kluin K, Martorello S & Heumann M. Effects of abstinence and relapse upon neuropsychological function and cerebral glucose metabolism in severe chronic alcoholism. *Journal of Clinical & Experimental Neuropsychology* (1997) **19**: pp. 378-385.

Jones A, Cunningham V, Ha-Kawa S, Fujiwara T, Luthra S, Silva S, Derbyshire S, Jones T. Changes in central opioid receptor binding in relation to inflammation and pain in patients with rheumatoid arthritis. *British Journal of Rheumatology* (1994) **33**: pp. 909-916.

Jones A, Friston K, Qi L, Harris M, Cunningham V, Jones T, Feinman C & Frackowiak R. Sites of action of morphine in the brain [letter]. *Lancet* (1991) **338**: p. 825.

Jones A, Kitchen N, Watabe H, Cunningham V, Jones T, Luthra S & Thomas D. Measurement of changes in opioid receptor binding in vivo during trigeminal neuralgic pain using [11C] diprenorphine and positron emission tomography. *Journal of Cerebral Blood Flow & Metabolism* (1999) **19**: pp. 803-808.

Jones A, Luthra S, Maziere B, Pike V, Loc'h C, Crouzel C, Syrota A & Jones T. Regional cerebral opioid receptor studies with [11C]diprenorphine in normal volunteers. *Journal of Neuroscience Methods* (1988) **23**: pp. 121-129.

Jucaite A, Odano I, Olsson H, Pauli S, Halldin C & Farde L. Quantitative analyses of regional [(11)C]PE2I binding to the dopamine transporter in the human brain: a PET study. *European Journal of Nuclear Medicine and Molecular Imaging* (2006) **33**: pp. 657-668.

Kaasinen V, Aalto S, Nagren K & Rinne J. Dopaminergic effects of caffeine in the human striatum and thalamus. *Neuroreport* (2004a) **15**: pp. 281-285.

Kaasinen V, Aalto S, Nagren K & Rinne J. Expectation of caffeine induces dopaminergic responses in humans. *The European Journal of Neuroscience* (2004b) **19**: pp. 2352-2356.

Kao C, Wang S, Yeh S. Presentation of regional cerebral blood flow in amphetamine abusers by 99Tcm-HMPAO brain SPECT. *Nuclear Medicine Communications* (1994) **15**: pp. 94-98.

Kapur S, Zipursky R, Remington G, Jones C, DaSilva J, Wilson A & Houle S. 5-HT2 and D2 receptor occupancy of olanzapine in schizophrenia: A PET investigation. *American Journal of Psychiatry* (1998) **155**: pp. 921-928.

Karlsson P, Farde L, Halldin C, Swahn C, Sedvall G, Foged C, Hansen, KT & Skrumsager B. PET examination of [11C]NNC 687 and [11C]NNC 756 as new radioligands for the D1-dopamine receptor. *Psychopharmacology* (1993) **113**: pp. 149-156.

Kaufman M, Levin J, Maas L, Rose S, Lukas B & Renshaw P. Cocaine decreases relative cerebral blood volume in humans: A dynamic susceptibility contrast magnetic resonance imaging study. *Psychopharmacology* (1998a) **138**: pp. 76-81.

Kaufman M, Levin J, Ross M, Lange N, Rose S, Kukes T, Mendelson, JH, Lukas S, Cohen B & Renshaw P. Cocaine-induced cerebral vasoconstriction detected in humans with magnetic resonance angiography. *JAMA* (1998b) **279**: pp. 376-380.

Kaufman M, Pollack M, Villafuerte R, Kukes T, Rose S, Mendelson J, Cohen B & Renshaw P. Cerebral phosphorus metabolite abnormalities in opiate-dependent polydrug abusers in methadone maintenance. *Psychiatry Research: Neuroimaging* (1999) **90**: pp. 143-152.

Kilts C, Schweitzer J, Quinn C, Gross R, Faber T, Muhammad F, Ely T, Hoffman J & Drexler K. Neural activity related to drug craving in cocaine addiction. *Archives of General Psychiatry* (2001) **58**: pp. 334-341.

Kim S, Lyoo I, Hwang J, Chung A, Hoon SY, Kim J, Kwon D, Chang K & Renshaw P. Prefrontal grey-matter changes in short-term and long-term abstinent methamphetamine abusers. *International Journal of Neuropsychopharmacology* (2006) **9**: pp. 221-228.

Kim S, Lyoo I, Hwang J, Sung Y, Lee H, Lee D, Jeong D & Renshaw P. Frontal glucose hypometabolism in abstinent methamphetamine users. *Neuropsychopharmacology* (2005) **30**: pp. 1383-1391.

Kinahan P, Rogers J. Analytic 3D image reconstruction using all detected events. *IEEE Transactions on Nuclear Science* (1989) **36**: pp. 964-968.

Kivisaari R, Kähkönen S, Puuskari V, Jokela O, Rapeli P & Autti T. Magnetic resonance imaging of severe, long-term, opiate-abuse patients without neurologic symptoms may show enlarged cerebrospinal spaces but no signs of brain pathology of vascular origin. *Archives of Medical Research* (2004) **35**: pp. 395-400.

Kiyatkin E, Wise R & Gratton A. Drug- and behavior-associated changes in dopamine-related electrochemical signals during intravenous heroin self-administration in rats. *Synapse* (1993) **14**: pp. 60-72.

Kling M, Carson R, Borg L, Zametkin A, Matochik J, Schluger J, Herscovitch P, Rice K, Ho A, Eckelman W & Kreek M. Opioid receptor imaging with positron emission tomography and [18F]cyclofoxy in long-term, methadone-treated former heroin addicts. *Journal of Pharmacology & Experimental Therapeutics* (2000) **295**: pp. 1070-1076.

Koepp M, Gunn R, Lawrence A, Cunningham V, Dagher A, Jones T, Brooks D, Bench C & Grasby P. Evidence for striatal dopamine release during a video game. *Nature* (1998) **393**: pp. 266-268.

Kohler C, Hall H, Ogren S & Gawell L. Specific in vitro and in vivo binding of 3H-raclopride. A potent substituted benzamide drug with high affinity for dopamine D-2 receptors in the rat brain. *Biochemical Pharmacology* (1985) **34**: pp. 2251-2259.

Kolb L & Himmelsbach C. Clinical studies of drug addiction III. A critical review of the withdrawal treatments with method of evaluating abstinence syndromes. *American Journal of Psychiatry* (1938) **94**: pp. 759-799.

Koob G. Drugs of abuse: anatomy, pharmacology and function of reward pathways. *Trends in Pharmacological Sciences* (1992) **13**: pp. 177-184.

Koob G. Neurobiology of addiction. Toward the development of new therapies. *Annals of the New York Academy of Sciences* (2000) **909**: pp. 170-185.

Koski L & Paus T. Functional Connectivity of the Anterior Cingulate Cortex within the Human Frontal Lobe: a Brain-mapping meta-analysis. *Experimental Brain Research* (2000) **133**: pp. 55-65.

Kosten T, Cheeves C, Palumbo J, Seibyl J, Price L & Woods S. Regional cerebral blood flow during acute and chronic abstinence from combined cocaine-alcohol abuse. *Drug & Alcohol Dependence* (1998) **50**: pp. 187-195.

Kosten TR, Scanley BE, Tucker KA, Oliveto A, Prince C, Sinha R, Potenza MN, Skudlarski P & Wexler BE. Cue-induced brain activity changes and relapse in cocaine-dependent patients. *Neuropsychopharmacology* (2006) **31**: pp. 644-650.

Kramer D, Schneider J, Rudin A, Lauterbur P. True three-dimensional nuclear magnetic resonance zeugmatographic images of a human brain. *Neuroradiology* (1981) **21**: pp. 239-244.

Krimer L, Muly E, Williams G & Goldman-Rakic P. Dopaminergic regulation of cerebral cortical microcirculation. *Nature Neuroscience* (1998) **1**: pp. 286-289.

Kroft C, Gescuk B, Woods B, Mello N, Weiss R & Mendelson J. Brain ventricular size in female alcoholics: An MRI study. *Alcohol* (1991) **8**: pp. 31-34.

Krystal J, Woods S, Kosten T, Rosen M, Seibyl J, van Dyck C, Price L, Zubal I, Hoffer P & Charney D. Opiate dependence and withdrawal: preliminary assessment using single photon emission computerized tomography (SPECT). *American Journal of Drug & Alcohol Abuse* (1995) **21**: pp. 47-63.

Kufahl P, Li Z, Wu G, Li S, Risinger R, Rainey C & Bloom A. Neural responses to acute cocaine administration in the human brain detected by fMRI. *NeuroImage* (2005) **28**: pp. 904-914.

Kuhl D, Reivich M, Alavi A, Nyary I, Staum M. Local cerebral blood volume determined by three-dimensional reconstruction of radionuclide scan data. *Circulation Research* (1975) **36**: pp. 610-619.

Kung H, Pan S, Kung M, Billings J, Kasliwal R, Reilley J, Alavi A. In vitro and in vivo evaluation of [123I]IBZM: a potential CNS D-2 dopamine receptor imaging agent. *Journal of Nuclear Medicine* (1989) **30**: pp. 88-92.

Kwong KK, Belliveau JW, Chesler DA, Goldberg IE, Weisskoff RM, Poncelet BP, Kennedy DN, Hoppel BE, Cohen MS, Turner R, Cheng H, Brady TJ, Rosen BR. Dynamic magnetic resonance imaging of human brain activity during primary sensory stimulation. *Proceedings of the National Academy of Science USA* (1992) **89**: pp. 5675-5679.

Laine T, Ahonen A, Rasanen P & Tiihonen J. Dopamine transporter availability and depressive symptoms during alcohol withdrawal. *Psychiatry Research* (1999) **90**: pp. 153-157.

Laine T, Ahonen A, Rasanen P & Tiihonen J. Dopamine transporter density and novelty seeking among alcoholics. *Journal of Addictive Diseases* (2001) **20**: pp. 91-96.

Laine T, Ahonen A, Torniainen P, Heikkila J, Pyhtinen J, Rasanen P, Niemela O & Hillbom M. Dopamine transporters increase in human brain after alcohol withdrawal. *Molecular Psychiatry* (1994) **4**: pp. 189-191.

Lammertsma A & Hume S. Simplified reference tissue model for PET receptor studies. *NeuroImage* (1996) **4**: pp. 153-158.

Lammertsma A, Bench C, Hume S, Osman S, Gunn K, Brooks D & Frackowiak R. Comparison of methods for analysis of clinical [11C]raclopride studies. *Journal of Cerebral Blood Flow & Metabolism* (1996) **16**: pp. 42-52.

Langleben D, Wang J, Gray J, Fornash A, O'Brien C & Childress A. Functional Magnetic Resonance Imaging (fMRI) of Regional Cerebral Blood Flow During Heroin-Related Cues in Opiate-Dependent Subjects. *Drug & Alcohol Dependence* (2002) **66**: p. S99.

Langleben DD, Ruparel K, Elman I, Busch-Winokur S, Pratiwadi R, Loughead J, O'Brien CP & Childress AR. Acute effect of methadone maintenance dose on brain FMRI response to heroin-related cues. *American Journal of Psychiatry* (2008a) **165**: pp. 390-394.

Langleben DD, Ruparel K, Elman I, Busch-Winokur S, Pratiwadi R, Loughead J, O'Brien CP, Childress AR. Acute Effect of Methadone Maintenance Dose on Brain fMRI Response to Heroin-Related Cues. *American Journal of Psychiatry* (2008b) **2008**: pp. 390-394.

Lartizien C, Kinahan PE, Swensson R, Comtat C, Lin M, Villemagne V, Trébossen R. Evaluating Image Reconstruction Methods for Tumor Detection in 3-Dimensional Whole-Body PET Oncology Imaging. *Journal of Nuclear Medicine* (2003) **44**: pp. 276-290.

Laruelle M. Imaging synaptic neurotransmission with in vivo binding competition techniques: a critical review. *Journal of Cerebral Blood Flow & Metabolism* (2000a) **20**: pp. 423-451.

Laruelle M. Imaging synaptic neurotransmission with in vivo binding competition techniques: a critical review. *Journal of Cerebral Blood Flow & Metabolism* (2000b) **20**: pp. 423-451.

Laruelle M, Abi-Dargham A, van Dyck C, Gil R, D'Souza C, Erdos J, McCance E, Rosenblatt W, Fingado C, Zoghbi S, Baldwin R, Seibyl J, Krystal J, Charney D & Innis R. Single photon emission computerized tomography imaging of amphetamine-induced dopamine release in drug-free schizophrenic subjects. *Proceedings of the National Academy of Sciences USA* (1996) **93**: pp. 9235-9240.

Laruelle M, Abi-Dargham A, van Dyck C, Rosenblatt W, Zea-Ponce Y, Zoghbi S, Baldwin R, Charney D, Hoffer P & Kung H. SPECT imaging of striatal dopamine release after amphetamine challenge. *Journal of Nuclear Medicine* (1995) **36**: pp. 1182-1190.

Laruelle M, D'Souza C, Baldwin R, Abi-Dargham A, Kanes S, Fingado C, Seibyl J, Zoghbi S, Bowers M, Jatlow P, Charney D & Innis R. Imaging D2 receptor occupancy by endogenous dopamine in humans. *Neuropsychopharmacology* (1997) **17**: pp. 162-174.

Law F, Bailey J, Allen D, Melichar J, Myles J, Mitcheson M, Lewis J & Nutt D. The feasibility of abrupt methadone-buprenorphine transfer in British opiate addicts in an outpatient setting. *Addiction Biology* (1997) **2**: pp. 191-200.

Lee TM, Zhou W, Luo X, Yuen K, Ruan X, Weng X. Neural activity associated with cognitive regulation in heroin users: A fMRI study.. *Neuroscience Letters* (2005) **382**: pp. 211-216.

Leppä M, Korvenoja A, Carlson S, Timonen P, Martinkauppi S, Ahonen J, Rosenberg PH, Aronen HJ & Kalso E. Acute opioid effects on human brain as revealed by functional magnetic resonance imaging. *NeuroImage* (2006) **31**: pp. 661-669.

Levin J, Holman B, Mendelson J, Teoh S, Garada B, Johnson K & Springer S. Gender differences in cerebral perfusion in cocaine abuse: technetium-99m-HMPAO SPECT study of drug-abusing women. *Journal of Nuclear Medicine* (1994) **35**: pp. 1902-1909.

Levin J, Mendelson J, Holman B, Teoh S, Garada B, Schwartz R & Mello N. Improved regional cerebral blood flow in chronic cocaine polydrug users treated with buprenorphine. *Journal of Nuclear Medicine* (1995) **36**: pp. 1211-1215.

Levin J, Ross M, Mendelson J, Kaufman M, Lange N, Maas L, Mello N, Cohen B & Renshaw P. Reduction in BOLD fMRI response to primary visual stimulation following alcohol ingestion. *Psychiatry Research* (1998) **82**: pp. 135-146.

Li S, Biswal B, Li Z, Risinger R, Rainey C, Cho J, Salmeron B & Stein E. Cocaine administration decreases functional connectivity in human primary visual and motor cortex as detected by functional MRI. *Magnetic Resonance in Medicine* (2000) **43**: pp. 45-51.

Lim K, Choi S, Pomara N, Wolkin A & Rotrosen J. Reduced frontal white matter integrity in cocaine dependence: a controlled diffusion tensor imaging study. *Biological Psychiatry* (2002) **51**: pp. 890-895.

Lingford-Hughes A, Acton P, Gacinovic S, Boddington S, Costa D, Pilowsky L, Ell P, Marshall E & Kerwin R. Levels of gamma-aminobutyric acid-benzodiazepine receptors in abstinent, alcohol-dependent women: preliminary findings from an 123I-iomazenil single photon emission tomography study. *Alcoholism: Clinical & Experimental Research* (2000) **24**: pp. 1449-1455.

Lingford-Hughes A, Acton P, Gacinovic S, Suckling J, Busatto G, Boddington S, Bullmore E, Woodruff P, Costa D, Pilowsky L, Ell P, Marshall E & Kerwin R. Reduced levels of GABA-benzodiazepine receptor in alcohol dependency in the absence of grey matter atrophy. *British Journal of Psychiatry* (1998) **173**: pp. 116-122.

Litton J, Neiman J, Pauli S, Farde L, Hindmarsh T, Halldin C & Sedvall G. PET analysis of [11C]flumazenil binding to benzodiazepine receptors in chronic alcohol-dependent men and healthy controls. *Psychiatry Research: Neuroimaging* (1993) **50**: pp. 1-13.

Liu X, Phillips R, Resnick S, Villemagne V, Wong D, Stapleton J & London E. Magnetic resonance imaging reveals no ventriculomegaly in polydrug abusers. *Acta Neurologica Scandinavica* (1995) **92**: pp. 83-90.

London E, Broussolle E, Links J, Wong D, Cascella N, Dannals R, Sano M, Herning R, Snyder F, Rippetoe L. Morphine-induced metabolic changes in human brain. Studies with positron emission tomography and [fluorine 18]fluorodeoxyglucose. *Archives of General Psychiatry* (1990a) **47**: pp. 73-81.

London E, Cascella N, Wong D, Phillips R, Dannals R, Links J, Herning R, Grayson R, Jaffe J, Wagner,HN,Jr. Cocaine-induced reduction of glucose utilization in human brain. A study using positron emission tomography and [fluorine 18]-fluorodeoxyglucose. *Archives of General Psychiatry* (1990b) **47**: pp. 567-574.

London E, Ernst M, Grant S, Bonson K & Weinstein A. Orbitofrontal cortex and human drug abuse: functional imaging. *Cerebral Cortex* (2000) **10**: pp. 334-342.

London E, Margolin R, Wong D, Links J, La France N, Cascella N, Broussolle E, Wagner J, Snyder F & Jasinski D. Cerebral glucose utilization in human heroin addicts: Case reports from a positron emission tomographic study. *Research Communications in Substances of Abuse* (1989) **10**: pp. 141-144.

Longoni R, Cadoni C, Mulas A, Di Chiara G & Spina L. Dopamine-dependent behavioural stimulation by non-peptide delta opioids BW373U86 and SNC 80: 2. Place-preference and brain microdialysis studies in rats. *Behavioural Pharmacology* (1998) **9**: pp. 9-14.

Lorenz IH, Kolbitsch C, Schocke M, Kremser C, Zschiegner F, Hinteregger M, Felber S, Hörmann C & Benzer A. Low-dose remifentanil increases regional cerebral blood flow and regional cerebral blood volume, but decreases regional mean transit time and regional cerebrovascular resistance in volunteers. *British Journal of Anaesthesia* (2000) **85**: pp. 199-204.

Lyoo I, Pollack M, Silveri M, Ahn K, Diaz C, Hwang J, Kim S, Yurgelun-Todd D, Kaufman M & Renshaw P. Prefrontal and temporal gray matter density decreases in opiate dependence. *Psychopharmacology* (2006) **184**: pp. 139-144.

Lyoo I, Streeter C, Ahn K, Lee H, Pollack M, Silveri M, Nassar L, Levin J, Sarid-Segal O, Ciraulo D, Renshaw P & Kaufman M. White matter hyperintensities in subjects with cocaine and opiate dependence and healthy comparison subjects. *Psychiatry Research: Neuroimaging* (2004) **131**: pp. 135-145.

Maas L, Lukas S, Kaufman M, Weiss R, Daniels S, Rogers V, Kukes, TJ & Renshaw P. Functional magnetic resonance imaging of human brain activation during cue-induced cocaine craving. *American Journal of Psychiatry* (1998) **155**: pp. 124-126.

MacKay S, Meyerhoff D, Dillon W, Weiner M, Fein G. Alteration of brain phospholipid metabolites in cocaine-dependent polysubstance abusers.. *Biological Psychiatry* (1993) **34**: pp. 261-264.

Malison R, Best S, van Dyck C, McCance E, Wallace E, Laruelle M, Baldwin R, Seibyl J, Price L, Kosten T & Innis R. Elevated striatal dopamine transporters during acute cocaine abstinence as measured by [123I] beta-CIT SPECT. *American Journal of Psychiatry* (1998) **155**: pp. 832-834.

Malison R, Best S, Wallace E, McCance E, Laruelle M, Zoghbi S, Baldwin R, Seibyl J, Hoffer P & Price L. Euphorigenic doses of cocaine reduce [123I]beta-CIT SPECT measures of dopamine transporter availability in human cocaine addicts. *Psychopharmacology* (1995) **122**: pp. 358-362.

Mander A, Young A, Chick J & Best J. The relationship of cerebral atrophy and T1 in alcoholics: an MRI study. *Drug & Alcohol Dependence* (1989) **24**: pp. 57-59.

Mann K, Mundle G, Langle G & Petersen D. The reversibility of alcoholic brain damage is not due to rehydration: a CT study. *Addiction* (1993) **88**: pp. 649-653.

Martin P, Rio D, Adinoff B, Johnson J, Bisserbe J, Rawlings R, Rohrbaugh J, Stapleton J & Eckardt M. Regional cerebral glucose utilization in chronic organic mental disorders associated with alcoholism. *Journal of Neuropsychiatry & Clinical Neurosciences* (1992) **4**: pp. 159-167.

Martin-Soelch C, Chevalley AF, Künig G, Missimer J, Magyar S, Mino A, Schultz W & Leenders KL. Changes in reward-induced brain activation in opiate addicts. *The European Journal of Neuroscience* (2001) **14**: pp. 1360-1368.

Martinez D, Gil R, Slifstein M, Hwang D, Huang Y, Perez A, Kegeles L, Talbot P, Evans S, Krystal J, Laruelle M & Abi-Dargham A. Alcohol dependence is associated with blunted dopamine transmission in the ventral striatum. *Biological Psychiatry* (2005) **58**: pp. 779-786.

Mathew R, Wilson W. Regional cerebral blood flow changes associated with ethanol intoxication. *Stroke* (1986) **17**: pp. 1156-1159.

Mathew R, Wilson W & Daniel D. The effect of nonsedating doses of diazepam on regional cerebral blood flow. *Biological Psychiatry* (1985) **20**: pp. 1109-1116.

Mathew R, Wilson W, Coleman R, Turkington T & De Grado T. Marijuana intoxication and brain activation in marijuana smokers. *Life Sciences* (1997) **60**: pp. 2075-2089.

Mathew R, Wilson W, Lowe J & Humphries D. Acute changes in cranial blood flow after cocaine hydrochloride. *Biological Psychiatry* (1996) **40**: pp. 609-616.

Matochik J, Nordahl T, Gross M, Semple W, King A, Cohen R & Zametkin A. Effects of acute stimulant medication on cerebral metabolism in adults with hyperactivity. *Neuropsychopharmacology* (1993) **8**: pp. 377-386.

Matthew E, Andreason P, Pettigrew K, Carson R, Herscovitch P, Cohen R, King C, Johanson C, Greenblatt D & Paul S. Benzodiazepine receptors mediate regional blood flow changes in the living human brain. *Proceedings of the National Academy of Sciences USA* (1995) **92**: pp. 2775-2779.

Mawlawi O, Martinez D, Slifstein M, Broft A, Chatterjee R, Hwang D, Huang Y, Simpson N, Ngo K, Van Heertum R & Laruelle M. Imaging human mesolimbic dopamine transmission with positron emission tomography: I. Accuracy and precision of D(2) receptor parameter measurements in ventral striatum. *Journal of Cerebral Blood Flow & Metabolism* (2001) **21**: pp. 1034-1057.

Maziere B, Coenen H, Halldin C, Nagren K & Pike V. PET radioligands for dopamine receptors and re-uptake sites: chemistry and biochemistry. *International Journal of Radiation Applications & Instrumentation - Part B, Nuclear Medicine & Biology* (1992) **19**: pp. 497-512.

McCann U, Szabo Z, Scheffel U, Dannals R & Ricaurte G. Positron emission tomographic evidence of toxic effect of MDMA ('Ecstasy') on brain serotonin neurons in human beings. *Lancet* (1998) **352**: pp. 1433-1437.

McClernon FJ, Hiott FB, Huettel SA & Rose JE. Abstinence-induced changes in self-report craving correlate with event-related FMRI responses to smoking cues. *Neuropsychopharmacology* (2005) **30**: pp. 1940-1947.

Mechelli A, Penny W, Price C, Gitelman D & Friston K. Effective connectivity and intersubject variability: using a multisubject network to test differences and commonalities. *NeuroImage* (2002) **17**: pp. 1459-1469.

Melichar J, Myles J, Eap C & Nutt D. Using saccadic eye movements as objective measures of tolerance in methadone dependent individuals during the hydromorphone challenge test. *Addiction Biology* (2003) **8**: pp. 59-66.

Melichar JK, Hume SP, Williams TM, Daglish MRC, Taylor LG, Ahmad R, Malizia AL, Brooks DJ, Myles JS, Lingford-Hughes A & Nutt DJ. Using [11C]diprenorphine to image opioid receptor occupancy by methadone in opioid addiction: clinical and preclinical studies. *Journal of Pharmacology & Experimental Therapeutics* (2005) **312**: pp. 309-315.

Mena I, Giombetti R, Miller B, Garrett K, Villanueva-Meyer J, Mody C, Goldberg M. Cerebral blood flow changes with acute cocaine intoxication: clinical correlations with SPECT, CT, and MRI. *NIDA Research Monograph* (1994) **138**: pp. 161-173.

Mettler FAJ, Wiest PW, Locken JA, Kelsey CA. CT scanning: patterns of use and dose. *Journal of Radiological Protection* (2000) **20**: pp. 353-359.

Meyerhoff D, MacKay S, Sappey-Marinier D, Deicken R, Calabrese G, Dillon W, Weiner M & Fein G. Effects of chronic alcohol abuse and HIV infection on brain phosphorus metabolites. *Alcoholism: Clinical & Experimental Research* (1995) **19**: pp. 685-692.

Mitrovic I & Napier TC. Mu and kappa opioid agonists modulate ventral tegmental area input to the ventral pallidum. *European Journal of Neuroscience* (2002) **15**: pp. 257-268.

Modell J & Mountz J. Focal cerebral blood flow change during craving for alcohol measured by SPECT. *Journal of Neuropsychiatry & Clinical Neurosciences* (1995) **7**: pp. 15-22.

Moeller F, Steinberg J, Dougherty D, Narayana P, Kramer L & Renshaw P. Functional MRI study of working memory in MDMA users. *Psychopharmacology* (2004) **177**: pp. 185-194.

Mukherjee J, Yang Z, Brown T, Roemer J & Cooper M. 18F-desmethoxyfallypride: a fluorine-18 labeled radiotracer with properties similar to carbon-11 raclopride for PET imaging studies of dopamine D2 receptors. *Life Sciences* (1996) **59**: pp. 669-678.

Newlin D, Golden C, Quaife M & Graber B. Effect of alcohol ingestion on regional cerebral blood flow. *International Journal of Neuroscience* (1982) **17**: pp. 145-150.

Nutt D. Addiction: brain mechanisms and their treatment implications. *Lancet* (1996) **347**: pp. 31-36.

Nyback H, Halldin C, Ahlin A, Curvall M, Eriksson L. PET studies of the uptake of (S)- and (R)-[11C]nicotine in the human brain: difficulties in visualizing specific receptor binding in vivo. *Psychopharmacology (Berlin)* (1994) **115**: pp. 31-36.

Oh J, Lyoo I, Sung Y, Hwang J, Kim J, Chung A, Park K, Kim S, Renshaw P & Song I. Shape changes of the corpus callosum in abstinent methamphetamine users. *Neuroscience Letters* (2005) **384**: pp. 76-81.

Oswald L, Wong D, McCaul M, Zhou Y, Kuwabara H, Choi L, Brasic J & Wand G. Relationships among ventral striatal dopamine release, cortisol secretion, and subjective responses to amphetamine. *Neuropsychopharmacology* (2005) **30**: pp. 821-832.

Pascual-Leone A, Dhuna A, Anderson D. Cerebral atrophy in habitual cocaine abusers: a planimetric CT study. *Neurology* (1991) **41**: pp. 34-38.

Pauli S, Liljequist S, Farde L, Swahn C, Halldin C, Litton J & Sedvall. PET analysis of alcohol interaction with the brain disposition of [11C]flumazenil. *Psychopharmacology* (1992) **107**: pp. 180-185.

Pearlson G, Jeffery P, Harris G, Ross C, Fischman M & Camargo E. Correlation of acute cocaine-induced changes in local cerebral blood flow with subjective effects. *American Journal of Psychiatry* (1993) **150**: pp. 495-497.

Penfield W & Rasmussen T. The cerebral cortex of man. Macmillan, New York, (1950).

Pezawas L, Fischer G, Diamant K, Schneider C, Schindler S, Thurnher M, Ploechl W, Eder H & Kasper S. Cerebral CT findings in male opioid-dependent patients: stereological, planimetric and linear measurements. *Psychiatry Research* (1998) **83**: pp. 139-147.

Pezawas L, Fischer G, Podreka I, Schindler S, Brcke T, Jagsch R, Thurnher M & Kasper S. Opioid addiction changes cerebral blood flow symmetry. *Neuropsychobiology* (2002) **45**: pp. 67-73.

Pfefferbaum A, Sullivan E, Hedehus M, Adalsteinsson E, Lim K & Moseley M. In vivo detection and functional correlates of white matter microstructural disruption in chronic alcoholism. *Alcoholism: Clinical & Experimental Research* (2000) **24**: pp. 1214-1221.

Pickens R & Johanson C. Craving: consensus of status and agenda for future research. *Drug & Alcohol Dependence* (1992) **30**: pp. 127-131.

Pontieri F, Tanda G & Di Chiara G. Intravenous cocaine, morphine, and amphetamine preferentially increase extracellular dopamine in the "shell" as compared with the "core" of the rat nucleus accumbens. *Proceedings of the National Academy of Sciences USA* (1995) **92**: pp. 12304-12308.

Ridenour T, Maldonado-Molina M, Compton W, Spitznagel E & Cottler L. Factors associated with the transition from abuse to dependence among substance abusers: Implications for a measure of addictive liability. *Drug & Alcohol Dependence* (2005) **80**: pp. 1-14.

Risinger R, Salmeron B, Ross T, Amen S, Sanfilipo M, Hoffmann R, Bloom A, Garavan H, Stein E. Neural correlates of high and craving during cocaine self-administration using BOLD fMRI. *NeuroImage* (2005) **26**: pp. 1097-1108.

Robinson T & Berridge K. The neural basis of drug craving: an incentive-sensitization theory of addiction. *Brain Research - Brain Research Reviews* (1993) **18**: pp. 247-291.

Rogers R, Everitt B, Baldacchino A, Blackshaw A, Swainson R, Wynne K, Baker N, Hunter J, Carthy T, Booker E, London M, Deakin J, Sahakian B & Robbins T. Dissociable deficits in the decision-making cognition of chronic amphetamine abusers, opiate abusers, patients with focal damage to prefrontal cortex, and tryptophan-depleted normal volunteers: evidence for monoaminergic mechanisms. *Neuropsychopharmacology*(1999) **20**: pp. 322-339.

Rolls E. The orbitofrontal cortex. *Philosophical Transactions of the Royal Society of London - Series B: Biological Sciences* (1996) **351**: pp. 1433-1443.

Rose J, Branchey M, Buydens-Branch L, Stapleton J, Chasten K, Werrell A & Maayan, M. Cerebral perfusion in early and late opiate withdrawal: a technetium-99m-HMPAO SPECT study. *Psychiatry Research: Neuroimaging* (1996) **67**: 39-47.

Rourke S, Dupont R, Grant I, Lehr P, Lamoureux G, Halpern S, Yeung D. Reduction in cortical IMP-SPET tracer uptake with recent cigarette consumption in a young group of healthy males. *European Journal of Nuclear Medicine* (1997) **24**: pp. 422-427.

Rumbaugh C, Fang H, Wilson G, Higgins R, Mestek M. Cerebral CT findings in drug abuse: clinical and experimental observations. *Journal Computer Assisted Tomography* (1980) **4**: pp. 330-334.

Sano M, Wendt P, Wirsen A, Stenberg G, Risberg J & Ingvar D. Acute effects of alcohol on regional cerebral blood flow in man. *Journal of Studies on Alcohol* (1993) **54**: pp. 369-376.

Schlaepfer T, Pearlson G, Wong D, Marenco S & Dannals R. PET study of competition between intravenous cocaine and [11C]raclopride at dopamine receptors in human subjects. *American Journal of Psychiatry* (1997) **154**: pp. 1209-1213.

Schlaepfer T, Strain E, Greenberg B, Preston K, Lancaster E, Bigelow G, Barta P & Pearlson G. Site of opioid action in the human brain: mu and kappa agonists' subjective and cerebral blood flow effects. *American Journal of Psychiatry* (1998) **155**: pp. 470-473.

Sell L, Morris J, Bearn J, Frackowiak R, Friston K & Dolan R. Activation of reward circuitry in human opiate addicts. *European Journal of Neuroscience* (1999) **11**: pp. 1042-1048.

Sell L, Morris J, Bearn J, Frackowiak R, Friston K & Dolan R. Neural responses associated with cue evoked emotional states and heroin in opiate addicts. *Drug & Alcohol Dependence* (2000) **60**: pp. 207-216.

Sell L, Simmons A, Lemmens G, Williams S, Brammer M & Strang J. Functional magnetic resonance imaging of the acute effect of intravenous heroin administration on visual activation in long-term heroin addicts: results from a feasibility study. *Drug & Alcohol Dependence* (1997) **49**: pp. 55-60.

Shalev U, Morales M, Hope B, Yap J & Shaham Y. Time-dependent changes in extinction behavior and stress-induced reinstatement of drug seeking following withdrawal from heroin in rats.. *Psychopharmacology* (2001) **156**: pp. 98-107.

Sharp P, Smith F, Gemmell H, Lyall D, Evans N, Gvozdanovic D, Davidson J, Tyrell D, Pickett R, Neirinckx R. Technetium-99m HM-PAO Stereoisomers as Potential Agents for Imaging Regional Cerebral Blood Flow: Human Volunteer Studies. *Journal of Nuclear Medicine* (1986) **27**: pp. 171-177.

Shi J, Zhao L, Copersino ML, Fang Y, Chen Y, Tian J, Deng Y, Shuai Y, Jin J & Lu L. PET imaging of dopamine transporter and drug craving during methadone maintenance treatment and after prolonged abstinence in heroin users. *European Journal of Pharmacology* (2008) **579**: pp. 160-166.

Siew KT, Mendelson J, Woods B, Mello N, Hallgring E, Anfinsen, Douglas A & Mercer G. Pituitary volume in men with concurrent heroin and cocaine dependence. *Journal of Clinical Endocrinology & Metabolism* (1993) **76**: pp. 1529-1532.

Silveri M, Anderson C, McNeil J, Diaz C, Lukas S, Mendelson J, Renshaw P & Kaufman M. Oral methylphenidate challenge selectively decreases putaminal T2 in healthy subjects. *Drug & Alcohol Dependence* (2004a) **76**: pp. 173-180.

Silveri M, Pollack M, Diaz C, Nassar L, Mendelson J, Yurgelun-Todd D, Renshaw P & Kaufman M. Cerebral phosphorus metabolite and transverse relaxation time abnormalities in heroin-dependent subjects at onset of methadone maintenance treatment. *Psychiatry Research* (2004b) **131**: pp. 217-226.

Small D, Jones-Gotman M & Dagher A. Feeding-induced dopamine release in dorsal striatum correlates with meal pleasantness ratings in healthy human volunteers. *NeuroImage* (2003) **19**: pp. 1709-1715.

Smith G, Schloesser R, Brodie J, Dewey S, Logan J, Vitkun S, Simkowitz P, Hurley A, Cooper T, Volkow N & Cancro R. Glutamate modulation of dopamine measured in vivo with positron emission tomography (PET) and 11C-raclopride in normal human subjects. *Neuropsychopharmacology* (1998a) **18**: pp. 18-25.

Smith J, Zubieta J, Price J, Flesher J, Madar I, Lever J, Kinter C, Dannals R & Frost J. Quantification of delta-opioid receptors in human brain with N1'-([11C]methyl) naltrindole and positron emission tomography. *Journal of Cerebral Blood Flow & Metabolism* (1999) **19**: pp. 956-966.

Smith Y, Zubieta J, del Carmen M, Dannals R, Ravert H, Zacur H & Frost J. Brain opioid receptor measurements by positron emission tomography in normal cycling women: relationship to luteinizing hormone pulsatility and gonadal steroid hormones. *Journal of Clinical Endocrinology & Metabolism* (1998b) **83**: pp. 4498-4505.

Sorge RE, Rajabi H & Stewart J. Rats maintained chronically on buprenorphine show reduced heroin and cocaine seeking in tests of extinction and drug-induced reinstatement. *Neuropsychopharmacology* (2005) **30**: pp. 1681-1692.

Spielberger C, Gorsuch R, Lushene R, Vagg P, Jacobs G. Manual for the State-Trait Anxiety Inventory. Consulting Psychologists' Press Inc. Palo Alto, CA., (1983).

Spinks T, Jones T, Bailey D, Townsend D, Grootoonk S, Bloomfield P, Gilardi M, Casey M, Sipe B & Reed J. Physical performance of a positron tomograph for brain imaging with retractable septa. *Physics in Medicine & Biology* (1992) **37**: pp. 1637-1655.

Spinks T, Jones T, Bloomfield P, Bailey D, Miller M, Hogg D, Jones W, Vaigneur K, Reed J, Young J, Newport D, Moyers C, Casey M & Nutt R. Physical characteristics of the ECAT EXACT3D positron tomograph. *Physics in Medicine & Biology* (2000) **45**: pp. 2601-2618.

Stapleton J, Gilson S, Wong D, Villemagne V, Dannals R, Grayson R, Henningfield J & London E. Intravenous nicotine reduces cerebral glucose metabolism: a preliminary study. *Neuropsychopharmacology* (2003) **28**: pp. 765-772.

Stapleton J, Morgan M, Phillips R, Wong D, Yung B, Shaya E, Dannals R, Liu X, Grayson R & London E. Cerebral glucose utilization in poly-substance abuse. *Neuropsychopharmacology* (1995) **13**: pp. 21-31.

Strang J & Gurling H. Computerized tomography and neuropsychological assessment in long-term high-dose heroin addicts. *British Journal of Addiction* (1989) **84**: pp. 1011-1019.

Streeter C, Ciraulo D, Harris G, Kaufman M, Lewis R, Knapp C, Ciraulo A, Maas L, Ungeheuer M, Szulewski S & Renshaw P. Functional magnetic resonance imaging of alprazolam-induced changes in humans with familial alcoholism. *Psychiatry Research* (1998a) **82**: pp. 69-82.

Streeter C, Ciraulo D, Harris G, Knapp C, Ann MC, Ungeheuer M, Szulewski S, Kaufman M, Maas L, Renshaw P & Lewis R. Functional magnetic resonance imaging of alprazolam-induced changes in humans with familial alcoholism. *Psychiatry Research: Neuroimaging* (1998b) **82**: pp. 69-82.

Streeter C, Hennen J, Ke Y, Jensen J, Sarid-Segal O, Nassar L, Knapp C, Meyer A, Kwak T, Renshaw P & Ciraulo D. Prefrontal GABA levels in cocaine-dependent subjects increase with pramipexole and venlafaxine treatment. *Psychopharmacology* (2005) **182**: pp. 516-526.

Studholme C, Hill DL & Hawkes DJ. An overlap invariant entropy measure of 3D medical image alignment. *Pattern Recognition* (1999) **32**: pp. 71-86.

Terry C & Pellens M. The Opium Problem. Bureau of Social Hygiene, New York, (1928).

Theodore W, Di Chiro G, Margolin R, Fishbein D, Porter R & Brooks R. Barbiturates reduce human cerebral glucose metabolism. *Neurology* (1986) **36**: pp. 60-64.

Thorpe S, Rolls E & Maddison S. The orbitofrontal cortex: neuronal activity in the behaving monkey. *Experimental Brain Research* (1983) **49**: pp. 93-115.

Tiihonen J, Kuikka J, Hakola P, Paanila J, Airaksinen J, Eronen M & Hallikainen T. Acute ethanol-induced changes in cerebral blood flow. *American Journal of Psychiatry* (1994) **151**: pp. 1505-1508.

Tsukada H, Nishiyama S, Kakiuchi T, Ohba H, Sato K, Harada N. Is synatpic dopamine concentration the exclusive factor which alters the in vivo binding of [11C]raclopride?: PET studies combined with microdialysis in conscious monkeys.. *Brain Research* (1999) **841**: pp. 160-169.

Tumeh S, Nagel J, English R, Moore M, Holman B. Cerebral abnormalities in cocaine abusers: demonstration by SPECT perfusion brain scintigraphy. Work in progress. *Radiology* (1990) **176**: pp. 821-824.

van Dyck C, Rosen M, Thomas H, McMahon T, Wallace E, O'Connor P, Sullivan M, Krystal J, Hoffer P, Woods S & Kosten T. SPECT Regional Cerebral Blood Flow Alterations in Naltrexone-Precipitated Withdrawal From Buprenorphine. *Psychiatry Research* (1994) **55**: pp. 181-191.

Veselis R, Reinsel R, Beattie B, Mawlawi O, Feshchenko V, Di Resta G, Larson S & Blasberg R. Midazolam changes cerebral blood flow in discrete brain regions: An H215O positron emission tomography study. *Anesthesiology* (1997) **87**: pp. 1106-1117.

Vila N & Chamorro A. Ballistic movements due to ischemic infarcts after intravenous heroin overdose: Report of two cases. *Clinical Neurology & Neurosurgery* (1997) **99**: pp. 259-262.

Villemagne V, Yuan J, Wong D, Dannals R, Hatzidimitriou G, Mathews W, Ravert H, Musachio J, McCann U & Ricaurte G. Brain dopamine neurotoxicity in baboons treated with doses of methamphetamine comparable to those recreationally abused by humans: evidence from [11C]WIN-35,428 positron emission tomography studies and direct in vitro determinations. *Journal of Neuroscience* (1998) **18**: pp. 419-427.

Volkow N & Fowler J. Addiction, a Disease of Compulsion and Drive: Involvement of the Orbitofrontal Cortex. *Cerebral Cortex* (2000) **10**: pp. 318-325.

Volkow N, Chang L, Wang G, Fowler J, Franceschi D, Sedler M, Gatley S, Hitzemann R, Ding Y, Wong C & Logan J. Higher cortical and lower subcortical metabolism in detoxified methamphetamine abusers. *American Journal of Psychiatry* (2001) **158**: pp. 383-389.

Volkow N, Ding Y, Fowler J, Wang G, Logan J, Gatley J, Dewey S, Ashby C, Liebermann J & Hitzemann R. Is methylphenidate like cocaine? Studies on their pharmacokinetics and distribution in the human brain. *Archives of General Psychiatry* (1995a) **52**: pp. 456-463.

Volkow N, Fowler J & Wang G. The addicted human brain viewed in the light of imaging studies: brain circuits and treatment strategies. *Neuropharmacology* (2004a) **47**: pp. 3-13.

Volkow N, Fowler J, Wang G, Hitzemann R, Logan J, Schlyer D, Dewey S & Wolf A. Decreased dopamine D2 receptor availability is associated with reduced frontal metabolism in cocaine abusers. *Synapse* (1993a) **14**: pp. 169-177.

Volkow N, Fowler J, Wolf A, Hitzemann R, Dewey S, Bendriem B, Alpert R & Hoff A. Changes in brain glucose metabolism in cocaine dependence and withdrawal. *American Journal of Psychiatry* (1991a) **148**: pp. 621-626.

Volkow N, Fowler J, Wolf A, Schlyer D, Shiue C, Alpert R, Dewey S, Logan J, Bendriem B & Christman D. Effects of chronic cocaine abuse on postsynaptic dopamine receptors. *American Journal of Psychiatry* (1990a) **147**: pp. 719-724.

Volkow N, Fowler J, Wolf A, Wang G, Logan J, MacGregor R, Dewey S, Schlyer D & Hitzemann R. Distribution and kinetics of carbon-11-cocaine in the human body measured with PET. *Journal of Nuclear Medicine* (1992a) **33**: pp. 521-525.

Volkow N, Gillespie H, Mullani N, Tancredi L, Grant C, Ivanovic M & Hollister L. Cerebellar metabolic activation by delta-9-tetrahydro-cannabinol in human brain: a study with positron emission tomography and 18F-2-fluoro-2-deoxyglucose. *Psychiatry Research: Neuroimaging* (1991b) **40**: pp. 69-78.

Volkow N, Gillespie H, Tancredi L, Grant C, Valentine A, Hollister L & Mullani N. Brain glucose metabolism in chronic marijuana users at baseline and during marijuana intoxication. *Psychiatry Research: Neuroimaging* (1996a) **67**: pp. 29-38.

Volkow N, Hitzemann R, Wang G, Fowler J, Burr G, Pascani K, Dewey S & Wolf A. Decreased brain metabolism in neurologically intact healthy alcoholics. *American Journal of Psychiatry* (1992b) **149**: pp. 1016-1022.

Volkow N, Hitzemann R, Wang G, Fowler J, Wolf A, Dewey S, Handlesman L. Long-term frontal brain metabolic changes in cocaine abusers. *Synapse* (1992c) **11**: pp. 184-190.

Volkow N, Hitzemann R, Wolf A, Logan J, Fowler J, Christman D, Dewey S, Schlyer D, Burr G & Vitkun S. Acute effects of ethanol on regional brain glucose metabolism and transport. *Psychiatry Research: Neuroimaging* (1990b) **35**: pp. 39-48.

Volkow N, Mullani N, Gould K, Adler S & Krajewski K. Cerebral blood flow in chronic cocaine users: a study with positron emission tomography. *British Journal of Psychiatry* (1988a) **152**: pp. 641-648.

Volkow N, Mullani N, Gould L, Adler S, Guynn R, Overall J & Dewey S. Effects of acute alcohol intoxication on cerebral blood flow measured with PET. *Psychiatry Research* (1988b) **24**: pp. 201-209.

Volkow N, Valentine A & Kulkarni M. Radiological and neurological changes in the drug abuse patient: a study with MRI. *Journal of Neuroradiology* (1988c) **15**: pp. 288-293.

Volkow N, Wang G, Begleiter H, Hitzemann R, Pappas N, Burr G, Pascani K, Wong C, Fowler J & Wolf A. Regional brain metabolic response to lorazepam in subjects at risk for alcoholism. *Alcoholism: Clinical & Experimental Research* (1995b) **19**: pp. 510-516.

Volkow N, Wang G, Fischman M, Foltin R, Fowler J, Abumrad N, Vitkun S, Logan J, Gatley S, Pappas N, Hitzemann R & Shea C. Relationship between subjective effects of cocaine and dopamine transporter occupancy. *Nature* (1997a) **386**: pp. 827-830.

Volkow N, Wang G, Fischman M, Foltin R, Fowler J, Franceschi D, Franceschi M, Logan J, Gatley S, Wong C, Ding Y, Hitzemann R & Pappas N. Effects of route of administration on cocaine induced dopamine transporter blockade in the human brain. *Life Sciences* (2000a) **67**: pp. 1507-1515.

Volkow N, Wang G, Fowler J, Franceschi D, Thanos P, Wong C, Gatley S, Ding Y, Molina P, Schlyer D, Alexoff D, Pappas N & Hitzemann R. Cocaine abusers show a blunted response to alcohol intoxication in limbic brain regions. *Life Sciences* (2000b) **66**: .

Volkow N, Wang G, Fowler J, Gatley S, Ding Y, Logan J, Dewey S, Hitzemann R & Lieberman J. Relationship between psychostimulant-induced "high" and dopamine transporter occupancy. *Proceedings of the National Academy of Sciences USA* (1996b) **93**: pp. 10388-10392.

Volkow N, Wang G, Fowler J, Gatley S, Logan J, Ding Y, Dewey S, Hitzemann R, Gifford A & Pappas N. Blockade of striatal dopamine transporters by intravenous methylphenidate is not sufficient to induce self-reports of "high". *Journal of Pharmacology & Experimental Therapeutics* (1999a) **288**: pp. 14-20.

Volkow N, Wang G, Fowler J, Gatley S, Logan J, Ding Y, Hitzemann R & Pappas N. Dopamine transporter occupancies in the human brain induced by therapeutic doses of oral methylphenidate. *American Journal of Psychiatry* (1998a) **155**: pp. 1325-1331.

Volkow N, Wang G, Fowler J, Hitzemann R, Angrist B, Gatley S, Logan J, Ding Y & Pappas N. Association of methylphenidate-induced craving with changes in right striato-orbitofrontal metabolism in cocaine abusers: implications in addiction. *American Journal of Psychiatry* (1999b) **156**: pp. 19-26.

Volkow N, Wang G, Fowler J, Hitzemann R, Gatley J, Ding Y, Wong C & Pappas N. Differences in regional brain metabolic responses between single and repeated doses of methylphenidate. *Psychiatry Research: Neuroimaging* (1998b) **83**: pp. 29-36.

Volkow N, Wang G, Fowler J, Hitzemann R, Gatley S, Dewey S & Pappas N. Enhanced sensitivity to benzodiazepines in active cocaine-abusing subjects: a PET study. *American Journal of Psychiatry* (1998c) **155**: pp. 200-206.

Volkow N, Wang G, Fowler J, Logan J, Angrist B, Hitzemann R, Lieberman J & Pappas N. Effects of methylphenidate on regional brain glucose metabolism in humans: relationship to dopamine D2 receptors. *American Journal of Psychiatry* (1997b) **154**: pp. 50-55.

Volkow N, Wang G, Fowler J, Logan J, Gatley S, Gifford A, Hitzemann R, Ding Y & Pappas N. Prediction of reinforcing responses to psychostimulants in humans by brain dopamine D2 receptor levels. *American Journal of Psychiatry* (1999c) **156**: pp. 1440-1443.

Volkow N, Wang G, Fowler J, Logan J, Gatley S, Hitzemann R, Chen A, Dewey S & Pappas N. Decreased striatal dopaminergic responsiveness in detoxified cocaine-dependent subjects. *Nature* (1997c) **386**: pp. 830-833.

Volkow N, Wang G, Fowler J, Logan J, Gatley S, Wong C, Hitzemann R & Pappas N. Reinforcing effects of psychostimulants in humans are associated with increases in brain dopamine and occupancy of D(2) receptors. *Journal of Pharmacology & Experimental Therapeutics* (1999d) **291**: pp. 409-415.

Volkow N, Wang G, Fowler J, Logan J, Hitzemann R, Ding Y, Pappas N, Shea C & Piscani K. Decreases in dopamine receptors but not in dopamine transporters in alcoholics. *Alcoholism: Clinical & Experimental Research* (1996c) **20**: pp. 1594-1598.

Volkow N, Wang G, Fowler J, Logan J, Hitzemann R, Gatley S, MacGregor R & Wolf A. Cocaine uptake is decreased in the brain of detoxified cocaine abusers. *Neuropsychopharmacology* (1996d) **14**: pp. 159-168.

Volkow N, Wang G, Fowler J, Telang F, Maynard L, Logan J, Gatley S, Pappas N, Wong C, Vaska P, Zhu W & Swanson J. Evidence that methylphenidate enhances the saliency of a mathematical task by increasing dopamine in the human brain. *American Journal of Psychiatry* (2004b) **161**: pp. 1173-1180.

Volkow N, Wang G, Fowler J, Thanos P, Logan J, Gatley S, Gifford A, Ding Y, Wong C & Pappas N. Brain DA D2 receptors predict reinforcing effects of stimulants in humans: replication study. *Synapse* (2002a) **46**: pp. 79-82.

Volkow N, Wang G, Franceschi D, Fowler J, Thanos P, Maynard L, Gatley S, Wong C, Veech R, Kunos G & Kai LT. Low doses of alcohol substantially decrease glucose metabolism in the human brain. *NeuroImage* (2006) **29**: pp. 295-301.

Volkow N, Wang G, Gatley S, Fowler J, Ding Y, Logan J, Hitzemann R, Angrist B & Lieberman J. Temporal relationships between the pharmacokinetics of methylphenidate in the human brain and its behavioral and cardiovascular effects. *Psychopharmacology* (1996e) **123**: pp. 26-33.

Volkow N, Wang G, Hitzemann R, Fowler J, Overall J, Burr G & Wolf A. Recovery of brain glucose metabolism in detoxified alcoholics. *American Journal of Psychiatry* (1994) **151**: pp. 178-183.

Volkow N, Wang G, Hitzemann R, Fowler J, Wolf A, Pappas N, Biegon A & Dewey S. Decreased cerebral response to inhibitory neurotransmission in alcoholics. *American Journal of Psychiatry* (1993b) **150**: pp. 417-422.

Volkow N, Wang G, Ma Y, Fowler J, Wong C, Ding Y, Hitzemann R, Swanson J & Kalivas P. Activation of orbital and medial prefrontal cortex by methylphenidate in cocaine-addicted subjects but not in controls: relevance to addiction. *Journal of Neuroscience* (2005) **25**: pp. 3932-3939.

Volkow N, Wang G, Ma Y, Maynard L, Telang F, Vaska P, Wong C, Fowler J, Ding Y, Zhu W & Swanson J. Expectation Enhances the Regional Brain Metabolic and the Reinforcing Effects of Stimulants in Cocaine Abusers. *Journal of Neuroscience* (2003) **23**: pp. 11461-11468.

Volkow N, Wang G, Maynard L, Fowler J, Jayne B, Telang F, Logan J, Ding Y, Gatley S, Wong C, Pappas N & Hitzemann R. Effects of alcohol detoxification on dopamine D2 receptors in alcoholics: A preliminary study. *Psychiatry Research: Neuroimaging* (2002b) **116**: pp. 163-172.

Volkow N, Wang G, Overall J, Hitzemann R, Fowler J, Pappas N, Frecska E & Piscani K. Regional brain metabolic response to lorazepam in alcoholics during early and late alcohol detoxification. *Alcoholism: Clinical & Experimental Research* (1997d) **21**: pp. 1278-1284.

Wagner KJ, Willoch F, Kochs EF, Siessmeier T, Tölle TR, Schwaiger M & Bartenstein P. Dose-dependent regional cerebral blood flow changes during remifentanil infusion in humans: a positron emission tomography study. *Anesthesiology* (2001) **94**: pp. 732-739.

Wallace E, Wisniewski G, Zubal G, VanDyck C, Pfau S, Smith E, Rosen, MI, Sullivan M, Woods S & Kosten T. Acute cocaine effects on absolute cerebral blood flow. *Psychopharmacology* (1996) **128**: pp. 17-20.

Walsh S, Gilson S, Jasinski D, Stapleton J, Phillips R, Dannals R, Schmidt J, Preston K, Grayson R & Bigelow G. Buprenorphine reduces cerebral glucose metabolism in polydrug abusers. *Neuropsychopharmacology* (1994) **10**: pp. 157-170.

Wang G, Volkow N, Chang L, Miller E, Sedler M, Hitzemann R, Zhu W, Logan J, Ma Y & Fowler J. Partial recovery of brain metabolism in methamphetamine abusers after protracted abstinence. *American Journal of Psychiatry* (2004) **161**: pp. 242-248.

Wang G, Volkow N, Fowler J, Cervany P, Hitzemann R, Pappas N, Wong C & Felder C. Regional brain metabolic activation during craving elicited by recall of previous drug experiences. *Life Sciences* (1999a) **64**: pp. 775-784.

Wang G, Volkow N, Fowler J, Ferrieri R, Schlyer D, Alexoff D, Pappas N, Lieberman J, King P & Warner D. Methylphenidate decreases regional cerebral blood flow in normal human subjects. *Life Sciences* (1994) **54**: p. L143-L146.

Wang G, Volkow N, Fowler J, Fischman M, Foltin R, Abumrad N, Logan J & Pappas N. Cocaine abusers do not show loss of dopamine transporters with age. *Life Sciences* (1997a) **61**: pp. 1059-1065.

Wang G, Volkow N, Fowler J, Logan J, Abumrad N, Hitzemann R, Pappas N, Pascani K. Dopamine D2 receptor availability in opiate-dependent subjects before and after naloxone-precipitated withdrawal. *Neuropsychopharmacology* (1997b) **16**: pp. 174-182.

Wang G, Volkow N, Fowler J, Pappas N, Wong C, Pascani K, Felder C & Hitzemann R. Regional cerebral metabolism in female alcoholics of moderate severity does not differ from that of controls. *Alcoholism: Clinical & Experimental Research* (1998) **22**: pp. 1850-1854.

Wang G, Volkow N, Franceschi D, Fowler J, Thanos P, Scherbaum N, Pappas N, Wong C, Hitzemann R & Felder A. Regional brain metabolism during alcohol intoxication. *Alcoholism: Clinical & Experimental Research* (2000) **24**: pp. 822-829.

Wang G, Volkow N, Levy A, Felder C, Fowler J, Pappas N, Hitzemann R & Wong C. Measuring reproducibility of regional brain metabolic responses to lorazepam using statistical parametric maps. *Journal of Nuclear Medicine* (1999b) **40**: pp. 715-720.

Wang G, Volkow N, Logan J, Fowler J, Schlyer D, MacGregor R, Hitzemann R, Gjedde A, Wolf A. Serotonin 5-HT2 receptor availability in chronic cocaine abusers.. *Life Sciences* (1995) **56**: p. PL299-303.

Weber D, Franceschi D, Ivanovic M, Atkins H, Cabahug C, Wong C, Susskind H. SPECT and planar brain imaging in crack abuse: iodine-123-iodoamphetamine uptake and localization. *Journal of Nuclear Medicine* (1993) **34**: pp. 899-907.

Weinstein A, Feldtkeller B, Malizia A, Wilson S, Bailey J & Nutt D. Integrating the cognitive and physiological aspects of craving. *Journal of Psychopharmacology* (1998) **12**: pp. 31-38.

Weinstein A, Wilson S, Bailey J, Myles J & Nutt D. Imagery of craving in opiate addicts undergoing detoxification. *Drug & Alcohol Dependence* (1997) **48**: pp. 25-31.

Wendt PE, Risberg J, Stenberg G, Rosén I & Ingvar DH. Ethanol reduces asymmetry of visual rCBF responses. *Journal of Cerebral Blood Flow & Metabolism* (1994) **14**: pp. 963-973.

Wexler B, Gottschalk C, Fulbright R, Prohovnik I, Lacadie C, Rounsaville B & Gore J. Functional magnetic resonance imaging of cocaine craving. *American Journal of Psychiatry* (2001) **158**: pp. 86-95.

Whalen P, Bush G, McNally R, Wilhelm S, McInerney S, Jenike M & Rauch S. The emotional counting Stroop paradigm: a functional magnetic resonance imaging probe of the anterior cingulate affective division. *Biological Psychiatry* (1998) **44**: pp. 1219-1228.

Wik G, Borg S, Sjogren I, Wiesel F, Blomqvist G, Borg J, Greitz T, Nyback H, Sedvall G & Stone-Elander S. PET determination of regional cerebral glucose metabolism in alcohol-dependent men and healthy controls using 11C-glucose. *Acta Psychiatrica Scandinavica* (1988) **78**: pp. 234-241.

Williams TM, Daglish MRC, Lingford-Hughes A, Taylor LG, Hammers A, Brooks DJ, Grasby P, Myles JS & Nutt DJ. Brain opioid receptor binding in early abstinence from opioid dependence: positron emission tomography study. *British Journal of Psychiatry* (2007) **191**: pp. 63-69.

Wise R. Neurobiology of addiction. *Current Opinion in Neurobiology* (1996) **6**: pp. 243-251.

Wise R & Hoffman D. Localization of drug reward mechanisms by intra-cranial injections. *Synapse* (1992) **10**: pp. 247-263.

Wise R, Leone P, Rivest R & Leeb K. Elevations of nucleus accumbens dopamine and DOPAC levels during intravenous heroin self-administration. *Synapse* (1995) **21**: pp. 140-148.

Wise RG, Rogers R, Painter D, Bantick S, Ploghaus A, Williams P, Rapeport G & Tracey I. Combining fMRI with a pharmacokinetic model to determine which brain areas activated by painful stimulation are specifically modulated by remifentanil. *NeuroImage* (2002) **16**: pp. 999-1014.

Wolkin A, Angrist B, Wolf A, Brodie J, Wolkin B, Jaeger J, Cancro R & Rotrosen J. Effects of amphetamine on local cerebral metabolism in normal and schizophrenic subjects as determined by positron emission tomography. *Psychopharmacology* (1987) **92**: pp. 241-246.

World Health Organization. International Statistical Classification of Diseases and Related Health Problems (ICD-10). World Health Organization, Geneva, (1992).

Wrase J, Grusser S, Klein S, Diener C, Hermann D, Flor H, Mann K, Braus D & Heinz A. Development of alcohol-associated cues and cue-induced brain activation in alcoholics. *European Psychiatry* (2002) **17**: pp. 287-291.

Wu J, Bell K, Najafi A, Widmark C, Keator D, Tang C, Klein E, Bunney B, Fallon J & Bunney W. Decreasing striatal 6-FDOPA uptake with increasing duration of cocaine withdrawal. *Neuropsychopharmacology* (1997) **17**: pp. 402-409.

Xiao Z, Lee T, Zhang JX, Wu Q, Wu R, Weng X & Hu X. Thirsty heroin addicts show different fMRI activations when exposed to water-related and drug-related cues. *Drug & Alcohol Dependence* (2006) **83**: pp. 157-162.

Young L, Wong D, Goldman S, Minkin E, Chen C, Matsumura K, Scheffel & Wagner H. Effects of endogenous dopamine on kinetics of [3H]N-methylspiperone and [3H]raclopride binding in the rat brain. *Synapse* (1991) **9**: pp. 188-194.

Yücel M, Lubman D, Harrison B, Fornito A, Allen N, Wellard R, Roffel K, Clarke K, Wood S, Forman S, Pantelis C. A combined spectroscopic and functional MRI investigation of the dorsal anterior cingulate region in opiate addiction.. *Molecular Psychiatry* (2007) **12**: pp. 691-702.

Zald DH, Boileau I, El-Dearedy W, Gunn R, McGlone F, Dichter GS & Dagher A. Dopamine transmission in the human striatum during monetary reward tasks. *Journal of Neuroscience* (2004) **24**: pp. 4105-4112.

Zubieta J, Dannals R & Frost J. Gender and age influences on human brain mu-opioid receptor binding measured by PET. *American Journal of Psychiatry* (1999) **156**: pp. 842-848.

Zubieta J, Gorelick D, Stauffer R, Ravert H, Dannals, RF & Frost J. Increased mu opioid receptor binding detected by PET in cocaine-dependent men is associated with cocaine craving. *Nature Medicine* (1996) **2**: pp. 1225-1229.

Zubieta J, Greenwald M, Lombardi U, Woods J, Kilbourn M, Jewett D, Koeppe R, Schuster C & Johanson C. Buprenorphine-induced changes in mu-opioid receptor availability in male heroin-dependent volunteers: a preliminary study. *Neuropsychopharmacology* (2000) **23**: pp. 326-334.

8 Appendices

8.1 Computer source code written for the thesis

8.1.1 Conventions used in presentation of source code

In order to aid readability the source code will be presented in a standardised format.

I will need to describe the format here.

Grey = comments
code = black
compiler pre-processing commands = green
type declarations = red
program language keywords = bold
numerical constants = blue
string constants = purple

8.1.2 Convolution

8.1.2.1 The re-implemented C-code

```
/* Re-implementation of mex_rogconv.c
  The original was created from mex_rogconv.m by MATLAB compiler.
  The original routine was written by Roger Gunn,
        while at MRC Cyclotron Unit, Hammersmith Hospital, London, UK.

  The matlab routine was:
        function convolution=rogconv(inp,k1,k2,t)
                ek2=exp(-k2);
                prev=0;
                for i=1:length(t)
                        prev=prev*ek2+k1*inp(i)*(1-ek2)/k2;
                        convolution(i)=prev;
                end
  Where inp is a column vector and t is a row-vectors of same length
  k1 & k2 are real numbers
  convolution is a vector of same length as inp & t
  For some reason Roger uses k2, where in the paper it is theta3.  Therefore,
  I will use theta as the variable name here.
  ==========
  Licensed under GPL, version of your choice.
  by:
  Dr. Mark Daglish
  Clinical Lecturer in Psychiatry
  Psychopharmacology Unit
  University of Bristol,UK
  mark.daglish@bris.ac.uk
  ==========
*/

/* $Revision: 0.1 $ */
/* include mex headers for matlab and math header for exponential */
#include "mex.h"
#include <math.h>

void conv( double *conv, const double *input, const double k1, const double theta, const int l)
/* The subroutine that does the work */
{
        double prev, et, factor;
        int i;
        prev = 0.0;
        et = exp(-theta);
        factor = k1*(1.0-et)/theta;
        for (i = 0; i < l; i++) {
                prev *= et;
                prev += (*(input+i)) * factor;
                *(conv+i) = prev;
        }
```

```
}

void mexFunction(
        int nlhs, mxArray *plhs[],
        int nrhs, const mxArray *prhs[])
/* The gateway routine called by Matlab */
{
        int inpM, inpN, tM, tN;
        double k1, theta;
        double *input, *solution, *td;

        /* Check input arguments. */
        if ( nrhs != 4 || nlhs != 1 ) {
                mexErrMsgTxt("Usage: convolution=conv(inp,k1,theta,t)");
        }
        inpM = mxGetM(prhs[0]);
        inpN = mxGetN(prhs[0]);
        tM = mxGetM(prhs[3]);
        tN = mxGetN(prhs[3]);
        if (!mxIsDouble(prhs[0]) || mxIsComplex(prhs[0]) ||
                !mxIsDouble(prhs[1]) || mxIsComplex(prhs[1]) ||
                !mxIsDouble(prhs[2]) || mxIsComplex(prhs[2]) ||
                !mxIsDouble(prhs[3]) || mxIsComplex(prhs[3])) {
                        mexErrMsgTxt("All arguments must be non-complex and double");
        }
        if ((inpM != 1) || (tN != 1)) {
                mexErrMsgTxt("inp must be a row vector and t a column vector");
        }
        if (inpN < tM) {
                        mexErrMsgTxt("inp must be the same size or longer than t");
        }
        /* Create matrix for the return argument. */
        plhs[0] = mxCreateDoubleMatrix(1,tM, mxREAL);

        /* Assign pointers to each input and output. */
        input = mxGetPr(prhs[0]);
        k1 = mxGetScalar(prhs[1]);
        theta = mxGetScalar(prhs[2]);
        td = mxGetPr(prhs[3]);
        solution = mxGetPr(plhs[0]);

        /* Call the convolution subroutine. */
        conv(solution,input,k1,theta,tM);
}
```

8.1.3 Basis pursuit solution

8.1.3.1 The original C++ code

8.1.3.1.1 rpm_ref.cpp

```
// Filename: rpm_ref.cpp
//
// Description: Calculates parameters for the simplified reference region model
//
// Classes:
//
// Comments: Mex implementation of rpm_ref.m
//
//function
[R1,k2,BP,index]=rpm_ref(bigm,W,no_basis_functions,lbeta1,weight,A,Cref,v(1).dim(2),mask(x,:),d,l
ambda)
//                      Wd=W*d;
//                      B=[Cref A(:,1)];
//                      for i=1:no_basis_functions
//                              B(:,2)=A(:,i);
//                              result=bigm((i*2-1):i*2,:)*Wd;
//                              ssq(i)=sum((weight).*(B*result-d).^2);
//                      end
//                      sol=find(min(ssq)==ssq);
//                      index=sol(1);
//                      result=bigm((index*2-1):index*2,:)*Wd;
//                      R1=result(1);
//                      k2=result(2)+(lbeta1(index)-lambda)*R1;
//                      BP=(k2)/(lbeta1(index)-lambda) - 1;
//
//                      mex -v -f ./gccopts.sh rpm_ref.cpp
//
// Author: Steve Gunn & Roger Gunn (c)

#include <cstdio>
#include "mex.h"
#ifndef _tensor_h_
        #include "tensor.h"
#endif

void mexFunction(int nlhs, mxArray *plhs[], int nrhs, const mxArray *prhs[])
{
        // Read in Variables
         precision *bigmP = (precision *)mxGetPr(prhs[0]);
         unsigned int bigmRow = mxGetM(prhs[0]);
         unsigned int bigmCol = mxGetN(prhs[0]);
        MATRIX<precision> bigm(bigmP,bigmRow,bigmCol);

         precision *WP = (precision *)mxGetPr(prhs[1]);
```

```
 unsigned int WRow = mxGetM(prhs[1]);
 unsigned int WCol = mxGetN(prhs[1]);
MATRIX<precision> W(WP,WRow,WCol);

 unsigned int no_basis_functions = (unsigned int)mxGetScalar(prhs[2]);

 precision *lbeta1P = (precision *)mxGetPr(prhs[3]);
 unsigned int lbeta1Row = mxGetM(prhs[3]);
 unsigned int lbeta1Col = mxGetN(prhs[3]);
VECTOR<precision> lbeta1(lbeta1P,lbeta1Col);

 precision *weightP = (precision *)mxGetPr(prhs[4]);
 unsigned int weightRow = mxGetM(prhs[4]);
 unsigned int weightCol = mxGetN(prhs[4]);
VECTOR<precision> weight(weightP,weightRow);

 precision *AP = (precision *)mxGetPr(prhs[5]);
 unsigned int ARow = mxGetM(prhs[5]);
 unsigned int ACol = mxGetN(prhs[5]);
MATRIX<precision> A(AP,ARow,ACol);

 precision *CrefP = (precision *)mxGetPr(prhs[6]);
 unsigned int CrefRow = mxGetM(prhs[6]);
 unsigned int CrefCol = mxGetN(prhs[6]);
VECTOR<precision> Cref(CrefP,CrefRow);

 unsigned int ydim = (unsigned int)mxGetScalar(prhs[7]);

 precision *maskP = (precision *)mxGetPr(prhs[8]);
 unsigned int maskRow = mxGetM(prhs[8]);
 unsigned int maskCol = mxGetN(prhs[8]);
VECTOR<precision> mask(maskP,maskCol);

 precision *dP = (precision *)mxGetPr(prhs[9]);
 unsigned int dRow = mxGetM(prhs[9]);
 unsigned int dCol = mxGetN(prhs[9]);
MATRIX<precision> d(dP,dRow,dCol);

 precision lambda = mxGetScalar(prhs[10]);

// Main Routine
 VECTOR<precision> R(ydim);
 VECTOR<precision> k(ydim);
 VECTOR<precision> BP(ydim);
 VECTOR<precision> ind(ydim);
 VECTOR<precision> temp(dRow), result(2), ssq(no_basis_functions), data(dRow);
 MATRIX<precision> B(dRow,2);
 VECTOR<precision> tempssq(dRow);
 B.putCol(Cref,0);
for(unsigned int y=0; y<ydim; y++)
{
        if (mask(y)!=0) {
                d.getCol(data, y);
```

```
                    VECTOR<precision> Wd=W*data;
                    for(unsigned int i=0; i<no_basis_functions; i++) {
                            A.getCol(temp, i);
                            B.putCol(temp, 1);
                            bigm.getRow(temp, i*2);
                            result(0) = temp*Wd;
                            bigm.getRow(temp, i*2 + 1);
                            result(1) = temp*Wd;
                            tempssq = (B*result - data);
                            ssq(i) = 0.0;
                            for(unsigned int j=0; j<dRow; j++)
                                    ssq(i) += weight(j)*tempssq(j)*tempssq(j);
                    }
                    unsigned int index = ssq.minIndex();
                    bigm.getRow(temp, index*2);
                    result(0) = temp*Wd;
                    bigm.getRow(temp, index*2 + 1);
                    result(1) = temp*Wd;
                    R(y) = result(0);
                    k(y) = result(1)+(lbeta1(index)-lambda)*result(0);
                    BP(y) = k(y)/(lbeta1(index)-lambda) - 1.0;
                    ind(y) = index;
            } else {
                    R(y) = 0.0;
                    k(y) = 0.0;
                    BP(y) = 0.0;
                    ind(y) = 100.0;                                    //Error here
            }
    }
    // Return Variables
    plhs[0] = mxCreateDoubleMatrix(1,ydim,mxREAL);
    precision *ptr0 = mxGetPr(plhs[0]);
    memcpy(ptr0,R.getdata(),ydim*sizeof(precision));
    plhs[1] = mxCreateDoubleMatrix(1,ydim,mxREAL);
    precision *ptr1 = mxGetPr(plhs[1]);
    memcpy(ptr1,k.getdata(),ydim*sizeof(precision));
    plhs[2] = mxCreateDoubleMatrix(1,ydim,mxREAL);
    precision *ptr2 = mxGetPr(plhs[2]);
    memcpy(ptr2,BP.getdata(),ydim*sizeof(precision));
    plhs[3] = mxCreateDoubleMatrix(1,ydim,mxREAL);
    precision *ptr3 = mxGetPr(plhs[3]);
    memcpy(ptr3,ind.getdata(),ydim*sizeof(precision));
}
```

8.1.3.1.2 tensor.cpp

```
// Filename: tensor.cpp
//
// Description: Routines for Tensors
//
// Classes: Tensor
//
// Comments: VECTOR and MATRIX are #defines which can be used to clarify
```

```
//                code to show show what type of tensor is intended.
//
// Author: Steve Gunn (srg@ecs.soton.ac.uk)
//
// Copyright: All rights reserved
#define _tensor_cpp_
#include <memory.h>
#include <stdio.h>
#include <assert.h>
#include <math.h>
#ifndef _tensor_h_
  #include "tensor.h"
#endif
using namespace std;
//////////////////// Private members ////////////////////////
template<class T>
void Tensor<T>::create()
{
        unsigned int i;
        if (rank)
        {
                length = 1;
                for(i=0; i<rank; i++) length *= size[i];
        }
        if (length!=0)
        {
                switch(rank)
                {
                case 1:
                        val = data = new T[length];
                        assert(data);
                        break;
                case 2:
                        val = new T*[size[0]];
                        assert(val);
                        ((T**)val)[0] = data = new T[length];
                        assert(data);
                        for(i=1; i<size[0]; i++) ((T**)val)[i] = ((T**)val)[i-1] + size[1];
                        break;
                case 3:
                        val = new T**[size[0]];
                        assert(val);
                        ((T***)val)[0] = new T*[size[0]*size[1]];
                        assert(((T***)val)[0]);
                        ((T***)val)[0][0] = data = new T[length];
                        assert(data);
                        for(i=1; i<size[0]*size[1]; i++) ((T***)val)[0][i] = (T *)
                                ((T***)val)[0][i-1] + size[2];
                        for(i=1; i<size[0]; i++) ((T***)val)[i] = (T **)
                                ((T***)val)[i-1] + size[2]*size[1];
                        break;
                default:
                        assert(rank <= MAX_TENSOR_RANK); // Tensor rank unsupported
```

```
                }
                // Initialise elements to zero
                T* p = data;
                for(unsigned long x=0L; x<length; x++) *p++ = (T)0.0;
        } else  {
                val = NULL;
                data = NULL;
        }
}
template<class T>
void Tensor<T>::destroy()
{
        if (rank == 0) return;
        if (length != 0) {
                switch(rank) {
                        case 1:
                                delete[] (T*)val;
                                break;
                        case 2:
                                delete[] ((T**)val)[0];
                                delete[] (T**)val;
                                break;
                        case 3:
                                delete[] ((T***)val)[0][0];
                                delete[] ((T***)val)[0];
                                delete[] (T***)val;
                                break;
                }
                length = 0;
        }
        delete[] size;
        size = NULL;
        rank = 0;
        data = NULL;
        val = NULL;
}
template<class T>
void Tensor<T>::copy(const Tensor<T> &t)
{
        if (t.rank) {
                rank = t.rank;
                size = new unsigned int[rank];
                assert(size);
                for(unsigned int i=0; i<rank; i++) size[i] = t.size[i];
                create();
                if (length) memcpy(data, t.data, (size_t)length*sizeof(T));
        } else {
                length = 0;
                rank = 0;
                size = NULL;
                data = NULL;
                val = NULL;
        }
```

```
}
////////////////////////// Constructors //////////////////////////
template<class T>
Tensor<T>::Tensor()
{
        rank = 0;           // It's a an uninitialised tensor
        length = 0;
        val = NULL;
        size = NULL;
        data = NULL;
}

template<class T>
Tensor<T>::Tensor(const unsigned int u)
{
        rank = 1;           // It's a vector
        size = new unsigned int[rank];
        assert(size);
        size[0] = u;
        create();
}

template<class T>
Tensor<T>::Tensor(const unsigned int u, const unsigned int v)
{
        rank = 2;           // It's a matrix
        size = new unsigned int[rank];
        assert(size);
        size[0] = u;
        size[1] = v;
        create();
}

template<class T>
Tensor<T>::Tensor(const unsigned int u, const unsigned int v, const unsigned int w)
{
        rank = 3;           // It's a 3tensor ... yeehah
        size = new unsigned int[rank];
        assert(size);
        size[0] = u;
        size[1] = v;
        size[2] = w;
        create();
}

// The following three member functions are required for the matlab
// interface. Implemented by KB 10/8/96
template<class T>
Tensor<T>::Tensor(T* t,const unsigned int l)
{
        rank = 1;           // It's a vector
        size = new unsigned int[rank];
        assert(size);
```

```
        size[0] = l;
        create();
        // do this the inefficient way as not to sure how this class works.
        for( unsigned int i = 0; i<l; i++) {
                ((T*)val)[i] = t[i];
        }
}

template<class T>
Tensor<T>::Tensor(T* t,const unsigned int nr, const unsigned int nc)
{
        rank = 2;           // It's a matrix
        size = new unsigned int[rank];
        assert(size);
        size[0] = nr;
        size[1] = nc;
        create();
//      do this the inefficient way as not to sure how this class works.
        for( unsigned int i = 0; i<nc; i++)
                for( unsigned int j = 0; j<nr; j++) ((T**)val)[j][i] = t[(i*nr) + j];
}

template<class T>
T* Tensor<T>::tensorPtr()
{
        T* ptr = NULL;
        unsigned int r,c;
        if (length != 0) {
                switch(rank) {
                        case 1: ptr = new T[size[0]];
                                for (c=0; c<size[0]; c++)
                                        ptr[c] = ((T*)val)[c];
                                break;
                        case 2: ptr = new T[size[1]*size[0]];
                                for (c=0; c<size[1]; c++) {
                                        for (r=0; r<size[0]; r++)
                                                ptr[c*(size[0])+r] = ((T**)val)[r][c];
                                }
                                break;
                        case 3:
                                cout << "\n help rank = 3 in tensorPtr \n";
                                break;
                }
        }
        return(ptr);
}

////////////////////// Overloaded Operators ////////////////////
template<class T>
Tensor<T>::operator T()
{
        return data[0];
}
```

```
template<class T>
Tensor<T>& Tensor<T>::operator=(const Tensor<T>& t)
{
	bool sameSize = true;
	if (this != &t) {  // if object is assigned to itself, do nothing
		if (rank != t.rank || length != t.length) sameSize = false;
		else
			for(unsigned int i=0; i<rank; i++)
				if (size[i] != t.size[i])
					sameSize = false;
		if (sameSize) {
			if (length)
				memcpy(data, t.data,  (size_t)length*sizeof(T));
		} else {
			if (rank) destroy();
			copy(t);
		}
	}
	return *this;
}

template<class T>
Tensor<T>& Tensor<T>::operator=(const T init)
{
	for(unsigned long i=0L; i<length; i++)
		data[i] = init;
	return *this;
}

template<class T>
bool Tensor<T>::operator==(const Tensor<T>& b)
{
	if (rank != b.rank) return false;
	if (length != b.length) return false;
	for(unsigned int i=0; i<rank; i++)
		if (dim(i) != b.dim(i)) return false;
	for(unsigned long j=0L; j<length; j++)
		if (data[j] != b.data[j]) return false;
	return true;
}

template<class T>
bool Tensor<T>::operator!=(const Tensor<T>& b)
{
	if (rank != b.rank) return true;
	if (length != b.length) return true;
	for(unsigned int i=0; i<rank; i++)
		if (dim(i) != b.dim(i)) return true;
	for(unsigned long j=0L; j<length; j++)
		if (data[j] != b.data[j]) return true;
	return false;
}
```

```
template<class T>
Tensor<T>& Tensor<T>::operator+=(const Tensor<T>& t)
{
        assert(same_size(t));
        T* d1 = data;
        T* d2 = t.data;
        for(unsigned long x=0L; x<length; x++) *d1++ += *d2++;
        return *this;
}

template<class T>
Tensor<T>& Tensor<T>::operator+=(const T add)
{
        T* d = data;
        for(unsigned long x=0L; x<length; x++) *d++ += T(add);
        return *this;
}

template<class T>
Tensor<T> Tensor<T>::operator+(const Tensor<T>& t)
{
        Tensor<T> sum =* this;
        sum += t;
        return sum;
}

template<class T>
Tensor<T> Tensor<T>::operator+(const T add)
{
        Tensor<T> sum = *this;
        sum += add;
        return sum;
}

template<class T>
Tensor<T> operator+(const T add, const Tensor<T>& t)
{
        Tensor<T> sum = t;
        sum += add;
        return sum;
}

template<class T>
Tensor<T>& Tensor<T>::operator-=(const Tensor<T>& t)
{
        assert(same_size(t));
        T* d1 = data;
        T* d2 = t.data;
        for(unsigned long x=0L; x<length; x++) *d1++ -= *d2++;
        return *this;
}
```

```
template<class T>
Tensor<T>& Tensor<T>::operator-=(const T sub)
{
        T* d = data;
        for(unsigned long x=0L; x<length; x++) *d++ -= T(sub);
        return *this;
}

template<class T>
Tensor<T> Tensor<T>::operator-(const Tensor<T>& t)
{
        Tensor<T> sum = *this;
        sum -= t;
        return sum;
}

template<class T>
Tensor<T> Tensor<T>::operator-(const T sub)
{
        Tensor<T> sum = *this;
        sum -= sub;
        return sum;
}

template<class T>
Tensor<T> operator-(const T sub, const Tensor<T>& t)
{
        Tensor<T> sum = t;
        sum -= sub;
        return sum;
}

template<class T>
Tensor<T>& Tensor<T>::operator*=(const Tensor<T>& t)
{
        Tensor<T> temp;
        temp = *this;
        *this = temp * t;
        return *this;
}

template<class T>
Tensor<T>& Tensor<T>::operator*=(const T mul)
{
        T* d = data;
        for(unsigned long x=0L; x<length; x++) *d++ *= T(mul);
        return *this;
}

template<class T>
Tensor<T> Tensor<T>::operator*(const Tensor<T>& t)
{
//      if (t.rank == 0) return *this * t.data[0];
```

```
//      if (rank == 0) return data[0] * t;
        assert(rank);
        assert(t.rank);  // Cannot multiply by uninitialised tensor
        assert(size[rank-1] == t.size[0]); // Incompatible Tensor dimensions
        Tensor<T> result;
        unsigned int newRank = rank+t.rank-2;
        unsigned int *newSize = NULL;
        if (newRank == 0) {
                newRank = 1;
                newSize = new unsigned int[newRank];
                newSize[0] = 1;
                assert(newSize);
        } else {
                newSize = new unsigned int[newRank];
                assert(newSize);
                unsigned int i1=0, j1=1;
                while(i1+1 < rank) {
                        newSize[i1] = size[i1];
                        i1++;
                }
                while(i1 < newRank)     {
                        newSize[i1] = t.size[j1];
                        i1++;
                        j1++;
                }
        }
        result.changeDim(newRank, newSize);
        delete[] newSize;
        T* rd = result.data;
        T* d = data;
        T* td = t.data;
        assert(rank < 3 && t.rank < 3); // tensor multiplication not tested for 3 tensors
        unsigned int i, j, k;
        unsigned long l, m;
        unsigned int t0, t1, t2;
        switch(t.rank) {
        case 1:
                t0 = t.size[0];
                m = (unsigned long) length/t0;
                for(l=0; l<m; l++, td = t.data, rd++)
                        for(i=0; i<t0; i++) *rd += *d++ * *td++;
                break;
        case 2:
                t0 = t.size[0];
                t1 = t.size[1];
                m = (unsigned long) length/t0;
                for(l=0; l<m; l++, rd += t1, td = t.data)
                        for(j=0; j<t0; j++, d++, rd -= t1)
                                for(i=0; i<t1; i++)
                                        *rd++ += *d * *td++;
                break;
        case 3:
                t0 = t.size[0];
```

```
                t1 = t.size[1];
                t2 = t.size[2];
                m = (unsigned long) length/t0;
                for(l=0; l<m; l++, rd += t2, td = t.data)
                        for(k=0; k<t0; k++)
                                for(j=0; j<t1; j++, d++, rd -= t2)
                                        for(i=0; i<t2; i++) *rd++ += *d * *td++;
                break;
        }

        return result;
}

template<class T>
Tensor<T> Tensor<T>::operator*(const T mul)
{
        Tensor<T> sum = *this;
        sum *= mul;
        return sum;
}

template<class T>
Tensor<T> operator*(const T mul, const Tensor<T>& t)
{
        Tensor<T> sum = t;
        sum *= mul;
        return sum;
}

template<class T>
Tensor<T>& Tensor<T>::operator/=(const Tensor<T>& t)
{
        assert(same_size(t));
        T* d1 = data;
        T* d2 = t.data;
        for(unsigned long x=0L; x<length; x++) if (*d2!=0.0) *d1++ /= *d2++;
        return *this;     // leave answer unchanged for division by zero
}

template<class T>
Tensor<T>& Tensor<T>::operator/=(const T div)
{
        assert(div != 0.0); // Tensor - division by zero
        T* d = data;
        for(unsigned long x=0L; x<length; x++) *d++ /= T(div);
        return *this;
}

template<class T>
Tensor<T> Tensor<T>::operator/(const Tensor<T>& t)
{
        Tensor<T> sum =* this;
        sum /= t;
```

```
        return sum;
}

template<class T>
Tensor<T> Tensor<T>::operator/(const T div)
{
        Tensor<T> sum =* this;
        sum /= div;
        return sum;
}

template<class T>
Tensor<T> operator/(const T div, const Tensor<T>& t)
{
        Tensor<T> sum = t;
        sum /= div;
        return sum;
}

////////////////////////////// IO Functions //////////////////////////
template<class T>
ostream& operator<<(ostream& out, const Tensor<T>& t)
{
        if (t.rank>0)
        {
                out << t.size[0];
                for(unsigned int i=1; i<t.rank; i++)
                        out << " " << t.size[i];
                out << endl;

                for(unsigned long x=0L; x<t.length; x++)
                        out << t.data[x] << " ";
        }
        out << endl;
        return out;
}

template<class T>
istream& operator>>(istream& in, Tensor<T>& t)
{
        unsigned int i = 0;
        unsigned int tempsize[MAX_TENSOR_RANK];
        char c;
        while( in.get(c) ) {
                if ( c == '\n' ) break;
                in.putback(c);
                in >> tempsize[i++];
                assert( i < MAX_TENSOR_RANK );
        }
        t.changeDim(i, tempsize);
        for(unsigned long x=0L; x<t.length; x++)
                in >> t.data[x];
        return in;
```

```
}

template<class T>
void Tensor<T>::fill(istream& in)
{
//      output matrix
        for(unsigned long x=0L; x<length && !in.eof(); x++)
        in >> data[x];
}

template<class T>
ostream& operator<<=(ostream& out, const Tensor<T>& t)
{
        if (t.rank>0) {
                out << t.size[0];
                for(int i=1; i<t.rank; i++)
                        out << " " << t.size[i];
                out     << endl;
        }
        out.write((char*)t.data, (int)t.length*sizeof(T));
        return out;
}

template<class T>
istream& operator>>=(istream& in, Tensor<T>& t)
{
        unsigned int i = 0;
        unsigned int tempsize[MAX_TENSOR_RANK];
        char c;
        while( in.get(c) ) {
                if ( c == '\n' ) break;
                in.putback(c);
                in >> tempsize[i++];
                assert( i < MAX_TENSOR_RANK );
        }
        t.changeDim(i, tempsize);
        in.read((char *)(t.data), (int)t.length*sizeof(T));
        return in;
}

////////////////////// Miscellaneous Functions ////////////////////////
template<class T>
Tensor<T> Tensor<T>::transpose()
{
        Tensor<T> trans = *this;
        switch(rank) {
        case 2:
                trans.changeDim(size[1], size[0]);
                for(unsigned int i=0; i< size[0]; i++)
                        for(unsigned int j=0; j< size[1]; j++) ((T**)trans.val)[j][i] = ((T**)val)[i]
[j];
        }
        return trans;
```

```
}

template<class T>
Tensor<T> Tensor<T>::concat(Tensor<T> &a)
{
//      concatenate two tensors.
        unsigned int i, newRank;
        Tensor<T> c;
        if (a.length == 0) return(*this);
        if (rank == 0 && a.rank == 0) return c;
        if (rank != 0 && a.rank !=0)
                for(i=1; i<rank; i++)
                        assert(size[i] == a.size[i] || size[i] == 0 || a.size[i] == 0);
                                        // dimensions incompatible for concat.
        if (rank == 0) newRank = a.rank;
        else newRank = rank;
        unsigned int *newSize = new unsigned int[newRank];
        assert(newSize);
        if (rank == 0) newSize[0] = a.size[0];
        else newSize[0] = size[0] + a.size[0];
        for(i=1; i<rank; i++)
                if (size[i] == 0) newSize[i] = a.size[i];
                else newSize[i] = size[i];
        c.changeDim(newRank, newSize);
        delete[] newSize;
        T *d = data;
        T *cd = c.data;
        for(i=0; i<length; i++) *cd++ = *d++;
        T *ad = a.data;
        for(i=0; i<a.length; i++) *cd++ = *ad++;
        return(c);
}

// This function should be combined with blockAdd
template<class T>
void Tensor<T>::add(Tensor<T> &a, const unsigned int startpos, const unsigned int offset)
{
        assert(a.rank == 1 && rank == 1);  // add currently only works on vectors
        // add the vector a to this vector putting it in the specified place
        assert((a.size[0]-1)*offset+startpos < size[0]);
        for (unsigned int i=0; i<a.size[0]; i++)
                ((T*)val)[i+startpos+i*offset] += ((T*)a.val)[i];
}

template<class T>
Tensor<T> Tensor<T>::subTensor(const unsigned int xStart, const unsigned int xEnd )
{
        assert(rank == 1);
                // subTensor(xstart,xend) only works on vectors
        assert(xStart <= xEnd && xEnd < size[0]);
                // illegal range in subTensor
        Tensor<T> result(xEnd - xStart + 1);
        for(unsigned long x=xStart, x1=0; x<xEnd + 1; x++, x1++)
```

```
                ((T*)result.val)[x1] = ((T*)val)[x];
        return(result);
}

template<class T>
Tensor<T> Tensor<T>::subTensor(const unsigned int xStart,
        const unsigned int xEnd, const unsigned int yStart, const unsigned int yEnd)
{
        assert(rank == 2);
                // subTensor(xstart,xend,ystart,yend) only works on matrices
        assert(xStart <= xEnd && xEnd < size[0] && yStart <= yEnd && yEnd < size[1]);
                // illegal range in subTensor
        Tensor<T> result(xEnd - xStart + 1, yEnd - yStart +1);

        for(unsigned long x=xStart, x1=0; x<xEnd + 1; x++, x1++)
                for(unsigned long y=yStart, y1=0; y<yEnd + 1; y++, y1++)
                        ((T**)result.val)[x1][y1] = ((T**)val)[x][y];

        return(result);
}

template<class T>
Tensor<T> Tensor<T>::subTensor(const unsigned int xStart, const unsigned int xEnd,
        const unsigned int yStart, const unsigned int yEnd, const unsigned int zStart,
        const unsigned int zEnd)
{
        assert(rank == 3);
                // subTensor(xstart,xend,ystart,yend, zstart, zend) only works on 3tensors. yeehah....
        assert(xStart <= xEnd && xEnd < size[0] && yStart <= yEnd && yEnd < size[1] && zStart
<= zEnd && zEnd < size[2]);
                // illegal range in subTensor
        Tensor<T> result(xEnd - xStart + 1, yEnd - yStart +1, zEnd - zStart +1);
        for(unsigned long x=xStart, x1=0; x<xEnd + 1; x++, x1++)
                for(unsigned long y=yStart, y1=0; y<yEnd + 1; y++, y1++)
                        for(unsigned long z=zStart, z1=0; z<zEnd + 1; z++, z1++)
                                ((T***)result.val)[x1][y1][z1] = ((T***)val)[x][y][z];
        return(result);
}

template<class T>
void Tensor<T>::insertSubTensor(Tensor<T> &m, const unsigned int x)
{
        assert(rank == 1);
        assert( x+m.dim() <= size[0] );
        for (unsigned int i=0; i<m.dim(0); i++) ((T*)val)[i+x] = ((T*)m.val)[i];
}

template<class T>
void Tensor<T>::insertSubTensor(Tensor<T> &m, const unsigned int x, const unsigned int y)
{
        assert(rank == 2);
        assert( (x+m.dim(0) <= size[0]) && (y+m.dim(1) <= size[1]) );
        for (unsigned int i=0; i<m.dim(0); i++)
```

```
                for (unsigned int j=0; j<m.dim(1); j++)
                        ((T**)val)[i+x][j+y] = ((T**)m.val)[i][j];
}

template<class T>
void Tensor<T>::insertSubTensor(Tensor<T> &m, const unsigned int x, const unsigned int y, const
unsigned int z)
{
        assert(rank == 3);
        assert( (x+m.dim(0) <= size[0]) && (y+m.dim(1) <= size[1]) && (z+m.dim(2) <= size[2]));
        for (unsigned int i=0; i<m.dim(0); i++)
                for (unsigned int j=0; j<m.dim(1); j++)
                        for (unsigned int k=0; k<m.dim(2); k++)
                                ((T***)val)[i+x][j+y][k+z] = ((T***)m.val)[i][j][k];
}

template<class T>
void Tensor<T>::addOuterProd(Tensor<T> &a)
{
        assert(a.rank == 1 && rank == 2); // addOuterProd currently only works on vectors
        // error if the vector is not the correct size is too large
        assert( (size[0]==a.size[0]) && (size[1]==a.size[0]) );
        T mult;
        T* ar = a.data;
        T* ac = a.data;
        for (unsigned int r=0; r<size[0]; r++, ar++, ac = &(a.data[r])) {
                for (unsigned int c=r; c<size[1]; c++) {
                        mult = *ar * *ac++;
                        ((T**)val)[r][c] += mult;
                        if (c!=r)  ((T**)val)[c][r] += mult;
                }
        }
}

template<class T>
Tensor<T>& Tensor<T>::OuterProduct(Tensor<T> &a, Tensor<T> &b)
{
        assert(a.rank == 1 && rank == 1);
                // OuterProduct currently only works on vectors
        assert( (size[0]==a.size[0]) && (size[1]==a.size[1]) );
                // error if the vector is not the correct size
        T* ar = a.data;
        T* bc = b.data;
        T* res = data;
        for (unsigned int r=0; r<size[0]; r++, ar++, bc = b.data)
                for (unsigned int c=0; c<size[1]; c++) *data++ = *ar * *bc++;
        return *this;
}

template<class T>
void Tensor<T>::blockAdd(Tensor<T> &A, const unsigned int rPos, const unsigned int cPos)
{
        assert(rank == 2);
```

```
        // BlockAdd currently only works on matrices
        // performs block addition, i.e. adds the matrix A into this
        // matrix where K(rPos,cPos) = A(0,0)
        // error if the matrix A is too large
        assert( (rPos+A.size[0]<=size[0]) && (cPos+A.size[1]<=size[1]) );
        for (unsigned int i=0; i<A.size[0]; i++)
                for (unsigned int j=0; j<A.size[0]; j++)
                        ((T**)val)[i+rPos][j+cPos] += ((T**)A.val)[i][j];
}

template<class T>
void Tensor<T>::diagonalAdd(T t)
{
        if (rank == 0 || rank == 1) { data[0] += t; return; }
        unsigned int i;
        unsigned long j;
        for(i=1; i<rank; i++) assert(size[0] == size[i]);
                //Cannot diagonal add to tensor with different dimensions
        unsigned int increment = size[0] + 1 + (rank-2)*size[0]*size[0];
        for (i=0, j=0L; i<size[0]; i++, j += increment) data[j] += t;
}

template<class T>
void Tensor<T>::swap(const unsigned int i, const unsigned int j)
{
        assert(rank == 1);
                // swap currently only works on vectors
        T c = ((T*)val)[i];
        ((T*)val)[i] = ((T*)val)[j];
        ((T*)val)[j] = c;
}

template<class T>
void Tensor<T>::changeDim(unsigned int newRank, unsigned int *newSize)
{
        if (rank && rank == newRank) {
                bool sameSize = true;
                for(unsigned int j=0; j<rank; j++)
                        if (size[j] != newSize[j]) sameSize = false;
                if (sameSize) {
                        (*this) = (T) 0;
                        return;
                }
        }
        if (rank) destroy();
        rank = newRank;
        if(rank) {
                size = new unsigned int[rank];
                assert(size != NULL);
                for (unsigned int i = 0; i < rank; i++) size[i] = newSize[i];
                create();
        }
}
```

```
template<class T>
void Tensor<T>::changeDim()
{
        if (rank == 0) return;
        destroy();
}

template<class T>
void Tensor<T>::changeDim(const unsigned int x)
{
        if (rank == 1 && x == size[0]) {
                (*this) = (T) 0;
                return;
        }
        destroy();
        size = new unsigned int[rank = 1];
        assert(size);
        size[0] = x;
        create();
}

template<class T>
void Tensor<T>::changeDim(const unsigned int x, const unsigned int y)
{
        if (rank == 2 && x == size[0] && y == size[1]) {
                (*this) = (T) 0;
                return;
        }
        destroy();
        size = new unsigned int[rank = 2];
        assert(size);
        size[0] = x;
        size[1] = y;
        create();
}

template<class T>
void Tensor<T>::changeDim(const unsigned int x, const unsigned int y, const unsigned int z)
{
        if (rank == 3 && x == size[0] && y == size[1] && z == size[2]) {
                (*this) = (T) 0;
                return;
        }
        destroy();
        size = new unsigned int[rank = 3];
        assert(size);
        size[0] = x;
        size[1] = y;
        size[2] = z;
        create();
}
```

```
template<class T>
void Tensor<T>::reorder(const unsigned int pt[])
{
        assert(rank == 1 || rank == 2);
        Tensor<T> temp = *this;
        unsigned int i;
        switch(rank) {
        case 1:
                for (i=0; i<size[0]; i++)
                        ((T*)val)[i] = ((T*)temp.val)[pt[i]];
                break;
        case 2:
                for (i=0; i<size[0]; i++)
                        for (unsigned int j=0; j<size[1]; j++)
                                ((T**)val)[i][j] = ((T**)temp.val)[pt[i]][j];
                break;
        }
}

template<class T>
bool Tensor<T>::same_size(const Tensor<T>& t)
{
        if (rank != t.rank) return false;
        for(unsigned int i=0; i<rank; i++) if (size[i] != t.size[i]) return false;
        return true;
}

template<class T>
void Tensor<T>::getRow(Tensor<T> &a, const unsigned int i)
{
        assert(rank == 2);
                // getRow currently only works on matrices
        a.changeDim(size[1]);
        for (unsigned int j=0; j<size[1]; j++) ((T*)a.val)[j] = ((T**)val)[i][j];
}

template<class T>
void Tensor<T>::putRow(Tensor<T> &a, const unsigned int i)
{
        assert(rank == 2);
                // putRow currently only works on matrices
        for (unsigned int j=0; j<size[1]; j++) ((T**)val)[i][j] = ((T*)a.val)[j];
}

template<class T>
void Tensor<T>::getCol(Tensor<T> &a, const unsigned int j)
{
        assert(rank == 2);
                // getCol currently only works on matrices
        a.changeDim(size[0]);
        for (unsigned int i=0; i<size[0]; i++) ((T*)a.val)[i] = ((T**)val)[i][j];
}
```

```
template<class T>
void Tensor<T>::putCol(Tensor<T> &a, const unsigned int j)
{
        assert(rank == 2);
                // putCol currently only works on matrices
        for (unsigned int i=0; i<size[0]; i++)
                ((T**)val)[i][j] = ((T*)a.val)[i];
}

template<class T>
void Tensor<T>::vecQSort(const int left, const int right)
{
        assert(rank == 1);
                // QSort currently only works on vectors
        // sort vector into ascending order. Taken from K&R p.87.
        if (right > left) {  // if array contains no elements, do nothing
                swap(left,(left+right)/2);
                unsigned int last = left;
                for (int i=left+1; i<=right; i++) {
                        if (((T*)val)[i] < ((T*)val)[left]) {
                        ++last;
                        swap(last,i);
                        }
                }
                swap(left,last);
                vecQSort(left,last-1);
                vecQSort(last+1,right);
        }
}

template<class T>
T Tensor<T>::euclidDist()
{
        precision s = 0.0;
        T *aval = data;
        for(unsigned long x=0L; x<length; x++) s += pow(*aval++,2.0);
        return T(pow(s,0.5));
}

template<class T>
T Tensor<T>::euclidDist(const Tensor<T>& t)
{
        precision s = 0.0;
        T *aval = data;
        T *bval = t.data;
        for(unsigned long x=0L; x<length; x++) s += pow(*aval++ - *bval++,2.0);
        return T(pow(s,0.5));
}

template<class T>
Tensor<T> Tensor<T>::abs()
{
        Tensor<T> result(*this);
```

```
        T* rptr = result.data;
        for(unsigned long x=0L; x<length; x++, rptr++) *rptr = fabs(*rptr);
        return result;
}

template<class T>
T Tensor<T>::minVal()
{
        T mindata = data[0];
        T* d = data;
        for(unsigned long x=1L; x<length; x++, d++) if (*d < mindata) mindata = *d;
        return mindata;
}

template<class T>
T Tensor<T>::maxVal()
{
        T maxdata = data[0];
        T* d = data;
        for(unsigned long x=1L; x<length; x++, d++) if (*d > maxdata) maxdata = *d;
        return maxdata;
}

template<class T>
unsigned long Tensor<T>::minIndex()
{       // absolute value
        T mindata = data[0];
        unsigned long minindex=0;
        T* d = data;
        for(unsigned long x=1L; x<length; x++, d++)
                if (*d < mindata) { mindata = *d; minindex=x; }
        return minindex;
}

template<class T>
unsigned long Tensor<T>::maxIndex()
{       // absolute value
        T maxdata = data[0];
        unsigned long maxindex=0;
        T* d = data;
        for(unsigned long x=1L; x<length; x++, d++)
                if (*d > maxdata){
                        maxdata = *d;
                        maxindex=x;
        }
        return maxindex;
}

template<class T>
void Tensor<T>::print()
{
        cout << "Tensor : Rank " << rank << endl << "Dimension : ";
        for(unsigned int i=0; i<rank; i++) cout << size[i] << " ";
```

```
        cout << endl;
        T* d = data;
        unsigned long x=0L;
        while( x++ < length ) {
                cout << *d++ << " ";
                if (x % size[rank-1] == 0) cout << endl;
        }
}

template<class T>
void Tensor<T>::clear()
{
        destroy();
}

template<class T>
void Tensor<T>::diag(Tensor<T> &d)
{
        assert(rank == 2);
        assert(size[0] == size[1]);
        for(unsigned int i=0; i<size[0]; i++) ((T**)val)[i][i] = d(i);
}

template<class T>
void Tensor<T>::diag(T &d)
{
        assert(rank == 2);
        assert(size[0] == size[1]);
        for(unsigned int i=0; i<size[0]; i++) ((T**)val)[i][i] = d;
}

template<class T>
Tensor<T> Tensor<T>::diag()
{
        assert(rank == 2);
        assert(size[0] == size[1]);
        VECTOR<precision> d(size[0]);
        for(unsigned int i=0; i<size[0]; i++) d(i) = ((T**)val)[i][i];
        return(d);
}

template<class T>
double Tensor<T>::sum()
{
        double result = 0.0;
        T* dptr = data;
        for(unsigned long x=0L; x<length; x++, dptr++) result += *dptr;
        return result;
}

template<class T>
Tensor<T> Tensor<T>::partialSum()
{
```

```
        Tensor<T> result;
        if (rank == 0) return result;
        unsigned int newRank = rank-1;
        unsigned int *newSize = NULL;
        if (newRank == 0) {
                newRank = 1;
                newSize = new unsigned int[newRank];
                newSize[0] = 1;
                assert(newSize);
        } else {
                newSize = new unsigned int[newRank];
                assert(newSize);
                unsigned int i=1;
                while(i < rank) {
                        newSize[i - 1] = size[i];
                        i++;
                }
        }
        result.changeDim(newRank, newSize);
        delete newSize;
        T* dptr = data;
        T* rptr = result.data;
        for(unsigned int y=0; y < (int)(length / size[0]); y++, rptr++)
                for(unsigned int x=0; x < size[0]; x++, dptr++) *rptr += *dptr;
        return result;
}

template<class T>
Tensor<T> Tensor<T>::inverse()
{       // Inverse of a matrix using SVD
        assert(rank == 2);
        VECTOR<T> w(size[1]);
        MATRIX<T> inv_w(size[1], size[1]);
        MATRIX<T> v(size[1], size[1]);
        MATRIX<T> u(*this);
        MATRIX<T> inverse;
        svdcmp(u, w, v);
        const precision threshold = 1.0e-8;
        for(unsigned int i=0; i<w.dim(); i++)
                if (w(i) < threshold) w(i) = 0.0;
                else w(i) = 1/w(i);
        inv_w.diag(w);
        inverse = v*inv_w*u.transpose();
        return(inverse);
}

////////////////////////// SVD Functions ////////////////////////////

template<class T>
void Tensor<T>::SVD(VECTOR<T> &b, VECTOR<T> &x)
{       // Solves Ax=b,  A.SVD(b,x)
        // where A is this matrix.
        assert(rank == 2 && b.rank == 1);
```

```
                // SVD operates on a matrix A and a vector b
        assert(size[0] == b.size[0]);
                // Incompatible Vector and Matrix dimensions for SVD.
        VECTOR<T> w(size[1]), y(size[1]);
        MATRIX<T> v(size[1], size[1]);
        MATRIX<T> A(*this);
        svdcmp(A, w, v);
        // This is where any singular values are 'edited'.
        const precision threshold = 1.0e-8;
        for(unsigned int j=0;j<A.size[1];j++)
                if(w(j) < threshold) { w(j) = 0.0;}
                svbksb(A, w, v, b, x);
}

template<class T>
void Tensor<T>::svdcmp(MATRIX<T> &A, VECTOR<T> &w, MATRIX<T> &v)
{       // constructs SVD of any matrix.
        // i.e.  A = U.W.V'
        // where for the output:
        //      A = U
        //      w = diag(W)
        //      V = V
        int m=A.dim(0);
        int n=A.dim(1);
        int flag,i,its,j,jj,k,l,nm;
        precision one = 1.0;
        precision anorm,c,f,g,h,s,scale,x,y,z;
        VECTOR<T> rv1(n);
        g=scale=anorm=0.0;
        for (i=0;i<n;i++) {
                l=i+1;
                ((T*)rv1.val)[i]=scale*g;
                g=s=scale=0.0;
                if (i < m) {
                        for (k=i;k<m;k++) scale += fabs(((T**)A.val)[k][i]);
                                if (scale) {
                                        for (k=i;k<m;k++) {
                                                ((T**)A.val)[k][i] /= scale;
                                                s += ((T**)A.val)[k][i] * ((T**)A.val)[k][i];
                                        }
                                        f = ((T**)A.val)[i][i];
                                        g = -ISISSIGN(sqrt(s),f);
                                        h = f * g - s;
                                        ((T**)A.val)[i][i] = f - g;
                                        for (j=l;j<n;j++) {
                                                for (s=0.0,k=i;k<m;k++)
                                                        s += ((T**)A.val)[k][i] * ((T**)A.val)
[k][j];

                                                f = s / h;
                                                for (k=i;k<m;k++)
                                                        ((T**)A.val)[k][j] += f * ((T**)A.val)
[k][i];
                                        }
```

```
                                        for (k=i;k<m;k++) ((T**)A.val)[k][i] *= scale;
                                }
                        }
                ((T*)w.val)[i] = scale * g;
                g = s = scale = 0.0;
                if (i < m && i != (n-1)) {
                        for (k=l;k<n;k++) scale += fabs(((T**)A.val)[i][k]);
                        if (scale) {
                                for (k=l;k<n;k++) {
                                        ((T**)A.val)[i][k] /= scale;
                                        s += ((T**)A.val)[i][k] * ((T**)A.val)[i][k];
                                }
                                f = ((T**)A.val)[i][l];
                                g = -ISISSIGN(sqrt(s),f);
                                h= f * g - s;
                                ((T**)A.val)[i][l] = f - g;
                                for (k=l;k<n;k++) ((T*)rv1.val)[k] = ((T**)A.val)[i][k] / h;
                                for (j=l;j<m;j++) {
                                        for (s=0.0,k=l;k<n;k++)
                                                s += ((T**)A.val)[j][k] * ((T**)A.val)[i][k];
                                        for (k=l;k<n;k++) ((T**)A.val)[j][k] += s * ((T*)rv1.val)
[k];
                                }
                                for (k=l;k<n;k++) ((T**)A.val)[i][k] *= scale;
                        }
                }
                anorm=ISISMAX(anorm,(fabs(((T*)w.val)[i])+fabs(((T*)rv1.val)[i])));
        }
        for (i=n-1;i>=0;i--) {
                if (i < (n-1)) {
                        if (g) {
                                for (j=l;j<n;j++)
                                        v(j,i)=(((T**)A.val)[i][j] / ((T**)A.val)[i][l])/g;
                                for (j=l;j<n;j++) {
                                        for (s=0.0,k=l;k<n;k++)
                                                s += ((T**)A.val)[i][k] * ((T**)v.val)[k][j];
                                        for (k=l;k<n;k++) ((T**)v.val)[k][j] += s * ((T**)v.val)
[k][i];
                                }
                        }
                        for (j=l;j<n;j++) ((T**)v.val)[i][j] = ((T**)v.val)[j][i] = 0.0;
                }
                ((T**)v.val)[i][i] = 1.0;
                g = ((T*)rv1.val)[i];
                l = i;
        }
        for (i=ISISMIN(m,n)-1;i>=0;i--) {
                l = i+1;
                g = ((T*)w.val)[i];
                for (j=l;j<n;j++) ((T**)A.val)[i][j] = 0.0;
                if (g) {
                        g = 1.0 / g;
                        for (j=l;j<n;j++) {
```

```
                        for (s=0.0,k=l;k<m;k++) s += ((T**)A.val)[k][i] * ((T**)A.val)[k]
[j];
                        f = (s / ((T**)A.val)[i][i]) * g;
                        for (k=i;k<m;k++) ((T**)A.val)[k][j] += f * ((T**)A.val)[k][i];
                    }
                    for (j=i;j<m;j++) ((T**)A.val)[j][i] *= g;
                }
                else for (j=i;j<m;j++) ((T**)A.val)[j][i] = 0.0;
                ++(((T**)A.val)[i][i]);
            }
            for (k=n-1;k>=0;k--) {
                for (its=1;its<=30;its++) {
                    flag = 1;
                    for (l=k;l>=0;l--) {
                        nm = l - 1;
                        if ((double)(fabs(((T*)rv1.val)[l])+anorm) == anorm) {
                            flag = 0;
                            break;
                        }
                        if ((double)(fabs(((T*)w.val)[nm])+anorm) == anorm) break;
                    }
                    if (flag) {
                        c = 0.0;
                        s = 1.0;
                        for (i=l;i<=k;i++) {
                            f = s * ((T*)rv1.val)[i];
                            ((T*)rv1.val)[i] = c * ((T*)rv1.val)[i];
                            if ((double)(fabs(f)+anorm) == anorm) break;
                            g = ((T*)w.val)[i];
                            h = pythag(f,g);
                            ((T*)w.val)[i] = h;
                            h = 1.0 / h;
                            c = g * h;
                            s = -f * h;
                            for (j=0;j<m;j++) {
                                y = ((T**)A.val)[j][nm];
                                z = ((T**)A.val)[j][i];
                                ((T**)A.val)[j][nm] = y * c + z * s;
                                ((T**)A.val)[j][i] = z * c - y * s;
                            }
                        }
                    }
                    z = ((T*)w.val)[k];
                    if (l == k) {
                        if (z < 0.0) {
                            ((T*)w.val)[k] = -z;
                            for (j=0;j<n;j++) ((T**)v.val)[j][k] = -((T**)v.val)[j][k];
                        }
                        break;
                    }
                    assert(its < 30); // SVD - no convergence in 30 svdcmp iterations
                    x = ((T*)w.val)[l];
                    nm = k - 1;
```

```
                        y = ((T*)w.val)[nm];
                        g = ((T*)rv1.val)[nm];
                        h = ((T*)rv1.val)[k];
                        f = ((y-z) * (y+z) + (g-h) * (g+h))/(2.0 * h * y);
                        g = pythag(f,one);
                        f = ((x-z) * (x+z) + h * ((y / (f + ISISSIGN(g,f))) - h)) / x;
                        c = s = 1.0;
                        for (j=l;j<=nm;j++) {
                                i = j + 1;
                                g = ((T*)rv1.val)[i];
                                y = ((T*)w.val)[i];
                                h = s * g;
                                g = c * g;
                                z = pythag(f,h);
                                ((T*)rv1.val)[j] = z;
                                c = f / z;
                                s = h / z;
                                f = x * c + g * s;
                                g = g * c - x * s;
                                h = y * s;
                                y *= c;
                                for (jj=0;jj<n;jj++) {
                                        x = ((T**)v.val)[jj][j];
                                        z = ((T**)v.val)[jj][i];
                                        ((T**)v.val)[jj][j] = x * c + z * s;
                                        ((T**)v.val)[jj][i] = z * c - x * s;
                                }
                                z = pythag(f,h);
                                ((T*)w.val)[j] = z;
                                if (z) {
                                        z = 1.0 / z;
                                        c = f * z;
                                        s = h * z;
                                }
                                f = c * g + s * y;
                                x = c * y - s * g;
                                for (jj=0;jj<m;jj++) {
                                        y = ((T**)A.val)[jj][j];
                                        z = ((T**)A.val)[jj][i];
                                        ((T**)A.val)[jj][j] = y * c + z * s;
                                        ((T**)A.val)[jj][i] = z * c - y * s;
                                }
                        }
                        ((T*)rv1.val)[l] = 0.0;
                        ((T*)rv1.val)[k] = f;
                        ((T*)w.val)[k] = x;
                }
        }
}

template<class T>
void Tensor<T>::svbksb(MATRIX<T> &u, VECTOR<T> &w, MATRIX<T> &v, VECTOR<T> &b,
VECTOR<T> &x)
```

```
{
        int m=u.dim(0);
        int n=u.dim(1);
        int jj,j,i;
        precision s;
        VECTOR<T> tmp(n);
//      find W^{-1} U^{T} b
        for (j=0;j<n;j++) {
                s = 0.0;
                if (((T*)w.val)[j]) {
                        for (i=0;i<m;i++) s += ((T**)u.val)[i][j] * ((T*)b.val)[i];
                        s /= ((T*)w.val)[j];
                }
                ((T*)tmp.val)[j] = s;
        }
//      find V . [W^{-1} U^{T} b]
        for (j=0;j<n;j++) {
                s = 0.0;
                for (jj=0;jj<n;jj++) s += ((T**)v.val)[j][jj] * ((T*)tmp.val)[jj];
                ((T*)x.val)[j] = s;
        }
}

template<class T>
double Tensor<T>::pythag(double &a, double &b)
{
        double absa,absb;
        absa=fabs(a);
        absb=fabs(b);
        if (absa > absb) return absa*sqrt(1.0+ISISSQR(absb/absa));
        else return (absb == 0.0 ? 0.0 : absb*sqrt(1.0+ISISSQR(absa/absb)));
}
```

8.1.3.1.3 tensor.h

```
// Filename: tensor.h
// Description: Routines for Tensors
// Classes: Tensor
// Comments: VECTOR and MATRIX are #defines which can be used to clarify
//                 code to show show what type of tensor is intended.
//
// Author: Steve Gunn (srg@ecs.soton.ac.uk) (c)
//
// Copyright: All rights reserved

#ifndef _tensor_h_
        #define _tensor_h_
        #include <assert.h>
        #include "defns.h"
        #define VECTOR Tensor
        #define MATRIX Tensor
        #define MAX_TENSOR_RANK 3
```

```
#ifdef _DEBUG
        #define RANGECHECKING(a)  a
#else
        #define RANGECHECKING(a)
#endif
template <class T> class Tensor;
template <class T> T operator +(Tensor<T>);
template <class T> T operator -(Tensor<T>);
template <class T> T operator *(Tensor<T>);
template <class T> T operator /(Tensor<T>, Tensor<T>);
template <class T> ostream& operator<<(Tensor<T>, Tensor<T>);
template <class T> istream& operator>>(Tensor<T>, Tensor<T>);
template <class T> ostream& operator<<=(Tensor<T>, Tensor<T>);
template <class T> istream& operator>>=(Tensor<T>, Tensor<T>);
template <class T>
class Tensor {
private:
        void create();
        void destroy();
        void copy(const Tensor& t);
protected:
        unsigned int rank;
        unsigned int* size;
        unsigned long length;       // total number of elements
        void* val;
        T* data;            // pointer to data
public:
        Tensor();
        Tensor(const unsigned int u);
        Tensor(const unsigned int u, const unsigned int v);
        Tensor(const unsigned int u, const unsigned int v, const unsigned int w);
        // required for matlab interface. Implemented by KB 10/8/96
        Tensor(T* t,const unsigned int l);
        Tensor(T* t,const unsigned int nr, const unsigned int nc);
        T* tensorPtr();
        ~Tensor() { destroy(); }
        operator T();
        Tensor(const Tensor<T>& t) { copy(t); }
        Tensor<T>& operator=(const Tensor<T>& t);
        Tensor<T>& operator=(const T init);
        bool operator==(const Tensor<T>& b);
        bool operator!=(const Tensor<T>& b);
        T& operator()(const unsigned int u)
        {
                RANGECHECKING(assert(u<size[0]);)
                return ((T*)val)[u];
        }
        T& operator()(const unsigned int u, const unsigned int v)
        {
                RANGECHECKING(assert(u<size[0] && v<size[1]);)
                return ((T**)val)[u][v];
        }
        T& operator()(const unsigned int u, const unsigned int v, const unsigned int w)
```

```
{
        RANGECHECKING(assert(u<size[0] && v<size[1] && w<size[2]);)
        return ((T***)val)[u][v][w];
}
bool same_size(const Tensor<T>& t);
Tensor<T>& operator+=(const Tensor<T>& t);
Tensor<T>& operator+=(const T add);
Tensor<T> operator+(const Tensor<T>& t);
Tensor<T> operator+(const T add);
friend Tensor<T> operator+<>(const T add, const Tensor<T>& t);
Tensor<T>& operator-=(const Tensor<T>& t);
Tensor<T>& operator-=(const T sub);
Tensor<T> operator-(const Tensor<T>& t);
Tensor<T> operator-(const T sub);
friend Tensor<T> operator-<>(const T sub, const Tensor<T>& t);
Tensor<T>& operator*=(const Tensor<T>& t);
Tensor<T>& operator*=(const T mul);
Tensor<T> operator*(const Tensor<T>& t);
Tensor<T> operator*(const T mul);
friend Tensor<T> operator*<>(const T mul, const Tensor<T>& t);
Tensor<T>& operator/=(const Tensor<T>& t);
Tensor<T>& operator/=(const T div);
Tensor<T> operator/(const Tensor<T>& t);
Tensor<T> operator/(const T div);
friend Tensor<T> operator/<>(const T div, const Tensor<T>& t);
friend ostream& operator<<<>(ostream& out, const Tensor<T>& t);
friend istream& operator>><>(istream& in, Tensor<T>& t);
friend ostream& operator<<=<>(ostream& out, const Tensor<T>& t);
friend istream& operator>>=<>(istream& in, Tensor<T>& t);
void fill(istream& in);
unsigned int ran() const { return rank; }
unsigned int dim() const {
        if (rank==0) return 0;
        return size[0]; }
unsigned int dim(const unsigned int d) const {
        if (d >= rank)  return 0;
        return size[d]; }
void* getval() const {return val; }
T* getdata() const {return data; }
unsigned long len() const { return length; }
Tensor<T> transpose();
Tensor<T> concat(Tensor<T> &a);
void add(Tensor<T> &a, const unsigned int startpos, const unsigned int offset);
Tensor<T> subTensor(const unsigned int xStart, const unsigned int xEnd );
Tensor<T> subTensor(const unsigned int xStart, const unsigned int xEnd, const
        unsigned int yStart, const unsigned int yEnd);
Tensor<T> subTensor(const unsigned int xStart, const unsigned int xEnd, const
        unsigned int yStart, const unsigned int yEnd, const unsigned int zStart,
const
        unsigned int zEnd);
void insertSubTensor(Tensor<T> &m, const unsigned int x);
void insertSubTensor(Tensor<T> &m, const unsigned int x, const unsigned int y );
void insertSubTensor(Tensor<T> &m, const unsigned int x, const unsigned int y,
```

```
                const unsigned int z );
        void addOuterProd(Tensor<T> &a);
        Tensor<T>& OuterProduct(Tensor<T> &a, Tensor<T> &b);
        void blockAdd(Tensor<T> &A, const unsigned int rPos, const unsigned int cPos);
        void diagonalAdd(T t);
        void swap(const unsigned int i, const unsigned int j);
        void changeDim(unsigned int newRank, unsigned int *newSize);
        void changeDim();
        void changeDim(const unsigned int x);
        void changeDim(const unsigned int x, const unsigned int y);
        void changeDim(const unsigned int x, const unsigned int y, const unsigned int z);
        void reorder(const unsigned int pt[]);
        void vecQSort(const int left, const int right);
        void getRow(Tensor<T> &a, const unsigned int i);
        void putRow(Tensor<T> &a, const unsigned int i);
        void getCol(Tensor<T> &a, const unsigned int j);
        void putCol(Tensor<T> &a, const unsigned int j);
        T euclidDist();
        T euclidDist(const Tensor<T>& t);
        Tensor<T> abs();
        T minVal();
        T maxVal();
        unsigned long minIndex();
        unsigned long maxIndex();
        void clear();
        void print();
        void diag(Tensor<T> &d);
        void diag(T &d);
        Tensor<T> diag();
        double sum();
        Tensor<T> partialSum();
        Tensor<T> inverse();
        void SVD(VECTOR<T> &b, VECTOR<T> &x);
        void svdcmp(MATRIX<T> &A, VECTOR<T> &w, MATRIX<T> &v);
        void svbksb(MATRIX<T> &u, VECTOR<T> &w, MATRIX<T> &v,
                VECTOR<T> &b, VECTOR<T> &x);
        double pythag(double &a, double &b);
};

#if defined(_MSC_VER) || defined(__BORLANDC__) || defined(__GNUC__) ||
        defined(__WATCOMC__)
        #include "tensor.cpp"
#endif
#endif
```

8.1.3.2 The new Matlab M-code program

```
function
[RI,k2,BP,index]=rpm_ref(bigm,W,no_basis_functions,lbeta1,weight,A,Cref,ydim,mask,d,lambda)
%       Pre-allocate arrays for speed, use 0 for R1,k2 & BP. Use signal value for index
        ssq=zeros(1,no_basis_functions);
        RI=zeros(1,ydim);
        k2=zeros(1,ydim);
```

```
        BP=zeros(1,ydim);
        index=ones(1,ydim)*(no_basis_functions);
        for y=1:ydim
                if mask(y) > 0
%                       Only do work if data exists
                        data=d(:,y);
                        Wd=W*data;
                        B=[Cref A(:,1)];
                        for i=1:no_basis_functions
                                B(:,2)=A(:,i);
                                result=bigm((i*2-1):i*2,:)*Wd;
                                ssq(i)=sum((weight).*(B*result-data).^2);
                        end
                        sol=find(min(ssq)==ssq);
                        ind=sol(1);
                        result=bigm((ind*2-1):ind*2,:)*Wd;
                        RI(y)=result(1);
                        k2(y)=result(2)+(lbeta1(ind)-lambda)*RI(y);
                        BP(y)=(k2(y))/(lbeta1(ind)-lambda) - 1;
                        index(y)=ind-1;
                end
        end
```

8.1.3.3 The new C program

```
/* Code to re-implement rpm_ref.cpp, tensor.cpp & tensor.h in C rather than C++
The original M-file and C++ code was written by Roger & Steve Gunn,
        while at MRC Cyclotron Unit, Hammersmith Hospital, London, UK.
================================================================================
function [RI,k2,BP,index] = rpm_ref(bigm, W, no_basis_functions, lbeta1, weight, A, Cref, ydim,
mask, d, lambda)
================================================================================
Where:
bigm double matrix (2*no_basis_functions,num_frames)
W double matrix (num_frames,num_frames)
no_basis_functions integer scalar
lbeta1 double row vector (1,no_basis_functions)
weight double column vector (num_frames,1)
A double matrix (num_frames,no_basis_functions)
Cref double column vector (num_frames,1)
ydim integer scalar
mask double coumn vector (1,ydim)
d double matrix (num_frames,ydim)
lambda double scalar
RI double row vector (1,ydim)
k2 double row vector (1,ydim)
BP double row vector (1,ydim)
index integer row vector (1,ydim)
================================================================================
Licensed under GPL, version of your choice.
  by:
Dr. Mark Daglish
Clinical Lecturer in Psychiatry
```

Psychopharmacology Unit
University of Bristol,UK
mark.daglish@bris.ac.uk

```
==========================================================
*/
/* $Revision: 0.1 $
  $Date: 2006-08-01 $*/
/* include the headers required by Matlab and the mathematics functions */
#include "mex.h"
#include "matrix.h"
#include <math.h>
void mexFunction(
        int nlhs, mxArray *plhs[], int nrhs, const mxArray *prhs[])
/* the gateway routine called by Matlab */
{
        int ydim, nobf, frames, M,N,i,j,bf,y,sol;
        double lambda, result[2], temp, *d, *Wd, *B;
        double *bigm, *W, *lbeta1, *A, *Cref, *mask, *data, ssq, minssq, *RI, *k2, *BP, *weight,
*index;
/* Check input arguments. */
        if ( nrhs != 11 || nlhs != 4 ) {
                mexErrMsgTxt("Usage: [RI,k2,BP,index] = markrpm_ref(bigm, W,
nobasisfunctions, lbeta1, weight,                    A, Cref, ydim, mask, d, lambda)");
        }
        for (i=0;i<11;i++) {
        if (!mxIsDouble(prhs[i]) || mxIsComplex(prhs[i])){
                mexErrMsgTxt("All arguments must be non-complex and double");
        }
}
nobf = (int)mxGetScalar(prhs[2]);
ydim = (int)mxGetScalar(prhs[7]);
frames = mxGetM(prhs[9]);
/* Argument dims   0      1      2  3      4          5        6      7  8      9        10 */
int Msize[11] = {2*nobf,frames,1,   1,  frames,frames,frames,1,  1,    frames,1};
int Nsize[11] = {frames, frames,1,nobf,     1,      nobf,     1,     1,ydim,  ydim ,1};

for (i = 0; i < 11; i++) {
        M = mxGetM(prhs[i]);
        N = mxGetN(prhs[i]);
        if ((M != Msize[i]) || (N != Nsize[i])) {
                mexErrMsgTxt("Matrix has wrong dimensions");
        }
}
/* Create matrices for the return argument. */
for (i = 0; i<4; i++) {
        plhs[i] = mxCreateDoubleMatrix(1,ydim, mxREAL);
        if (plhs[i] == NULL) {
                mexErrMsgTxt("Failed to allocate memory for return value");
        }
}

/* Assign pointers to each input and output. */
bigm = mxGetPr(prhs[0]);
```

```
W = mxGetPr(prhs[1]);
lbeta1 = mxGetPr(prhs[3]);
weight = mxGetPr(prhs[4]);
A = mxGetPr(prhs[5]);
Cref = mxGetPr(prhs[6]);
mask = mxGetPr(prhs[8]);
d = mxGetPr(prhs[9]);
lambda = mxGetScalar(prhs[10]);
RI = mxGetPr(plhs[0]);
k2 = mxGetPr(plhs[1]);
BP = mxGetPr(plhs[2]);
index = mxGetPr(plhs[3]);

/* Allocate space for working variables */
Wd = mxCalloc(frames,sizeof(double));
if (Wd == NULL) {
        mexErrMsgTxt("Failed to allocate memory (Wd)");
}
data = mxCalloc(frames,sizeof(double));
if (data == NULL) {
        mexErrMsgTxt("Failed to allocate memory (data)");
}
B = mxCalloc(frames*2,sizeof(double));
if (B == NULL) {
        mexErrMsgTxt("Failed to allocate memory (B)");
}
/* From here the comments reproduce the M-code we are copying */
/* B(:,1)=Cref; */
/* This factor doesn't change for each basis function, therefore pre-load the first column of the matrix
*/
for (i=0;i<frames;i++) {
        *(B+i) = Cref[i];
}
for (y = 0; y<ydim; y++) {
        /* if mask = 0 then we have no usable data in this voxel */
        if (mask[y] > 0.0) {
                /* data=d(:,y);
                Extract the data for the voxel we want
                Wd=W*data;
                And also calculate the weighted data */
                for (i = 0; i<frames; i++) {
                        *(data+i) = *(d+y*frames+i);
                        *(Wd+i) = *(data+i) * *(W+i*frames+i);
                }
                sol = 0;
                minssq = 0.0;
                for (bf=0 ; bf<nobf;bf++) {
                        /* B(:,2)=A(:,bf);
                        For each basis function in turn extract the required parameters */
                        for (i=0;i<frames;i++) {
                                *(B+frames+i)=*(A+bf*frames+i);
                        }
                        /* result=bigm((bf*2-1):bf*2,:)*Wd; */
```

```
                        result[0] = 0.0;
                        result[1] = 0.0;
                        for (i=0; i<2;i++) {
                                for (j=0; j<frames; j++) {
                                        result[i] += *(bigm+j*2*nobf+(bf*2+i)) * Wd[j];
                                }
                        }
/*ssq(bf) = sum((weight).*(B*result-data).^2);
and calculate the sum of squares difference  between the predicted data from the parameters and the
observed data */
                        ssq = 0.0;
                        for (i=0; i<frames;i++) {
                                temp = *(B+i)*result[0] + *(B+frames+i)*result[1] - data[i];
                                ssq += temp*temp*weight[i];
                        }
/* sol = find(min(ssq)==ssq); */
/* Brought finding the minimum sum of squares solution inside the same loop to cut computational
time */
                        if (bf == 0) {
/* Skip checking first time round as minssq starts at 0.0 */
                                minssq=ssq;
                                sol = bf;
                        } else if (ssq < minssq) {
                                sol = bf;
                                minssq = ssq;
                        }
                }
/* result = bigm((sol*2-1):sol*2,:) * Wd;
and copy the solution into the returned parameters */
                result[0] = 0.0;
                result[1] = 0.0;
                for (i=0; i<2;i++) {
                        for (j=0; j<frames; j++) {
                                result[i] += *(bigm+j*2*nobf+sol*2+i) * Wd[j];
                        }
                }
                RI[y]=result[0];
                k2[y]=result[1]+(lbeta1[sol]-lambda)*RI[y];
                BP[y]=k2[y]/(lbeta1[sol]-lambda)-1.0;
                index[y]=sol;
        } else {
/* if there is no data set the return values to zero */
                RI[y] = 0.0;
                k2[y] = 0.0;
                BP[y] = 0.0;
/* except the index which should be a signal value of max+1 */
                index[y] = nobf;
        }
}
/* free the working memory before we exit */
mxFree(data);
mxFree(Wd);
mxFree(B);
```

```
}
```

8.2 Appendix 2: Questionnaires used

8.2.1 Heroin Craving Questionnaire (HCQ)

Indicate how much you agree or disagree with each of the following statements by placing a single cross (like this: X) along each line between STRONGLY DISAGREE and STRONGLY AGREE. The closer you place your cross to one end or the other indicates the strength of your agreement or disagreement. Please complete every item. We are interested in how you are thinking or feeling RIGHT NOW as you are filling out the questionnaire.

RIGHT NOW

1. If there was heroin right here in front of me, it would be hard not to use it.

   STRONGLY DISAGREE |___|___|___|___|___|___|___| STRONGLY AGREE

2. Using heroin would not be pleasant.

   STRONGLY DISAGREE |___|___|___|___|___|___|___| STRONGLY AGREE

3. I would feel less sick now if I used heroin.

   STRONGLY DISAGREE |___|___|___|___|___|___|___| STRONGLY AGREE

4. If I had the chance to use heroin right now, I don't think I would use it.

   STRONGLY DISAGREE |___|___|___|___|___|___|___| STRONGLY AGREE

5. Using heroin would not sharpen my concentration.

   STRONGLY DISAGREE |___|___|___|___|___|___|___| STRONGLY AGREE

6. Even if it were possible, I probably wouldn't use heroin right now.

   STRONGLY DISAGREE |___|___|___|___|___|___|___| STRONGLY AGREE

7. I am not missing heroin now.

   STRONGLY DISAGREE |___|___|___|___|___|___|___| STRONGLY AGREE

8. I am going to use heroin as soon as possible.

   STRONGLY DISAGREE |___|___|___|___|___|___|___| STRONGLY AGREE

9. My aches and stiffness would not go away if I used heroin right now.

   STRONGLY DISAGREE |___|___|___|___|___|___|___| STRONGLY AGREE

10. Using heroin now would make things seem just perfect.

STRONGLY DISAGREE |___|___|___|___|___|___|___| STRONGLY AGREE

11. My desire to use heroin seems overpowering.

STRONGLY DISAGREE |___|___|___|___|___|___|___| STRONGLY AGREE

12. Right now, I am not making plans to use heroin.

STRONGLY DISAGREE |___|___|___|___|___|___|___| STRONGLY AGREE

13. I could control things better right now if I could use heroin.

STRONGLY DISAGREE |___|___|___|___|___|___|___| STRONGLY AGREE

14. Using heroin right now would make me feel less tired.

STRONGLY DISAGREE |___|___|___|___|___|___|___| STRONGLY AGREE

15. I could not stop myself from using heroin if I had some here now.

STRONGLY DISAGREE |___|___|___|___|___|___|___| STRONGLY AGREE

16. If I tried a little heroin now, I would not be able to stop using more of it.

STRONGLY DISAGREE |___|___|___|___|___|___|___| STRONGLY AGREE

17. I want heroin so bad I can almost taste it.

STRONGLY DISAGREE |___|___|___|___|___|___|___| STRONGLY AGREE

18. Nothing would be better than using heroin right now.

STRONGLY DISAGREE |___|___|___|___|___|___|___| STRONGLY AGREE

19. I would do almost anything for heroin now.

STRONGLY DISAGREE |___|___|___|___|___|___|___| STRONGLY AGREE

20. I would feel so good and happy if I used heroin now.

STRONGLY DISAGREE |___|___|___|___|___|___|___| STRONGLY AGREE

21. I don't want to use heroin now.

STRONGLY DISAGREE |___|___|___|___|___|___|___| STRONGLY AGREE

22. I would be less irritable now if I could use heroin.

STRONGLY DISAGREE |____|____|____|____|____|____|____| STRONGLY AGREE

23. All I want to use now is heroin.

STRONGLY DISAGREE |____|____|____|____|____|____|____| STRONGLY AGREE

24. It would be difficult to turn down heroin now.

STRONGLY DISAGREE |____|____|____|____|____|____|____| STRONGLY AGREE

25. Starting now, I could go without using heroin for a long time.

STRONGLY DISAGREE |____|____|____|____|____|____|____| STRONGLY AGREE

26. Using heroin would not be very satisfying now.

STRONGLY DISAGREE |____|____|____|____|____|____|____| STRONGLY AGREE

27. If I used heroin right now, it would not help me calm down.

STRONGLY DISAGREE |____|____|____|____|____|____|____| STRONGLY AGREE

28. I would not enjoy using heroin right now.

STRONGLY DISAGREE |____|____|____|____|____|____|____| STRONGLY AGREE

29. I would not be able to control how much heroin I used if I had some here.

STRONGLY DISAGREE |____|____|____|____|____|____|____| STRONGLY AGREE

30. I would feel energetic if I used heroin

STRONGLY DISAGREE |____|____|____|____|____|____|____| STRONGLY AGREE

31. If I had some heroin with me right now, I probably wouldn't use it.

STRONGLY DISAGREE |____|____|____|____|____|____|____| STRONGLY AGREE

32. My hot and cold flushes would not get better if I used heroin now.

STRONGLY DISAGREE |____|____|____|____|____|____|____| STRONGLY AGREE

33. I do not need to use heroin now.

STRONGLY DISAGREE |____|____|____|____|____|____|____| STRONGLY AGREE

34. I will use heroin as soon as I get the chance.

STRONGLY DISAGREE |___|___|___|___|___|___|___| STRONGLY AGREE

35. I have no desire to use heroin right now.

STRONGLY DISAGREE |___|___|___|___|___|___|___| STRONGLY AGREE

36. If I were using heroin, I would feel less tense.

STRONGLY DISAGREE |___|___|___|___|___|___|___| STRONGLY AGREE

37. Using heroin right now would make me content.

STRONGLY DISAGREE |___|___|___|___|___|___|___| STRONGLY AGREE

38. It would be easy to pass up the chance to use heroin.

STRONGLY DISAGREE |___|___|___|___|___|___|___| STRONGLY AGREE

39. I crave heroin right now.

STRONGLY DISAGREE |___|___|___|___|___|___|___| STRONGLY AGREE

40. If I were offered some heroin, I would use it immediately.

STRONGLY DISAGREE |___|___|___|___|___|___|___| STRONGLY AGREE

41. Using heroin would make me feel less depressed.

STRONGLY DISAGREE |___|___|___|___|___|___|___| STRONGLY AGREE

42. I have an urge for heroin.

STRONGLY DISAGREE |___|___|___|___|___|___|___| STRONGLY AGREE

43. I am thinking of ways to get heroin.

STRONGLY DISAGREE |___|___|___|___|___|___|___| STRONGLY AGREE

44. I could easily control how much heroin I used right now.

STRONGLY DISAGREE |___|___|___|___|___|___|___| STRONGLY AGREE

45. I think that I could resist using heroin now.

STRONGLY DISAGREE |___|___|___|___|___|___|___| STRONGLY AGREE

8.2.2 Eysenck Personality Questionnaire – Revised (EPQ-R)

INSTRUCTIONS: Please answer each question by putting a circle around the 'YES' or 'NO' following the question. There are no right or wrong answers, and no trick questions. Work quickly and do not think too long about the exact meaning of the questions.

PLEASE REMEMBER TO ANSWER EACH QUESTION

1. Do you have many different hobbies? YES / NO
2. Do you stop to think things over before doing anything? YES / NO
3. Does your mood often go up and down? YES / NO
4. Have you ever taken praise for something you knew someone else had really done? YES / NO
5. Do you take much notice of what people think? YES / NO
6. Are you a talkative person? YES / NO
7. Would being in debt worry you? YES / NO
8. Do you ever feel 'just miserable' for no reason? YES / NO
9. Do you give money to charities? YES / NO
10. Were you ever greedy by helping yourself to more than your share of anything? YES / NO
11. Are you rather lively? YES / NO
12. Would it upset you a lot to see a child or an animal suffer? YES / NO
13. Do you often worry about things you should not have done or said? YES / NO
14. Do you dislike people who don't know how to behave themselves? YES / NO
15. If you say you will do something, do you always keep your promise no matter how inconvenient it might be? YES / NO
16. Can you usually let yourself go and enjoy yourself at a lively party? YES / NO
17. Are you an irritable person? YES / NO
18. Should people always respect the law? YES / NO
19. Have you ever blamed someone for doing something you knew was really your fault? YES / NO

20. Do you enjoy meeting new people? YES / NO
21. Are good manners very important? YES / NO
22. Are your feelings easily hurt? YES / NO
23. Are *all* your habits good and desirable ones? YES / NO
24. Do you tend to keep in the background on social occasions? YES / NO
25. Would you take drugs which may have strange or dangerous effects? YES / NO
26. Do you often feel 'fed-up'? YES / NO
27. Have you ever taken anything (even a pin or button) that belonged to someone else? YES / NO
28. Do you like going out a lot? YES / NO
29. Do you prefer to go your own way rather than act by the rules? YES / NO
30. Do you enjoy hurting people you love? YES / NO
31. Are you often troubled about feelings of guilt? YES / NO
32. Do you sometimes talk about things you know nothing about? YES / NO
33. Do you prefer reading to meeting people? YES / NO
34. Do you have enemies who want to harm you? YES / NO
35. Would you call yourself a nervous person? YES / NO
36. Do you have many friends? YES / NO
37. Do you enjoy practical jokes that can sometimes really hurt people? YES / NO
38. Are you a worrier? YES / NO
39. As a child, did you do as you were told immediately and without grumbling? YES / NO
40. Would you call yourself happy-go-lucky? YES / NO
41. Do good manners and cleanliness matter much to you? YES / NO
42. Have you often gone against your parents' wishes? YES / NO
43. Do you worry about awful things that might happen? YES / NO
44. Have you ever broken or lost something belonging to someone else? YES / NO
45. Do you usually take the initiative in making new friends? YES / NO
46. Would you call yourself tense or 'highly-strung'? YES / NO
47. Are you mostly quiet when you are with other people? YES / NO
48. Do you think marriage is old fashioned and should be done away with?

YES / NO

49. Do you sometimes boast a little? YES / NO
50. Are you more easy-going about right and wrong than most people? YES / NO
51. Can you easily get some life in to a rather dull party? YES / NO
52. Do you worry about your health? YES / NO
53. Have you ever said anything bad or nasty about anyone? YES / NO
54. Do you enjoy co-operating with others? YES / NO
55. Do you like telling jokes and funny stories to your friends? YES / NO
56. Do most things taste the same to you? YES / NO
57. As a child, were you ever cheeky to your parents? YES / NO
58. Do you like mixing with people? YES / NO
59. Does it worry you if you know there are mistakes in your work? YES / NO
60. Do you suffer from sleeplessness? YES / NO
61. Have people said that you sometimes act too rashly? YES / NO
62. Do you always wash before a meal? YES / NO
63. Do you nearly always have a 'ready-answer' when people take to you? YES / NO
64. Do you like to arrive at appointments in plenty of time? YES / NO
65. Have you often felt listless and tired for no reason? YES / NO
66. Have you ever cheated at a game? YES / NO
67. Do you like doing things in which you have to act quickly? YES / NO
68. Is (or was) your mother a good woman? YES / NO
69. Do you often make decisions on the spur of the moment? YES / NO
70. Do you often feel life is very dull? YES / NO
71. Have you ever taken advantage of someone? YES / NO
72. Do you often take on more activities than you have time for? YES / NO
73. Are there several people who keep trying to avoid you? YES / NO
74. Do you worry a lot about your looks? YES / NO
75. Do you think people spend too much time safeguarding their future with savings and insurance? YES / NO
76. Have you ever wished that you were dead? YES / NO

77. Would you dodge paying taxes if you knew you could never be found out? YES / NO
78. Can you get a party going? YES / NO
79. Do you try not to be rude to people? YES / NO
80. Do you worry too long after an embarrassing experience? YES / NO
81. Do you generally 'look before you leap'? YES / NO
82. Have you ever insisted on having your own way? YES / NO
83. Do you suffer from 'nerves'? YES / NO
84. Do you often feel lonely? YES / NO
85. Can you on the whole trust people to tell the truth? YES / NO
86. Do you always practise what you preach? YES / NO
87. Are you easily hurt when people find fault with you or the work you do? YES / NO
88. Is it better to follow society's rules than go your own way? YES / NO
89. Have you ever been late for an appointment or work? YES / NO
90. Do you like plenty of bustle and excitement around you? YES / NO
91. Would you like other people to be afraid of you? YES / NO
92. Are you sometimes bubbling over with energy and sometimes very sluggish? YES / NO
93. Do you sometimes put off until tomorrow what you ought to do today? YES / NO
94. Do other people think of you as being very lively? YES / NO
95. Do people tell you a lot of lies? YES / NO
96. Do you believe one has special duties to one's family? YES / NO
97. Are you touchy about some things? YES / NO
98. Are you always willing to admit it when you have made a mistake? YES / NO
99. Would you feel sorry for an animal caught in a trap? YES / NO
100. When your temper rises, do you find it difficult to control? YES / NO
101. Do you lock up your house carefully at night? YES / NO
102. Do you believe insurance schemes are a good idea? YES / NO
103. Do people who drive carefully annoy you? YES / NO
104. When you catch a train, do you often arrive at the last minute? YES / NO

105.Do your friendships break up easily with out it being your fault? YES / NO

106.Do you sometimes feel like teasing animals? YES / NO

8.2.3 Eysenck Personality Questionnaire – Impulsiveness, Venturesomeness, Empathy (EPQ-IVE)

INSTRUCTIONS: Please answer each question by putting a circle around the YES or NO following the question. There are no right or wrong answers, and no trick questions. Work quickly and do not think too long about the exact meaning of the questions. **PLEASE ANSWER EACH QUESTION**

1. Would you enjoy water skiing? YES NO

2. Usually do you prefer to stick to brands you know are reliable, to trying new ones on the chance of finding something better? YES NO

3. Would you feel sorry for a lonely stranger? YES NO

4. Do you quite enjoy taking risks? YES NO

5. Do you often get emotionally involved with your friends' problems? YES NO

6. Would you enjoy parachute jumping? YES NO

7. Do you often buy things on impulse? YES NO

8. Do unhappy people who are sorry for themselves irritate you? YES NO

9. Do you generally do and say things without stopping to think? YES NO

10. Are you inclined to get nervous when others around you seem to be nervous? YES NO

11. Do you often get into a jam because you do things without thinking? YES NO

12. Do you think hitchhiking is too dangerous a way to travel? YES NO

13. Do you find it silly for people to cry out of happiness? YES NO

14. Do you like diving off the high board? YES NO

15. Do people you are with have a strong influence on your moods? YES NO

16. Are you an impulsive person? YES NO

17. Do you welcome new and exciting experiences and sensations, even if they are a little frightening and unconventional? YES NO

18. Does it affect you very much when one of your friends seems upset? YES NO

19. Do you usually think carefully before doing anything? YES NO

20. Would you like to learn to fly an aeroplane? YES NO

21. Do you ever get deeply involved with the feelings of a character in a film, play or novel? YES NO

22. Do you often do things on the spur of the moment? YES NO

23. Do you get very upset when you see someone cry? YES NO

24. Do you sometimes find someone else's laughter catching? YES NO

25. Do you mostly speak without thinking things out? YES NO

26. Do you often get involved in things you later wish you could get out of? YES NO

27. Do you get so "carried away" by new and exciting ideas, that you never think of possible snags? YES NO

28. Do you find it hard to understand people who risk their necks climbing mountains? YES NO

29. Can you make decisions without worrying about other people's feelings? YES NO

30. Do you sometimes like doing things that are a bit frightening? YES NO

31. Do you need to use a lot of self-control to keep out of trouble? YES NO

32. Do you become more irritated than sympathetic when you see someone cry? YES NO

33. Would you agree that almost everything enjoyable is illegal or immoral? YES NO

34. Generally do you prefer to enter cold sea water gradually, to diving or jumping straight in? YES NO

35. Are you often surprised at people's reactions to what you do or say? YES NO

36. Would you enjoy the sensation of skiing very fast down a high mountain slope? YES NO

37. Do you like watching people opening presents? YES NO

38. Do you think an evening out is more successful if it is unplanned or arranged at the last moment? YES NO

39. Would you like to go scuba diving? YES NO

40. Would you find it very hard to break bad news to someone? YES NO

41. Would you enjoy fast driving? YES NO

42. Do you usually work quickly without bothering to check? YES NO

43. Do you often change your interests? YES NO

44. Before making up your mind, do you consider all the advantages and disadvantages? YES NO

45. Can you get very interested in your friends' problems? YES NO

46. Would you like to go pot-holing? YES NO

47. Would you be put off a job involving quite a bit of danger? YES NO

48. Do you prefer to "sleep on it" before making decisions? YES NO

49. When people shout at you, do you shout back? YES NO

50. Do you feel sorry for very shy people? YES NO

51. Are you happy when you are with a cheerful group and sad when the others are glum? YES NO

52. Do you usually make up your mind quickly? YES NO

53. Can you imagine what it must be like to be very lonely? YES NO

54. Does it worry you when others are worrying and panicky? YES NO

8.2.4 Severity of Dependence Scale (SDS)

Please can you answer the following questions for each drug you used in the month before entering Oakwood House. Each question refers to how you felt in the month before entering Oakwood House.

1 = Never, or almost never
2 = Sometimes
3 = Often
4 = Always, or almost always

Drug Name	Did you ever think your drug use was out of control?	Did the prospect of missing a fix or dose make you anxious or worried?	Did you worry about your drug use?	Did you wish you could stop?	How difficult did you find it to stop or go without your drug?
Alcohol					

8.2.5 General Health MOS- Short form 36 (SF-36) UK version

Instructions: The questions below ask you about your health, including how you feel and how well you are able to do your usual activities. If you are unsure how to answer, please give the best answer you can. Thank you.

1. In general, would you say your health is: (circle one)

Excellent	1
Very good	2
Good	3
Fair	4
Poor	5

2. Compared to one year ago, how would you rate your health in general now?

(circle one)

Much better now than one year ago	1
Somewhat better now than one year ago	2
About the same as one year ago	3
Somewhat worse now than one year ago	4
Much worse now than one year ago	5

3. The following questions are about activities you might do during a typical day. Does your health now limit you in these activities? If so, how much?

(circle one number on each line)

Activities	Yes, Limited a lot	Yes, Limited a little	No, Not limited at all
a. **Vigorous activities**, such as running, lifting heavy objects, participating in strenuous sports, etc.	1	2	3
b. **Moderate activities**, such as moving a table, pushing a vacuum cleaner, bowling, or playing golf, etc.	1	2	3
c. Lifting or carrying groceries.	1	2	3
d. Climbing **several** flights of stairs.	1	2	3
e. Climbing **one** flight of stairs.	1	2	3
f. Bending, kneeling or stooping.	1	2	3
g. Walking **more than a mile**	1	2	3

h. Walking **half a mile**	1	2	3
i. Walking **one hundred yards.**	1	2	3
j. Bathing or dressing yourself.	1	2	3

4. During the past 4 weeks, have you had any of the following problems with your work or other regular daily activities as a result of your physical health?

circle one number on each line)

	YES	NO
a. Cut down on the amount of time you spent on work or other activities.	1	2
b. Accomplished less than you would like.	1	2
c. Were limited in the kind of work or other activities	1	2
d. Had difficulty performing the work or other activities (for example it took extra effort).	1	2

5. During the past 4 weeks, have you had any of the following problems with your work or other regular daily activities as a result of any emotional problems (such as feeling depressed or anxious)?

(circle one number on each line)

	YES	NO
a. Cut down on the amount of time you spent on work or other activities.	1	2
b. Accomplished less than you would like.	1	2
c. Didn't do work or other activities as carefully as usual.	1	2

6. During the past 4 weeks, to what extent has your physical health or emotional problems interfered with your normal social activities with family, friends, neighbours or groups?

(circle one)

Not at all	1
Slightly	2
Moderately	3
Quite a bit	4
Extremely	5

7. How much bodily pain have you had during the past 4 weeks?

	(circle one)
None	1
Very Mild	2
Mild	3
Moderate	4
Severe	5
Very severe	6

8. During the past 4 weeks, how much did pain interfere with your normal work (including both work outside the home and housework)?

	(circle one)
Not at all	1
Slightly	2
Moderately	3
Quite a bit	4
Extremely	5

9. These questions are about how you feel and how things have been with you during the past 4 weeks. For each question, please give the one answer that comes closest to the way you have been feeling.

How much of the time during the past 4 weeks:- (circle one number on each line)

	All of the time	Most of the time	A good bit of the time	Some of the time	A little of the time	None of the time
a. Did you feel full of life?	1	2	3	4	5	6
b. Have you been a very nervous person?	1	2	3	4	5	6
c. Have you felt so down in the dumps that nothing could cheer you up?	1	2	3	4	5	6
d. Have you felt calm and peaceful?	1	2	3	4	5	6
e. Did you have a lot of	1	2	3	4	5	6

energy?						
f. Have you felt downhearted and low?	1	2	3	4	5	6
g. Did you feel worn out?	1	2	3	4	5	6
h. Have you been a happy person?	1	2	3	4	5	6
h. Did you feel tired?	1	2	3	4	5	6

10. During the past 4 weeks, how much of the time has your physical health or emotional problems interfered with you social activities (like visiting friends, relatives etc.)?

(circle one)

All of the time	1
Most of the time	2
Some of the time	3
A little of the time	4
None of the time	5

11. How TRUE or FALSE is each of the following statements for you?

(circle one number on each line)

	Definitely true	Mostly true	Don't know	Mostly false	Definitely false
a. I seem to get ill more easily than other people	1	2	3	4	5
b. I am as healthy as anyone I know	1	2	3	4	5
c. I expect my health to get worse	1	2	3	4	5
d. My health is excellent	1	2	3	4	5

8.2.6 Spielberger State-Trait Anxiety Inventory (STAI)

Instructions: Please circle a number on the left to indicate the score which best describes how you are feeling **RIGHT NOW**, that is **AT THIS MOMENT**.

1 = Not at all 2 = Somewhat 3 = Moderately so 4 = Very much so

1. I feel calm	1	2	3	4	
2. I feel secure (safe)	1	2	3	4	
3. I am tense	1	2	3	4	
4. I feel strained	1	2	3	4	
5. I feel at ease (at rest)	1	2	3	4	
6. I feel upset	1	2	3	4	
7. I am presently worrying over possible misfortunes	1	2	3	4	
8. I feel satisfied (happy enough)	1	2	3	4	
9. I feel frightened	1	2	3	4	
10. I feel comfortable	1	2	3	4	
11. I feel self-confident (confident in myself)	1	2	3	4	
12. I feel nervous	1	2	3	4	
13. I feel jittery (shaky)	1	2	3	4	
14. I feel indecisive (unable to make decisions)	1	2	3	4	
15. I feel relaxed	1	2	3	4	
16. I feel content (quietly happy)	1	2	3	4	
17. I feel worried	1	2	3	4	
18. I feel confused (mixed up)	1	2	3	4	
19. I feel steady (stable)	1	2	3	4	
20. I feel pleasant	1	2	3	4	

Instructions: Please circle a number on the left to indicate the score which best describes how you are feeling **GENERALLY**, that is **NOT** just how you feel at this moment.

1 = Not at all 2 = Somewhat 3 = Moderately so 4 = Very much so

12. I feel pleasant	1	2	3	4
13. I feel nervous and restless	1	2	3	4
14. I feel satisfied with myself	1	2	3	4
15. I wish I could be as happy as others seem to be	1	2	3	4
16. I feel like a failure	1	2	3	4
17. I feel rested	1	2	3	4
18. I am "calm, cool and collected"	1	2	3	4
19. I feel that difficulties are piling up so that I cannot overcome them	1	2	3	4
20. I worry too much over something that really doesn't matter	1	2	3	4
21. I am happy	1	2	3	4
22. I have disturbing thoughts	1	2	3	4
23. I lack self-confidence	1	2	3	4
24. I feel secure	1	2	3	4
25. I make decisions easily	1	2	3	4
26. I feel inadequate	1	2	3	4
27. I am content	1	2	3	4
28. Some unimportant thought runs through my mind and bothers me	1	2	3	4
29. I take disappointments so keenly that I can't put them out of my mind	1	2	3	4
30. I am a steady person	1	2	3	4
31. I get in a state of tension or turmoil as I think over my recent concerns and interests	1	2	3	4

Thank you.

8.2.7 Beck Depression Inventory (BDI)

On this questionnaire are groups of statements. Please read each group of statements carefully. Then pick out the one statement in each group which best describes the way you have been feeling in the **past week, including today.** Circle the number beside the statement you picked. If several statements in the group seem to apply equally well, circle each one. Be sure to read all the statements in each group before making your choice.

1.	I do not feel sad.	0
	I feel sad.	1
	I am sad all the time and I can't snap out of it.	2
	I am so sad or unhappy that I can't stand it.	3
2.	I am not particularly discouraged about my future.	0
	I feel discouraged about the future.	1
	I feel I have nothing to look forward to.	2
	I feel the future is hopeless and that things cannot improve.	3
3.	I do not feel like a failure.	0
	I feel I have failed more than an average person.	1
	As I look back on my life, all I can see is a lot of failures.	2
	I feel I am a complete failure as a person.	3
4.	I get as much satisfaction out of things as I used to.	0
	I don't enjoy things the way I used to.	1
	I don't get real satisfaction out of anything any more.	2
	I am dissatisfied or bored with everything.	3
5.	I don't feel particularly guilty.	0
	I feel guilty a good part of the time.	1
	I feel quite guilty most of the time.	2
	I feel guilty all of the time.	3
6.	I don't feel I am being punished.	0
	I feel I may be punished.	1
	I expect to be punished.	2
	I feel I am being punished.	3
7.	I don't feel disappointed in myself.	0
	I am disappointed in myself	1
	I am disgusted with myself	2
	I hate myself	3

8.	I don't feel I am worse than anybody else	0
	I am critical of myself for my weaknesses or mistakes	1
	I blame myself all the time for my faults	2
	I blame myself for everything bad that happens	3
9.	I don't have any thoughts of killing myself	0
	I have thoughts of killing myself but I would not carry them out	1
	I would like to kill myself	2
	I would kill myself if I had the chance	3
10.	I don't cry any more than usual	0
	I cry more than I used to	1
	I cry all the time now	2
	I used to be able to cry, but now I can't cry even though I want to	3
11.	I am no more irritated now than I ever am	0
	I get annoyed or irritated more easily than I used to	1
	I feel irritated all the time now	2
	I don't get irritated at all by the things which used to irritate me	3
12.	I have not lost interest in other people	0
	I am less interested in other people	1
	I have lost most of my interest in other people	2
	I have lost all my interest in other people	3
13.	I make decisions as well now as I ever could	0
	I put off making decisions more than I used to	1
	I have greater difficulty in making decisions than before	2
	I can't make decisions at all any more	3
14.	I don't feel I look any worse than I used to	0
	I am worried that I am looking old or unattractive	1
	I feel there are permanent changes in my appearance that make me look unattractive	2
	I believe I look ugly	3
15.	I can work about as well as before	0
	It takes an extra effort to get started at doing something	1
	I have to push myself very hard to do anything	2
	I can't do any work at all	3
16.	I can sleep as well as usual	0
	I don't sleep as well as I used to	1
	I wake up 1-2 hours earlier	2
	I wake up several hours earlier than I used to and cannot get back to sleep	3

17.	I don't get more tired than usual	0
	I get tired more easily than I used to	1
	I get tired from doing almost anything	2
	I am too tired to do anything	3
18.	My appetite is no worse than usual	0
	My appetite is not as good as usual	1
	My appetite is much worse now	2
	I have no appetite at all any more	3
19.	I haven't lost much weight, if any, lately	0
	I have lost more than 5lbs	1
	I have lost more than 10lbs	2
	I have lost more than 15lbs	3
	I am purposely trying to lose weight by eating less:	Yes / No
20.	I am no more worried about my health than usual	0
	I am worried about physical problems such as aches and pains, upset stomach, or constipation	1
	I am worried about physical problems and it's hard to think of much else	2
	I am so worried about my physical problems that I cannot think about anything else	3
21.	I have not noticed any recent change in my interest in sex	0
	I am less interested in sex than I used to be	1
	I am much less interested in sex now	2
	I have lost interest in sex completely	3

8.2.8 Addition Research Centre Inventory (ARCI)

These 49 items may or may not describe how you feel **RIGHT NOW**. Mark T (for True) next to each item that does describe how you feel, and mark F (for False) for the items that do not describe how you feel. You must mark either T or F for each statement.

1. My speech is slurred.	T	F	18. I can completely appreciate what others are saying when I am in this mood.	T	F
2. I am not as active as usual.	T	F	19. I would be happy all the time if I feel as I feel now.	T	F
3. I have a feeling of things being an uphill struggle rather than plain sailing	T	F	20. I feel so good that I know other people can tell it.	T	F
4. I feel sluggish.	T	F	21. I feel as if something pleasant had just happened to me.	T	F
5. My head feels heavy.	T	F	22. I would be happy all the time if I felt as I do now.	T	F
6. I feel like avoiding people although I usually do not feel this way.	T	F	23. I feel more clear headed than dreamy.	T	F
7. I feel dizzy.	T	F	24. I feel as if I am popular with people today.	T	F
8. It seems harder than usual to move around.	T	F	25. I feel a very pleasant emptiness.	T	F
9. I am moody.	T	F	26. My thoughts come more easily than usual.	T	F
10. People might say that I'm a little dull today.	T	F	27. I feel less discouraged than usual.	T	F
11. I feel drowsy.	T	F	28. I am in the mood to talk about the feelings I have.	T	F
12. I am full of energy.	T	F	29. I feel more excited than dreamy.	T	F
13. Today I find it easy to express myself.	T	F	30. Answering these questions was very easy today.	T	F
14. Things around me seem more pleasing than usual.	T	F	31. My memory seems sharper to me than usual.	T	F

15. I have a pleasant feeling in my stomach.	T	F	32. I feel as if I could write for hours.	T	F
16. I fear I will lose the contentment that I have now.	T	F	33. I feel very patient.	T	F
17. I feel in complete harmony with the world and those about me.	T	F	34. Some parts of my body are tingling.	T	F
35. I had a weird feeling.	T	F	43. I notice my hand shakes when I try to write.	T	F
36. My movements seem faster than usual.	T	F	44. I have a disturbance in my stomach.	T	F
37. I have better control over myself than usual.	T	F	45. I feel an increasing awareness of bodily sensations	T	F
38. My movements seem slower than usual.	T	F	46. I feel anxious and upset.	T	F
39. I find it hard to keep my mind on a task or job.	T	F	47. I have an unusual weakness of my muscles.	T	F
40. I do not feel like reading anything right now.	T	F	48. A thrill has gone through me one or more times since I started the test.	T	F
41. It seems I am spending longer than I should on each of these questions.	T	F	49. My movements are free, relaxed and pleasurable.	T	F
42. My hands feel clumsy.	T	F			

8.2.9 Adjective Checklist (AC)

For each item below, indicate how you feel **RIGHT NOW** using the scale below.

0 = not at all 1 = a little 2 = moderately 3 = quite a bit 4 = extremely

Normal	0 1 2 3 4	Restless	0 1 2 3 4
Stomach churning	0 1 2 3 4	Watery eyes	0 1 2 3 4
Nodding off to sleep	0 1 2 3 4	Runny nose	0 1 2 3 4
Skin itchy	0 1 2 3 4	Chills or gooseflesh	0 1 2 3 4
Heavy or sluggish feeling	0 1 2 3 4	Sick to stomach	0 1 2 3 4
Relaxed	0 1 2 3 4	Sneezing	0 1 2 3 4
Dry mouth	0 1 2 3 4	Abdominal cramps	0 1 2 3 4
"Coasting along"	0 1 2 3 4	Irritable	0 1 2 3 4
Carefree	0 1 2 3 4	Backache	0 1 2 3 4
Talkative	0 1 2 3 4	Tense and jittery	0 1 2 3 4
Friendly	0 1 2 3 4	Sweating	0 1 2 3 4
Good mood	0 1 2 3 4	Depressed / sad	0 1 2 3 4
Pleasant sick	0 1 2 3 4	Sleepy	0 1 2 3 4
Energetic	0 1 2 3 4	Shaky (hands)	0 1 2 3 4
Drive / Enthusiasm	0 1 2 3 4	Hot or cold flushes	0 1 2 3 4
Drunken	0 1 2 3 4	Bothered by noises	0 1 2 3 4
Nervous	0 1 2 3 4	Skin clammy and damp	0 1 2 3 4
Muscle cramps	0 1 2 3 4	Painful joints	0 1 2 3 4
Flushing	0 1 2 3 4	Yawning	0 1 2 3 4

8.2.10 Modified Himmelsbach Opiate Withdrawal Scale – Observer Rated (OWS)

Lacrimation: ☐

0 = None. 1 = manually induced. 2 = spontaneous

Rhinorrhoea: ☐

0 = None. 1 = watery sound on sniffing 2 = spontaneous runny nose

Piloerection: ☐

0 = None. 1 = can feel bumps 2 = visible without touching

Perspiration: ☐

0 = None. 1 = can palpate sweat 2 = visible sweating

Restlessness: (in past 15 minutes) ☐

0 = None. 1 = one behavioural sign 2 = more than one behavioural sign

Yawning: ☐

0 = None. 1 = one yawn 2 = more than one yawn

Total: ☐

8.2.11 Mood Profile

Instructions: Please make a mark on the line to indicate how you have felt **IN THE LAST 24 HOURS**, compared to your usual self over the last few weeks or months. The closer you make a mark to either end of the line, the greater the change in your feelings. Making a mark in the shaded area, means you felt no different from usual.

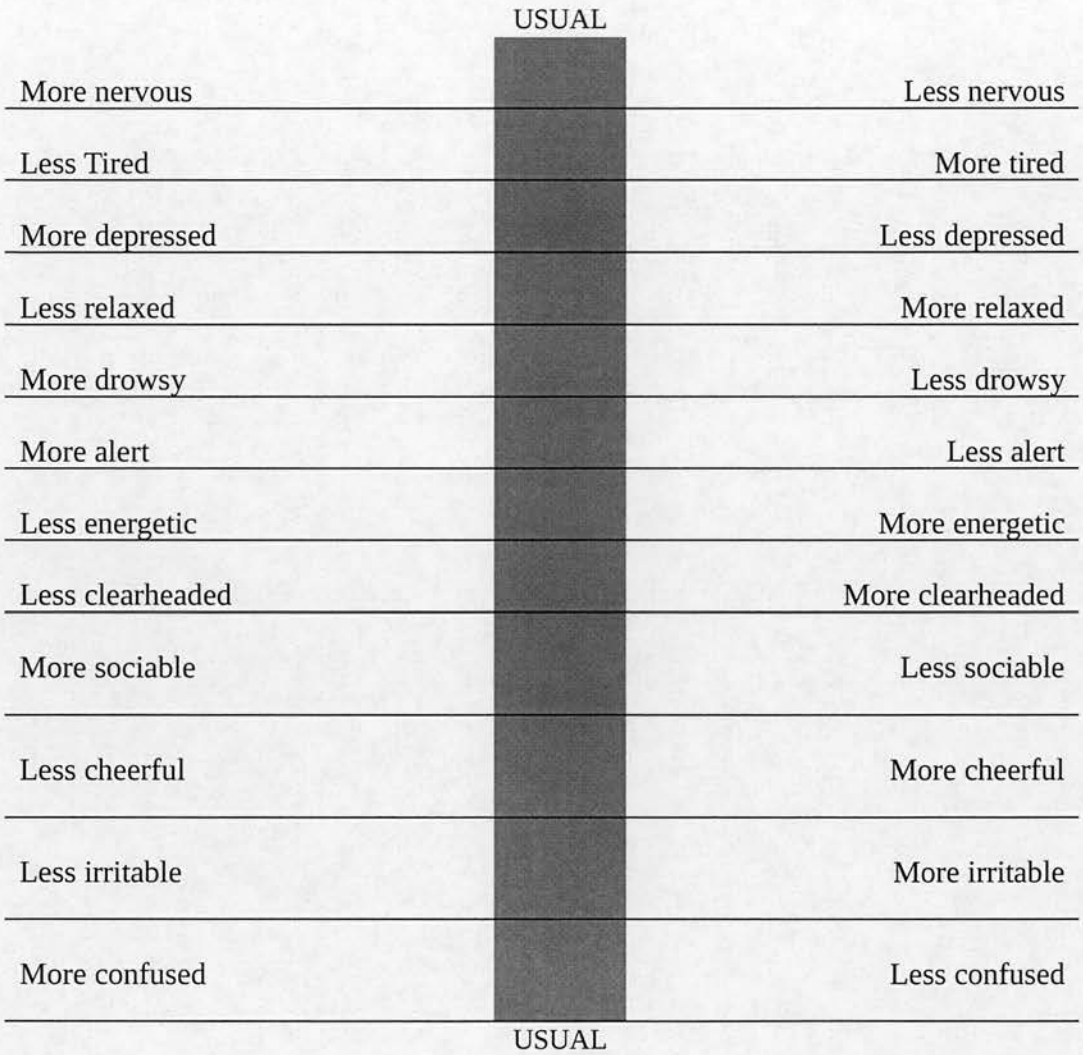

8.2.12 Obsessive Compulsive Drinking Scale modified for opiates

Instructions: The questions below ask about your opiate (e.g. heroin, methadone, codeine etc) use, and your attempts to control your opiate use. Please circle the number next to the statement that best applies to you. Thank you.

1. How much of your time when you're not actually under the influence of opiates is occupied by ideas, thoughts, impulses, or images relating to opiate use?

0 = None
1 = Less than 1 hour a day
2 = 1-3 hours a day
3 = 4-8 hours a day
4 = Greater than 8 hours a day

2. How frequently do these thoughts occur?

0 = Never
1 = No more than 8 times a day
2 = More than 8 times a day, but most hours of the day are free of those thoughts
3 = More than 8 times a day, and during most hours of the day
4 = Thoughts are too numerous to count, and an hour rarely passes without several such thoughts occurring

3. How much do these ideas, thoughts, impulses, or images related to opiate use interfere with your social or work (or role) functioning? Is there anything you don't or can't do because of them? (If you are not currently working, how much of your performance would be affected if you were working?)

0 = Thoughts of opiate use *never* interfere - I can function normally
1 = Thoughts of opiate use *slightly* interfere with my social or occupational activities (what occupies me, e.g. work), but my overall performance is not impaired
2 = Thoughts of opiate use *definitely* interfere with my social or occupational performance, but I can still manage
3 = Thoughts of opiate use cause *substantial* (considerable) impairment in my social or occupational performance
4 = Thoughts of opiate use interfere *completely* with my social or work performance

4. How much distress or disturbance do these ideas, thoughts, impulses, or images related to opiate use cause you when you're not actually under the influence of opiates?

0 = None
1 = Mild, infrequent, and not too disturbing
2 = Moderate, frequent, and disturbing, but still manageable
3 = Severe, very frequent, and very disturbing
4 = Extreme, nearly constant, and disabling distress

5. How much of an effort do you make to resist these thoughts or try to disregard or turn your attention away from these thoughts as they enter your mind when you're not actually under the influence of opiates? (please rate *your effort made to resist these thoughts*, not your success or failure in actually controlling them)

0 = My thoughts are so minimal, I don't need to actively resist. If I have thoughts, I make an effort to *always* resist
1 = I try to resist most of the time
2 = I make some effort to resist
3 = I give in to all such thoughts without attempting to control them, but I do so with some reluctance (unwillingness)
4 = I completely and willingly give in to all such thoughts

6. How successful are you in stopping or diverting these thoughts when you're not actually under the influence of opiates?

0 = I am completely successful in stopping or diverting such thoughts
1 = I am usually able to stop or divert such thoughts with some effort and concentration
2 = I am sometimes able to stop or divert such thoughts
3 = I am rarely successful in stopping such thoughts and can only divert such thoughts with difficulty
4 = I am rarely able to divert such thoughts even momentarily (for a moment)

7. How many times do you INJECT opiates each day (include injecting and skin popping)?

0 = None
1 = Less than one injection per day

2 = 1 injection per day
3 = 2-3 injections per day
4 = 4 or more injections per day

8. How many times do you USE opiates each day (include injecting, skin popping, smoking and swallowing)?

0 = None
1 = Less than one use per day
2 = 1-2 uses per day
3 = 3-7 uses per day
4 = 8 or more uses per day

9. How many days each week do you use opiates?

0 = None
1 = No more than 1 day per week
2 = 2-3 days per week
3 = 4-5 days per week
4 = 6-7 days per week

10. How much does your opiate use interfere with your work functioning? Is there anything you don't or can't do because of your opiate use? (If you are not currently working, how much of your performance would be affected if you were working?)

0 = Opiate use *never* interferes - I can function normally
1 = Opiate use *slightly* interferes with my occupational activities (what occupies me, e.g. work), but my overall performance is not impaired
2 = Opiate use *definitely* interferes with my occupational performance, but I can still manage
3 = Opiate use causes *substantial* (considerable) impairment in my occupational performance
4 = Problems caused by opiate use interfere *completely* with my work performance

11. How much does your opiate use interfere with your social functioning? Is there anything you don't or can't do because of your opiate use?

0 = Opiate use *never* interferes - I can function normally
1 = Opiate use *slightly* interferes with my social activities, but my overall performance is not impaired
2 = Opiate use *definitely* interferes with my social performance, but I can

still manage

3 = Opiate use causes *substantial* (considerable) impairment in my social performance

4 = Problems caused by opiate use interfere *completely* with my social performance

12. If you were prevented from using opiates when you desired opiates, how anxious or upset would you become?

0 = I would not experience any anxiety or irritation

1 = I would become only slightly anxious or irritated

2 = The anxiety or irritation would mount, but remain manageable

3 = I would experience a prominent and very disturbing increase in anxiety or irritation

4 = I would experience incapacitating (disabling) anxiety or irritation

13. How much of an effort do you make to resist using opiates? (Only rate *your effort to resist,* not your success or failure in actually controlling your opiate use)

0 = My opiate use is so minimal, I don't need to actively resist. If I use opiates, I make an effort to *always* resist

1 = I try to resist most of the time

2 = I make some effort to resist

3 = I give in to almost all my opiate use without attempting to control it, but I do so with some reluctance (unwillingness)

4 = I completely and willingly give in to all opiate use

14. How strong is the drive (internal pressure) to use opiates?

0 = No drive

1 = Some pressure to use opiates

2 = Strong pressure to use opiates

3 = Very strong pressure to use opiates

4 = The drive to use opiates is completely involuntary (not under my own control) and overpowering

15. How much control do you have over the use of opiates?

0 = I have complete control

1 = I am usually able to exercise voluntary control over it

2 = I can control it only with difficulty

3 = I must use opiates and can only delay using with difficulty

4 = I am rarely able to delay using opiates even momentarily (for a moment)

8.2.13 Drug Profile

DRUG PROFILE - OPIATES: If you circle "YES" in the first column, please complete the rest of that row, including each opiate that you have taken.

	PREVIOUS OPIATE USE				RECENT OPIATE USE		
	Have you EVER used this drug? If "yes", please also fill in the rest of that row	**How old were you when you FIRST took it?**	**How long ago when you LAST took it (OR how old were you if not in the last year)?**	**For how many months or years did you use it regularly (OR if not regularly how many times)?**	**How many days have you used it out of the last 28 days? (N = None)**	**On average how much have you used daily in the last 28 days? (N = None)**	**How are/were you taking it? O = Oral S = Smoked I = Injected Other (pl. state)**
Opiates							
Heroin by smoking	Yes No Unsure						
Heroin by injection	Yes No Unsure						
Prescribed methadone mixt.	Yes No Unsure						
Street methadone mixture	Yes No Unsure						
Methadone tablets	Yes No Unsure						
Buprenorphine (Temgesic)	Yes No Unsure						
Morphine or MST	Yes No Unsure						
Diconal or Palfium	Yes No Unsure						
DF118, Dihydrocodiene	Yes No Unsure						
Codeine, galcodeine	Yes No Unsure						
Co-proxamol (Distalgesic)	Yes No Unsure						
Nalbuphine (Nu-bain)	Yes No Unsure						
Kaolin and Morphine	Yes No Unsure						
Cough mixtures (codeine etc)	Yes No Unsure						
Dr Collis Brown's	Yes No Unsure						
Gee's linctus	Yes No Unsure						
Opium	Yes No Unsure						
Poppy seeds or heads	Yes No Unsure						
Other opioids (please state) 1.	Yes No Unsure						

DRUG PROFILE – NON-OPIATE DRUGS: If you circle "YES" in the first column, please complete the rest of that row. Thank you.

	OTHER PREVIOUS DRUG USE				OTHER RECENT DRUG USE		
	Have you EVER used this drug? If "yes", please also fill in the rest of that row	**How old were you when you FIRST took it?**	**How old were you when you LAST took it (OR how long ago if in the last 12 months)?**	**For how many months or years did you use it regularly (OR if not regularly how many times)?**	**How many days have you used it out of the last 28 days? (N = None)**	**On average how much have you used daily in the last 28 days? (N = None)**	**How are/were you taking it? O = Oral S = Smoked I = Injected Other (pl. state)**
Non-opiate drugs							
Alcohol	Yes No Unsure						
Cannabis	Yes No Unsure						
Amphetamines	Yes No Unsure						
Cocaine	Yes No Unsure						
Crack	Yes No Unsure						
Prescribed tranquillisers e.g. valium, mogodon	Yes No Unsure						
Street tranquillisers	Yes No Unsure						
Barbiturates	Yes No Unsure						
Ecstacy (MDMA)	Yes No Unsure						
LSD (acid)	Yes No Unsure						
Magic mushrooms	Yes No Unsure						
Poppers	Yes No Unsure						
Glue, solvents, aerosols	Yes No Unsure						
Tobacco	Yes No Unsure						
Steroids	Yes No Unsure						
Others (please specify):							
1.	Yes No Unsure						
2.	Yes No Unsure						
3.	Yes No Unsure						

8.2.14 Injection questionnaire

Please answer the following few questions about the injection you had just before the scan started. Please remember that you may have an injection of hydromorphone for both, one or neither of your two scans. Please circle the option that most closely matches your answer.

1. This time I received an injection of **Hydromorphone / Water**.

2. The effects of this injection were roughly the same as how much street heroin?

   Zero / £10 bag / 2 x £10 bags / ½ gram / 1 gram / 1½ grams / 2 grams

   Injected / Smoked

3. The effects of this injection were roughly the same as how much methadone?

0mg 10mg 20mg 30mg 40mg 50mg 60mg 70mg 80mg 90mg 100mg

8.2.15 Visual Analogue Scales (Craving Study)

1. **At this moment the intensity of my craving for heroin is .....**

0	10	20	30	40	50	60	70	80	90	100
Not at all strong		A little strong			Quite strong		Very strong			The strongest ever

2. **At this moment my urge to take heroin is .....**

0	10	20	30	40	50	60	70	80	90	100
Not at all strong		A little strong			Quite strong		Very strong			The strongest ever

3. **At this moment I feel this happy .....**

0	10	20	30	40	50	60	70	80	90	100
Not at all		A little			Quite a bit		Very			The most I could be

4. **At this moment I feel this sad .....**

0	10	20	30	40	50	60	70	80	90	100
Not at all		A little			Quite a bit		Very			The most I could be

5. **At this moment I feel this anxious .....**

0	10	20	30	40	50	60	70	80	90	100
Not at all		A little			Quite a bit		Very			The most I could be

6. **At this moment I the vividness of the script is .....**

0	10	20	30	40	50	60	70	80	90	100
Not at all		A little			Quite a bit		Very			The most I could be

8.2.16 Visual Analogue Scales (Raclopride Study)

1. **At this moment I feel this sleepy .....**

0	10	20	30	40	50	60	70	80	90	100
Not at all		A little			Quite a bit		Very			The most I could be

2. **At this moment my urge to take heroin is .....**

0	10	20	30	40	50	60	70	80	90	100
Not at all strong		A little strong			Quite strong		Very strong			The strongest ever

3. **At this moment the intensity of my craving for heroin is..**

0	10	20	30	40	50	60	70	80	90	100
Not at all strong		A little strong			Quite strong		Very strong			The strongest ever

4. **At this moment I feel this gouched out .....**

0	10	20	30	40	50	60	70	80	90	100
Not at all		A little			Quite a bit		Very			The most I could be

5. **At this moment I feel I am withdrawing .....**

0	10	20	30	40	50	60	70	80	90	100
Not at all		A little			Quite a bit		Very			The most I could be

6. **At this moment I feel this high .....**

0	10	20	30	40	50	60	70	80	90	100
Not at all		A little			Quite a bit		Very			The most I could be

7. **At this moment I feel this much of a rush .....**

0	10	20	30	40	50	60	70	80	90	100
Not at all		A little			Quite a bit		Very			The most I could be